



UNIVERSIDAD DE CHILE  
FACULTAD DE CIENCIAS FÍSICAS Y MATEMÁTICAS  
DEPARTAMENTO DE INGENIERÍA QUÍMICA, BIOTECNOLOGÍA Y  
MATERIALES

BIOPROSPECTION AND PEPTIDOGENOMICS OF NOVEL  
*STREPTOMYCES* SPECIES FROM SALAR DE HUASCO

TESIS PARA OPTAR AL GRADO DE DOCTOR EN CIENCIAS DE LA INGENIERÍA  
MENCIÓN INGENIERÍA QUÍMICA Y BIOTECNOLOGÍA

CARLOS JAVIER CORTÉS ALBAYAY

PROFESORES GUIAS

JUAN ASENJO DE LEUZE DE LANCIZOLLE  
BARBARA ANDREWS FARROW

MIEMBROS DE LA COMISION

ORIANA SALAZAR AGUIRRE  
BERNARDO GONZALEZ OJEDA  
BRUCE CASSELS NIVEN

[PROYECTO FINANCIADO POR PFCHA/DOCTORADO BECAS CHILE/2016-21160585]

SANTIAGO DE CHILE  
2019

**SUMMARY OF THE THESIS FOR THE DEGREE IN:** PhD. in Engineering Sciences, mention Chemical Engineering and Biotechnology  
**BY:** Carlos Javier Cortés Albayay  
**DATE:** August 2019  
**SUPERVISORS:** PhD. Juan A. Asenjo and PhD. Barbara Andrews

## **BIOPROSPECTION AND PEPTIDOGENOMICS OF NOVEL *STREPTOMYCES* SPECIES FROM SALAR DE HUASCO**

Over the last decade the Atacama Desert has become one of the most studied extremobiosphere biomes for the microbial bioprospection focused on novel actinobacterial species. Many of the habitats found in Atacama Desert, including those defined as hyper-arid and -saline have demonstrated a dominance of actinobacteria, of which many have been the source of a novel chemodiversity of natural products and biosynthetic gene clusters for specialized metabolites of valuable pharmaceutical interest.

The Salar de Huasco is an athalassohaline and poly-extreme high altitude wetland in the Chilean Altiplano of the Atacama Desert, characterized for its high levels of solar radiation, aridity and high salinity of its soils. Our first culture-dependent study carried out on this ecosystem for the selective isolation of new *Streptomyces* species from arid soil samples of the Salar de Huasco shoreline, showed the presence of a high number of phenotypically and genotypically different *Streptomyces* strains. Some of them successfully inhibited the growth of Gram-positive and Gram-negative pathogens, fungal pathogens and showed cytotoxicity against hepatocellular carcinoma (HepG2) and mouse fibroblast cell lines (NIH-3T3).

Two of the most promising *Streptomyces* strains demonstrated genetic, phenotypic and chemotaxonomic features that distinguished them from their closest type strains and were validly described as the novel alkalitolerant species *Streptomyces altiplanensis* HST21<sup>T</sup> and *Streptomyces huasconensis* HST28<sup>T</sup>.

A protein-centric genome mining analysis for these new species revealed a high number of biosynthetic gene clusters (BGCs) including lasso peptides and lanthipeptides. *Streptomyces huasconensis* HST28<sup>T</sup> showed 4 lasso peptide BGCs of the classes II and IV of which a new class II lasso peptide was successfully detected in vitro by means of a peptidogenomic approach. This new lasso peptide, named huascopeptin, showed the first seven-membered macrolactam ring motif structure, the smallest ring currently described in a lasso peptide. Our findings suggest that poly-extreme environments like the Salar de Huasco are promising sources for exploring novel and valuable producers of natural products with pharmaceutical potential.

**RESUMEN DE LA TESIS PARA OPTAR AL GRADO DE:** Doctor en Ciencias de la Ingeniería, mención Ingeniería Química y Biotecnología  
**POR:** Carlos Javier Cortés Albayay  
**FECHA:** Agosto 2019  
**SUPERVISORES:** Dr. Juan A. Asenjo y Dra. Barbara Andrews

## **BIOPROSPECCIÓN Y PEPTIDOGENÓMICA DE NUEVAS ESPECIES DE *STREPTOMYCES* DEL SALAR DE HUASCO**

Durante la última década, el Desierto de Atacama se ha convertido en uno de los más estudiados biomas de la extremobiosfera para la bioprospección microbiana enfocada en nuevas especies de actinobacterias. Muchos de estos hábitats encontrados en el Desierto de Atacama, incluyendo aquellos definidos como hiperáridos e hiper-salinos han demostrado una dominancia de actinobacterias, de las cuales muchas han sido fuente de una nueva quimiodiversidad de productos naturales y clusters de genes biosintéticos de metabolitos especializados de gran interés farmacéutico.

El Salar de Huasco es un humedal de altura, atalasohalino y poliextremo en el altiplano Chileno del Desierto de Atacama, caracterizado por sus altos niveles de radiación solar, aridez y alta salinidad de sus suelos. Nuestro primer estudio dependiente de cultivo llevado a cabo en este ecosistema, para el aislamiento selectivo de nuevas especies de *Streptomyces*, desde muestras de suelo áridas de la orilla del Salar de Huasco, mostró la presencia de un alto número de cepas de *Streptomyces* fenotípica y genotípicamente diferentes. Algunas de ellas inhibieron exitosamente el crecimiento de patógenos Gram-positivos y –negativos, patógenos fúngicos y mostraron citotoxicidad contra líneas celulares de carcinoma hepatocelular (HepG2) y fibroblastos de ratón (NIH-3T3).

Dos de las cepas de *Streptomyces* más prometedoras demostraron características fenotípicas, genéticas y quimiotaxonómicas que las distinguieron de sus cepas tipo más cercanas y fueron válidamente descritas como las nuevas especies alcali-tolerantes *Streptomyces altiplanensis* HST21<sup>T</sup> y *Streptomyces huasconensis* HST28<sup>T</sup>.

Un análisis de minería de genomas centrado en proteínas, de estas nuevas especies, reveló un alto número de clusters de genes biosintéticos (CGBs) incluyendo péptidos lazo y lantipéptidos. *Streptomyces huasconensis* HST28<sup>T</sup> mostró 4 CGBs de péptidos lazo, de las clases II y IV, de los cuales un nuevo péptido lazo clase II fue exitosamente detectado in vitro por medio de una aproximación peptidogenómica. Este nuevo péptido lazo, denominado huascopeptina, mostró el primer motivo estructural de anillo macrolactámico de siete miembros, el anillo más pequeño actualmente descrito en un péptido lazo. Nuestros hallazgos sugieren que los ambientes poliextremos como el Salar de Huasco son fuentes prometedoras para explorar nuevos y valiosos productores de productos naturales con potencial farmacéutico.

***Dedicado a mi Madre...***

***-. Madre, contra todo, lo logramos!!!...***

***Gracias por todo, te amo mucho!!!...***

# Acknowledgments

I would like to start thanking to my supervisors, Juan A. Asenjo and Barbara Andrews for their support to this project and all the guidance and fruitful discussions that led to the achievement of all the objectives proposed on this research.

Also thanks to the members of the evaluation committee: Prof. Oriana Salazar, Prof. Bruce Cassels and Prof. Bernardo Gonzalez. I'm extremely grateful for the valuable time spent in reviewing and evaluating my thesis project. I'm really glad to be evaluated for all of you and receive your valuable feedback.

I would also like to thanks to the sponsor of my thesis project Prof. Cristina Dorador for kindly supporting my thesis project, giving me the exclusive opportunity to work with my *Streptomyces* strains isolated from Salar de Huasco, during my first step of this research line in my undergraduate program at the University of Antofagasta, which are part of the strains collection of the Laboratory of Microbial Complexity and Functional Ecology. Also thanks for all your help and support during my scientific career.

Many thanks to all the members of the Laboratory of Microbial Complexity and Functional Ecology, for housed and supported me during my first steps in Science; to Pablo Aguilar for his good hand in the collection of the soil samples from Salar de Huasco; To my best friend Diego Cornejo, for your technical support, trust and always believe in this work, even in my extremely bad moments; To my friends and colleagues: Daniel Chacana, Franco Colón, Gonzalo Fuentes, Gonzalo Icaza and Nicolas Cornejo, for all the scientific discussions and being always present contributing to my work and life in the University of Antofagasta.

Many thanks to all who are part of the Centre for Biotechnology and Bioengineering (CeBiB), with special thanks to: Gina Madariaga, Irene Roman, Paz Zañartu, Nancy Carrasco, Juan Luis Gonzalez, Juan Guillermo Navarro, Hector Figueroa and all the people that is behind of each detail to make that the gears of the CeBiB works perfectly.

To all my lab colleagues, because I learn something from all of you, even with the bad experiences, which helped me to be more secure and stronger.

To Prof. Marcel Jaspars, thanks for receiving me during my internship at the University of Aberdeen and provide all the equipment and support necessary for the characterization of the new peptide described in this study. Also thanks to the PhD. student Scott Jarmusch for the support in the isolation and purification of this peptide and complete the structure elucidation.

To my second sponsor and supervisor during my internship Prof. Imen Nouioui. I feel honoured to have worked with the best youngest taxonomist of the world. You have

been the best supervisor that someone could have and I will be everlastingly grateful for all your support and kindness, thanks for show me the honest and altruistic side in the world of the science. Many thanks for your hospitality, time, patience and for the finance of big part of this work.

Finally, the most important, all the members of my family, mainly to my aunt Ruth, my uncle Wilson, my cousin Vicente, my uncle Carlos Andres and all his family, my father and the two most important persons of my life my Mother and my Partner, the loves of my life. All this is thanks to you and for you, in each word written here there is a piece of my love for all of you and you were in my heart and mind during all this long and hard process.

Thanks to god!! And thanks to the Universe!! Because the day that we assume that we are nothing more than an small particle of dust in this immense universe, no more important than the last and simplest bacterial cell in the soil, this world will be completely different.

## Contributions statement

The presented idea and theory were conceived and developed by the PhD. candidate Carlos Cortés Albayay with guidance of his supervisors Prof. Juan Asenjo and Prof. Barbara Andrews at the University of Chile, Santiago, Chile.

The PhD. candidate carried out the treatment of soil samples, selective isolation, characterization, culture maintenance and phylogenetic analysis of the *Streptomyces* strains from Salar de Huasco with the supervision of Prof. Cristina Dorador (Chapter 2); The phenotypic characterization, Scanning electron microscope, phylogenetic analysis and MLST, genome analysis and annotation, digital DNA:DNA hybridization, polar lipids analysis, whole-cell sugars analysis and diaminopimelic acid isomers detection of the two novel *Streptomyces* species with the guidance and support of Prof. Imen Nouioui (Chapter 3-4); The fermentations and their optimization, all the in silico genome analysis, prediction of the peptides fragmentation patterns, analysis of tandem mass spectra and discovery of huascopeptin in the culture extracts with the supervision of Prof. Marcel Jaspars (Chapter 5). In addition, the PhD. candidate drafted the four manuscripts presented in this thesis with inputs of all the researchers that participate in the current publications.

Prof. Cristina Dorador, kindly provided the *Streptomyces* strains isolated from Salar de Huasco at the University of Antofagasta, Antofagasta, Chile, to continue this research line.

Prof. Johannes Imhoff and PhD. Johanna Silber carried out the preliminary HPLC-MS analysis of the *Streptomyces* crude extracts and the subsequent bioassays at GEOMAR Helmholtz-Zentrum für Ozeanforschung Ozeanforschung, Kiel, Germany (Chapter 2).

Prof. Paul Herron and PhD. Jana Schniete carried out the genome sequencing of *Streptomyces huasconensis* HST28<sup>T</sup> and *Streptomyces altiplanensis* HST21<sup>T</sup> at Strathclyde University, Glasgow, UK (Chapter 3-4).

Prof. Imen Nouioui actively supervised, guided and financed all the experiments for the taxonomic description and genomic characterization of *S. huasconensis* HST28<sup>T</sup> and *S. altiplanensis* HST21<sup>T</sup> at Newcastle University, Newcastle upon Tyne, UK (Chapter 3-4).

Prof. Peter Schumann carried out the menaquinones and fatty acids analysis of *S. huasconensis* HST28<sup>T</sup> and *S. altiplanensis* HST21<sup>T</sup> and their corresponding closest

type strains at Leibniz Institute DSMZ-German Collection of Microorganisms and Cell Cultures, Braunschweig, Germany (Chapter 3-4).

Prof. Marcel Jaspars supervised the huascopeptin detection, isolation and purification; his PhD. student Scott Jarmusch carried out the structure elucidation and characterization by NMR experiments at the University of Aberdeen, Aberdeen, UK (Chapter 5).

PhD. Jeanette Andersen, PhD. Kirsti Helland and PhD. Marte Albrigsten carried out the biological assays for huascopeptin bioactivity at Marbio, UiT – The Arctic University of Norway, Tromsø, Norway (Chapter 5).



# Contents

<b>Chapter 1</b>	<b>Introduction</b> .....	1
1.1	The <i>Streptomyces</i> genus and its bioactive potential.....	1
1.2	Bioprospecting <i>Streptomyces</i> of the Atacama Desert.....	3
1.3	Peptidic natural products (PNPs).....	4
1.4	Lasso peptides.....	6
1.5	Genome mining and Peptidogenomics.....	10
	<b>Objectives</b> .....	14
<b>Chapter 2</b>	<b>Bioprospection of new <i>Streptomyces</i> from the poly-extreme ecosystem Salar de Huasco</b> .....	15
2.1	Abstract.....	15
2.2	Introduction.....	16
2.3	Materials and methods.....	17
2.3.1	Selective isolation of <i>Streptomyces</i> .....	17
2.3.2	Identification of bacterial isolates.....	18
2.3.2.1	Morphological characterization based on colour grouping.....	18
2.3.2.2	16S rRNA gene-based phylogenetic analysis.....	19
2.3.3	Evaluations of pharmaceutical potentials.....	20
2.3.3.1	Genotyping of Non-ribosomal peptide synthetase (NRPS).....	20
2.3.3.2	Preparation of crude extracts and bioactivity assessments.....	20
2.3.3.3	Profiling of metabolites in crude extracts.....	21
2.4	Results and discussion.....	21
2.4.1	Selective isolation and identification of the isolates.....	21
2.4.2	Secondary metabolite analysis.....	28
2.5	Conclusion.....	32
<b>Chapter 3</b>	<b>Taxonomic description of the new species <i>Streptomyces huasconensis</i> HST28<sup>T</sup></b> .....	33
3.1	Abstract.....	33
3.2	Introduction.....	34
3.3	Materials and methods.....	35
3.3.1	Isolation, culture and maintenance.....	35
3.3.2	Phenotypic characterization.....	35
3.3.3	Scanning electron microscope.....	36
3.3.4	Phylogenetic analysis.....	36
3.3.5	Genome sequencing and dDDH.....	37

3.3.6	Chemotaxonomy methods.....	37
3.4	Results and discussion.....	38
3.5	Description of <i>Streptomyces huasconensis</i> sp. nov.....	46
3.6	Conclusion.....	47
<b>Chapter 4</b>	<b>Taxonomic description of the new species <i>Streptomyces altiplanensis</i> HST21<sup>T</sup></b> .....	<b>48</b>
4.1	Abstract.....	48
4.2	Introduction.....	49
4.3	Materials and methods.....	49
4.3.1	Isolation, culture and maintenance.....	49
4.3.2	Phenotypic characterization.....	50
4.3.3	Scanning Electron Microscope.....	50
4.3.4	Phylogenetic analysis.....	50
4.3.5	Genome sequencing, dDDH and ANI calculations.....	51
4.3.6	Chemotaxonomy methods.....	53
4.4	Results and discussion.....	53
4.5	Description of <i>Streptomyces altiplanensis</i> sp. nov.....	61
4.6	Emended description of <i>Streptomyces chryseus</i> (Krasil'nikov et al. 1965) Pridham 1970 (Approved Lists 1980) .....	61
4.7	Conclusion.....	62
<b>Chapter 5</b>	<b>Peptidogenomics of the new class II lasso peptide Huascopeptin</b> .....	<b>63</b>
5.1	Abstract.....	63
5.2	Introduction.....	64
5.3	Materials and methods.....	65
5.3.1	Isolation, culture and maintenance.....	65
5.3.2	Molecular analysis.....	65
5.3.3	Genome mining.....	65
5.3.4	General experimental procedures.....	66
5.3.5	Fermentation, detection and isolation.....	66
5.3.6	3D-modelling of huascopeptin.....	67
5.3.7	Biological assays.....	67
5.3.8	Spectroscopic data.....	68
5.4	Results and discussion.....	68
5.5	Conclusion.....	76
	<b>General conclusions</b> .....	<b>77</b>
	<b>Future perspectives</b> .....	<b>79</b>
	<b>Bibliography</b> .....	<b>80</b>
	<b>Appendices</b> .....	<b>92</b>
	<b>Published papers</b> .....	<b>118</b>

# List of tables

1	Actinobacteria-derived peptide antibiotic products in market and clinical trials.....	5
2	Lasso peptides with antibiotic activities discovered between 2000-2018.....	9
3	16S rRNA gene-based identification of all bacteria isolated from Salar de Huasco.....	22
4	Morphological and molecular characteristics of some <i>Streptomyces</i> spp. isolated from Salar de Huasco.....	23
5	Antibacterial activity of crude extracts derived from <i>Streptomyces</i> spp. isolates.....	29
6	Antifungal activity of crude extracts derived from <i>Streptomyces</i> spp. isolates.....	30
7	Cytotoxic activity of crude extracts derived from <i>Streptomyces</i> spp. isolates.....	31
8	Growth and cultural features of strain HST28 <sup>T</sup> after 7 days of incubation at 28°C.....	38
9	Phenotypic features that distinguish strain HST28 <sup>T</sup> from its nearest phylogenetic neighbours <i>Streptomyces aureus</i> DSM 41785 <sup>T</sup> and <i>Streptomyces kanamyceticus</i> DSM 40500 <sup>T</sup> .....	43
10	Fatty acid profiles for strain HST28 <sup>T</sup> and its closest relatives.....	46
11	Accession numbers of the sequences used for the MLST analysis in the present study.....	52
12	Growth and cultural features of strain HST21 <sup>T</sup> after 10 days of incubation at 28°C.....	53
13	Phenotypic features that distinguish strain HST21 <sup>T</sup> from its nearest phylogenetic neighbours <i>S. albidochromogenes</i> DSM 41800 <sup>T</sup> and <i>S. flavidovirens</i> DSM40150 <sup>T</sup> .....	55
14	Fatty acid profiles for strain HST21 <sup>T</sup> and its closest phylogenetic relatives.....	58

# List of figures

1	<i>Streptomyces coelicolor</i> life cycle.....	2
2	Natural product diversity of Actinomycetes isolated from the Atacama Desert soils...	3
3	Generic biosynthetic pathway for bacterial RiPPs.....	6
4	Lasso peptide structural features and common residues.....	7
5	General overview of lasso peptide biosynthesis.....	8
6	Lasso peptide classes and topologies.....	9
7	The protein-centric method for lasso peptide genome mining.....	12
8	Salar de Huasco and sampling sites images.....	18
9	Neighbour-joining phylogenetic tree based on almost complete 16S RNA sequences of the 19 <i>Streptomyces</i> isolates derived from Salar de Huasco and their closely related species.....	25
10	Scanning electron micrograph of strain HST28 <sup>T</sup> .....	39
11	Maximum-likelihood phylogenetic tree based on the 16S rRNA gene sequences showing the phylogenetic relationships between the isolate HST28 <sup>T</sup> and its closest phylogenetic relatives.....	40
12	Maximum-likelihood multi-locus sequence analysis (MLSA) tree based on the concatenated partial sequences of five housekeeping genes: <i>atpD</i> ; <i>gyrB</i> ; <i>recA</i> ; <i>rpoB</i> and <i>trpB</i> .....	41
13	Two-dimensional thin layer chromatography (TLC) for polar lipids extracted from strain HST28 <sup>T</sup> and its closest relatives.....	45
14	Scanning electron micrograph of strain HST21 <sup>T</sup> .....	54
15	Two-dimensional thin layer chromatography (TLC) for polar lipids extracted from strain HST21 <sup>T</sup> and its closest type strains.....	57
16	Maximum-likelihood phylogenetic tree based on almost complete 16S rRNA gene sequences showing the phylogenetic relationship between strain HST21 <sup>T</sup> and its relatives within the genus <i>Streptomyces</i> .....	59
17	Maximum-likelihood phylogenetic tree based on concatenated sequences of five housekeeping genes showing the phylogenetic relationship between isolate HST21 <sup>T</sup> and its relatives within the genus <i>Streptomyces</i> .....	60
18	Huascopeptin biosynthetic gene cluster.....	69
19	High-resolution mass spectra for <i>Streptomyces huasconensis</i> HST28 <sup>T</sup> small-scale culture extracts.....	71
20	High-resolution tandem mass spectrum (HRESIMS/MS) for purified huascopeptin 1.	72
21	Key nuclear Overhauser spectroscopy (NOESY) correlations (blue) confirming the majority of the connectivities for huascopeptin 1 peptide sequence.....	73
22	In silico structural model for huascopeptin 1.....	76

# List of the papers that make up this thesis

Chapter	Title of the paper	Status
2	The Polyextreme Ecosystem, Salar de Huasco at the Chilean Altiplano of the Atacama Desert Houses Diverse <i>Streptomyces</i> spp. with Promising Pharmaceutical Potentials.	Published in: Diversity journal.  Cortés-Albayay et al., 2019. doi: 10.3390/d11050069
3	Taxonomic description of <i>Streptomyces huasconensis</i> sp. nov., an haloalkalitolerant actinobacterium isolated from a high altitude saline wetland at the Chilean Altiplano.	Published in: International Journal of Systematic and Evolutionary Microbiology.  Cortés-Albayay et al., 2019. doi: 10.1099/ijsem.0.003468.
4	A novel species of alkalitolerant <i>Streptomyces</i> isolated from Chilean Altiplano soil, <i>Streptomyces altiplanensis</i> sp. nov. and emended description of <i>Streptomyces chryseus</i> Krasil'nikov et al. 1965.	Published in: International Journal of Systematic and Evolutionary Microbiology.  Cortés-Albayay et al., 2019 doi: 10.1099/ijsem.0.003468
5	Downsizing class II lasso peptides: peptidogenomic-guided isolation of huascopeptin containing a novel seven-membered macrocycle.	Submitted to Organic letters Journal.  * Cortés-Albayay et al., 2019

\* : This paper was developed with equal contribution of the PhD. Student Scott Jarmush from the University of Aberdeen, Aberdeen, Scotland, UK.

# Chapter 1

## Introduction

### 1.1 The *Streptomyces* genus and its bioactive potential

The Streptomycetes are aerobic Gram-positive bacteria from the Actinomycetales order within the actinobacterial class (Stackebrandt et al., 1997). The genus comprises more than 800 species with validly published names (<http://www.bacterio.net/streptomyces.html>). These microorganisms are chemoorganotrophic and have an oxidative type of metabolism, being many of them able to degrade substrates as: casein, gelatine, hypoxanthine, starch and cellulose (Kampfer et al., 1991; Williams et al., 1983). The nutritional requirements are mostly restricted to an organic carbon source (starch, glucose, glycerol, lactate, etc.) and an inorganic nitrogen source ( $\text{NH}_4^+$  or  $\text{NO}_3^-$ ), in addition to essential mineral salts (Balows, 1992). Its optimal growth temperature is between 25°C – 35°C and the optimal pH range for its growth is around 6.5-8.0.

Its biological development has been widely studied based on the *Streptomyces coelicolor* species life cycle (Chater and Horinouchi, 2003) and consist mainly of a vegetative growth which produces branched filaments that only septate occasionally, forming long cells that contain multiple nucleoids (Angert et al., 2005). Subsequently and in response to nutrient depletion some species alter their pattern of growth to produce aerial mycelia and spores able to easily disperse between ecosystems (Antony-Babu and Goodfellow, 2008) (Fig. 1). Also these spores can stay alive but inactive during many years even in unfavourable environments (Bull et al., 2000).

Between the unicellular prokaryotes, the Actinomycetes are considered the major producers of bioactive compounds in nature (Bérdy, 2005). It is estimated that about 70% of the clinical use antibiotics are derived from natural products produced by this class of bacteria (Pimentel-Elardo et al., 2010). Within this great bioactive potential, the *Streptomyces* genus is the major contributor with more than 80% of all the bioactive

compounds of microbial origin (Bérdy, 2005; Watve et al., 2001). Although the major bioactive potential found in *Streptomyces* correspond to a high number antibiotics that have been discovered for decades, an uncountable amount of strains belonging to this genus with antiproliferative and/or antitumoral activity have been also found as the case of *Streptomyces griseorubens* WBF9, which was isolated from marine sediments in China and that presented an strong antitumoral activity against Hela, KB and SMMC7721 cell lines (Ye et al., 2009); the metabolites produces by *Streptomyces* sp. 23-2B, isolated from the marine clam *Donax trunculus* at the Mediterranean sea, which showed an strong antitumoral activity against the Ehrlich ascites carcinoma, selectivity against solid tumours and high cytotoxicity against hepatocellular carcinoma (HepG2), cervix carcinoma (HELGA) and breast carcinoma (MCF7) (El-Shatoury et al., 2009). Even more, a great diversity of new molecules with antitumoral potential has been discovered in members of *Streptomyces* genus (Dharmaraj, 2010). Interestingly, many of these molecules had a peptidic nature as the case of the of the piperazimycins A-C, that correspond to hexapeptides of non-ribosomal origin and which showed an strong in vitro cytotoxic activity (Miller et al., 2007), or allophycocyanin, that is one of the most important marine bioactive peptides, isolated from the *Streptomyces* strain M097 (Hou et al., 2006). Allophycocyanin has an strong inhibitory activity over the murine sarcoma cancer cell line S-180 showing its potential pharmaceutical use.

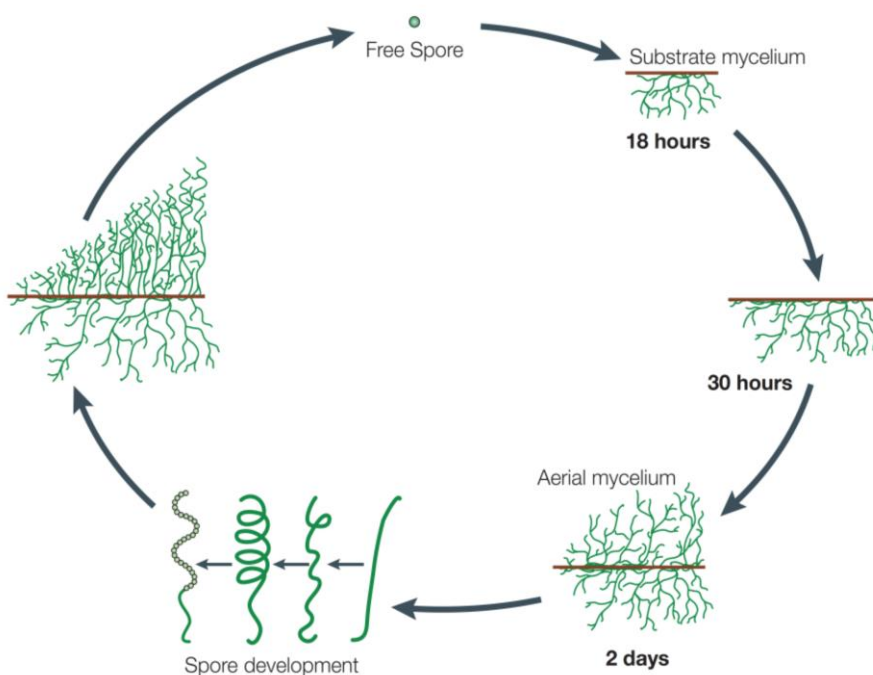


**Figure 1. *Streptomyces coelicolor* life cycle.** A vegetative hypha emerges from a germinating spore and the hyphal filament grows by tip extension. Occasionally, cell division occurs and the filament branches, which produces a thick network of hyphae, known as the substrate mycelium. As local nutrients are depleted, a complex signalling cascade triggers the production of a surfactant that coats some emerging filaments, which allows them to grow away from the substrate. These aerial filaments are developmentally different from those of the substrate mycelium. The unbranched cell at the ends of some of these aerial filaments differentiates. Each cell divides synchronously at many sites along its length forming uninucleoid cells that further develop into spores (Angert et al., 2005).

## 1.2 Bioprospecting *Streptomyces* of the Atacama Desert

The search and discovery of novel bacterial strains producers of bioactive compounds also known as “Microbial Bioprospection” (Pandian, 2004), mainly focused in the search of novel Actinomycetes has led the researchers to study ecosystems so complex in their abiotic conditions such as the Mariana trench, the deepest point on the earth, placed in the Pacific ocean (Pathom-aree et al., 2006); polar soils and permafrost (Lyutskanova et al., 2009; Steven et al., 2008) and the hyper saline and extremely arid soils of the Atacama Desert (Okoro et al., 2009). The last one has a huge diversity of ecosystems with extreme conditions in which it has been developed a broad and successful search of novel Actinomycetes and novel natural products of valuable pharmaceutical interest produced by these microorganisms (Rateb et al., 2018) (Fig. 2).

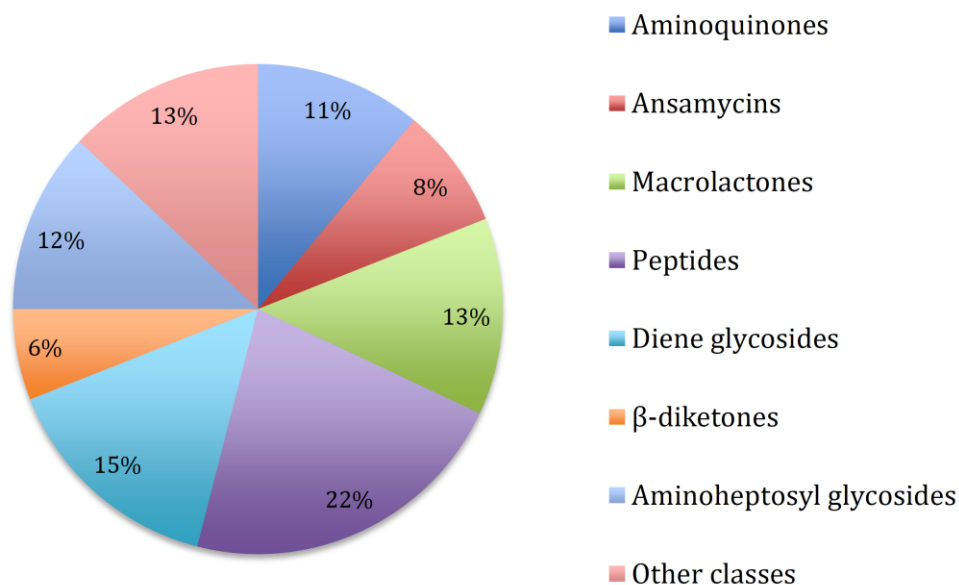


**Figure 2.** Natural product diversity of Actinomycetes isolated from the Atacama Desert soils (Modified from Rateb et al., 2018).

Examples are the studies carried out in the Salar de Atacama (Laguna de Chaxa) and Valle de la Luna (Okoro et al., 2009) from which were obtained five new *Streptomyces* species: *Streptomyces atacamensis* (Santhanam et al., 2012b), *Streptomyces desertii* (Santhanam et al., 2012a), *Streptomyces bulli* (Santhanam et al., 2013), *Streptomyces leeuwenhoekii* (Busarakam et al., 2014) and *Streptomyces asenjonii* (Goodfellow et al., 2017). The most prolific of these *Streptomyces* species has been *S. leeuwenhoekii*, whose strains C34, C38 and C58 produced four novel natural products: the chaxamycins, with antimicrobial activity against *Staphylococcus aureus* ATCC 25923 and an important inhibitory effect on the Hsp90 chaperon protein (Rateb et al., 2011a); chaxalactins, with antimicrobial activity against Gram-positive bacteria as *Listeria monocytogenes* and *Bacillus subtilis* (Rateb et al., 2011b); atacamycins, with moderate antiproliferative activity and an inhibitory activity over the phosphodiesterase



PDE-4B2 (Nachtigall et al., 2011); and the chaxapeptin, which showed an important growth inhibitory activity of the lung cancer cell line A549 (Elsayed et al., 2015).

Studies like these aroused our interest in the search for novel *Streptomyces* strains with bioactive potential from extreme and unexplored ecosystems like the salt-lakes placed in the Chilean highlands (Altiplano) of the Atacama Desert, which distinguished from each other in their mineral salts concentration and composition, aridity (Risacher et al., 2003) solar radiation levels and in the great diversity of existent microbial communities strongly influenced by the predominant physicochemical conditions (Dorador et al., 2013). One of the best representatives of these ecosystems is the Salar de Huasco, a salt-lake of athalossohaline origin, which receives this denomination because it is a continental lake of marine origin, which has an ionic composition markedly different from the sea water (Demergasso et al., 2004). This salt-lake is located in the Chilean altiplano of the Atacama Desert at an altitude of 3800 meters at sea level (m.a.s.l) and presents limiting abiotic conditions such as: high salinity, low temperatures (annual average  $>5^{\circ}\text{C}$ ), low atmospheric pressure (40% less than at the sea level), high solar radiation ( $<1100\text{ w m}^{-2}$ ), negative water balance and an important microbial diversity of archaea and extremophile bacteria (Dorador et al., 2010; Dorador et al., 2013).

### **1.3 Peptidic natural products (PNPs)**

The peptidic natural products (PNPs) are widely present in nature accomplishing biological functions associated with development, defence and communication (Daffre et al., 2008), in a large variety of microorganisms (Donadio et al., 2007; Velásquez and Van der Donk, 2011). These peptides have been the target of studies for many decades, mainly because of their high specificity (Kersten et al., 2011). The non-linear peptides also known as cyclic peptides (ring motif structures), are mostly sought and studied because they are much more stable and resistant to human proteases what makes them more reliable to apply in human therapies even for oral treatments (Nolan and Walsh, 2009).

The chemical structure of these peptides contains, in many cases, a great variety of non-proteinogenic aminoacids or/and Posttranslational modifications that give them unique characteristics that can be used in pharmaceutical applications (McIntosh et al., 2009). In addition, their ability to join in highly specific way to their targets in vivo confers them a valuable advantage over other natural products, resulting in a high potency and relatively few secondary effects (Fosgerau and Hoffmann, 2014). The peptides derived from natural sources have been finely regulated to interact specifically with their biological targets (Craik et al., 2013). In principle, the peptides could have many valuable applications in medicine, considering all the advantages that they possess: high selectivity, high potency, wide range of targets, lower toxicity than other molecules, low accumulation in tissues, high chemical and biological diversity and the possibility of discovery at both chemical and genetic level (Fosgerau and Hoffmann, 2014). Some of

these peptides, mainly isolated from Actinobacterial species, are currently commercialized or approved for clinical trials (Zhao et al., 2018) (Table 1).

**Table 1.** Actinobacteria-derived peptide antibiotic products in market and clinical trials (Zhao et al., 2018).

Name	Source	Biological target	Current status	References
Viomycin	<i>Streptomyces puniceus</i>	Anti-tuberculosis	Not marketed but widely used	Bartz et al., 1951 Barkei et al., 2009
Capreomycin	<i>Streptomyces capreolus</i>	Anti-tuberculosis	WHO <sup>b</sup> recommended drugs	Lougheed et al., 2009
Tuberactinomycin	<i>Streptomyces griseoverticillatus</i>	Anti-tuberculosis	WHO recommended drugs	Nagata et al., 1968 Thomas et al., 2003
Vancomycin	<i>Amycolatopsis orientalis</i>	MRSA <sup>a</sup>	WHO recommended drugs	Levine et al., 2006 Gardete et al., 2014
Teicoplanin	<i>Actinoplanes teichomyeticus</i>	Gram-positive bacteria	WHO recommended drugs	Butler et al., 2014 Jung et al., 2009
Daptomycin	<i>Streptomyces roseosporus</i>	Gram-positive bacteria	FDA <sup>c</sup> approval	Tally et al., 2000 Kerry et al., 2013

a : MRSA: methicillin-resistant *Staphylococcus aureus*

b : WHO: World Health Organization (<https://www.who.int/>).

c : FDA: Food and Drugs Administration. (<https://www.fda.gov/>)

There are two different biosynthesis pathways: the ribosomal and non-ribosomal biosynthesis (Nolan and Walsh, 2009). The first group correspond to the Ribosomally synthesized and Posttranslationally modified Peptides (RiPPs), which follow an homologous synthesis process to other cellular proteins (Oman and van der Donk, 2010). This precursor peptide consist of a leader region, which serves as a scaffold that contains the recognition sites for the processing enzymes that introduce posttranslational modifications; and the core region that constitutes the primary sequence of the peptide natural product that is modified (Kersten et al., 2011) (Fig. 3).

The modifications that the peptide can undergo can often be extensive and can provide a wealth of structural diversity rendering these peptides unrecognizable as ribosomally synthesized molecular entities (Moore, 2008). Some modifications such as dehydrations, cyclizations and oxidations of the aminoacidic residues in the core peptide give as product lanthipeptides (Willey and van der Donk, 2007), thiopeptides (Li and Kelly, 2010), cyanobactins (Donia et al., 2008), microcins (Duquesne et al., 2007) and lasso peptides (Maksimov and Link, 2014).

In the second group are the non-ribosomal peptides (NRPs) which are synthesized by a multifunctional protein assembly line that selects its aminoacidic precursors by mean of an adenilating enzyme that selects and transfer its substrates to transporter proteins facilitating the peptide synthesis by the non-ribosomal peptide synthetases (NRPS) (Challis et al., 2000).

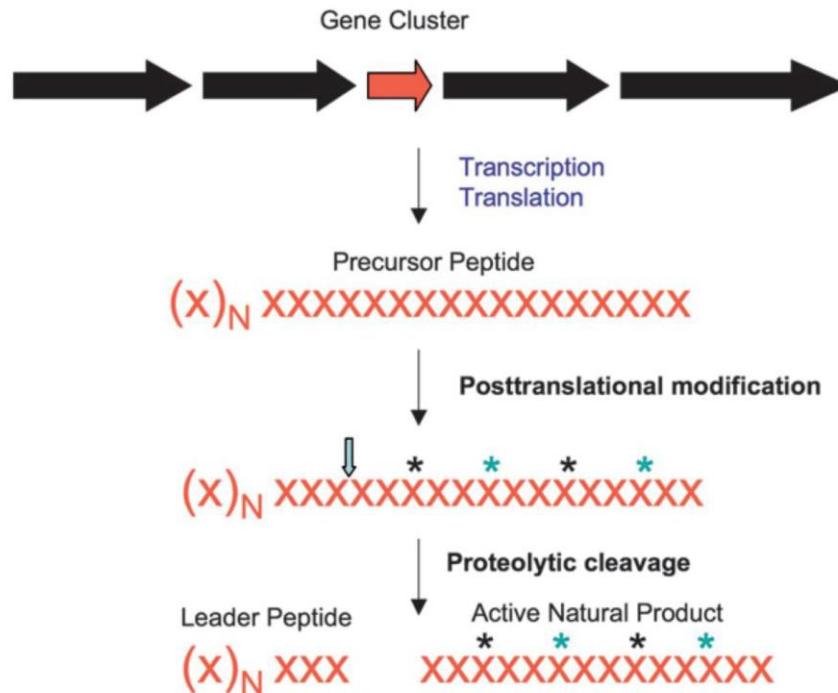


**Figure 3. Generic biosynthetic pathway for bacterial RiPPs.** In bacteria, a gene for a precursor peptide (orange) is often clustered with its modifying enzymes. The precursor peptide is translated and then posttranslationally modified by the encoded enzymes. Commonly, Posttranslational modifications include both side chain modifications and main chain modifications such as proteolysis to generate the mature natural product (McIntosh et al., 2009).

## 1.4 Lasso peptides

Within the wide variety of RiPPs existing in nature, one of the most studied groups of these natural products is the lasso peptides. The lasso peptide topology was first described in 1994 with the characterization of the RP-71955 (aborycin) structure, which was isolated from *Streptomyces griseoflavus* during an anti-HIV-1 screening program (Frechet et al., 1994). However, the first lasso peptide identified was the anantin, a lasso peptide isolated from *Streptomyces coeruleus* during bio-guided screening of natural products for antagonist of the atrial natriuretic factor receptor in 1991, but its structure has not been elucidated yet (Weber et al., 1991; Wyss et al., 1991). Until 2017 more than 40 different lasso peptides and some of their BGCs have been identified from bioactivity screenings or genome mining approaches (Maksimov and Link, 2014; Hegemann et al., 2015). Currently, this number has increased to ~3000 biosynthetic gene clusters belonging this group, found using genome mining tools (Sikandar and Koehnke, 2019). The chemical features of these natural products correspond to aminoacidic sequences of about 16-21 residues, with a characteristic “lariat-knot” structure formed by a macrolactam ring that irreversibly traps the carboxylic terminal inside the macrocycle (Arnison et al., 2012). This configuration is acquired due to the formation of an isopeptide bond between the N-terminal  $\alpha$ -amino group of

cysteine, glycine, alanine or serine and the carboxylic group located in the side chain of an aspartic acid or a glutamic acid (Maksimov et al., 2012) (Fig. 4).

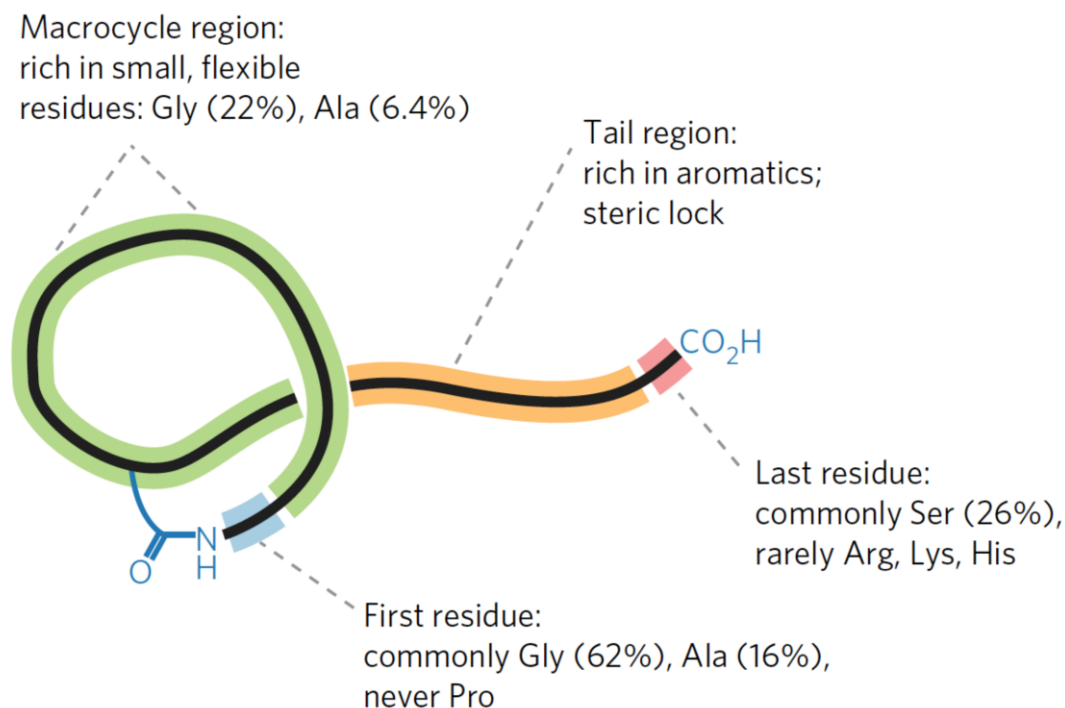


**Figure 4. Lasso peptide structural features and common residues** (Modified from Tietz et al., 2017).

The biosynthesis and maturation of lasso peptides is mediated mainly by two key enzymes: an asparagine synthetase B-like protein, encoded by a *lasC* gene responsible for the lasso peptide cyclization by mean of the isopeptide bond formed and a transglutaminase-like protease, encoded by the *lasB2* gene, which catalyses the cleavage of the leader peptide from the precursor (Duquesne et al., 2007; Severinov et al., 2007). Figure 5 shows a general overview of lasso peptide biosynthesis.

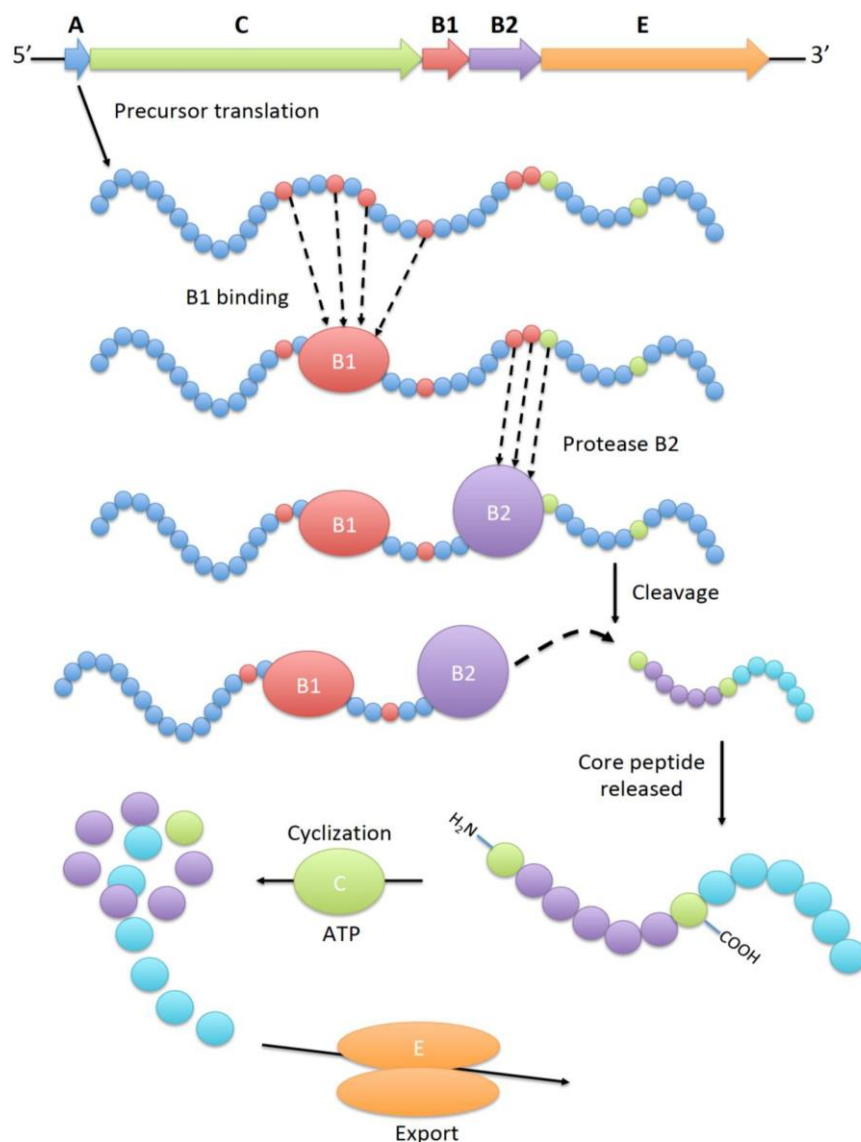


**Figure 5. General Overview of lasso peptide biosynthesis.** The encoding genes of the enzymatic machinery for the biosynthesis of the lasso peptides, is clustered together with the precursor peptide (gene A). The biosynthesis begins with the direct translation of the precursor peptide to which the protein “B1” (RRE) binds to the conserved motif YxxPxLx3Gx5Tx (small red spheres) of the leader sequence and delivers the peptide to the peptidase B2, which in turn recognizes the TxG motif (small red-green spheres) and cleave-off the core peptide from the leader sequence. Subsequently, the lasso peptide cyclase C, catalyse the isopeptide bond formation between the N-terminal α-amino group of the first residue and the radical carboxylic group of an aspartic acid or a glutamic acid to form the macrolactam ring and the typical lariat-knot structure.

The different classes of lasso peptides are distinguished from each other in the way in which the knot structures are stabilized, specifically how the tail is maintained threaded through of the macrocycle (Arnison et al., 2012). This stabilization is achieved through one or two disulphide bonds formed by cysteine residues, connecting the tail and ring in the classes I and III; exerting a steric impediment (steric lock) by the side chains (aromatic or long aliphatic chains) of certain amino acids of the tail in lasso

peptides class II (Hegemann et al., 2015); and the most recently discovered class IV that possess one disulphide bond formed by two cysteine residues that resides in the tail of the peptide conforming a handcuff motif structure (Tietz et al., 2017) (Fig. 6).

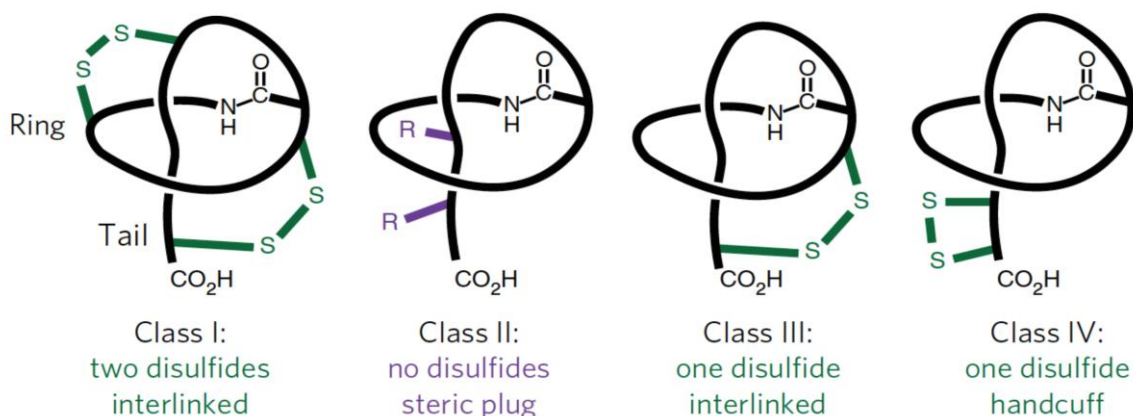


**Figure 6. Lasso peptide classes and topologies** (Modified from Tietz et al., 2017).

The lasso peptides have exhibited a broad range of biological activities from antimicrobial (Iwatsuki et al., 2006, Ducasse et al., 2012, Gavrish et al., 2014; Zhao et al., 2018) (Table 1), antiviral (Chokekijchai et al. 1995) to enzymatic inhibition (Yano et al., 1996). They have been widely found in the genus *Streptomyces*, with important antimicrobial activities (Weber et al., 1991, Potterat et al. 1994 and Tsunakawa et al. 1995). The best example correspond to the previously mentioned chaxapeptin, the first lasso peptide obtained from the novel species *Streptomyces leeuwenhoekii* C58, isolated from an extreme environment of the Atacama Desert (Elsayed et al., 2015).

**Table 2. Lasso peptides with antibiotic activities discovered between 2000-2018** (Zhao et al., 2018).

Name	Sequence	Antibiotic activity	DIZ/MIC	Reference
Achromosin	Gly <sup>*</sup> -Ile-Gly-Ser-Gln-Thr-Trp-Asp <sup>*</sup> -Thr-Ile-Trp-Leu-Trp-Asp	Antibacterial	11 mm <sup>a</sup>	Kaweewan et al., 2017
Chaxapeptin	Gly <sup>*</sup> -Phe-Gly-Ser-Lys-Pro-Leu-Asp <sup>*</sup> -Ser-Phe-Gly-Leu-Asn-Phe-Phe	Antibacterial	30-35 µg/mL <sup>b</sup>	Elsayed et al., 2015
Lariat A	Gly <sup>*</sup> -Ser-Gln-Leu-Val-Tyr-Arg-Glu <sup>*</sup> -Trp-Val-Gly-His-Ser-Asn-Val-Ile-Lys-Pro	Antituberculosic	3.13-6.25 µg/mL <sup>b</sup> 18 - 19 mm <sup>a</sup>	Iwatsuki et al., 2006, 2007
Lariat B	Gly <sup>*</sup> -Ser-Gln-Leu-Val-Tyr-Arg-Glu <sup>*</sup> -Trp-Val-Gly-His-Ser-Asn-Val-Ile-Lys-Gly-Pro-Pro			
Lassomycin	Gly <sup>*</sup> -Leu-Arg-Arg-Leu-Phe-Ala-Asp <sup>*</sup> -Gln-Leu-Val-Gly-Arg-Arg-Asn-Ile-CO <sub>2</sub> -Me	Antituberculosic and Antibacterial	0.1-3.1 µg/mL <sup>b</sup>	Gavrish et al., 2014

**Table 2. Continued**

Name	Sequence	Antibiotic activity	DIZ/MIC	Reference
Actinokineosin	Gly <sup>*</sup> -Tyr-Pro-Phe-Trp-Asp-Asn-Arg-Asp <sup>*</sup> -Ile-Phe-Gly-Gly-Tyr-Thr-Phe-Ile-Gly	Antibacterial	8-8.5 mm <sup>a</sup>	Takasaka et al., 2017
Sphaericin	Gly <sup>*</sup> -Leu-Pro-Ile-Gly-Trp-Trp-Ile-Glu <sup>*</sup> -Arg-Pro-Ser-Gly-Trp-Tyr-Phe-Pro-Ile	Antibacterial	50 µg/disk	Kodani et al., 2017
Sviceucin	Cys <sup>**</sup> -Val-Trp-Gly-Gly-Asp-Cys <sup>**</sup> -Thr-Asp <sup>+</sup> -Phe-Leu-Gly-Cys <sup>*</sup> -Gly-Thr-Ala-Trp-Ile-Cys <sup>**</sup> -Val	Antibacterial	2.6 - 5.2 µg/mL <sup>b</sup>	Li et al., 2015
Streptomomicin	Ser <sup>*</sup> -Leu-Gly-Ser-Ser-Pro-Tyr-Asn-Asp <sup>*</sup> -Ile-Leu-Gly-Tyr-Pro-Ala-Leu-Ile-Val-Ile-Tyr-Pro	Antibacterial	4 - 128 µg/mL <sup>b</sup>	Metelev et al., 2015

<sup>\*</sup>, <sup>\*\*</sup>, <sup>+</sup>: Denote the linkage position of the first, second and third ring formation, respectively.

<sup>a</sup>: DIZ: Diameter of inhibition zone.

<sup>b</sup>: MIC: Minimum inhibitory concentration.

## 1.5 Genome mining and Peptidogenomics

For much of its history, the natural products discovery has been a process driven in large part by chance. In most cases, discovery of new natural products has been driven either by bioactivity-guided fractionation of crude fermentation broth extracts, or via chemical screening (isolation of chromatographically resolvable metabolites with ‘interesting’ spectroscopic properties) (Bachmann et al., 2014). In 2000, Gregory Challis and coworkers discovered the coelichelin based on its biosynthetic gene cluster, in the partial genome sequence of *S. coelicolor*, obtaining for first time a new natural product using genome information (Challis et al., 2000). Since these studies, genome mining has appeared as a radical “re-envisioning” of the process of natural products discovery, which has the theoretical potential to eliminate all chance from discovery approaches and has quickly becoming in the most used approach for characterization of a great amount of natural products (Challis, 2008).

The most classic definition for this methodology is related to the search for specific genes that encode the enzymatic machinery involved in the biosynthesis of specialized metabolites within a sequenced genome (Ziemert et al., 2016). This approach can be roughly divided into two successive steps: first, the identification of the target proteins involved in the biosynthesis of natural products from the translated genomic sequences, based on their homology with characterized representatives or the presence of conserved motifs; and second, the detailed analysis of the genomic vicinity of the detected hits in order to assign its function within a biosynthetic gene cluster (Nett et al., 2014).

The advantages of the genome mining discovery approaches over the traditional chemistry guided discovery relies on the possibility of addressing a vast and valuable chemical diversity hidden in cryptic BGCs and lead the analysis to specific target molecules, based on the genomic information obtained, making the discovery of novel compounds faster and efficient (Corre and Challis, 2009; Choi et al., 2015).

However, there exist some difficulties with this methodology at the moment of completely predicting the structure and organization of the gene clusters for the biosynthesis of these peptides, for example in the case of the RiPPs, their BGCs are often too small, which make difficult their prediction and annotation by mean of the existing bioinformatics platforms such as: ClustScan (Starcevic et al., 2008), NP.searcher (Li et al., 2009), NRPSpredictor (Rausch et al., 2005), NRPSpredictor2 (Röttig et al., 2011), AntiSmash (Weber et al., 2015) and PRISM (Skinnider et al., 2015). In addition, as these peptides have multiple and variable unusual posttranslational modifications, they fragment poorly, obtaining spectra with very few peaks that makes impossible their identification only by tandem mass spectrometry (Mohimani and Pevzner, 2016).

The Peptidogenomics approaches incorporates the identification of these peptidic natural products and the characterization of their biosynthetic genes, making possible the connection of the mass spectra data of molecules detected in a culture or metabolic extract to their corresponding genotypes i.e to the genes involved in the biosynthesis of these molecules (Kersten et al., 2011; Liu et al., 2010).

In practice, this methodology can follow three possible ways; the first, consists of a precursor-centric approach focused on the screening of all the short open reading frames present in the genome for possible lasso peptide precursors, using patterns of conserved elements (conserved motifs) in known lasso peptide precursors to then analyse the genomic neighbourhood looking for the maturation enzymes and finally evaluate the in vitro production of the peptide by Mass spectrometry. The second corresponds to a protein-homology based approach as described in Figure 7. The third is an MS-guided approach which is based on an exhaustive analysis of mass spectra of microbial extracts in such way that interesting molecules are then fragmented by MS<sup>2</sup> to generate short peptide tags that are later compared with translated short open reading frames corresponding to putative precursor peptides (Maksimov and Link, 2014).



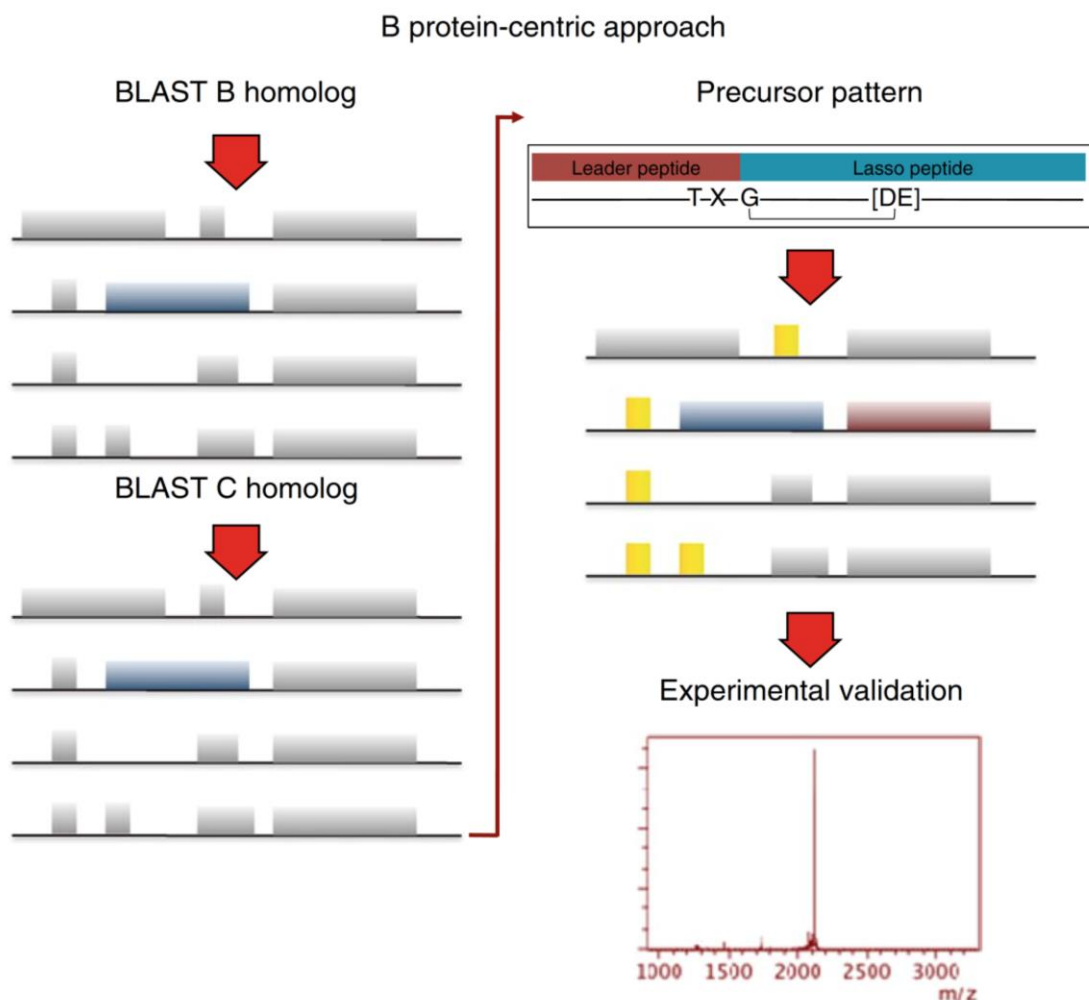


**Figure 7. The protein-centric method for lasso peptide genome mining.** This method is based in an iterative BLAST search to find homologs of the B maturation enzyme (protease) in bacterial genomes. C-homologs (cyclase) and precursor peptides are then identified in the vicinity of the putative B-homolog (Maksimov and Link, 2014).

The success of the genome mining approach applied to new Atacama Desert microorganisms was previously demonstrated with the discovery of the chaxapeptin and its biosynthetic gene cluster from *S. leeuwenhoekii* C53 (Elsayed et al., 2015). This study opened the only perspective about the discovery of RiPPs from Atacama Desert novel species.

In addition, previous studies have demonstrated that novel actinobacterial species isolated from Atacama Desert extremobiosphere are considered “gifted” microorganisms due to their large genomes (> 8 Mb) that can harbour between 25-50 BGCs for specialized metabolites (Baltz et al., 2017; Goodfellow et al., 2018). Therefore, bioprospecting strategies and subsequent genomic approaches should remain focused on the detection of these novel microorganisms with large genomes given their propensity to produce novel natural products (Bull and Goodfellow 2019).

The question that arises now in light of this evidence lies in whether it is possible to find a new chemodiversity of RiPPs in novel *Streptomyces* species obtained from other interesting Atacama Desert extreme ecosystems such as salt-lakes of Chilean altiplano (highlands).

To address this question, the present study developed a complete bioprospection pipeline, which involved the isolation, characterization and evaluation of the bioactive potential of new *Streptomyces* species from Salar de Huasco, in the Chilean altiplano of Atacama Desert, with a further peptidogenomics approach directed to the discovery of novel lasso peptides produced by these new species.

The first stage of this study (Chapter 2) concerns the new cultivable diversity of *Streptomyces* species from the Salar de Huasco, obtaining novel strains with important antimicrobial and cytotoxic activities.

The second stage (Chapter 3 and 4), involved the taxonomic characterization and description of the two novel species *Streptomyces huasconensis* HST28<sup>T</sup> and *Streptomyces altiplanensis* HST21<sup>T</sup>, two of the most promising *Streptomyces* isolated in the first stage of this study.

The third and final stage (Chapter 4) corresponds to the discovery of the new class II lasso peptide “huascopeptin” produced by *S. huasconensis* HST28<sup>T</sup>, through a protein-centric peptidogenomics approach.

# Objectives

## Main objective

To discover new bioactive Ribosomally synthesized and Posttranslationally modified peptides produced by novel *Streptomyces* species isolated from Salar de Huasco.

## Specific objectives

1. To isolate selectively new *Streptomyces* strains from Salar de Huasco arid soil samples.
2. To evaluate the antimicrobial and cytotoxic activities of the *Streptomyces* strains crude extracts.
3. To describe taxonomically the putative novel *Streptomyces* species by a polyphasic approach.
4. To map and predict the RiPPs biosynthetic gene clusters and their precursor peptides in the genomes of the novel *Streptomyces* species.
5. To detect the RiPPs in the mass spectra of microbial extracts through their theoretical mass/charge and fragmentation pattern.
6. To evaluate the bioactivity of purified RiPPs by antimicrobial and cytotoxic assays.

# Chapter 2

## Bioprospection of new *Streptomyces* from the poly-extreme ecosystem Salar de Huasco

### Objectives

1. To isolate selectively new *Streptomyces* strains from Salar de Huasco arid soil samples.
2. To evaluate the antimicrobial and cytotoxic activities of the *Streptomyces* strains crude extracts.

### 2.1 Abstract

Salar de Huasco at the Chilean Altiplano of the Atacama Desert is considered a poly-extreme environment, where solar radiation, salinity and aridity are extremely high and occur simultaneously. In this study, a total of 76 bacterial isolates were discovered from soil samples collected at two different sites in the east shoreline of Salar de Huasco, including H0 (base camp next to freshwater stream in the north part) and H6 (saline soils in the south part). All isolated bacteria were preliminarily identified using some of their phenotypic and genotypic data into the genera *Streptomyces* (86%), *Nocardiopsis* (9%), *Micromonospora* (3%), *Bacillus* (1%), and *Pseudomonas* (1%). *Streptomyces* was found dominantly in both sites (H0 = 19 isolates and H6 = 46 isolates), while the other genera were found only in site H0 (11 isolates). Based on the genotypic and phylogenetic analyses using the 16S rRNA gene sequences of all *Streptomyces* isolates, 18% (12 isolates) revealed <98.7% identity of the gene

sequences compared to those in the publicly available databases and were identified as possible novel species with a high probability. Further studies suggested that many *Streptomyces* isolates possess the non-ribosomal peptide synthetases-coding gene, and some of which could inhibit growth of at least two test microbes (i.e., Gram-positive and Gram-negative bacteria and fungi) and showed also the cytotoxicity against hepatocellular carcinoma and or mouse fibroblast cell lines. The antimicrobial activity and cytotoxicity of these *Streptomyces* isolates were highly dependent upon the nutrients used for their cultivation. Moreover, the HPLC-UV-MS profiles of metabolites produced by the selected *Streptomyces* isolates unveiled apparent differences when compared to the public database of existing natural products. With our findings, the poly-extreme environments like Salar de Huasco are promising sources for exploring novel and valuable bacteria with pharmaceutical potentials.

## 2.2 Introduction

Actinomycetes are the most important bacteria that are capable of producing bioactive compounds. The majority of natural products for new pharmaceutical applications are derived from actinomycetes (Bérdy, 2005), while the notable member of actinomycetes, the genus *Streptomyces* is the major producer (Watve et al., 2001). Many of these specialized metabolites biosynthesized by actinomycetes correspond to polyketides and non-ribosomal peptides, which may act as antibiotics, immunosuppressant, anticancer/antitumor agents, toxins, and siderophores (Amoutzias et al., 2016). The members of the genus *Streptomyces* are widely distributed across various habitats and geographical locations (Antony-Babu et al., 2008). *Streptomyces* produces spores that are characteristically resistant, allowing this bacterium to persist in the extreme environments and to maintain its viability for many years (Bull et al., 2005). Previous studies showed that bacteria isolated from the extreme environments, such as the Mariana Trench (Pathom-aree et al., 2006), the polar and permafrost soils in the Arctic (Steven et al., 2008; Lyutskanova et al., 2009), and the extremely dry and saline soils of the Atacama Desert (Okoro et al., 2009) are unique sources for the discovery of new bioactive compounds and many of them are possibly novel species (Bull et al., 2005; Fiedler et al., 2005; Goodfellow et al., 2018).

The Atacama Desert is the driest place in the world located in South America, precisely in Chile, covering a 1000-km strip of land on the Pacific coast, west of the Andes Mountains. It is bordering Peru in the north and extending to the Copiapó River in the south. Nowadays, five novel *Streptomyces* species derive from this extreme desert, including *Streptomyces atacamensis* (Santhanam et al., 2012a), *Streptomyces desertii* (Santhanam et al., 2012b), *Streptomyces bulli* (Santhanam et al., 2013), and *Streptomyces leeuwenhoekii* (Busarakam et al., 2014). *S. leeuwenhoekii* is the producer of two newly bioactive compounds comprised of (i) chaxamycins, showing antagonism against *Staphylococcus aureus* ATCC 25923, inhibiting the heat shock protein 90, and degrading proteins involved in cell proliferation (Rateb et al., 2011a) and (ii) chaxalactins, the anti-Gram-positive bacterial agents (Rateb et al., 2011b). Two more novel compounds, atacamycins and chaxapeptin, each derive respectively from

*Streptomyces* sp., C38 (Nachtigall et al., 2011) and *Streptomyces leeuwenhoekii* C58 (Elsayed et al., 2015) isolated from hyper-arid soil of the Laguna de Chaxa of Salar de Atacama in the north of Chile (a lagoon located in the commune of San Pedro de Atacama, province of El Loa). These two compounds correspond to a macrolactone and a lasso peptide produced by ribosomal biosynthesis with posttranslational modification, with moderate antiproliferative activity and capable of inhibiting human lung cancer cell line A549 respectively. Another group of new compounds with antimicrobial activity, the abenquines A–D, were obtained from *Streptomyces* sp. DB634 isolated from the Salar de Tara in the Chilean Altiplano (>4000 m.a.s.l.) (Schulz et al., 2011).

In Chile, the Chilean Altiplano of the Atacama Desert, is considered the highest plateau of the Andes Mountains (>3000 m.a.s.l.) with 14° to 22° S of latitude. In addition, it is exposed to strong climatic variation over different temporal scales (Risacher et al., 2003; Dorador et al., 2013). This site offers a unique ecosystem with highly extreme conditions, such as changes in daily temperature from –10 to +25 °C (Dorador et al., 2013) and it is divided into different sites, for instance, Salar de Tara (at 150 km east of the town of San Pedro de Atacama, in the Province of El Loa, region Antofagasta) and Salar de Huasco (in the south of the town of Parinacota in the Arica and Parinacota regions). The Salar de Huasco is known by its poly-extreme conditions, i.e., salinity gradient (from freshwater to saturation), elevated levels of solar radiation (<1100 W/m<sup>2</sup>), and negative water balance, which differs from the other locations previously studied in the Atacama Desert. Some areas of the Salar de Huasco have been found to house diverse microbes (Dorador et al., 2010; Molina et al., 2016). However, there is no study regarding the cultivable actinomycetes from this poly-extreme ecosystem and their pharmaceutical potentials. The present work aims to isolate bacteria with a focus on actinomycetes from different sites of the Salar de Huasco and to assess their pharmaceutical potential in possession of non-ribosomal peptide synthases (NRPS)-coding gene, antimicrobial activity and cytotoxicity.

## 2.3 Materials and methods

### 2.3.1 Selective isolation of *Streptomyces*

Six soil samples were collected from sites H0 (base camp; freshwater stream) and H6 (saline soils) located in the northern and southern parts of the eastern shoreline of the Salar de Huasco, respectively (Dorador et al., 2010) (Fig. 8). Sites H0 and H6 were characterized as meso-saline and hyper saline sites with pH 7.6 and pH 8.6, respectively (Dorador et al., 2009). The samples were taken at 5 cm depth from the ground surface using sterile polypropylene tubes and transferred to the laboratory. These samples were stored at ambient temperature for a period not exceeding 5 days. One g of soil sample was suspended in 9 ml of ¼ strength Ringer's solution and 1 ml of the soil suspension was diluted 100-fold and mixed in an orbital shaker at 150 rpm for 1 h. The diluted soil suspension was pretreated by heating at 55 °C for 6 min in a thermo-regulated bath (Antony-Babu et al., 2008). The heated aliquot (0.1 mL) was spread over the surface of starch casein agar medium (SCA), supplemented with 50 µg/ml nystatin and 50 µg/mL cycloheximide to prevent fungal contamination (Kuester and Williams,

1964). All seeded agar plates were prepared in triplicate and incubated at 28 °C for 14-21 days (Vickers et al., 1984). Colonies with rough appearance, powdery or tough texture and branching filaments with and without aerial mycelia were subcultured on SCA plates and incubated at 28 °C for 14 days. A subculture of each isolate was grown in International *Streptomyces* Project III (ISP3) medium (Shirling and Gottlieb, 1966) under the same conditions cited above. The purity of the each isolate was checked using light microscope.

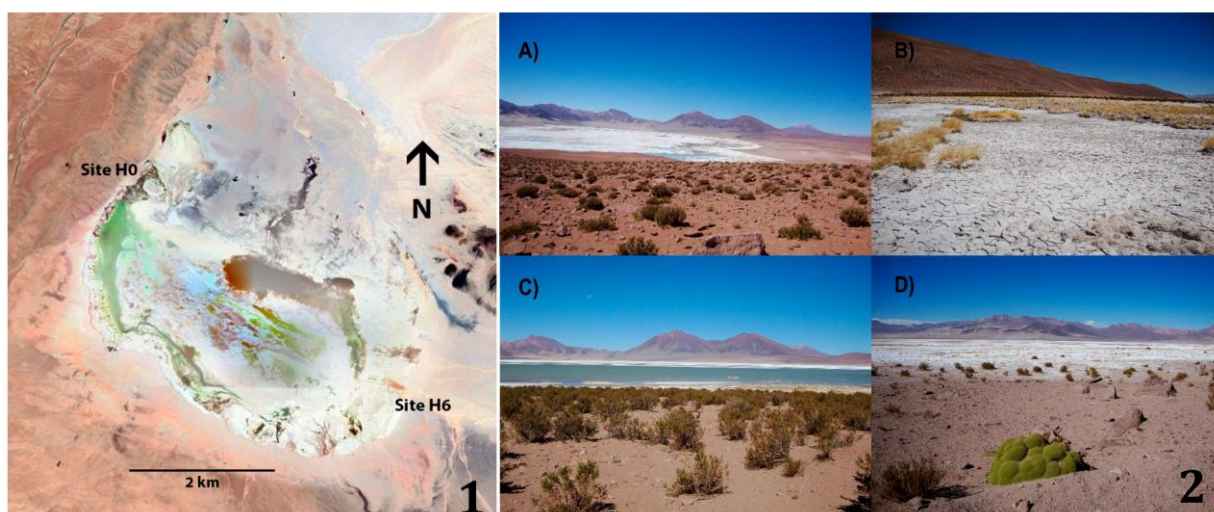


**Figure 8. Salar de Huasco and sampling sites images.** (1) Satellite image of Salar de Huasco indicating sampling sites. Image Google Earth V 7.3.2.5776. (March 3, 2019). Salar de Huasco, Chile. 20°16'22.68" S, 68°52'54.08" W, Eye alt 14.35 mi. CNES/Airbus 2019 [March 30, 2019]. <https://earth.google.com/web/@20.29749527,68.84083051,3780.51679815a,17347.67437889d,35y,360h,0t,0r>. (2) Sampling sites at Salar de Huasco, Northern Chile. (A) Panoramic view of Salar de Huasco, Chilean Altiplano; (B) Site H0, saline crusts; (C) Site H6, soils; (D) Site H6, saline soils.

## 2.3.2 Identification of bacterial isolates

### 2.3.2.1 Morphological characterization based on colour grouping

The morphological characteristics of all bacterial isolates such as aerial spore mass colour, substrate (vegetative) mycelium pigmentation and the production of diffusible exopigments were examined and registered after incubation on ISP3 agar medium at 28°C for 14 days. The colours of the aerial and substrate mycelium of the isolates were described referring to the National Bureau of Standards (NBS) Colour Name Charts (Kelly, 1964) and subsequently the isolates with common morphological characteristics were classified into a same colour group, in order to select . Each isolate was maintained on glucose yeast extract and malt extract (GYM) medium and stored as spore suspensions and hyphae in 25% (v/v) glycerol at -80 °C.

### 2.3.2.2 16S rRNA gene-based phylogenetic analysis

Bacterial cultures were prepared in 2 ml of tryptone yeast extract (ISP1) broth at 28 °C for 7 days and then transferred to vials containing 0.5 mm glass beads (BioSpec Products Inc, Bartlesville, Oklahoma, USA) to breakdown mechanically the bacterial cells (Mini Bead Beater, Bead Homogenizer, BioSpec Products Inc, Bartlesville, Oklahoma, USA). Total genomic DNA was extracted from the homogenized bacterial suspension using the AxyPrep Bacterial Genomic DNA Miniprep kit (Axygen Biosciences, Union city, New Jersey, USA) as recommended by the manufacturer.

The 16S rRNA gene was amplified by PCR using the universal primers for bacteria, Eub9-27F and Eub1542R (Stackebrandt and Liesack, 1993). Every reaction was performed in a final volume of 50 µL, containing 50-100 ng of genomic DNA, 2.0 µM of each primer, 19 µl of nuclease-free MilliQ-H<sub>2</sub>O (Merck Millipore, Burlington, Massachusetts, USA), and 25 µL of SapphireAmp® Fast PCR Master Mix (TaKaRa, Japan). PCR was carried out in a thermocycler under the following conditions: Initial denaturation at 94 °C for 5 min; 30 cycles of denaturation at 94 °C for 45 s; annealing at 54 °C for 45 s; extension at 72 °C for 1.5 min; and a final extension at 72 °C for 5 min. The PCR (Polymerase chain reaction) products were checked by 1% (w/v) agarose gel electrophoresis and subsequently sequenced by capillary sequencing using an ABI Prism 3730XL automated DNA sequencer (Applied Biosystems, Macrogen Inc., Korea), with the same universal PCR primers for the genus-level assignment and the two additional internal primers 341F and 1492R (Muyzer et al., 1993) to obtain the nearly complete 16S rRNA gene sequences.

The 16S rRNA gene sequences were analysed and edited using the software DNA Baser Sequence Assembler version 3.5 (Heracle BioSoft SRL, 2014). The partial 16S rRNA gene sequences of the isolates were aligned using RDP II (Wang et al., 2007). EzTaxon (Kim et al., 2012) was used to retrieve the nearest phylogenetic neighbours of all bacterial isolates. The nearly completed 16S rRNA gene sequences (> 1300 nt) of the isolates were deposited in the GenBank database with the accession numbers KX130868-KX130886. The phylogenetic tree was constructed using Neighbour-Joining algorithms (Saitou and Nei, 1987) with a Tamura-Nei substitution model using MEGA 7.0 software (Kumar et al., 2016). The multiple alignments of all the 16S rRNA gene sequences were performed using MUSCLE (MULTiple Sequence Comparison by Log- Expectation) algorithm (Edgar, 2004). The robustness of the tree was evaluated using 1000 Bootstrap (Felsenstein, 1981).



## 2.3.3 Evaluations of pharmaceutical potentials

### 2.3.3.1 Genotyping of Non-ribosomal peptide synthetase (NRPS)

*Streptomyces* isolates with nearly complete 16S rRNA gene sequences were screened for the presence of non-ribosomal peptide synthetase (NRPS) domains using the primers A3F (5'-GCSTACSYSATSTACACSTCSGG-3') and A7R (5'-SASGTCVCCSGTSCGGTAS-3') (Y = C or T; S = G or C) following a method described by Ayuso-Sacido and Genilloud, 2005.

### 2.3.3.2 Preparation of crude extracts and bioactivity assessments

The secondary metabolites were extracted from *Streptomyces* isolates possessing NRPS domains following a protocol described by Schneemann et al., 2010 with some modifications. Each isolate was grown in 100 mL of GYM (pH 7.2) and in starch-soy peptone (SPM, pH 7.0) liquid media supplemented with 2% NaCl and incubated at 28°C for one week, with shaking at 135 rpm, in an orbital shaking incubator (MaxQ 4000, Thermo Fisher Scientific, Waltham, Massachusetts, USA). Extraction of metabolites from the whole culture broths started with the addition of 150 mL of ethyl acetate to each flask, followed by stirring and sonication cycles and kept at 4 °C overnight for effective phase separation. The lower aqueous phase was discarded, and the ethyl acetate phase (supernatant) was dried in a rotary evaporator (Büchi, Flawil, Switzerland) at ambient temperature.

The antimicrobial activity of the crude extracts was evaluated by bioassays using stocks solutions with a concentration of 1% w/v (equivalent to 10 mg/mL in methanol). The bioassays of antibacterial and antifungal activities were performed following a procedure described by Schneemann et al., 2010. Aliquot of 5 µL of each crude extract was added in each well of the 96-well microtiter plate and then the solvent was evaporated using vacuum centrifuge (Biotage SPE Dry, Sweden) before append 195 µL of the test microbial suspension. The final concentration of each crude extract in the bioassays was 250 µg/mL. The test organisms comprised of Gram-positive bacteria: *Staphylococcus epidermidis* DSM 20044<sup>T</sup>, methicillin-resistant *Staphylococcus aureus* DSM 18827, *Pseudomonas aeruginosa* DSM 50071<sup>T</sup> and *Propionibacterium acnes* DSM 1897<sup>T</sup>; Gram-negative bacteria: *Xanthomonas campestris* DSM 2405 and *Erwinia amylovora* DSM 50901; and fungi: *Candida albicans* DSM 1386, *Trichophyton rubrum*, *Septoria tritici* and *Phytophthora infestans*. *Trichophyton rubrum* was obtained from F. Horter (Department of Dermatology, Allergology, and Venerology, University Hospital Schleswig-Holstein, Kiel, Germany while *Septoria tritici* and *Phytophthora infestans* were obtained from Dr. J. B. Speakman (BASF, Ludwigshafen, Germany). The positive control for the test bacteria was 100 µg/well of chloramphenicol and for the test fungi was 200 µg/well of cycloheximide, while the negative control was no compound applied.

The cytotoxicity test was performed following a method described by Schulz et al., 2011. Aliquot (1  $\mu$ L) of each crude extract was added in a final assay volume of 100  $\mu$ L of the mouse fibroblasts (NIH-3T3) and hepatocellular carcinoma (HepG2 ACC 180) cell lines. NIH-3T3 cell line was provided by G. Rimbach, University of Kiel, Germany while HepG2 ACC 180 was obtained from Leibniz Institute DSMZ-German collection of microorganisms and cell cultures, Braunschweig, Germany. The final concentration of each crude extract in the bioassays was 100  $\mu$ g/mL. The positive control for these assays was tamoxifen with a final concentration of 40  $\mu$ M. No compound was added for the negative control.

### **2.3.3.3 Profiling of metabolites in crude extracts**

The crude extracts dissolved in methanol were elucidated by analytical reversed-phase HPLC-UV-MS (High-Performance Liquid Chromatography with UV detector coupled to Mass Spectrometry), in a VWR-Hitachi La-Chrom Elite System, coupled to a diode array detector and a Phenomenex Onyx Monolithic column (C<sub>18</sub>, 100 x 3.00 mm) according to the conditions described by Silber et al., 2013. For the mass detection, the HPLC system was coupled to an ion trap detector (Esquire4000, Bruker Daltonics, Billerica, Massachusetts, USA). The UV-Vis spectra of peaks obtained from each bacterial crude extract were compared with the Dictionary of Natural Products 2012 (Buckingham, 2012).

## **2.4 Results and discussion**

### **2.4.1 Selective isolation and identification of the isolates**

30 and 46 isolates were obtained from soils samples of sites H0 and H6 respectively (Table 3). These isolates were obtained from plates with 10 fold dilutions and 97% (74 isolates) of them were found affiliated with the phylum Actinobacteria based on the 16S rRNA gene sequence similarity. 65 of these isolates belong to *Streptomyces* genus and most of them (40) were recovered from the soil sample of the hyper saline site H6, which also has a pH 8.6 (Table 3). In contrast, the eleven non-*Streptomyces* isolates were found only in the soil sample with neutral pH 7.6 collected from site H0. These results evidenced that the majority of *Streptomyces* isolates came from soils with extreme conditions and therefore these strains should be the focus of interest given their propensity to produce novel natural products in response to these harsh conditions (Bull and Goodfellow 2019).

**Table 3.** 16S rRNA gene-based identification of all bacteria isolated from Salar de Huasco.

Class	Family	Genus	Number of isolates (%)	Site of Isolation
<i>Actinobacteria</i>	<i>Streptomycetaceae</i>	<i>Streptomyces</i>	65 (86%)	H0 and H6
	<i>Nocardiopsaceae</i>	<i>Nocardiopsis</i>	7 (9%)	H0
	<i>Micromonosporaceae</i>	<i>Micromonospora</i>	2 (3%)	H0
<i>Bacilli</i>	<i>Bacillaceae</i>	<i>Bacillus</i>	1 (1%)	H0
<i>Gammaproteobacteria</i>	<i>Pseudomonadaceae</i>	<i>Pseudomonas</i>	1 (1%)	H0

All 65 *Streptomyces* isolates showed leathery or butyrous colonies during the first stages of growth and a granular or powdery pigmented aerial mycelium, consistent with the typical morphology of the genus *Streptomyces* (Lechevalier and Lechevalier, 1970). Most of these isolates also produced diffusible pigments and excreted coloured aqueous droplets on the hydrophobic surface of their colonies (Shirling and Gottlieb, 1966) after the incubation ISP3 agar medium. Nineteen out of 65 *Streptomyces* classified into single- and multi-membered colour groups were selected for further study based on its morphological differentiation and the similarity of the nearly complete 16S rRNA gene sequences (>1300 bp) (Table 4).

**Table 4.** Morphological and molecular characteristics of some *Streptomyces* spp. <sup>a</sup> isolated from Salar de Huasco.

Isolate code	Site of isolation	Morphological characteristics <sup>b</sup>			Molecular characteristics			
		Aerial spore mass	Substrate mycelium	Diffusible pigments	Closest type strain	16 rDNA sequences <sup>c</sup>	Similarity (%)	NRPS <sup>d</sup>
HST05	H6	White	Light yellowish pink	-	<i>Streptomyces canus</i> DSM 40017 <sup>T</sup>	KQ948708	96.8	+
HST09	H6	Dark greyish blue	Deep purplish red	-	<i>Streptomyces lienomycini</i> LMG 20091 <sup>T</sup>	AJ781353	99.6	+
HST14	H6	White	Pale violet	Light greyish brown	<i>Streptomyces atroolivaceus</i> NRRL ISP-5137 <sup>T</sup>	JNXG01000049	96.0	-
HST18	H6	-	Dark olive green	Moderate yellow green	<i>Streptomyces alboniger</i> NRRL B-1832 <sup>T</sup>	LIQN01000245	96.7	+
HST19	H6	Dark greyish blue	Dark greenish yellowish green	Dark greyish yellowish brown	<i>Streptomyces collinus</i> NBRC 12759 <sup>T</sup>	AB184123	99.2	+
HST21	H6	White	Greyish yellow	Moderate olive brown	<i>Streptomyces albidochromogenes</i> NBRC 101003 <sup>T</sup>	AB249953	99.1	+
HST22	H6	White	Deep orange yellow	Moderate olive brown	<i>Streptomyces albidochromogenes</i> NBRC 101003 <sup>T</sup>	AB249953	99.0	+
HST23	H6	Light pink	Light orange yellow	Dark yellow	<i>Streptomyces purpureus</i> NBRC 13927 <sup>T</sup>	AB184547	98.8	-
HST28	H6	White	Light olive brown	Dark brown	<i>Streptomyces kanamyceticus</i> NBRC 13414 <sup>T</sup>	AB184388	98.8	+
HST50	H6	White	Greyish reddish brown	-	<i>Streptomyces ambofaciens</i> ATCC 23877 <sup>T</sup>	CP012382	96.0	-
HST51	H6	Light pink	Strong yellowish brown	-	<i>Streptomyces alboniger</i> NRRL B-1832 <sup>T</sup>	LIQN01000245	98.6	+
HST54	H6	White	Deep red	Light greyish brown	<i>Streptomyces griseolus</i> NRRL B-2925 <sup>T</sup>	JOFC01000069	97.6	-
HST61	H6	Pale yellowish pink	Pale orange yellow	-	<i>Streptomyces kanasensis</i> ZX01 <sup>T</sup>	JN572690	99.6	-

**Table 4. Continued**

Isolate code	Site of isolation	Morphological characteristics <sup>b</sup>			Molecular characteristics			
		Aerial spore mass	Substrate mycelium	Diffusible pigments	Closest type strain	16 rDNA sequences <sup>c</sup>	Similarity (%)	NRPS <sup>d</sup>
HST66	H6	White	Deep greenish yellow	-	<i>Streptomyces fumanus</i> NBRC 13042 <sup>T</sup>	AB184273	96.9	+
HST68	H6	Greyish blue	Pinkish grey	-	<i>Streptomyces ambofaciens</i> ATCC 23877 <sup>T</sup>	CP012382	96.0	+
HST69	H0	White	Brilliant yellow	-	<i>Streptomyces chlorus</i> BK125 <sup>T</sup>	LIQN01000245	98.1	+
HST72	H0	White	Strong yellowish brown	Strong brown	<i>Streptomyces microflavus</i> NBRC 13062 <sup>T</sup>	AB184284	97.9	-
HST82	H0	White	Pale yellowish pink	-	<i>Streptomyces cyaneofuscatus</i> NRRL B-2570 <sup>T</sup>	JOEM01000050	95.6	-
HST83	H0	White	Strong yellowish brown	Strong brown	<i>Streptomyces pratensis</i> ch24 <sup>T</sup>	JQ806215	97.8	+

a: *Streptomyces* isolates were selected according to their distinctive morphological characteristics and 16S rRNA gene similarities (>1300 nt).

b: The morphological characteristics were observed after growing *Streptomyces* isolates on ISP3 agar medium at 28 °C for 14 days.

c: GeneBank accession number.

d: 700 bp fragment of adenylation domain A3-A7 region.

These 19 isolates were widely distributed across the phylogenetic tree of the genus *Streptomyces* supported by high bootstrap values as shown in figure 9. A total of 12 isolates showed a 16S rRNA gene sequence similarity below the 98.7% threshold for proposing as novel species (Chun et al., 2018) (Table 4), while the other seven (HST09, HST19, HST21, HST22, HST23, HST28, and HST61) found to occupy distinct phylogenetic positions from their closest relatives with no close relationship with any species and type strains of the genus *Streptomyces* from the Atacama Desert described so far (Santhanam et al., 2012a,b,c; Busarakam et al., 2014; Goodfellow et al., 2018) (Fig. 9).

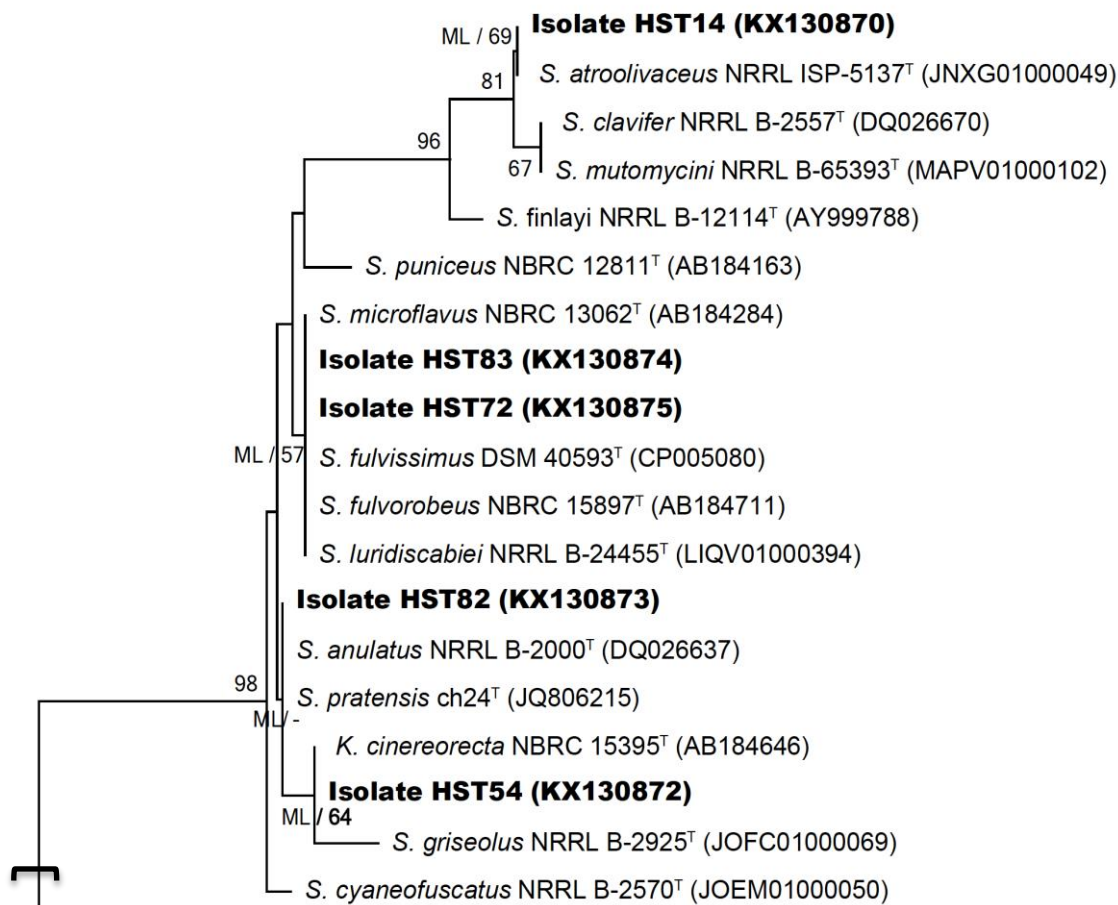


Figure 9. Continued

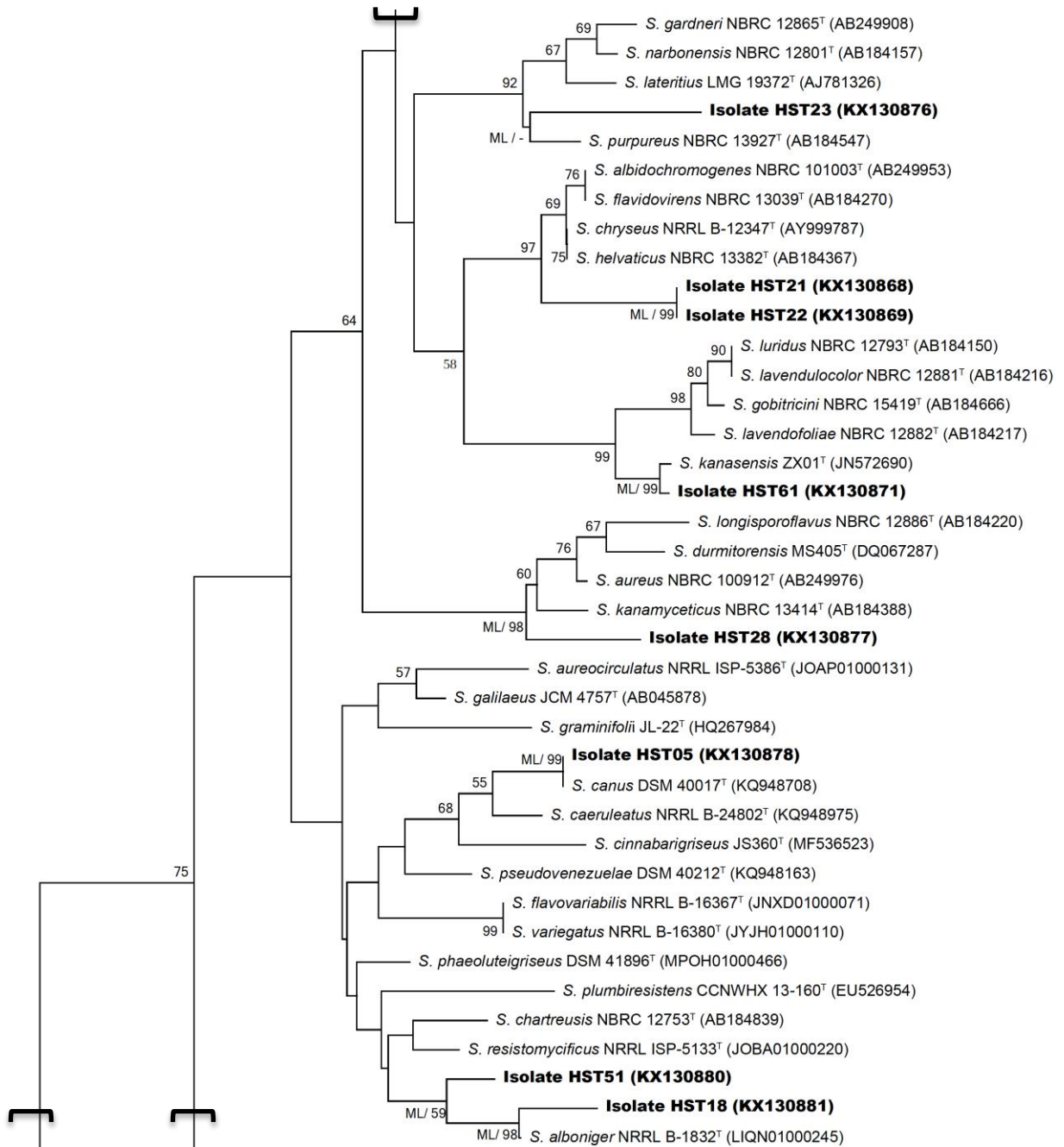
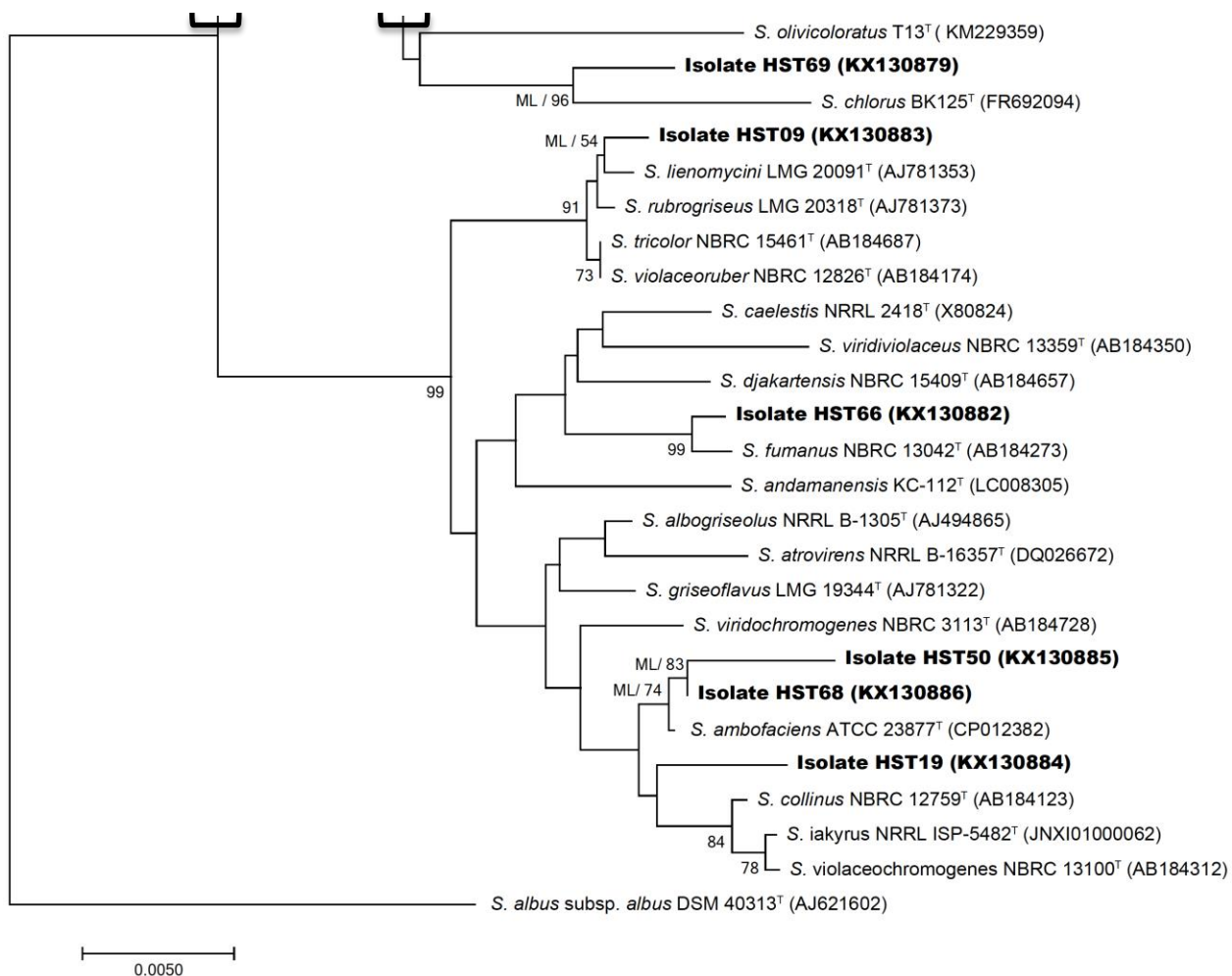


Figure 9. Continued



**Figure 9. Neighbour-joining phylogenetic tree based on almost complete 16S RNA sequences (>1300 nt) of the 19 *Streptomyces* isolates derived from Salar de Huasco and their closely related species.** The tree was constructed using the Neighbor-Joining algorithm and the Jukes–Cantor substitution model. The scale bar indicates 0.005 substitutions per nucleotide, and *Streptomyces albus* subsp. *albus* DSM 40313<sup>T</sup> was used as outgroup. Bootstrap values above 50% are present.

Isolate HST19 forms a distinct branch closely related to the type strain of *Streptomyces collinus* NBRC 12759<sup>T</sup> (99.2%) (Lindenbein, 1952), *Streptomyces iakyrus* NRRL ISP-5482<sup>T</sup> (98.8%) (De Querioz and Albert, 1962), and *Streptomyces violaceochromogenes* NBRC 13100<sup>T</sup> (99.3%) (Ryabova et al., 1957). Isolates HST21 and HST22 form a well-supported sub-clade closely associated to *Streptomyces albidochromogenes* NBRC 101003<sup>T</sup> (99.0%) (Gause et al., 1983). Strain HST61 occupied a phylogenetic position close to “*Streptomyces kanasensis*” ZX01 (99.6%) which is a producer of a novel antiviral glycoprotein (Han et al., 2015). Isolate HST28 showed close phylogenetic relationship with *Streptomyces kanamyceticus* NBRC 13414<sup>T</sup> (98.8%) (Okami and Umezawa, 1957), while isolate HST23 had close relatedness to *Streptomyces purpureus* NBRC 13927<sup>T</sup> (98.8%) (Goodfellow et al., 1986). Isolates HST09 occupied distant subclade closely related to *Streptomyces lienomycini* LMG 20091<sup>T</sup> (99.6%) (Gause et al., 1983).



The length of the branch of all *Streptomyces* isolates in the phylogenetic tree and the assignment of these isolates to completely different clades from each other, except for isolates HST21 and HST22, highlight the divergence of them from their closely related neighbours. Further studies as MLST (Multi locus sequence typing) and dDDH (Digital DNA:DNA hybridization) need to be performed to confirm the right affiliations of these isolates to the novel species within the evolutionary radiation of the genus *Streptomyces* (Stackebrandt et al., 2002).

Most isolates (except for isolates HST83, HST72, HST21, and HST22) showed divergent phylogenetic positions compared to the type species of the genus *Streptomyces* (Fig. 9). Therefore, these strains should be designed for further taxonomic and analytical chemistry analyses to confirm their novelty at species rank and as a source of novel chemical entities (Bull and Goodfellow et al., 2019)

#### **2.4.2 Secondary metabolite analysis**

The NRPSs multimodular enzymatic complexes are constituted by three main catalytic domains: The adenylation (A) domain, responsible for the recognition and activation of a specific amino acid, the condensation (C) domain catalyses the formation of the peptidic bond (C-N) between different modules, and the peptidyl-carrier (T) domain which transfers the activated amino acids from the A domain to the C domain of the same module (Phatom-aree et al., 2006). The presence of A domain in actinobacterial genomes reflects the biosynthesis of secondary metabolites. The products of the NRPS biosynthetic pathway are diverse secondary metabolites including several antitumor compounds (Onaka, 2006; Sánchez et al., 2006). A total of 12 *Streptomyces* isolates (63%) (Table 4) revealed the possession of NRPS A domain.

A correlation has been previously observed between the numbers of isolates with the positive NRPS-PCR reaction and the production of bioactive compounds (Schneemann et al., 2010). The 12 NRPS-holding isolates were tested further for their bioactivities. Isolates HST05, HST14, HST18 and HST51 were discarded from this analysis due to their low growth rate on the test media. From the pairs of isolates HST83-HST72 and HST21-HST22 that occupied the same phylogenetic position (Fig. 9), only the isolates HST21 and HST72 were included in bioactivity tests.

The crude extracts obtained from *Streptomyces* isolates grown previously in GYM or SPM broth demonstrated different HPLC profiles (Appx. 1). These isolates have a wide range of metabolites in their chromatograms (Appx. 1). The UV-Vis and MS data of the crude extracts in comparison with the Dictionary of Natural Products Database exhibited a low similarity to the known compounds, which highlights the novelty of these natural entities.

The majority of the isolates showed important antifungal, antibacterial and cytotoxic activities (Table 5-7). In the case of the antibacterial activity, the crude extracts from GYM media showed greater percentages of inhibition than extracts from SPM media and a broader spectrum of activity against the pathogens tested (Table 5). In addition, most strains showed levels of growth inhibition >90% in GYM extracts. However, these levels of growth inhibition were also obtained in SPM extracts for the strains HST21, HST23 and HST72 against *S. epidermis*, MRSA and *P. acnes*. In summary, the strains that displayed growth inhibition >90% were HST09, HST21, HST23, HST28, HST72, HST82, HST50, HST54 and HST68 against MRSA; strains HST23, HST28, HST50, HST54 and HST72 against *P. acnes*; strains HST21, HST23, HST28, HST50, HST54 and HST68 against *X. campestris*; and strains HST21 and HST23 against *E. amylovora* (Table 5).

**Table 5.** Antibacterial activity of crude extracts derived from *Streptomyces* spp. of Salar de Huasco.

Crude <sup>b</sup> extracts	Growth inhibition (%) <sup>a</sup>					
	<i>Staphylococcus epidermidis</i> DSM 20044 <sup>T</sup>	MRSA <sup>c</sup> DSM 18827	<i>Pseudomonas aeruginosa</i> DSM 50071 <sup>T</sup>	<i>Propionibacterium acnes</i> DSM 1897 <sup>T</sup>	<i>Xanthomonas campestris</i> DSM 2405	<i>Erwinia amylovora</i> DSM 50901
<b>GYM media</b>						
HST09	96	92	-	27	96	-
HST14	-	-	-	-	-	-
HST19	-	-	57	55	-	-
HST21	99	98	-	84	99	91
HST23	93	92	100	97	93	71
HST28	97	98	100	100	97	22
HST50	96	-	90	97	96	92
HST54	96	95	96	78	96	-
HST61	73	-	-	76	73	63
HST68	93	-	90	97	93	91
HST72	95	97	98	35	95	-
HST82	100	97	90	92	100	-
<b>SPM media</b>						
HST09	-	-	-	-	-	-
HST14	-	-	30	-	-	-
HST19	-	-	-	-	-	-
HST21	96	-	100	-	53	96
HST23	97	76	100	100	49	97
HST28	-	39	29	89	25	-
HST50	-	-	57	30	-	-
HST54	-	-	47	-	35	-
HST61	68	-	43	62	26	68
HST68	-	-	45	-	-	-
HST72	-	-	50	96	28	-
HST82	-	-	26	-	-	-

a: These results correspond to the mean  $\pm$  SEM of triplicate experiments, expressed as the inhibition percentage (%) of growth for the test bacterial strains, calculated based on the control. The negative results are shown with (-).

b: GYM and SPM refer respectively to glucose yeast extract plus malt extract medium and starch-soy peptone medium, in which the *Streptomyces* isolates were grown before the preparation of their crude extracts.

c: methicillin-resistant *Staphylococcus aureus*.

For the case of the antifungal activity, the crude extracts of GYM and SPM showed almost similar percentages of inhibition and spectrum of activity against the tested pathogens (Table 6). However, a greater number of strains with inhibition levels >90% was obtained in the GYM media. The percentages of inhibition >90% were mainly obtained against *T. rubrum* (HST21 and HST23) and *S. tritici* (HST23, HST28 and HST72) (Table 6).

**Table 6.** Antifungal activity of crude extracts derived from *Streptomyces* spp. of Salar de Huasco.

Crude extracts <sup>b</sup>	Growth inhibition (%) <sup>a</sup>			
	<i>Candida albicans</i> DSM 1386	<i>Trichophyton</i> <i>rubrum</i>	<i>Septoria</i> <i>tritici</i>	<i>Phytophthora</i> <i>infestans</i>
<b>GYM media</b>				
HST09	-	72	-	-
HST14	-	33	-	-
HST19	-	58	-	-
HST21	-	86	22	50
HST23	77	100	100	49
HST28	45	37	94	27
HST50	-	41	29	-
HST54	-	48	-	39
HST61	-	59	59	22
HST68	-	30	21	-
HST72	28	60	100	47
HST82	-	41	-	-
<b>SPM media</b>				
HST09	-	-	-	-
HST14	-	30	-	-
HST19	-	-	-	-
HST21	-	100	-	53
HST23	76	100	100	49
HST28	39	29	89	25
HST50	-	57	30	-
HST54	-	47	-	35
HST61	-	43	62	26
HST68	-	45	-	-
HST72	-	50	96	28
HST82	-	26	-	-

a: These results correspond to the mean  $\pm$  SEM of triplicate experiments, expressed as the inhibition percentage (%) of growth for the test bacterial strains, calculated based on the control. The negative results are shown with (-).

b: GYM and SPM refer respectively to glucose yeast extract plus malt extract medium and starch-soy peptone medium, in which the *Streptomyces* isolates were grown before the preparation of their crude extracts.

The cytotoxic activity of GYM and SPM crude extracts, at a final extract concentration of 100  $\mu$ g/ml, showed almost the same percentages of growth inhibition for all the isolates, with exception of the isolate HST09, which showed important cytotoxic activity only with GYM extract (Table 7). The isolates HST21, HST23, HST28 and HST72 showed levels of growth inhibition >99% against the tumour cell line HepG2 and mouse fibroblasts NIH-3T3 (Table 7).

**Table 7.** Cytotoxic activity of crude extracts derived from *Streptomyces* spp. of Salar de Huasco.

Crude extracts <sup>b</sup>	Growth inhibition (%) <sup>a</sup>	
	NIH-3T3 <sup>c</sup>	HepG2 <sup>d</sup>
<b>GYM media</b>		
HST09	99	79
HST14	50	40
HST19	57	34
HST21	99	99
HST23	99	99
HST28	100	100
HST50	43	38
HST54	53	24
HST61	-	-
HST68	-	21
HST72	97	69
HST82	50	40
<b>SPM media</b>		
HST09	36	-
HST14	51	42
HST19	57	34
HST21	99	99
HST23	99	99
HST28	100	100
HST50	43	38
HST54	53	24
HST61	-	-
HST68	-	21
HST72	97	69
HST82	39	38

a: a: These results correspond to the mean  $\pm$  SEM of triplicate experiments, expressed as the inhibition percentage (%) of growth for the test bacterial strains, calculated based on the control. The negative results are shown with (-).

b: GYM and SPM refer respectively to glucose yeast extract plus malt extract medium and starch-soy peptone medium, in which the *Streptomyces* isolates were grown before the preparation of their crude extracts.

c: Mouse fibroblasts cell line

d: Hepatocellular carcinoma cell line

Based on the overall bioassays, isolates HST21, HST23, and HST28 were the producers of the broadest spectrum of bioactivities. These results are coherent with those described for *Streptomyces* spp. isolated from the other Salar sites of the Atacama Desert, e.g., *Streptomyces* sp. C38 from Salar de Atacama that produces atacamycins A–C (Nachtigall et al., 2011) and *Streptomyces* sp. DB634 from Salar de Tara that produces abenquines A–D (Schulz et al., 2011).

It seems that polyextreme ecosystems as Salar de Huasco forces the microorganisms to adapt to it (Bowers et al., 2009), which led to the development of unique *Streptomyces* taxa that are clearly different from the other sites in the Atacama Desert and the Altiplano (Okoro et al., 2009) and probably vary due to the spatial heterogeneity within the same area (Dorador et al., 2008).

## 2.5 Conclusion

*Streptomyces* spp. isolated from the Salar de Huasco at the Chilean Altiplano showed taxonomic divergences from the validly published species and capabilities to produce novel secondary metabolites with interesting pharmaceutical potentials. These findings open up the prospect for novel drug discovery. Further analytical and chemical analyses should be carried out to elucidate these microbial products in order to be exploited for future biotechnological applications.

# Chapter 3

## Taxonomic description of the new species *Streptomyces huasconensis* HST28<sup>T</sup>

### Objectives

- 3 To describe taxonomically the putative novel *Streptomyces* species by a polyphasic approach.

### 3.1 Abstract

*Streptomyces* strain HST28<sup>T</sup> isolated from the Salar de Huasco, an athalassohaline and poly-extreme high altitude saline wetland located in northern Chile, was the subject of a polyphasic taxonomic study. Strain HST28<sup>T</sup> showed morphological and chemotaxonomic features in line with its classification in the genus *Streptomyces*. Optimal growth of strain HST28<sup>T</sup> was obtained at 28°C, pH 8-9 and up to 10% (w/v) NaCl. Single (16S rRNA) and multi-locus gene sequence analyses showed that strain HST28<sup>T</sup> had a distinct phylogenetic position from its closest relatives, the type strains of *Streptomyces aureus* and *Streptomyces kanamyceticus*. Digital DNA–DNA hybridization (23.3 and 31.0 %) and average nucleotide identity (79.3 and 85.6 %) values between strain HST28<sup>T</sup> and its corresponding relatives mentioned above were below the threshold of 70 and 96 %, respectively, defined for assigning a prokaryotic strains to the same species. Strain HST28<sup>T</sup> was characterised by the presence of LL-diaminopimelic acid in its peptidoglycan layer; galactose, glucose, ribose and traces of arabinose and mannose as whole-cell sugars; phosphatidylmethylethanolamine, phosphatidylinositol, aminolipid, glycerophospholipid and an unidentified lipid as polar lipids; and the predominating menaquinones MK-9(H<sub>6</sub>), MK-9(H<sub>8</sub>) and MK-9(H<sub>4</sub>) (>20 %) as well as

C<sub>15:0</sub> *anteiso* and C<sub>17:0</sub> *anteiso* as major fatty acids (>15 %). Based on the phenotypic and genetic results, strain HST28<sup>T</sup> (DSM 107268<sup>T</sup> = CECT 9648<sup>T</sup>) merits recognition as a new species named *Streptomyces huasconensis* sp.

## 3.2 Introduction

The genus *Streptomyces* encompasses more than 800 species with validly published names (<http://www.bacterio.net/streptomyces.html>) which were grouped in different clusters based on single gene (Kampfer, 2012, Labeda et al., 2012) multi-locus sequence analysis (Labeda et al., 2017) and genome sequence (Nouioui et al., 2018). The monophyly of the genus *Streptomyces* was recently questioned and a taxonomic revision of this taxon was performed based on genome sequence and led to transfer the species *Streptomyces scabrisporus* (Ping et al., 2004) and *Streptomyces aomiensis* (Nagai et al., 2011) to two novel genera, *Embleya* and *Yinghuangia* (Nouioui et al., 2018). *Streptomyces* strains are aerobic, Gram-stain positive and heterotrophic microorganisms characterized by extensive branched substrate and aerial mycelia which differentiate into spore chains (Angert, 2005); peptidoglycan-rich mainly in LL-diaminopimelic acid (A<sub>2</sub>pm), but *meso*-A<sub>2</sub>pm was also detected in certain species; major amounts of saturated *iso*- and *anteiso*-fatty acids; diphosphatidylglycerol, phosphatidylethanolamine; phosphatidylinositol and phosphatidylinositol mannosides as major polar lipids; hexa- and octa-hydrogenated menaquinones with nine isoprene units as predominant isoprenologues (Kroppenstedt, 1985; Kampfer, 2012). Members of this taxon were abundant in soil including composts and some species are pathogenic for animal and human, and others are phytopathogens (Kampfer, 2012).

This taxon has been the main target of several bioprospecting strategies due to its significant ability to produce secondary metabolites compared to the other actinobacterium taxa (Watve et al., 2001). The genus *Streptomyces* is well known by its high G+C content (69-78 mol%) and a large genome size (≈8.0 Mb), which contains a high number of biosynthetic gene clusters (BGCs). In this context, the hyper-arid soils of the Atacama Desert were the target for bioprospecting studies (Bull et al., 2013). Forty six natural products were obtained from diverse microorganisms isolated from the Atacama Desert (Rateb et al., 2018) including 14 compounds with novel chemical structures identified from *Streptomyces* species: (i) *Streptomyces leeuwenhoekii*, isolated from the Laguna Chaxa (Okoro et al., 2009; Busarakam et al., 2014) produces metabolites, atacamycins A-C (Nachtigall et al., 2011), chaxalactins A-C (Rateb et al., 2011a), chaxamycins A-D (Rateb et al., 2011b) and chaxapeptin (Elsayed et al., 2015), with antibacterial and cytotoxic activities; (ii) *Streptomyces asenjonii*, isolated from the Salar de Atacama (Goodfellow et al., 2017), produces novel natural compounds, asenjonamides A-C (Abdelkader et al., 2018), with antibiotic and anti-ageing activities. These findings have reinforced the continued search for novel *Streptomyces* species from these ecosystems, mainly from unexploited sites such as high altitude soils and salt-lakes of the Atacama Desert located at the Altiplano (3000-5000 m.a.s.l.).

In this present study, *Streptomyces* strain HST28<sup>T</sup> isolated from the Salar de Huasco (Cortés-Albayay et al., 2019a), an athalosaline and poly-extreme high altitude saline wetland (3800 m.a.s.l) located in the Altiplano, the high plateau of the Andes (Dorador et al., 2009), was the subject of a polyphasic taxonomic study. The resultant data showed that the isolate HST28<sup>T</sup> represents a new species within the evolutionary radiation of the genus *Streptomyces* for which the name *Streptomyces huasconensis* sp. nov. is proposed.

### 3.3 Materials and methods

#### 3.3.1 Isolation, culture and maintenance

The isolate HST28<sup>T</sup> was recovered from arid soil samples, site H6 (-20.328611 S, -68.838611 W) (Dorador et al., 2009), collected at a location in the Salar de Huasco (Cortés-Albayay et al., 2019a) in complete absence of vegetation. This site has a wide range of salinity that reaches the maximum of 49.1 PSU (practical salinity units) above the oceanic average, high daily temperature changes (-10 to 25°C) and one of the highest solar radiation levels registered worldwide (>1200 Wm<sup>-2</sup>) (Hernandez et al., 2016).

The soil sample and the isolation procedures were performed following Okoro *et al.*, 2009. Strain HST28<sup>T</sup> was isolated as described by Cortés-Albayay *et al.*, 2019a and maintained together with its nearest phylogenetic neighbours, *Streptomyces aureus* DSM 41785<sup>T</sup> (Manfio et al., 2003) and *Streptomyces kanamyceticus* DSM 40500<sup>T</sup> (Umezawa et al., 1957) [both obtained from the German Collection of Microorganisms and Cell Cultures (DSMZ)], on GYM (medium 65, DSMZ) medium. All the strains were stored as spore suspensions and hyphae in 25% v/v glycerol at -80°C. *S. aureus* DSM 40500<sup>T</sup> and *S. kanamyceticus* DSM 41785<sup>T</sup> were originally deposited in DSMZ by Professor Michael Goodfellow and Dr. Elwood B. Shirling, respectively.

#### 3.3.2 Phenotypic characterization

Cultural features of the strain were determined on GYM, yeast extract-malt extract agar, tryptone-yeast extract, oatmeal, inorganic salts-starch, glycerol-asparagine and tyrosine agar plates (International *Streptomyces* Project [ISP1-7] (Shirling and Gottlieb, 1966). The ability of strain HST28<sup>T</sup> to grow at different temperatures, 4, 10, 15, 25, 28, 37 and 45°C as well as in a wide range of pH (5, 6, 7, 8, 9, 11 and 12) was examined on GYM medium after incubation for 7 days at 28°C. The tolerance of the studied strain HST28<sup>T</sup> to salinity was evaluated after incubation on GYM medium supplemented with different concentrations of NaCl (2, 4, 8, 10, 12, 15 and 20%) for 7 days at 28°C.



The biomass of strain HST28<sup>T</sup> used for all the molecular and phenotypic tests was prepared on GYM agar plates after incubation for 7 days at 28°C. Strain HST28<sup>T</sup> together with its nearest phylogenetic neighbours, type strains *S. aureus* and *S. kanamyceticus*, were examined for their ability to use a wide range of carbon and nitrogen sources as well as for their susceptibility to grow in the presence of different inhibitory compounds using GENIII microplates in an Omnilog device (BIOLOG Inc., Haywood, USA). The tests were carried out in duplicate and the resultant data were exported and analysed using the opm package for R (Staneck and Roberts, 1974; Vaas et al., 2013) version 1.06.

### 3.3.3 Scanning electron microscope

The cell structures including spore chain ornamentation and spore surface morphology of the studied strain were recorded after incubation for 14 days on GYM medium at 28°C, using a field-emission scanning electron microscope (Tescan Vega 3 LMU: Tescan, Wellbrook Court, Girtton, Cambridge, CB3 0NA).

### 3.3.4 Phylogenetic analysis

Genomic DNA of strain HST28<sup>T</sup> was extracted using the UltraClean® Microbial DNA isolation kit (MoBio Labs, Carlsbad, CA), following the instructions of the manufacturer. The 16S rRNA-PCR amplification was evaluated using the primers Eub9-27F and Eub1542R and according to the conditions cited by Stackebrandt and Liesack, 1993. A BLAST of the complete 16S rRNA gene sequence (1517 bp; accession number KX130877) of strain HST28<sup>T</sup> was performed using the EzTaxon server (Yoon et al., 2017).

The pairwise sequence similarities were calculated based on the method recommended by Meier-Kolthoff *et al.*, 2013a. The multiple sequence alignments were performed using MUSCLE (Edgar, 2004). The Maximum-likelihood (ML) (Kimura, 1980) and Maximum-parsimony (MP) phylogenetic trees (Fitch, 1971) were constructed using the DSMZ phylogenomics pipeline (Meier-Kolthoff et al., 2014) available at Genome-to-Genome distance calculator (GGDC) web server (Meier-Kolthoff et al., 2013b) (<http://ggdc.dsmz.de/>). ML and MP trees were inferred using RAxML (Stamatakis, 2014) and TNT (Goloboff et al., 2008), respectively. The search for the best topology for the resultant ML tree was obtained from a rapid bootstrapping method in combination with the autoMRE bootstopping criterion (Pattengale et al., 2010) while a bootstrapping method of 1000 iterations, in combination with a tree-bisection-and-reconnection branch swapping method with ten additional random sequence replicates has been used for the MP tree. The tree was rooted using *Cryptosporangium arvum* DSM 44712<sup>T</sup> (Tamura et al., 1998) and the sequences were checked for a compositional bias using the X2 test as implemented in PAUP\* (Swofford, 2003). Multi-locus sequence analysis (MLSA) was performed based on five well-known housekeeping genes in refining the phylogeny of

the genus *Streptomyces*: *atpD* (ATP synthase F1, beta subunit), *gyrB* (DNA gyrase B subunit), *rpoB* (RNA polymerase beta subunit), *recA* (recombinase A) and *trpB* (tryptophan synthase beta chain) genes sequences (Busarakam et al., 2014; Labeda, 2016; Idris et al., 2017; Labeda et al., 2017). All the partial housekeeping sequences of the nearest phylogenetic neighbours were retrieved from GenBank database and the ARS Microbial Genome Sequence Database server, respectively (<http://199.133.98.43>); those of the studied strain HST28<sup>T</sup> were extracted from the draft genome sequence (accession number RBWT00000000). ML and MP algorithms were used to establish a MLSA phylogenetic tree based on the phylogenomic pipeline of DSMZ cited above. The genetic distance between the loci of the studied strain and its closest phylogenetic neighbours was estimated with Kimura 2-parameter (Kimura, 1980) using MEGA 7.0 software (Kumar et al., 2016).

### 3.3.5 Genome sequencing and dDDH

For genome sequencing, the genomic DNA extraction for strain HST28<sup>T</sup> was performed according to Schniete *et al.*, 2017. The draft genome was sequenced using an Ion Torrent PGM (Personal Genome Machine) sequencer, and the Ion PGM Hi-Q Sequencing Kit (Life Technologies, Inc., United States) on a 318 v2 chip type (Life Technologies, Inc., United States). The genome was assembled using the SPAdes software (Bankevich et al., 2012), annotated through RAST server (Aziz et al., 2008; Overbeek et al., 2014) and deposited in GenBank database under accession number RBWT00000000.

Digital DNA:DNA hybridization (dDDH) between the draft genome sequence of strain HST28<sup>T</sup> and its closest neighbours, *S. aureus* NRRL B-2808<sup>T</sup> (GenBank accession number LIPQ00000000) and *S. kanamyceticus* NRRL B-2535<sup>T</sup> (GenBank accession number LIQU00000000) were calculated using the GGDC server with the recommended formula 2 (Meier-Kolthoff et al., 2013). In addition, the average nucleotide identity (ANI) values between the strains cited above were also estimated using an OrthoANlu algorithm of the ANI Calculator (Lee et al., 2016; Yoon et al., 2017).

### 3.3.6 Chemotaxonomy methods

Chemotaxonomic markers of strain HST28<sup>T</sup> and its closest neighbours, type strains *S. aureus* and *S. kanamyceticus*, were identified using standard procedures. Cells were harvested, from cultures after shaking at 250 r.p.m, washed twice with sterile distilled water and freeze-dried. Thin-layer chromatography (TLC) was used to determine A<sub>2</sub>pm isomers (Staneck and Roberts, 1974), whole cell sugars (Lechevalier and Lechevalier, 1970) and polar lipids profiles (Minnikin et al., 1984).

Menaquinones were extracted as described by Tindall, 1990 and analysed by using an Agilent 1260 Infinity II HPLC system. The analytical column 125/2 Nucleosil 120-3 C<sub>18</sub> column (length 125 mm, diameter 2 mm, particle size 3 µm) was thermostatted at 35°C. An isocratic solvent system (acetonitrile/isopropanol, 65:35, v/v; 0.4 ml min<sup>-1</sup>) was used.

Fatty acids extraction was carried out for all the strains cited above following the protocol of Miller, 1982 and Kuykendall *et al.*, 1988. The fatty acid extracts were analysed using gas chromatography (Agilent 6890N instrument) and identified using the standard microbial identification (MIDI) system version 4.5 and the ACTIN 6 database (Sasser, 1990).

### 3.4 Results and discussion

Strain HST28<sup>T</sup> was able to grow on ISP1-5 (Table 8) and in a temperature range between 25-37°C as well as in a wide range of pH (6-11) and up to 10% (w/v) NaCl. Optimal growth of strain HST28<sup>T</sup> was observed on GYM medium at temperature 28°C, pH 8-9 and up to 10% (w/v) NaCl. The strain formed a pinkish white aerial mycelium with no diffusible pigment after incubation for 7 days at 28°C.

**Table 8.** Growth and cultural features of strain HST28<sup>T</sup> after 7 days of incubation at 28°C.

Medium	Growth	Substrate mycelium colour	Aerial mycelium colour
Tryptone-yeast extract agar (ISP1)	++	Strong yellow	Pale yellowish green
Yeast extract-malt extract agar (ISP 2)	+	Deep yellow	Pinkish white
Oatmeal agar (ISP 3)	++	Grayish green	Pale green
Inorganic salts-starch agar (ISP 4)	++	Strong yellowish brown	White
Glycerol-asparagine agar (ISP 5)	++	Moderate yellow	Yellowish white
Tyrosine agar (ISP 7)	++	Dark yellow	Greenish white
GYM (DSMZ 65)	+++	Dark brown	Pinkish white

Strain HST28<sup>T</sup> showed rectiflexible spore chains in section with hairy spore surfaces (Fig. 10) while the nearest phylogenetic neighbours, *S. kanamyceticus* DSM 40500<sup>T</sup> and *S. aureus* DSM 41758<sup>T</sup>, were identified by their smooth spore surface (Kampfer, 2012).

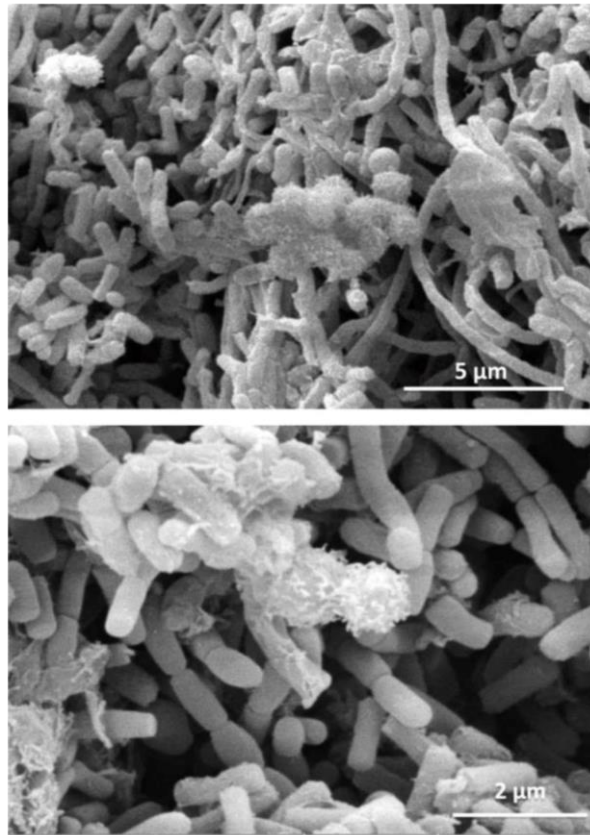


**Figure 10. Scanning electron micrograph of strain HST28<sup>T</sup>.** The micrograph shows the strain HST28<sup>T</sup> after incubation on GYM agar plates at 28°C for 14 days, showing “rectiflexible” spore chains section and spores with a hairy surface.

BLAST results of the complete 16S rRNA gene sequence of strain HST28<sup>T</sup> showed values of 99.0% (14 nt of difference) and 98.9% (16 nt of difference) of similarity to *S. kanamyceticus* NRRL B-2535<sup>T</sup> and *S. aureus* NRRL B-2808<sup>T</sup>, respectively. These results are in line with the phylogenetic position of strain HST28<sup>T</sup> in the 16S rRNA gene tree (Fig. 11) where it formed a distinct branch loosely associated to a well-supported clade housing the type strains of *S. aureus*, *Streptomyces durmitorensis* (Savic et al., 2007), *S. kanamyceticus*, *Streptomyces longisporoflavus* (Waksman and Lechevalier, 1953), *Streptomyces rectiviolaceus* (Gause et al., 1983) and *Streptomyces rosealbus* (Xu et al., 2005); the type strains of *S. aureus* and *S. kanamyceticus* appeared in the phylogenetic tree as the closest phylogenetic neighbours of strain HST28<sup>T</sup> (Fig. 11).

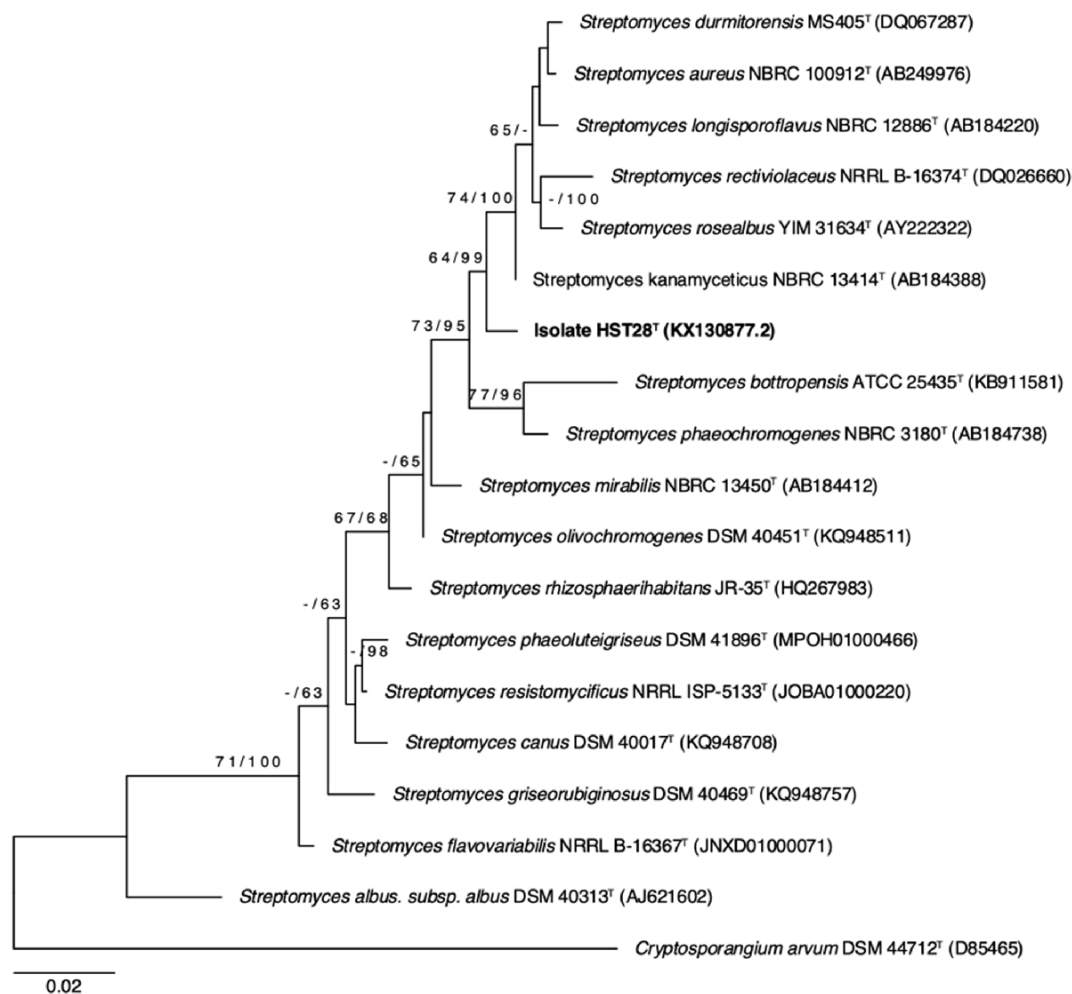


**Figure 11. Maximum-likelihood phylogenetic tree based on the 16S rRNA gene sequences showing the phylogenetic relationships between the isolate HST28<sup>T</sup> and its closest phylogenetic relatives.** The tree was inferred using the GTR+GAMMA model and rooted using the 16S rRNA sequence of *Cryptosporangium arzum* DSM 44712<sup>T</sup>. The branches were scaled in terms of the expected number of substitutions per site and the numbers above the nodes correspond to the support values for Maximum-likelihood (left) and Maximum-parsimony (right).

The resultant sequenced genome of the Strain HST28<sup>T</sup> showed a coverage of 78x with 468 contigs, a size of 8.6 Mb, 71.5 mol% as an in silico G+C content, 67 RNAs and 8211 coding sequences. Similarly, the type strains of *S. kanamyceticus* and *S. aureus* have genome sizes of 9.8Mb and 7.9Mb and in silico 71.0% and 71.8% G+C content, respectively. In silico genome analysis revealed the genetic potential of strain HST28<sup>T</sup> in producing new secondary metabolites well known by their antimicrobial and anticancer activities (Cortés-Albayay et al., 2019a).

The dDDH values between the draft genome sequences of strain HST28<sup>T</sup> and its closest relatives, *S. aureus* NRRL B-2808<sup>T</sup> (23.3% [21 - 25.8%]) and *S. kanamyceticus* NRRL B-2535<sup>T</sup> (31.0% [28.6 - 33.5%]), were well below the 70% cut-off point recommended for assigning prokaryotic strains to the same species (Wayne et al., 1987). These results are coherent with the corresponding ANI values of 79.3% and

85.6%, which are well below the threshold of 95-96% used to delineate prokaryotic species (Goris et al., 2007; Richter and Roselló-Móra, 2009; Chun and Rainey, 2014).

In the MLSA tree, the isolate HST28<sup>T</sup> formed a well-supported subclade closely related to the type strain of *S. kanamyceticus* and next to the *S. aureus* species (Fig. 12). The evolutionary genetic distances, based on the concatenated sequences, between strain HST28<sup>T</sup> and its closest neighbours cited above were above the threshold of 0.007 (Appx. 2) for the conspecific assignation (Rong and Huang, 2012, 2014).

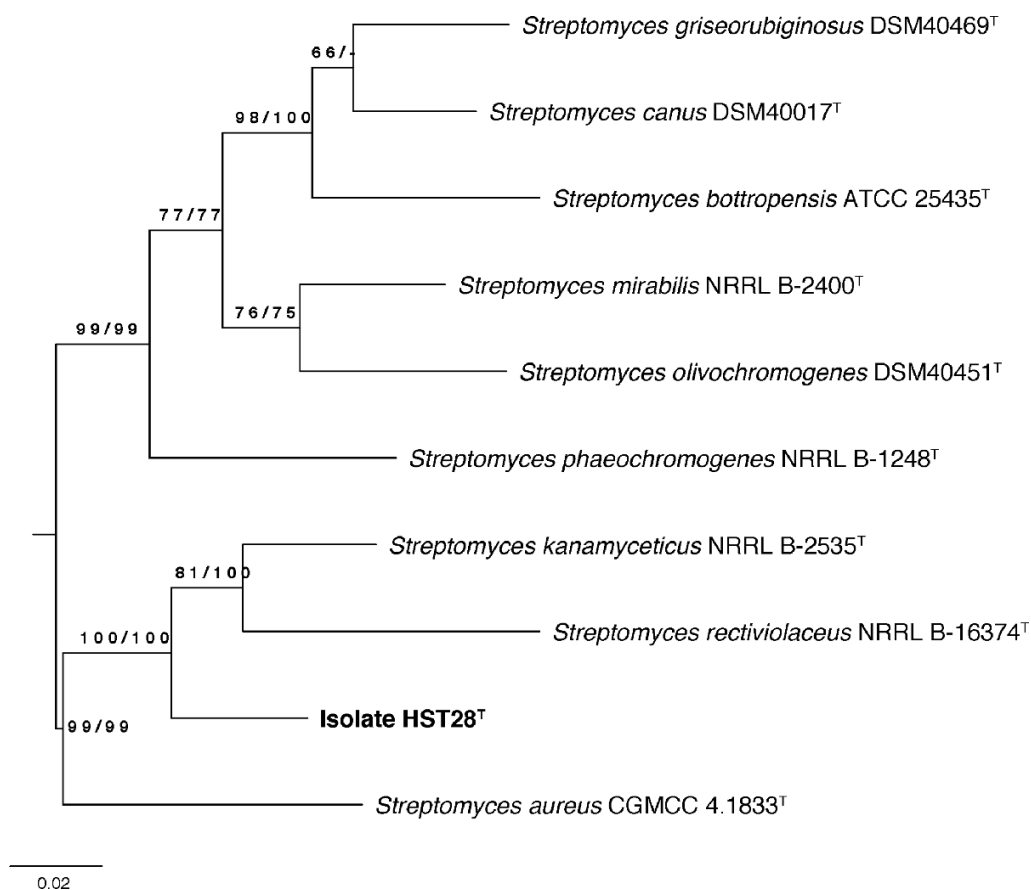


**Figure 12. Maximum-likelihood multilocus sequence analysis (MLSA) tree based on the concatenated partial sequences of five housekeeping genes: *atpD*; *gyrB*; *recA*; *rpoB* and *trpB*.** The tree was inferred using the GTR+GAMMA model and rooted by midpoint-rooting. The branches were scaled in terms of the expected number of substitutions per site and the numbers above the nodes correspond to the support values for Maximum-likelihood (left) and Maximum-parsimony (right).

Strain HST28<sup>T</sup> together with its closest phylogenetic neighbour, *S. kanamyceticus* DSM 40500<sup>T</sup>, were able to metabolise D-fructose, D-fructose-6-phosphate and myo-inositol (carbon sources); L-arginine and L-alanine (nitrogen sources); acetoacetic acid (organic acid); however, *S. kanamyceticus* DSM 40500<sup>T</sup> was able to oxidise a large

number of carbon and nitrogen substrates in addition to its tolerance to several inhibitory compounds unlike strain HST28<sup>T</sup> (Table 9).

The chemotaxonomic features of strain HST28<sup>T</sup> were in line with those of the genus *Streptomyces*. Whole-cell hydrolysates of the strain HST28<sup>T</sup> were rich in LL-A<sub>2</sub>pm and galactose, glucose, ribose and traces of arabinose and mannose as whole cell sugars. However, the type strain of *S. kanamyceticus* contained traces of mannose and xylose while *S. aureus* DSM 41785<sup>T</sup> lacks galactose and had traces of mannose.

The predominant isoprenologs for strain HST28<sup>T</sup> corresponded to hexahydrogenated menaquinones with nine isoprene units [MK-9(H<sub>6</sub>) (45%)] and octahydrogenated menaquinones with nine isoprene units [MK-9(H<sub>8</sub>) (34%)] (Table 8). The closest type strains *S. kanamyceticus* DSM 40500<sup>T</sup> and *S. aureus* DSM 41758<sup>T</sup> had the same major types than the strain HST28<sup>T</sup>, with the difference that MK-9(H<sub>8</sub>) was found to be the predominant isoprenolog (48 and 54% respectively) (Table 9).

**Table 9.** Phenotypic features that distinguish strain HST28<sup>T</sup> from its nearest phylogenetic neighbours *Streptomyces aureus* DSM 41785<sup>T</sup> and *Streptomyces kanamyceticus* DSM 40500<sup>T</sup>.

	HST28 <sup>T</sup>	<i>S. aureus</i> DSM 41785 <sup>T</sup>	<i>S. kanamyceticus</i> DSM 40500 <sup>T</sup>
<b>Carbon source utilization</b>			
α-D-lactose, D-galacturonic acid, D-maltose, D-salicin and N-acetyl-neuraminic acid	-	+	+
β-methyl-D-glucoside, D-fucose, D-raffinose, D-sorbitol, D-glucose-6-phosphate, inosine, N-acetyl-β-D-mannosamine, N-acetyl-D-galactosamine, pectin sucrose, turanose, stachyose and 3-O-methyl-D-glucose	-	-	+
D-arabitol, D-melibiose, L-fucose and L-rhamnose	-	w	+
D-fructose, D-fructose-6-phosphate and myo-inositol	+	-	+
<b>Aminoacids</b>			
D-aspartic acid, D-serine 1, D-serine 2 and L-serine	-	-	+
Gly-Pro and L-pyroglutamic acid	-	w	+
L-arginine and L-alanine	+	-	+
<b>Organic acids</b>			
Acetoacetic acid	+	-	+
Bromo-succinic acid	-	w	+
Butyric acid, citric acid, D-glucuronic acid, sodium formate, γ-amino-n-butyric acid and mucic acid	-	+	+
D-Lactic acid methyl ester, D-malic acid, L-lactic acid, p-hydroxy-phenylacetic acid and quinic acid	-	-	+
D-saccharic acid	-	w	+
Methyl pyruvate	+	w	w
<b>Inhibitory compounds</b>			
Guanidine hydrochloride	-	w	+



**Table 9. Continued**

	HST28 <sup>T</sup>	<i>S. aureus</i> DSM 41785 <sup>T</sup>	<i>S. kanamyceticus</i> DSM 40500 <sup>T</sup>
Lincomycin, rifamycin SV and sodium bromate	-	-	+
Minocycline and 1% sodium lactate	-	+	+
Potassium tellurite	+	-	+
<b>Isoprenologs pattern</b>	MK-9(H <sub>6</sub> ) 45%, MK-9(H <sub>8</sub> ) 34%, MK-9(H <sub>4</sub> ) 11%, MK-10 6% and MK-8(H <sub>2</sub> ) 4%	MK-9(H <sub>8</sub> ) 48%, MK-9(H <sub>6</sub> ) 26%, MK-9(H <sub>4</sub> ) 12%, MK-9(H <sub>2</sub> ) 4%, MK-10(H <sub>2</sub> ) 3%, MK-10 2%, MK-9 1% and MK-8(H <sub>4</sub> ) 1%	MK-9(H <sub>8</sub> ) 54%, MK-9(H <sub>6</sub> ) 20%, MK-9(H <sub>4</sub> ) 9%, MK-9(H <sub>2</sub> ) 4%, MK-10(H <sub>2</sub> ) 7%, MK-10 2%, MK-9 2% and MK-8(H <sub>4</sub> ) 2%

+ Positive reaction; -, negative reaction. All the strains oxidised D-glucose, D-mannose, D-galactose, trehalose, cellobiose, β-gentibiose, D-mannitol, glycerol, N-acetyl-D-glucosamine, Tween 40, dextrin and gelatin (carbon source); L-aspartic acid, L-glutamic acid and L-histidine (amino acids); acetic acid, α-hydroxy-butyric acid, α-ketobutyric acid, α-keto-glutaric acid, β-hydroxy-butyric acid, D-gluconic acid, L-malic acid and propionic acid (organic acids); and growth in presence of aztreonam, lithium chloride, nalidixic acid, tetrazolium blue (inhibitory compounds) and NaCl (1-8%w/v). In contrast none of the strains metabolised glucuronamide and L-galactonic acid- γ-lactone, and grew in presence of fusidic acid, Niaproof, tetrazolium violet, troleandomycin and vancomycin (inhibitory compounds).

The observed polar lipids in the Strain HST28<sup>T</sup> corresponded to phosphatidylethanolamine (PE), phosphatidylinositol (PI), aminolipid (AL), glycopospholipid (GPL) and unidentified lipid (L) (Fig. 13). The closest type strains showed these same polar lipids in addition to hydroxyphosphatidylethanolamine (OH-PE) and unidentified phospholipid (PL) in *S. aureus*; amino-glycophospholipid (AGPL) and glycolipids (GL) in *S. kanamyceticus*; phosphatidylmethyl-ethanolamine (PME) and diphosphatidylglycerol (DPG) in both type strains (Fig. 13).

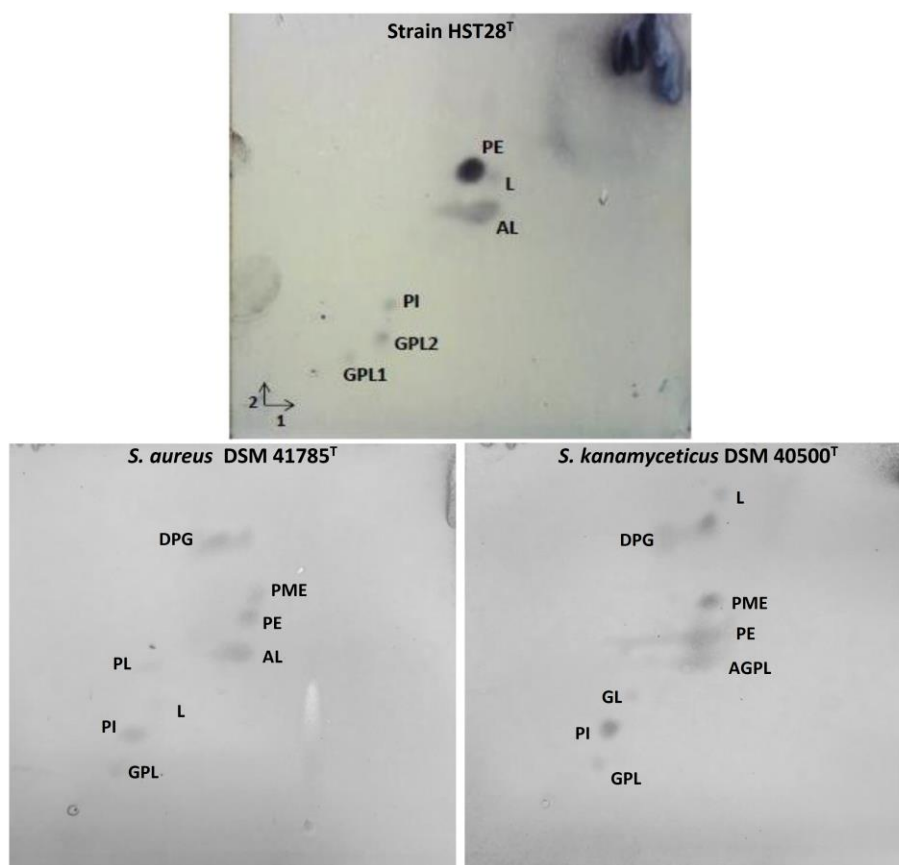


**Figure 13. Two-dimensional thin layer chromatography (TLC) for polar lipids extracted from strain HST28<sup>T</sup> and its closest relatives.** The plates were stained with molybdato-phosphoric acid to identify total lipid content. Key: PE, phosphatidylethanolamine; PI, phosphatidylinositol; GL, glycolipids, GPL, glycopospholipid; AL, aminolipid; L, unidentified lipid; AGPL, amino-glycophospholipid; PME, phosphatidylmethyl-ethanolamine; and DPG, diphosphatidylglycerol. >Solvent 1: chloroform: methanol: distilled water (65:25:4 by vol); ^Solvent 2: chloroform: glacial acetic acid: methanol: distilled water (80:12:15:4 by vol).

The major fatty acids (>15%) for strain HST28<sup>T</sup> and its nearest neighbour *S. kanamyceticus* DSM 40500<sup>T</sup>, had similar compositions [*C*<sub>15:0</sub> *anteiso* (~31.8%) and *C*<sub>17:0</sub> *anteiso* (~18.3%)], while the type strain of *S. aureus* DSM 41785<sup>T</sup> was characterized by the presence of *C*<sub>16:0</sub> *iso* (26.5%) and *C*<sub>15:0</sub> *anteiso* (20.8%) (Table 10).

**Table 10.** Fatty acid profiles for strain HST28<sup>T</sup> and its closest relatives.

Fatty acids	Abundance (%)		
	Strain HST28 <sup>T</sup>	<i>S. kanamyceticus</i> DSM 40500 <sup>T</sup>	<i>S. aureus</i> DSM 41785 <sup>T</sup>
C <sub>11:0</sub> <i>iso</i>	0.4	-	-
C <sub>13:0</sub> <i>iso</i>	0.2	0.2	0.3
C <sub>13:0</sub> <i>anteiso</i>	0.2	0.2	0.3
C <sub>14:0</sub> <i>iso</i>	1.2	1.4	7.7
C <sub>14:0</sub>	0.3	0.3	0.3
C <sub>15:0</sub> <i>iso</i>	8.2	9.3	10.7
C <sub>15:0</sub> <i>anteiso</i>	31.8	31.7	20.8
C <sub>15:0</sub>	1.0	1.1	3.2
C <sub>16:1</sub> <i>iso</i> H	1.6	0.7	3.1
C <sub>16:0</sub> <i>iso</i>	10.1	11.3	26.5
C <sub>16:1</sub> <i>cis</i> 9	3.3	2.0	0.9
C <sub>16:0</sub>	4.97	9.3	4.1
C <sub>16:0</sub> 9? methyl	4.3	2.0	2.4
C <sub>17:1</sub> <i>anteiso</i> C	8.1	2.1	1.7
C <sub>17:0</sub> <i>iso</i>	4.1	8.1	5.4
C <sub>17:0</sub> <i>anteiso</i>	18.3	18.7	9.0
C <sub>17:1</sub> <i>cis</i> 9	0.4	0.3	0.5
C <sub>17:0</sub> <i>cyclo</i>	0.7	1.0	0.7
C <sub>17:0</sub>	0.3	0.5	0.8

### 3.5 Description of *Streptomyces huasconensis* sp. nov.

*Streptomyces huasconensis* (hu.as.co.nen'sis. N.L. masc. adj. huasconensis referring to the site, Salar de Huasco, where the strain was isolated).

Aerobic, Gram-stain-positive actinobacterium producing a pinkish-white aerial mycelium on GYM agar plates after 7 days at 28 °C. Optimal growth of strain HST28<sup>T</sup> is obtained at 28°C, pH 8-9 and up to 10% (w/v) NaCl. It was able to metabolise D-fructose, D-fructose-6-phosphate and myo-inositol (carbon sources); L-arginine and L-alanine (nitrogen sources); acetoacetic acid (organic acid) and to grow in the presence of aztreonam, lithium chloride, nalidixic acid and tetrazolium blue. It is characterised by LL-diaminopimelic acid in its peptidoglycan layer and galactose, glucose, ribose and traces of arabinose and mannose as whole-cell sugars; the polar lipid profile contains phosphatidylmethylethanolamine, phosphatidylinositol, aminolipid, glycopospholipid

and an unidentified lipid. MK-9(H<sub>6</sub>), MK-9(H<sub>8</sub>) and MK-9(H<sub>4</sub>) are the predominating isoprenologs. The fatty acid profile contains major amounts of C<sub>15:0</sub> *anteiso*, C<sub>16:0</sub> *iso* and C<sub>17:0</sub> *anteiso*.

The genome size is 8.6Mb with an in silico G+C content of 71.5 mol%. The type strain, HST28<sup>T</sup> (DSM 107268<sup>T</sup>=CECT 9648<sup>T</sup>), was isolated from hyper arid soil of Salar de Huasco in the Atacama Desert, Chile.

### 3.6 Conclusion

The resultant phenotypic, genetic and genomic data of the strain HST28<sup>T</sup> allowed to distinguish this isolate from its nearest phylogenetic neighbours and form a new taxonomic centre within the evolution of the genus *Streptomyces*. Therefore it merits the recognition as a new species, namely *Streptomyces huasconensis* sp. nov.

# Chapter 4

## Taxonomic description of the new species *Streptomyces altiplanensis* HST21<sup>T</sup>

### Objectives

- 3 To describe taxonomically the putative novel *Streptomyces* species by a polyphasic approach.

### 4.1 Abstract

A polyphasic approach was used for evaluating the taxonomic status of strain HST21<sup>T</sup> isolated from, Salar de Huasco, in the Atacama Desert. The 16S rRNA gene and multi-locus sequence phylogenetic analyses assigned strain HST21<sup>T</sup> to the genus *Streptomyces* with *Streptomyces albidochromogenes* DSM 41800<sup>T</sup> and *Streptomyces flavidovirens* DSM 40150<sup>T</sup> as the nearest neighbours. Digital DNA-DNA hybridization (dDDH) and average nucleotide identity (ANI) between the genome sequences of strain HST21<sup>T</sup> and *S. albidochromogenes* DSM 41800<sup>T</sup> (35.6% and 88.2%) and *S. flavidovirens* DSM 40105<sup>T</sup> (47.2% and 88.8%) were below the thresholds of 70% and 95-96% for prokaryotic conspecific assignment. Phenotypic, chemotaxonomic and genetic results distinguish strain HST21<sup>T</sup> from its closest neighbours. Strain HST21<sup>T</sup> is characterised by the presence of LL-diaminopimelic acid in its peptidoglycan layer; glucose and ribose as whole cell sugars; diphosphatidylglycerol (DPG), hydroxy-phosphatidylethanolamine (OH-PE), phosphatidylethanolamine (PE), phosphatidylinositol (PI), glycopospholipids (GPL1-2), unknown lipids (L1-2) and

phospholipids (PL1-2) as polar lipids; C<sub>15:0</sub> *anteiso* (21.6%) and C<sub>17:0</sub> *anteiso* (20.5%) as major fatty acids (>15%). Based on these results, strain HST21<sup>T</sup> merits the recognition as a novel species for which the name *Streptomyces altiplanensis* sp. nov. is proposed. The type strain is HST21<sup>T</sup> = DSM 107267<sup>T</sup> = CECT 9647<sup>T</sup>.

While analysing the phylogeny of the strain HST21<sup>T</sup>, *Streptomyces chryseus* DSM 40420<sup>T</sup> and *Streptomyces helveticus* DSM 40431<sup>T</sup> found to have 100% 16S rRNA gene sequence similarity with dDDH and ANI values of 95.3% and 99.4%, respectively. Therefore, *S. helveticus* is considered as a later heterotypic synonym of *S. chryseus* and consequently, description of *S. chryseus* was emended.

## 4.2 Introduction

Members of the genus *Streptomyces* (Waksman and Henrici, 1945; Witt and Stackebrandt, 1990) of the family *Streptomycetaceae* (Kim et al., 2003; Zhi et al., 2009) are well known as a preeminent source of secondary metabolites and antibiotic production (Watve et al., 2001). This taxon encompasses Gram-positive, aerobic and heterotrophic microorganisms with extensive branched substrate and aerial mycelia (Angert, 2005). Over 800 *Streptomyces* species have been validly named and characterised by the presence of LL-diaminopimelic acid (A<sub>2</sub>pm) in their peptidoglycan layer; diphosphatidylglycerol, phosphatidylethanolamine, phosphatidylinositol and phosphatidylinositol mannosides as major polar lipids; saturated *iso*- and *anteiso*-fatty acids as the major fatty acids; *hexa*- and *octa*- hydrogenated menaquinones with nine isoprene units as predominant isoprenologs (Kroppenstedt, 1985; Kampfer, 2012) and a G+C content range between 69-78 mol%. The genus *Streptomyces* is widely distributed in various ecosystems, such as soil, fresh and marine waters and clinical samples (Kapadia et al., 2007) and they are also found in extreme or poly-extreme environments, (Hong et al., 2009; Tiwari and Gupta, 2012; Guo et al., 2015). In this context and during our investigation of *Streptomyces* biodiversity in poly-extreme high altitude saline wetland (3800 m.a.s.l) of the Atacama Desert, *Streptomyces* strain HST21<sup>T</sup> was isolated and characterised (Cortés-Albayay et al., 2019 a,b; Dorador et al., 2009) based on polyphasic taxonomic approach. The isolate HST21<sup>T</sup> was found to be a new species within the evolutionary radiation of the genus *Streptomyces* for which the name *Streptomyces altiplanensis* sp. nov. is proposed.

## 4.3 Materials and Methods

### 4.3.1 Isolation, culture and maintenance

*Streptomyces* strain HST21<sup>T</sup> was isolated from arid soil samples location (site H6) in the Salar de Huasco (Cortés-Albayay et al., 2019a) of the Atacama Desert. The characteristic of site H6 and the isolation procedures were carried out as described by Cortés-Albayay *et al.*, 2019 a,b. Isolate HST21<sup>T</sup> was maintained on GYM (DSMZ; Medium 65) agar plates, for 10 days of incubation at 28°C, together with its closest phylogenetic relatives, *Streptomyces albidochromogenes* DSM 41800<sup>T</sup> (Gause et al.,

1983), *Streptomyces flavidovirens* DSM 40150<sup>T</sup> (Kudrina, 1957; Pridham, 1958), *Streptomyces chryseus* DSM 40420<sup>T</sup> (Pridham, 1958; Krasil'nikov et al., 1965), and *Streptomyces helveticus* DSM 40431<sup>T</sup> (Pridham, 1958; Krasil'nikov et al., 1965), which were obtained from the DSMZ German culture collection (<https://www.dsmz.de/>). All strains were preserved in 25% v/v glycerol at -80°C.

### 4.3.2 Phenotypic characterization

Cultural properties of strain HST21<sup>T</sup> were examined using different agar media: International *Streptomyces* Project [ISP1-7] (Shirling and Gottlieb, 1966) and GYM (DSMZ medium 65). A range of temperatures of 4°C, 10°C, 15°C, 25°C, 28°C, 37°C and 45°C as well as pH ranges from 6 to 12 were tested on HST21<sup>T</sup> culture using GYM media.

The ability of strain HST21<sup>T</sup> to use different carbon and nitrogen sources and to grow in presence of inhibitory compounds was examined using GENIII microplates in an Omnilog device (BIOLOG Inc., Haywood, USA). The type strains *S. albidochromogenes* and *S. flavidovirens* species were included in this test, which was carried out in duplicate. Opm package for R (Vaas et al., 2012, 2013) version 1.06 was used to analyse the resultant data.

### 4.3.3 Scanning Electron Microscope

A field-emission scanning electron microscope (Tescan Vega 3 LMU: Tescan, Wellbrook Court, Girton, Cambridge, CB3 0NA) was used to describe the spore chain ornamentation and spore surface morphology of strain HST21<sup>T</sup> grown for 10 days on GYM media at 28°C.

### 4.3.4 Phylogenetic analysis

The genomic DNA extraction of strain HST21<sup>T</sup> and 16S rDNA-PCR amplification were carried out as described by Cortés-Albayay *et al.*, 2019b. The retrieval of the nearest phylogenetic neighbours of strain HST21<sup>T</sup> was performed following the alignment of the complete 16S rRNA gene sequence (1517 bp; accession number KX130868) of isolate HST21<sup>T</sup> against those available in the EzTaxon database (Yoon et al., 2017). The phylogenetic trees were inferred from the DSMZ phylogenomics pipeline (Meier-Kolthoff et al., 2014) available at the Genome-to-Genome distance calculator (GGDC) web server (Meier-Kolthoff et al., 2013a) (<http://ggdc.dsmz.de/>). Pairwise sequence similarities of 16S rRNA gene were estimated based on the method of Meier-Kolthoff *et al.*, 2013. MUSCLE (Edgar, 2004) program was used for multiple sequence alignments. RAXML (Stamatakis, 2014) and TNT (Goloboff et al., 2008) were used for

the construction of Maximum-likelihood (ML) (Felsenstein, 1981) and Maximum-parsimony (MP) phylogenetic trees (Fitch, 1971), respectively. A rapid bootstrapping method together with the autoMRE bootstopping criterion (Pattengale et al., 2010) was used for the resultant ML tree. However the resultant best topology of the MP tree was obtained based on a combination of the bootstrapping method with 1000 iterations with a tree-bisection-and-reconnection branch swapping method in addition to the use of ten additional random sequence replicates. The X2 test of the PAUP program (Swofford, 2002) was used to check the sequences for a compositional bias. All the trees were rooted using the type species of the genus, *Cryptosporangium arvum* DSM 44712<sup>T</sup> (Waksman and Henrici, 1945; Tamura et al., 1998).

Multi locus sequence analyses (MLSA) was carried out based on five partial housekeeping gene sequences, *atpD* (ATP synthase F1, beta subunit), *gyrB* (DNA gyrase B subunit), *rpoB* (RNA polymerase beta subunit), *recA* (recombinase A) and *trpB* (tryptophane B, beta subunit) (Busarakam et al., 2014; Labeda, 2016; Labeda et al., 2017; Idris et al., 2017). All the genes of strain HST21<sup>T</sup> were taken from the draft genome sequence (accession number RHMC00000000) and those of the reference strains were retrieved from the ARS Microbial Genome Sequence (<http://199.133.98.43>) and the GenBank databases (Table 11). A ML phylogenetic tree was inferred using the DSMZ phylogenomics pipeline cited above while the neighbour joining tree was constructed using the MEGA software version 7 and the Kimura 2-parameter (Kimura, 1980) was used to estimate the genetic distance between the loci of strain HST21<sup>T</sup> and its closest phylogenetic neighbours.

#### 4.3.5 Genome sequencing, dDDH and ANI calculations

The genomic DNA of strain HST21<sup>T</sup> was sequenced using Ion Torrent PGM (Personal Genome Machine) sequencer technology as described by Cortés-Albayay *et al.*, 2019b while the *S. albidochromogenes* DSM 41800<sup>T</sup>, *S. chryseus* DSM 40420<sup>T</sup> and *S. helveticus* DSM 40431<sup>T</sup> genomes were sequenced using Illumina next-generation sequencing technology (MicrobesNG, Birmingham, UK). The RAST server (Aziz et al., 2008; Overbeek et al., 2014) was used for annotation of these genome sequences.

The GGDC server with the recommended formula 2 (Meier-Kolthoff et al., 2013b) was used to estimate the digital DNA:DNA hybridization (dDDH) between the draft genome sequence of strain HST21<sup>T</sup> and its closest phylogenetic relatives, *S. albidochromogenes* DSM 41800<sup>T</sup>, *S. chryseus* DSM 40420<sup>T</sup>, *S. flavidovirens* DSM 40105<sup>T</sup> and *S. helveticus* DSM 40431<sup>T</sup>. The OrthoANIu algorithm of the ANI Calculator (Lee et al., 2016; Yoon et al., 2017) was used to calculate the average nucleotide identity (ANI) values between the strains cited above.



**Table 11.** Accession numbers of the sequences used for the MLST analysis in the present study.

Species	Type strain	Genome	Genebank accession number				
			<i>trpB</i>	<i>atpD</i>	<i>gyrB</i>	<i>rpoB</i>	<i>recA</i>
<i>Streptomyces altiplanensis</i>	HST21 <sup>T</sup>	RHMC00000000	-	-	-	-	-
<i>Streptomyces flavidovirens</i>	DSM 40150 <sup>T</sup>	AUBE00000000	-	-	-	-	-
<i>Streptomyces albidochromogenes</i>	DSM 41800 <sup>T</sup>	VBVX00000000	-	-	-	-	-
<i>Streptomyces helveticus</i>	DSM 40431 <sup>T</sup>	VBVY00000000	-	-	-	-	-
<i>Streptomyces chryseus</i>	DSM 40420 <sup>T</sup>	VBVW00000000	-	-	-	-	-
<i>Streptomyces violaceorectus</i>	NRRL B-1218 <sup>T</sup>	-	KT389419	KT384750	KT385098	KT389070	KT385452
<i>Streptomyces xanthochromogenes</i>	NRRL B-5410 <sup>T</sup>	-	KT389432	KT384763	KU721027	KT389083	KT385465
<i>Streptomyces cyaneofuscatus</i>	CGMCC 4.1612 <sup>T</sup>	-	EF055143	EF031291	EF054980	EF055088	EF055033
<i>Streptomyces anulatus</i>	NRRL B-2000 <sup>T</sup>	-	EF055137	EF031285	KT384816	EF055082	EF055027
<i>Streptomyces mauvecolor</i>	NRRL B-24302 <sup>T</sup>	-	KT389307	KT384638	KT384987	KT388958	KT385338
<i>Streptomyces hypolithicus</i>	NRRL B-24669 <sup>T</sup>	-	KT389268	KT384599	KT384948	KT388919	KT385297
<i>Streptomyces litmocidini</i>	NRRL B-3635 <sup>T</sup>	-	KT389294	KT384625	KT384974	KT388945	KT385325
<i>Streptomyces puniceus</i>	NRRL ISP-5083 <sup>T</sup>	-	EF661808	EF031273	EF661745	EF055070	EF661766
<i>Streptomyces hundertgensis</i>	BH38 <sup>T</sup>	CP032698	-	-	-	-	-
<i>Streptomyces laurentii</i>	ATCC 31255 <sup>T</sup>	AP017424	-	-	-	-	-
<i>Streptomyces gelaticus</i>	CGMCC 4.1444 <sup>T</sup>	-	EF661799	EF661715	HQ823589	EF661778	EF661757
<i>Streptomyces albus</i> subsp. <i>albus</i>	NRRL B-1811 <sup>T</sup>	JODR01000001	-	-	-	-	-

### 4.3.6 Chemotaxonomy methods

Standard procedures for chemotaxonomic analyses were used to characterise strains HST21<sup>T</sup>, *S. albidochromogenes* DSM 41800<sup>T</sup> and *S. flavidovirens* DSM 40150<sup>T</sup>. Diaminopimelic acids isomers (Staneck and Roberts, 1974), whole-cell sugars (Lechevalier and Lechevalier, 1970), polar lipids profiles (Minnikin et al., 1984) and menaquinones (Tindall, 1990) were determined using freeze dried cells obtained following the same procedure of Cortés-Albayay *et al.*, 2019b. The menaquinones were analysed using an Agilent 1260 Infinity II high performance liquid chromatography (HPLC) system with. 125/2 Nucleosil 120-3 C<sub>18</sub> column (length 125 mm, diameter 2 mm, particle size 3µm) and an isocratic solvent system (acetonitrile/isopropanol, 65:35, v/v; 0.4 ml/min). Fatty acids analyses were performed for strain HST21<sup>T</sup> and all the reference strains cited above, following the protocols of Miller, 1982 and Kuykendall *et al.*, 1988 and using a gas chromatography (Agilent 6890 N) instrument. The extracts were identified using the standard microbial identification (MIDI) system Version 4.5 and the ACTIN 6 database (Sasser, 1990).

## 4.4 Results and discussion

Strain HST21<sup>T</sup> was able to grow in all the tested media but with moderate growth on ISP2. Growth was detected after 10 days of incubation at 28°C and 37°C, pH from 7 to 11. It formed a white aerial mycelium and brownish substrate mycelia with diffusible pigment after 10 days of incubation at 28°C on GYM medium. More details about the cultural characteristics of strain HST21<sup>T</sup> were given in Table 12.

**Table 12.** Growth and cultural features of strain HST21<sup>T</sup> after 10 days of incubation at 28°C.

Medium	Growth	Substrate mycelium colour	Aerial mycelium colour	Diffusible pigments
Tryptone-yeast extract agar (ISP1)	++	Deep reddish brown	Dark brown	Strong reddish brown
Yeast extract-malt extract agar (ISP 2)	+	White	White	-
Oatmeal agar (ISP 3)	+++	-	White	Deep reddish brown
Inorganic salts-starch agar (ISP 4)	++	Dark grayish yellow	Light grayish olive	Vivid greenish yellow
Glycerol-asparagine agar (ISP 5)	++	Light olive brown	Strong yellowish brown	Strong yellow
Tyrosine agar (ISP 7)	++	Dark yellowish brown	Light olive brown	Dark Yellow
GYM (DSMZ 65)	+++	Strong brown	White	Deep reddish brown

It is characterised by the presence of rectiflexible spore chains in section with spiny spore surfaces (Fig. 14) while *S. albidochromogenes* DSM 41800<sup>T</sup> and *S. flavidovirens* DSM 40150<sup>T</sup>, the nearest phylogenetic neighbours, have spiral and rectiflexible spore chains with a smooth spore surface, respectively (Kampfer, 2012).

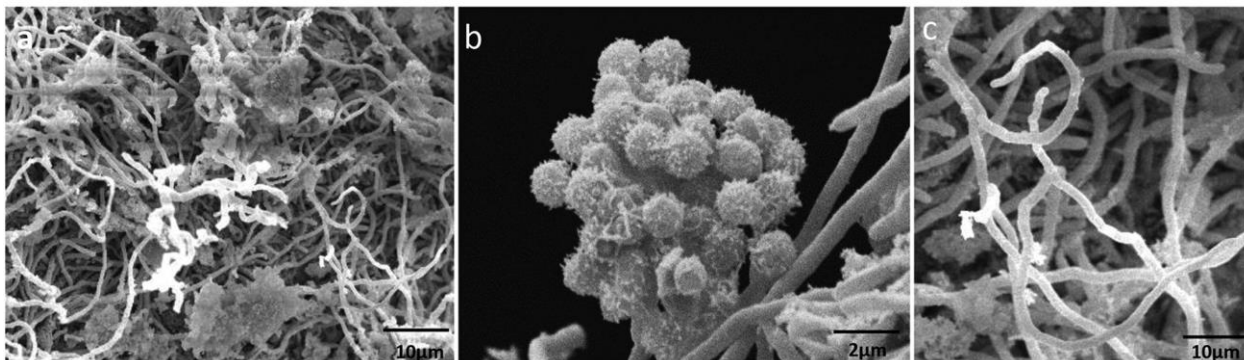


**Figure. 14. Scanning electron micrograph of strain HST21<sup>T</sup>.** The micrograph showed “rectiflexible” spore chains in section and spores with a spiny surface, after incubation on GYM agar plates at 28°C.

Strain HST21<sup>T</sup> could be distinguished from its relatives cited above by its ability to metabolise rhamnose (carbon source) and quinic acid (organic acid) (Table 13) while strain DSM 40150<sup>T</sup> was able to oxidise D-fucose, N-acetyl-D-galactosamine, D-melibiose and methyl pyruvate (carbon sources), D-lactic acid methyl ester, L-galactonic acid-γ-lactone and L-lactic acid (organic acids). However strain DSM 41800<sup>T</sup> could use N-acetyl-neuraminic acid (organic acid), D-serine 2 and L-serine (Table 13). In addition, HST21<sup>T</sup> like its closest neighbour *S. flavidovirens* DSM 40150<sup>T</sup>, has MK-9(H<sub>6</sub>) and MK-9(H<sub>8</sub>) as the predominant menaquinones (>20%) while *S. albidochromogenes* DSM 41800<sup>T</sup> has MK-9(H<sub>8</sub>) (Table 13).

**Table 13.** Phenotypic features that distinguish strain HST21<sup>T</sup> from its nearest phylogenetic neighbours *S. albidochromogenes* DSM 41800<sup>T</sup> and *S. flavidovirens* DSM 40150<sup>T</sup>.

	Strain HST21 <sup>T</sup>	<i>S. albidochromogenes</i> DSM 41800 <sup>T</sup>	<i>S. flavidovirens</i> DSM 40150 <sup>T</sup>
<b>Carbon utilization</b>			
D-arabitol, D-fructose, α-D-lactose, <i>myo</i> -inositol, D-mannitol, D-raffinose, pectin, stachyose and turanose	+	-	+
D-fucose, N-Acetyl-D-galactosamine and D-melibiose	-	-	+
L-rhamnose	+	-	-
Methyl pyruvate	-	-	+
<b>Aminoacids</b>			
D-Serine 2, L-Serine	-	+	-
Glycine-proline	+	+	-
<b>Organic Acids</b>			
Bromo-succinic acid, citric acid and l-pyroglutamic acid	+	-	+
D-lactic acid methyl ester, L-galactonic acid-γ-lactone and L-lactic acid	-	-	+
D-malic acid and sodium formate	+	+	-
N-acetyl-neuraminic acid	-	+	-
Quinic acid	+	-	-
<b>Inhibitory compounds</b>			
Rifamycin sv, 1% sodium lactate	+	+	-
8% NaCl	+	-	-

**Table 13. Continued**

	<b>Strain HST21<sup>T</sup></b>	<b><i>S. albidochromogenes</i> DSM 41800<sup>T</sup></b>	<b><i>S. flavidovirens</i> DSM 40150<sup>T</sup></b>
<b>Isoprenologs pattern</b>	MK-9(H <sub>6</sub> ) 26%, MK-9(H <sub>8</sub> ) 25%, MK-9(H <sub>4</sub> ) 8%, MK-7(H <sub>2</sub> ) 8%, MK-8(H <sub>2</sub> ) 6%, MK-9(H <sub>2</sub> ) 3%, MK-10 2%	MK-9(H <sub>8</sub> ) 76%, MK-9(H <sub>6</sub> ) 7%, MK-9(H <sub>4</sub> ) 7%, MK-9(H <sub>2</sub> ) 6%, MK-10(H <sub>2</sub> ) 1%	MK-9(H <sub>8</sub> ) 52%, MK-9(H <sub>6</sub> ) 22%, MK- 9(H <sub>4</sub> ) 11%, MK-9(H <sub>2</sub> ) 9%, MK-10(H <sub>2</sub> ) 3%, MK-8(H <sub>4</sub> ) 2%, MK-9 1%

+, Positive reaction; -, negative reaction. All the strains were able to metabolise dextrin, D-maltose, L-fucose, D-trehalose, N-acetyl-β-D-mannosamine, D-cellobiose, β-gentobiose, methyl-β-D-glucoside, D-salicin, N-acetyl-D-glucosamine, D-glucose, D-mannose, D-galactose, inosine, glycerol, D-glucose-6-phosphate, D-fructose-6-phosphate, gelatin and sucrose (carbon source); L-arginine, L-alanine, L-aspartic acid, L-glutamic acid and L-histidine (aminoacids); butyric acid, β-hydroxy-butyric acid, D-gluconic acid, α-keto glutaric acid, L-malic acid, γ-amino-n-butyric acid, α-hydroxy-butyric acid, α-keto-butyric acid, acetoacetic acid, propionic acid and acetic acid (organic acids); to grow in presence of aztreonam, nalidixic acid, lithium chloride, potassium tellurite, sodium bromate and tween 40 (inhibitory compounds); and at 1-4% (w/v) NaCl and pH 6-8. In contrast none of the strains used D-sorbitol, 3-O-methyl-D-glucose and glucuronamide (carbon source); D-aspartic acid and D-serine 1 (aminoacids); D-glucuronic acid, D-galacturonic acid, p-hydroxy-phenylacetic acid, D-saccharic acid and mucic acid (organic acids); and were unable to grow in presence of guanidine hydrochloride, tetrazolium blue and violet, troleandomycin, vancomycin, minocycline, lincomycin, Niaproof, fusidic acid and pH 5.

Whole-cell hydrolysates of strain HST21<sup>T</sup> were rich in LL-diaminopimelic acid, glucose, and ribose as whole-cell sugars while the type strains of *S. albidochromogenes* and *S. flavidovirens* have in addition mannose. Strain HST21<sup>T</sup> contained, in its polar lipid profile, diphosphatidylglycerol (DPG), hydroxy-phosphatidylethanolamine (OH-PE), phosphatidylethanolamine (PE), phosphatidylinositol (PI), glycopospholipids (GPL1-2), unknown lipids (L1-2) and phospholipids (PL1-2). The same profile was obtained for *S. flavidovirens* DSM 40150<sup>T</sup> and *S. albidochromogenes* DSM 41800<sup>T</sup> but devoid of OH-PE (Fig. 15) and with unidentified aminolipids (AL1-2) and glycolipids (GL1-4) for strain DSM 41800<sup>T</sup>. *S. chryseus* DSM 40420<sup>T</sup> and *S. helveticus* DSM 40431<sup>T</sup> contained DPG, PE, PI, GPL as major polar lipids, but only strain DSM 40420<sup>T</sup> had PME and PL while strain DSM 40431<sup>T</sup> showed unknown aminolipids (Fig. 15).

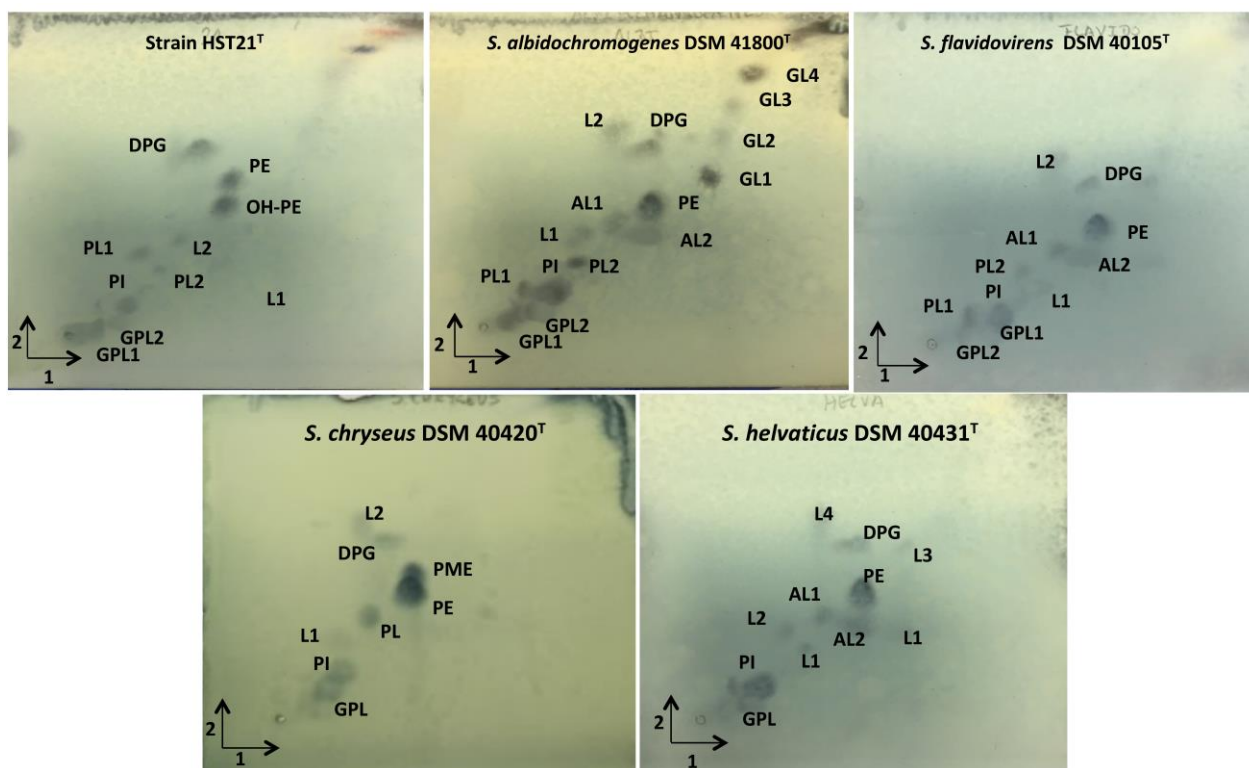


**Figure 15. Two-dimensional thin layer chromatography (TLC) for polar lipids extracted from strain HST21<sup>T</sup> and its closest type strains.** The TLC plates were stained with molybdotophosphoric acid to identify total lipid content. Key: DPG, diphosphatidylglycerol; PE, phosphatidylethanolamine; PME, phosphatidylmethyl-ethanolamine; PI, phosphatidylinositol; GPL, glycopospholipid; AL1-2, aminolipids, AGPL, amino-glycopospholipid; GL1-4, glycolipids and L1-2, lipids and PL1-4, phospholipids. >Solvent (1): chloroform: methanol: distilled water (65:25:4); ^Solvent (2): chloroform: glacial acetic acid: methanol: distilled water (80:12:15:4).

Similarly to its close phylogenetic relatives; C<sub>15:0 anteiso</sub> (21.6%) and C<sub>17:0 anteiso</sub> (20.5%) were detected as the major fatty acids (>15%) of strain HST21<sup>T</sup>; However its nearest relatives *S. flavidovirens* DSM 40150<sup>T</sup> and *S. albidochromogenes* DSM 41800<sup>T</sup> had C<sub>15:0 anteiso</sub> (38.7%) and C<sub>15:0 anteiso</sub> (27.0%) and C<sub>16:0</sub> (16.0%), respectively (Table 14). While the major fatty acids for strains *S. chryseus* DSM 40420<sup>T</sup>

and *S. helvaticus* DSM 40431<sup>T</sup> were C<sub>15:0</sub> *anteiso* (19.9%) and C<sub>16:0</sub> *iso* (19.3%) (Table 14).

**Table 14.** Fatty acid profiles for strain HST21<sup>T</sup> and its closest phylogenetic relatives.

Fatty acids	Abundance (%)				
	Strain HST21 <sup>T</sup>	<i>S. albidochromogenes</i> DSM 41800 <sup>T</sup>	<i>S. flavidovirens</i> DSM 40150 <sup>T</sup>	<i>S. chryseus</i> DSM 40420 <sup>T</sup>	<i>S. helvaticus</i> DSM 40431 <sup>T</sup>
C <sub>15:0</sub> <i>iso</i>	7.0	8.6	5.6	8.6	4.4
C <sub>15:0</sub> <i>anteiso</i>	21.6	26.9	38.7	19.9	23.5
C <sub>16:0</sub> <i>iso</i>	8.7	15.7	13.9	19.3	18.3
C <sub>16:1</sub> <i>cis</i> 9	10.4	7.5	4.6	6.9	7.3
C <sub>16:0</sub>	8.5	9.4	6.0	5.7	6.0
C <sub>16:0</sub> methyl 9	6.1	-	-	5.9	4.23
C <sub>17:1</sub> <i>anteiso</i> C	7.4	2.6	4.6	4.0	6.0
C <sub>17:0</sub> <i>anteiso</i>	20.5	10.5	11.4	12.5	14.9

Strain HST21<sup>T</sup> showed 16S rRNA gene sequence similarity values of 99.2% with *S. albidochromogenes* NBRC 101003<sup>T</sup> (12 nt of difference) and *S. flavidovirens* NBRC 13039<sup>T</sup> (12 nt of difference) and 99.1% with *S. chryseus* NRRL B-12347<sup>T</sup> (13 nt of difference) and *S. helvaticus* NBRC 13382<sup>T</sup> (13 nt of difference). These results were reflected in the 16S rRNA phylogenetic tree (Fig. 16), where strain HST21<sup>T</sup> formed together with all the strains cited above a well-supported clade next to *Streptomyces hypolithicus* HSM10<sup>T</sup> (Le Roes-Hill et al., 2009) (Fig. 16).

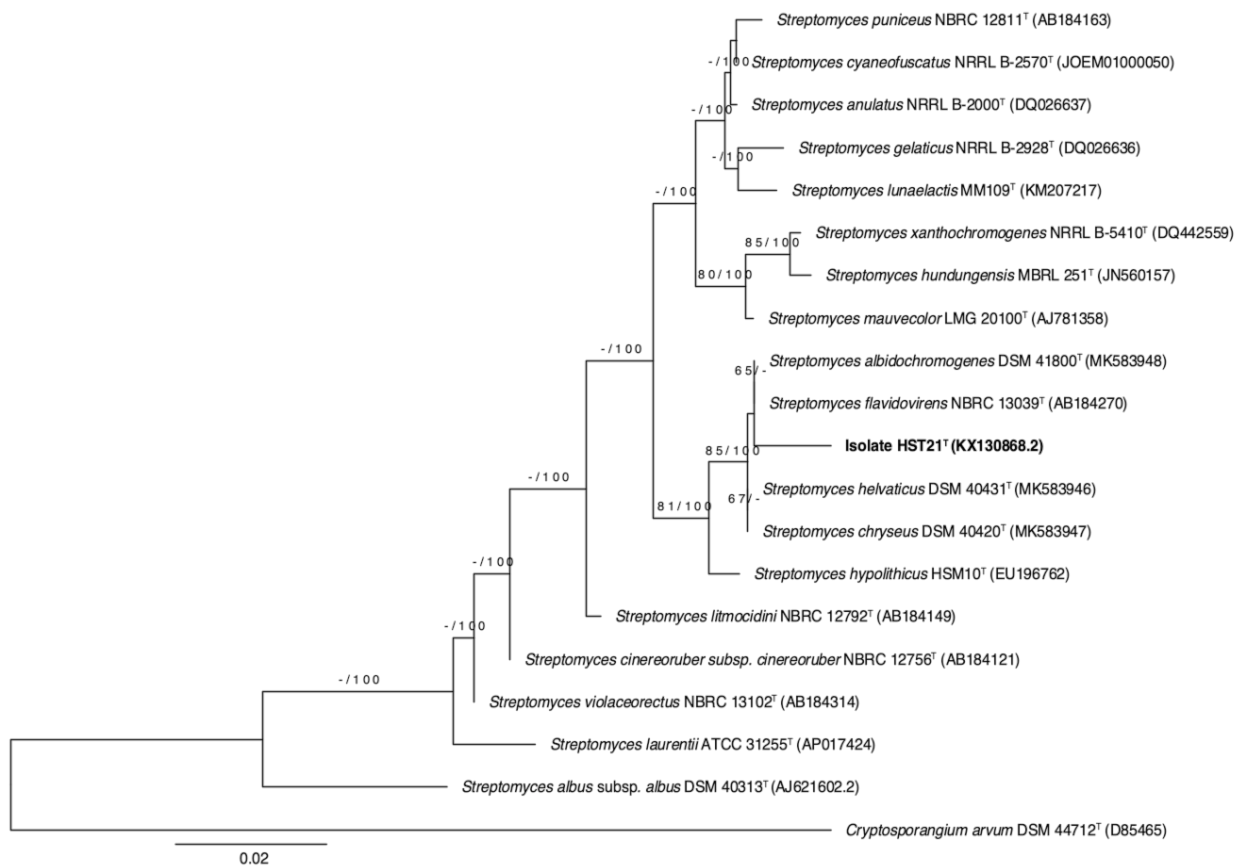


**Figure 16. Maximum-likelihood phylogenetic tree based on almost complete 16S rRNA gene sequences showing the phylogenetic relationship between strain HST21<sup>T</sup> and its relatives within the genus *Streptomyces*.** The numbers above the branches are bootstrap support values greater than 60% for maximum-likelihood (left) and maximum-parsimony (right).

The phylogenetic position of *S. albidochromogenes* NBRC 101003<sup>T</sup>, *S. chryseus* NRRL B-12347<sup>T</sup>, *S. flavidovirens* NBRC 13039<sup>T</sup> and *S. helvaticus* NBRC 13382<sup>T</sup> (16S rRNA gene sequence similarities between 99.9% and 100%) in the same branch, which is in line with previous studies (Kampfer, 2012; Labeda et al., 2017; Nouioui et al., 2018), indicate the need for taxonomic revision of the status of these species based on MLSA and genomic analyses.

In the MLSA tree, strain HST21<sup>T</sup> formed a subclade with *S. flavidovirens* DSM 40150<sup>T</sup> next to the one that encompasses the representative strains of *S. albidochromogenes*, *S. chryseus* and *S. helvaticus* species. These two latter occupied the same branch unlike *S. albidochromogenes* (Fig. 17). The topologies of the ML and NJ MLSA trees as well as the 16S rRNA gene tree are in concordance (Fig. 16-17). These results are consistent with the MLSA evolutionary genetic distances, which showed value above the threshold of 0.007 for the assigning *Streptomyces* strains to the same species (Rong and Huang, 2012, 2014) between strain HST21<sup>T</sup> and the rest of its closest phylogenetic neighbours (Appx. 3). However, a genetic distance value of 0.0% was obtained between *S. chryseus* DSM 40420<sup>T</sup> and *S. helvaticus* DSM 40431<sup>T</sup> (appx. 3).



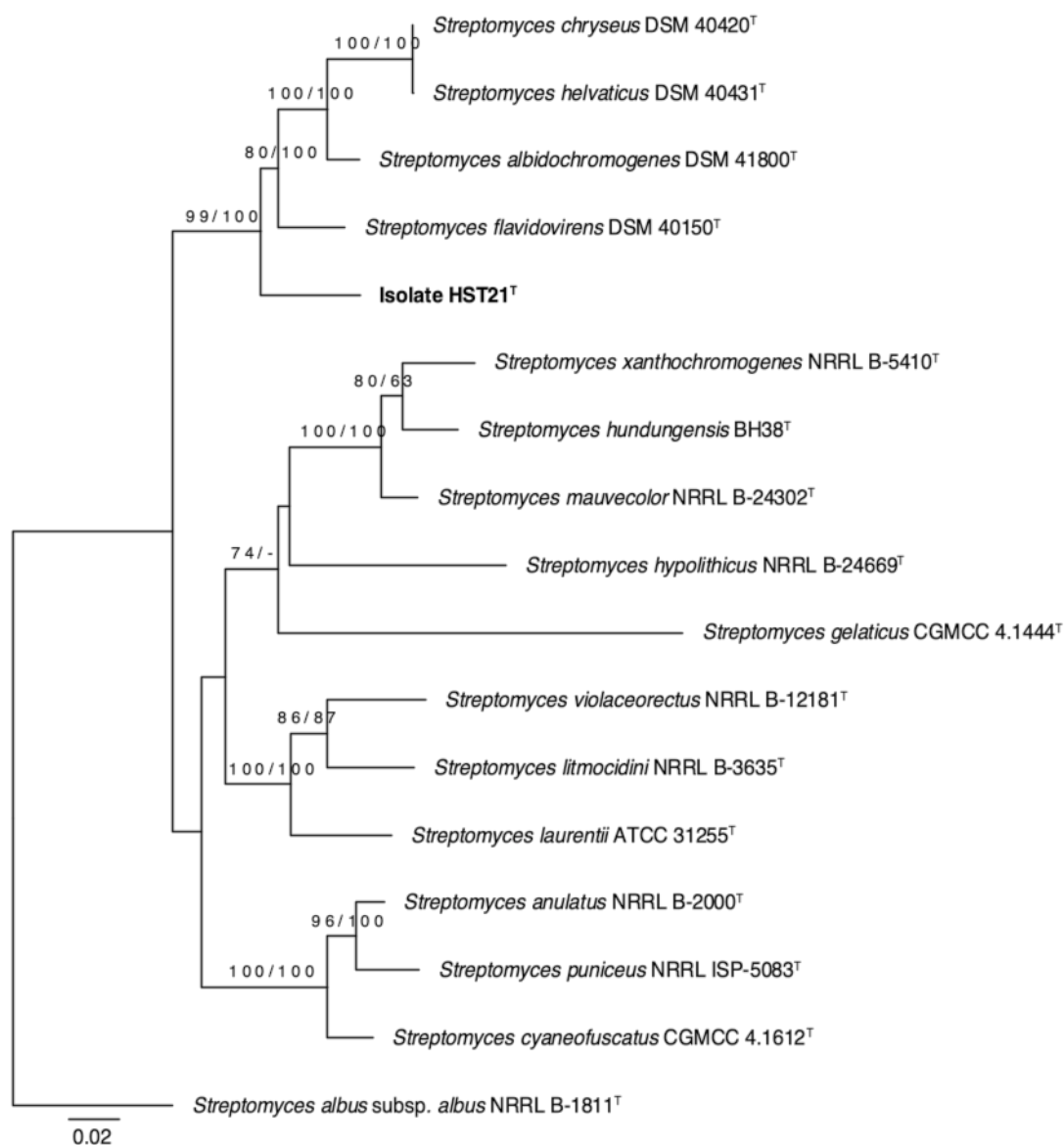


**Figure 17. Maximum-likelihood phylogenetic tree based on concatenated sequences of five housekeeping genes showing the phylogenetic relationship between isolate HST21<sup>T</sup> and its relatives within the genus *Streptomyces*.** The numbers above the branches are bootstrap support values greater than 60% for maximum-likelihood (left) and maximum-parsimony (right).

The dDDH values obtained between the genome of the HST21<sup>T</sup> and its closest relatives *S. albidochromogenes* DSM 41800<sup>T</sup> (35.6 %), *S. chryseus* DSM 40420<sup>T</sup> (36.5 %), *S. flavidovirens* DSM 40105<sup>T</sup> (47.2 %) and *S. helveticus* DSM 40431<sup>T</sup> (36.0 %), with which the 16S rRNA gene sequence similarities values are above 99.0 %, were well below the threshold of 70% for conspecific assignment (Wayne et al., 1987). These results are in concordance with the corresponding ANI values of 88.2%, 88.4%, 88.8% and 88.2 %; values below the cut-off point of 95–96% for delineation of prokaryotic species (Goris et al., 2007; Chun and Rainey, 2014).

The comparison of the dDDH and ANI values estimated between the pairs of the closest phylogenetic neighbours showed that only *S. chryseus* DSM 40420<sup>T</sup> and *S. helveticus* DSM 40431<sup>T</sup> have dDDH (95.3%) and ANI (99.4%) values above the described threshold of 70% and 96%, respectively. These results are coherent with their phylogenetic position in the 16S rRNA gene and MLSA tree and also with their phenotypic features.

#### **4.5 Description of *Streptomyces altiplanensis* sp. nov.**

*Streptomyces altiplanensis* (al.ti.pla.nen'sis N.L. masc. adj. altiplanensis referring to the site in the Chilean Altiplano where the strain was isolated).

Aerobic, Gram-positive actinobacterium, which produce white aerial mycelium and a brownish substrate mycelia, with diffusible pigments production observed after 10 days of incubation at 28°C on GYM media. It has rectiflexible spore chains in section with spiny spore surfaces. Strain HST21<sup>T</sup> was able to grow on GYM media and at a range of temperature between 28°C and 37°C; poor growth was observed at 25°C and 45°C. Optimal growth of strain HST21<sup>T</sup> was observed on GYM agar medium, pH 9-11, after 10 days of incubation at 28°C. Strain HST21<sup>T</sup> was able to metabolise sucrose, stachyose, D-raffinose, D-fructose, D-galactose (carbon sources); L-pyrroglutamic acid, quinic acid, β-hydroxy-butyric acid, α-keto-butyric acid, butyric acid (organic acids); L-arginine (amino acid); and grow in presence of aztreonam, lithium chloride and tween 40 (inhibitory compounds) and sodium bromate, 1% sodium lactate (salts) (Table 13). Whole-cell hydrolysates of strain HST21<sup>T</sup> were rich in LL-diaminopimelic acid in its peptidoglycan and, glucose, and ribose in its cell wall sugars. It is characterised by the presence of diphosphatidylglycerol, phosphatidylmethylethanolamine, phosphatidylethanolamine, phosphatidylinositol, glycerophospholipids and unknown lipids and phospholipids as polar lipids; C<sub>15:0</sub> *anteiso* and C<sub>17:0</sub> *anteiso* as major fatty acids. The menaquinone profile contained MK-9(H<sub>6</sub>), MK-9(H<sub>8</sub>), MK-9(H<sub>4</sub>), MK-7(H<sub>2</sub>), MK-8(H<sub>2</sub>), MK-9(H<sub>2</sub>), MK-10.

The genome size is 7.9 Mb with an in silico G+C content of 71.0%. The type strain HST21<sup>T</sup> (DSM 107267<sup>T</sup> = CECT 9647<sup>T</sup>) was isolated from hyper arid soil of the Salar de Huasco in the Atacama Desert, Chile. The accession numbers of the 16S rRNA gene and genome sequences of strain HST21<sup>T</sup> are KX130868 and RHMC00000000, respectively.

#### **4.6 Emended description of *Streptomyces chryseus* (Krasil'nikov et al. 1965) Pridham 1970 (Approved Lists 1980)**

The description is as given by Kämpfer (2012) with the following modifications and additions after inclusion of *S. helveticus*. Spore chains in section *Retinaculiaperti* to *Spirales* but rectiflexible spore chains may also be common; spore surface is smooth.

The major fatty acids (>15%) are C<sub>15:0</sub> *anteiso* and C<sub>16:0</sub> *iso*. Polar lipids pattern has DPG, PE, PI, GPL, AL, L1-2 and PL.

The genome size is 7.1-7.6 Mb with an in silico G+C content of 71.2-71.3%. The type strain is AS 4.1694, ATCC 19829, CBS 678.72, DSM 40420, NBRC 13377, JCM 4737, NCIMB 10041, NRRL B-12347, NRRL-ISP 5420, RIA 1338, VKM Ac-200.

## 4.7 Conclusion

The strain HST21<sup>T</sup> showed phenotypic, genetic and genomic data distinct from its closest phylogenetic relatives and consequently, it merits the recognition as a new species, namely *Streptomyces altiplanensis* sp. nov. In parallel, the two phylogenetic neighbours *Streptomyces chryseus* and *Streptomyces helveticus* presented common phenotypic, genetic and genomic features, which allowed to conclude that the later one, correspond to a heterotypic synonym of *S. chryseus*.

# Chapter 5

## Peptidogenomics of the new class II lasso peptide huascopeptin

### Objectives

4. To map and predict the RiPPs biosynthetic gene clusters and their precursor peptides in the genomes of the novel *Streptomyces* species.
5. To detect the RiPPs in the mass spectra of microbial extracts through their theoretical mass/charge and fragmentation pattern.
6. To evaluate the bioactivity of purified RiPPs by antimicrobial and cytotoxic assays.

### 5.1 Abstract

The novel lasso peptide, huascopeptin, was isolated following peptidogenomic discovery of a new biosynthetic gene cluster in extremotolerant *Streptomyces huasconensis* HST28<sup>T</sup> from Salar de Huasco, Atacama Desert, Chile. Huascopeptin **1** is a thirteen-residue class II lasso peptide containing a novel Gly-Asp macrolactam ring, a three-residue loop, and a three-residue tail, making it the smallest lasso peptide isolated to date. The lasso structure was confirmed using Nuclear Overhauser enhancement restrained molecular dynamics simulations.

## 5.2 Introduction

The development of high-throughput sequencing methods coupled with modern genome mining approaches, has provided universal access to the biosynthetic potential of microbes and subsequently the potential to discover new chemistry (Challis, 2008; Gomez-Escribano et al., 2015; Ziemert et al., 2016). Ribosomally synthesized and posttranslationally modified peptides (RiPPs) have conserved protein domains involved in the posttranslational modification of the precursor peptide. Structural characteristics and putative structures can be determined based on the predicted precursor peptides and the Posttranslational modification enzymes (Hetrick and van der Donk, 2017), making RiPPs an ideal target for genome mining. Lasso peptides, characterised by their unique lariat-knot conformation, have increasingly drawn attention due to their broad range of biological activities including antimicrobial (Iwatsuki et al., 2006; Gavrish et al., 2014; Li et al., 2015), antiviral (Chokekijchai et al., 1995) and enzymatic inhibition (Yano et al., 1996). Intriguingly, software tools such as RODEO, predict that the overall chemical space of lasso peptides has barely been scratched (Tietz et al., 2017; Hudson et al., 2019). *Streptomyces* species are prolific sources of antimicrobial lasso peptides (Weber et al., 1991; Potterat et al., 1994; Detlefsen et al., 1995). Lasso peptides are unique due to the formation of a macrolactam ring as a result of an isopeptide bond between the N-terminal  $\alpha$ -amino group and the carboxylic group located in the side chain of an aspartic acid or a glutamic acid (Maksimov et al., 2012). The lariat-knot is formed enzymatically when the macrolactam ring cyclises around the tail, locking the carboxylic acid terminus (Arnison et al., 2013). This conformation is stabilized by disulphide bonds in lasso peptides class I and III, by steric hindrance in class II and by “handcuffing” in class IV (Weber et al., 1991; Potterat et al., 1994; Tietz et al., 2017). Extreme conditions in the Atacama Desert favours the development of unique actinobacterial diversity, forming a basis for new chemistry (Goodfellow et al., 2018; Rateb et al., 2018). In continuation of our previous studies, the new species *Streptomyces huasconensis* HST28<sup>T</sup> (Cortés-Albayay et al., 2019b) was isolated from Salar de Huasco, an athalossohaline high altitude wetland (3800 m.a.s.l.), located in the Atacama Desert (Cortés-Albayay et al., 2019a). Genome mining was used to mine *S. huasconensis* HST28<sup>T</sup> for RiPPs, which evidenced the presence of one new lasso peptide biosynthetic gene cluster (BGC) named “*hpt*”, encoding for the production of a novel class II chemotype. In silico predictions were confirmed *in vivo*, leading to the isolation and structure elucidation of huascopeptin **1** using tandem mass spectrometry (MS2) and nuclear magnetic resonance (NMR) spectroscopy. Compound **1** contains a novel Gly-Asp seven-membered macrolactam ring. Furthermore, the lasso nature of the molecule was evaluated by nuclear Overhauser enhancement (NOE) and subsequently modelling, confirming the lasso motif laid out for the xanthomonins (Hegemann et al., 2014).

## 5.3 Materials and methods

### 5.3.1 Isolation, culture and maintenance

*Streptomyces huasconensis* HST28<sup>T</sup> was isolated from an arid soil sample collected in sectors surrounding a salt-lake (-20.328611, -68.838611) in complete absence of vegetation (Cortés-Albayay et al., 2019a). This site is marked by a negative water balance, a salinity gradient from freshwater to saturation and elevated levels of solar radiation (<1100 W/m<sup>2</sup>) (Dorador et al., 2010). The soil samples were treated according to the procedure described by Cortés-Albayay et al, 2019a and strain HST28<sup>T</sup> was recovered from Starch-Casein-KNO<sub>3</sub> agar plates supplemented with 50 µg/ml of nystatin and 50 µg/ml of cycloheximide as selective agents (Kuester and Williams, 1964). A pure culture was obtained and maintained on Starch-Casein-KNO<sub>3</sub> agar plates at 28°C for 5 days.

### 5.3.2 Molecular analysis

Genomic DNA of *S. huasconensis* was extracted from 10 ml of GYM liquid culture incubated for 5 days at 30°C whilst shaking at 150 rpm (glucose, yeast extract, malt extract and CaCO<sub>3</sub>) media. DNA extraction was completed using the UltraClean® Microbial DNA isolation kit (MoBio Labs, Carlsbad, CA) following the manufacturer procedure. The 16S rRNA-PCR amplification was evaluated using the primer Eub9-27F and Eub1542R and according to the conditions cited by Stackebrandt and Liesack, 1993. A BLAST of an almost complete 16S rRNA gene sequence (1517 bp; accession number KX130877) of strain HST28<sup>T</sup> was performed using the EzTaxon server (Yoon et al., 2017). The assignment of the strain HST28<sup>T</sup> to the genus *Streptomyces* was confirmed with a 99.0% of 16S rRNA gene sequence similarity with *S. kanamyceticus* NRRL B-2535<sup>T</sup>.

### 5.3.3 Genome mining

The whole genome of strain HST28<sup>T</sup> was sequenced using an Ion Torrent PGM system at the Strathclyde Institute of Pharmacy and Biomedical Sciences (SIPBS, Glasgow, United Kingdom). The genome sequences were assembled using the SPAdes software (Bankevich et al., 2012), annotated through RAST server (Aziz et al., 2008; Overbeek et al., 2014) and submitted in GenBank under accession RBWT00000000.

The prediction of BGCs for specialized metabolites, including lasso peptides BGCs and their putative final chemical structures was completed using RiPP-PRISM and compared against combinatorial structure libraries (Skinnider et al., 2016, 2017) The mapping and identification of the BGC for huascopeptin **1**, was developed using ARTEMIS (Carver et al., 2012) to identify the ORFs corresponding to all the genes

present in the BGC and the web tool “CDS search” of NCBI (Marchler-Bauer et al., 2015), to find the conserved protein domains corresponding to all the enzymes involved in the class II lasso peptides.

The amino acid sequence of the core peptide was used to calculate the molecular weight and the web tool Protein Prospector (<http://prospector.ucsf.edu>) (Chalkley et al., 2005) was used to predict the potential fragments from MS<sup>2</sup>, considering the loss of one water molecule as result of the isopeptide bond formed during the cyclization (appx. 4).

### 5.3.4 General experimental procedures

High-resolution electrospray ionisation mass spectrometry (HRESIMS) was performed using a MAXIS II Quadrupole-time of flight (Q-TOF) (Bruker) and a LTQ XL Orbitrap (Thermo) mass spectrometers, both coupled to an ultra high-pressure liquid-chromatographer (UHPLC) Agilent 1290 Infinity to achieve the separations. Both mass spectrometers utilized a Phenomenex Kinetex XB-C<sub>18</sub> column (2.6 μM, 100 x 2.1 mm) with a mobile phase of 5% Acetonitrile (ACN) + 0.1% formic acid to 100% ACN + 0.1% formic acid in total times of 11 min for Q-TOF and 25 min for LTQ XL Orbitrap.

Optical rotations were measured using a polarimeter. UV was measured using a UV/vis spectrometer. NMR spectra were recorded on a 2.5 mM sample of **1** and obtained with an 800 MHz Bruker spectrometer with 5 mm TCI He <sup>1</sup>H/<sup>13</sup>C/<sup>15</sup>N CryoProbe and <sup>1</sup>H-<sup>15</sup>N heteronuclear single-quantum correlation (HSQC) data was collected using 600 MHz Bruker spectrometer with TCI He <sup>1</sup>H/<sup>13</sup>C/<sup>15</sup>N CryoProbe. NMR solvents were purchased from VWR international as well as all chromatography solvents.

Semi-preparative high performance liquid chromatography (HPLC) separations were conducted in an Agilent 1200 HPLC, using a Waters SunFire semi-preparative C<sub>18</sub> column (5 μM, 100 Å 250 × 10 mm column) with a solvent system of **A**: MeOH/H<sub>2</sub>O (95:5) and **B**: MeOH (100%), connected to a binary pump and monitored using a photodiode array detector.

### 5.3.5 Fermentation, detection and isolation

To evaluate the production of in silico predicted lasso peptides, a single colony of *S. husconensis* HST28<sup>T</sup> was inoculated in 50 ml (x3) of GYM and SPM (Starch, Soy peptone and CaCl<sub>2</sub> x H<sub>2</sub>O) liquid media supplemented with 2% of artificial sea salts and incubated for 7 days at 30°C with shaking at 150 rpm. The resultant cultures were centrifuged at 4600 rpm for 20 min; the wet biomass was washed twice with sterile Milli-Q water and then homogenized and extracted with methanol while the resultant supernatants were shaken at 130 rpm overnight with 20 g/l of HP-20 resin at room

temperature. The resin was filtered and washed twice with Milli-Q water, extracted with methanol (MeOH) to exhaustion and all resultant extracts analysed by LC-QTOF-MS.

For the large-scale culture, 2 l baffled flasks (x8) containing 500 ml of GYM media, were inoculated with 100 ml of the seed culture and incubated for 10 days at 30°C with shaking at 150 rpm. Extraction was performed using HP-20 resin as explained above, except no centrifugation was completed as compound **1** retained on the resin. Crude extract was partitioned using modified Kupchan partitioning method (Morris et al., 2000) yielding 5 fractions. Solid-phase extraction (SPE) using 10g C<sub>18</sub> cartridge (Phenomenex) was conducted on the sec-butanol fraction, yielding 5 fractions eluted with increasing MeOH. The MeOH/water (50:50) fraction was then separated using reverse-phase flash chromatography (RP-FPLC) (Biotage, 12g C<sub>18</sub>) where huascopeptin **1** was detected in fraction 6 at a retention time (t<sub>R</sub>) of 50 min. Lastly, fraction 6 was re-purified, using a solvent gradient of 30% B to 100% B at a flow rate of 2.5 mL/min over 85 minutes to obtain pure compound. Pure Huascopeptin **1** was recovered at a t<sub>R</sub> of 63.5 min with an overall yield of 0.6 mg/4 l.

### 5.3.6 3D-modelling of huascopeptin

The structure of huascopeptin **1** was modelled using the lasso peptide chaxapeptin **1** as structural template with YASARA WhatIf (version 11.12.31) (Vriend, 1990). Final cyclisation was done by deleting one HN of Gly1, one Oδ (OD) atom of the side chain of Asp7 and inserting a single bond in trans between N of Gly1 and CG of Asp7 to mimic the isopeptide bond of the lasso peptide. The length of the newly created isopeptide bond and position of the replaced amino acids after modelling were corrected by energy minimization with YASARA2 force field. In total, 3 models differing in the position of the tail through the ring were generated (Figure 22A-C). With all models, molecular dynamics (MD) simulations were performed with AMBER03 over 100 ns in a cubic box (30 Å length) with periodic boundaries and drift correction at 298 K with pH 7.4, 0.9 % NaCl, a van der Waals cutoff of 7.86 Å, and PME for long-range Coulomb forces. Hydrogen bonds were analysed with YASARA WhatIf (version 11.12.31). The flexibility was visualised by colour coding the RMSF (Root Mean Square Fluctuation) value over 100 ns and mapping on the structure of huascopeptin **1** for each atom.

### 5.3.7 Biological assays

Assays of the Minimum inhibitory concentration (MIC) were completed on *P. aeruginosa* ATCC 27853 and methicillin-resistant *Staphylococcus aureus* (MRSA) ATCC 33591 using the methodology established by Ingebrigtsen *et al.*, 2016, with the exception that MRSA was cultivated in Brain heart infusion instead of Mueller-Hinton broth.



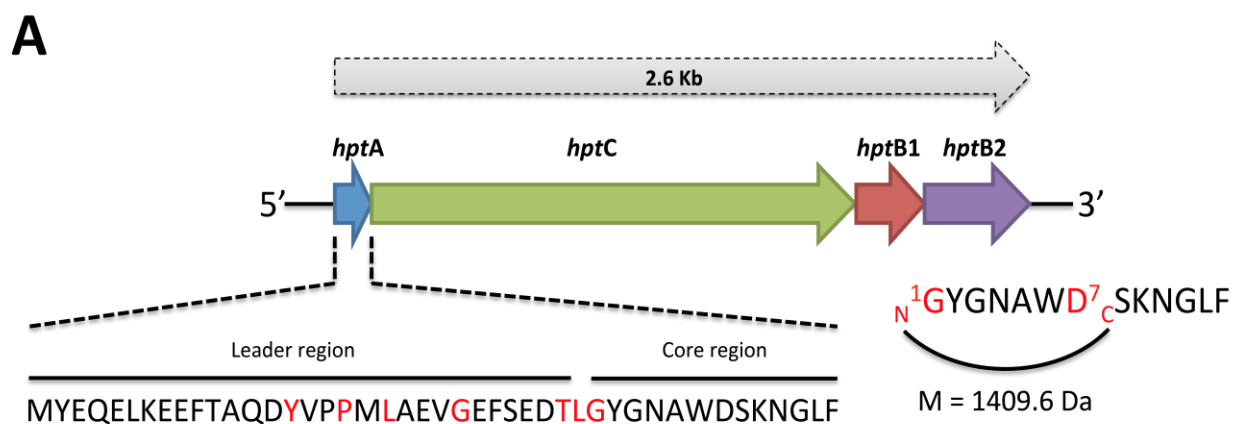
The cytotoxic activity of huascopeptin **1** was evaluated on a MRC5 (lung fibroblast) cell line (ATCC CCL-171), using the colorimetric MTS (3-(4,5-dimethylthiazol-2-yl)-2,5-diphenyltetrazolium bromide) assay and according to the protocol described by Ingebrigtsen *et al.*, 2016. The cell lines were seeded in 96-well microtiter plates at a concentration of 4000 cells/well in Minimum Essential Medium Eagle with Earle's salts (EMEM), supplemented with 10 % fetal bovine serum, 10 µg/ml gentamycin, 1 % non-essential amino acids, 1% L-glutamine, 1% sodium pyruvate and 1% sodium bicarbonate.

### 5.3.8 Spectroscopic data

Huascopeptin **1**: colourless amorphous solid.  $[\alpha]^{25D} + 20$  (c 0.05, MeOH); UV (MeOH)  $\lambda_{\max}$  228 nm<sup>-1</sup>, 279 nm<sup>-1</sup>. <sup>1</sup>H and <sup>13</sup>C NMR data in appendix 5. HRESIMS m/z 1410.6429 [M+H]<sup>+</sup> (calcd for C<sub>65</sub>H<sub>88</sub>N<sub>17</sub>O<sub>19</sub>, m/z 1410.644,  $\Delta = -0.7$  ppm).

## 5.4 Results and discussion

In silico analysis of the *S. huasconensis* HST28<sup>T</sup> genome showed 39 putative secondary metabolite BGCs amongst which polyketides, nonribosomal peptides and RiPPs were found (Unpublished). The latter included four new lasso peptide BGCs, among which the huascopeptin *hpt* BGC assumed to be responsible for the production of huascopeptin **1**. This cluster has a total size of 2.6Kb (accession number MK636692). The *hpt* BGC houses the four main genes involved in class II lasso peptide biosynthesis and maturation (Maksimov *et al.*, 2014): (I) the *hptA* gene encodes for 44 amino acid residues including the precursor peptide of huascopeptin **1**. HptA product consists of 31 and 13 amino acid residues in the leader (N-terminal) and in the core peptide regions (C-terminal), respectively; (II) the *hptC* gene encodes for an asparagine synthetase-like protein domain (HptC) which is responsible for the isopeptide formation and subsequent cyclisation of the macrolactam ring (Maksimov *et al.*, 2013); (III) the HptB1 gene product contains a pyrroloquinoline quinone protein domain D (PqqD), also known as the RiPP recognition element (RRE), which binds to the leader region and delivers the precursor peptide to the protease HptB2 for the further processing (Burkhart *et al.*, 2015; Zhu *et al.*, 2016) (Figure 18); (IV) the HptB2 gene encodes a transglutaminase-like protease which is involved in the cleavage of the leader region in the precursor peptide (Burkhart *et al.*, 2015).



**B**

ORF	Size (aa)	Chaxapeptin Homologue	Identity/Similarity %	Protein Domain	Proposed function
HptA	44	CptA	51/60	-	Precursor peptide
HptC	613	CptC	49/63	Asparagine synthetase	Cyclase
HptB1	86	CptB1	42/57	Coenzyme PqqD	Recognition element
HptB2	134	CptB2	68/77	Transglutaminase	Protease

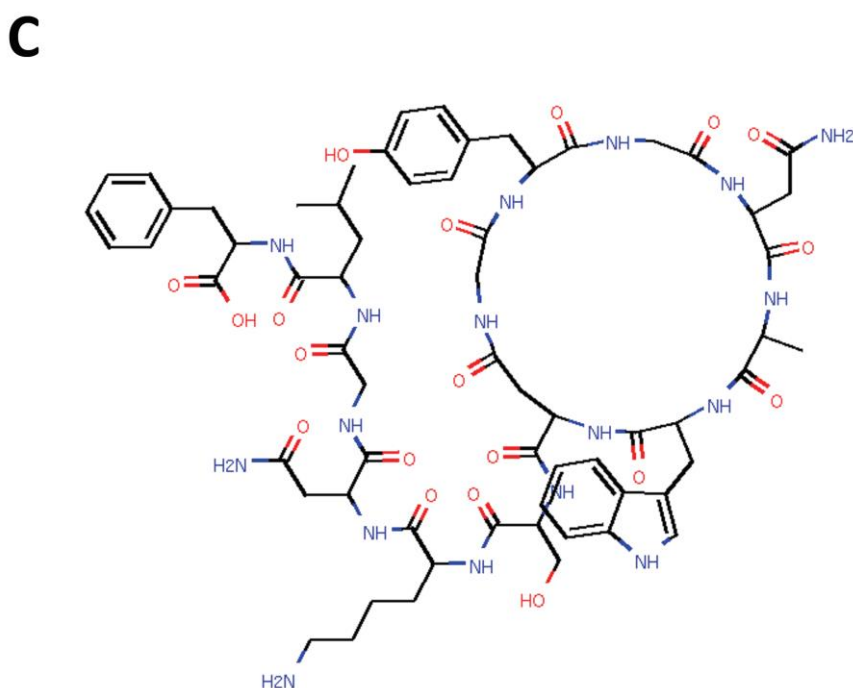


**Figure 18. Huascopeptin biosynthetic gene cluster. (A)** Genetic map of *hpt* gene cluster (accession number MK636692) in the genome of *S. huasconensis* HST28<sup>T</sup>. The residues in red correspond to the conserved cleavage motif. **(B)** The functions and relatedness of the proteins encoded by the *hpt* genes with their homologs of the *cpt* gene cluster for chaxapeptin (Elsayed et al., 2015). **(C)** Huascopeptin combinatorial structure prediction.

The core region amino acid sequence, GYGNAWDSKNGLF, was predicted to have an accurate mass of 1409.636 Da. The leader and core regions are divided by the characteristic TxG motif (Fig. 18A) needed to remove the leader peptide during lasso peptide maturation (Pan et al., 2012). The four genes of the *hpt* cluster (*hptACB1B2*) were found to be closely related to the *cptACB1B2* biosynthetic gene cluster of chaxapeptin (Elsayed et al., 2015). The HptA precursor peptide and HptC cyclase showed 51% and 49% identity with CptA and CptC while HptB1 protease and HptB2 had 42% and 68% of identity with CptB1 and CptB2, respectively (Fig. 18B). Although was not possible to find any protein involved in the export of the huascopeptin next to its BGC, an ABC multidrug transporter commonly involved in the self-immunity and export of lasso peptides (Maksimov et al., 2014) was found approximately 5Kb downstream of this BGC, so is not possible to discard that could be involved with huascopeptin export. However previous studies have reported that some lasso peptides lacks of these transporters (Hegemann et al., 2015).

A putative structure for huascopeptin (Fig. 18C) was obtained based in the only cyclization reaction found to occur between Gly1 and Asp7 residues of the core aminoacid sequence and the previously mentioned enzymatic machinery detected in the BGC (Skinnider et al., 2016).

The extracts obtained from *S. huasconensis* HST28<sup>T</sup> small-scale cultures, grown in SPM and GYM liquid media, showed two peaks at  $t_R$  3.9 and 4.1 respectively, which contained  $m/z$  1410.6 and  $m/z$  705.8 corresponding to the singly  $[M+H]^+$  and doubly  $[M+2H]^{2+}$  charged ions for huascopeptin **1** (Fig. 19). In addition to these results are consistent with the previously calculated molecular ion for the core aminoacidic sequence of huascopeptin and its post-tranlationally modification ( $-H_2O$ ); the fragmentation of  $[M+2H]^{2+}$  and  $[M+H]^+$  ions showed several of the ion fragments predicted for this molecule in the theoretical fragmentation (appx. 4).

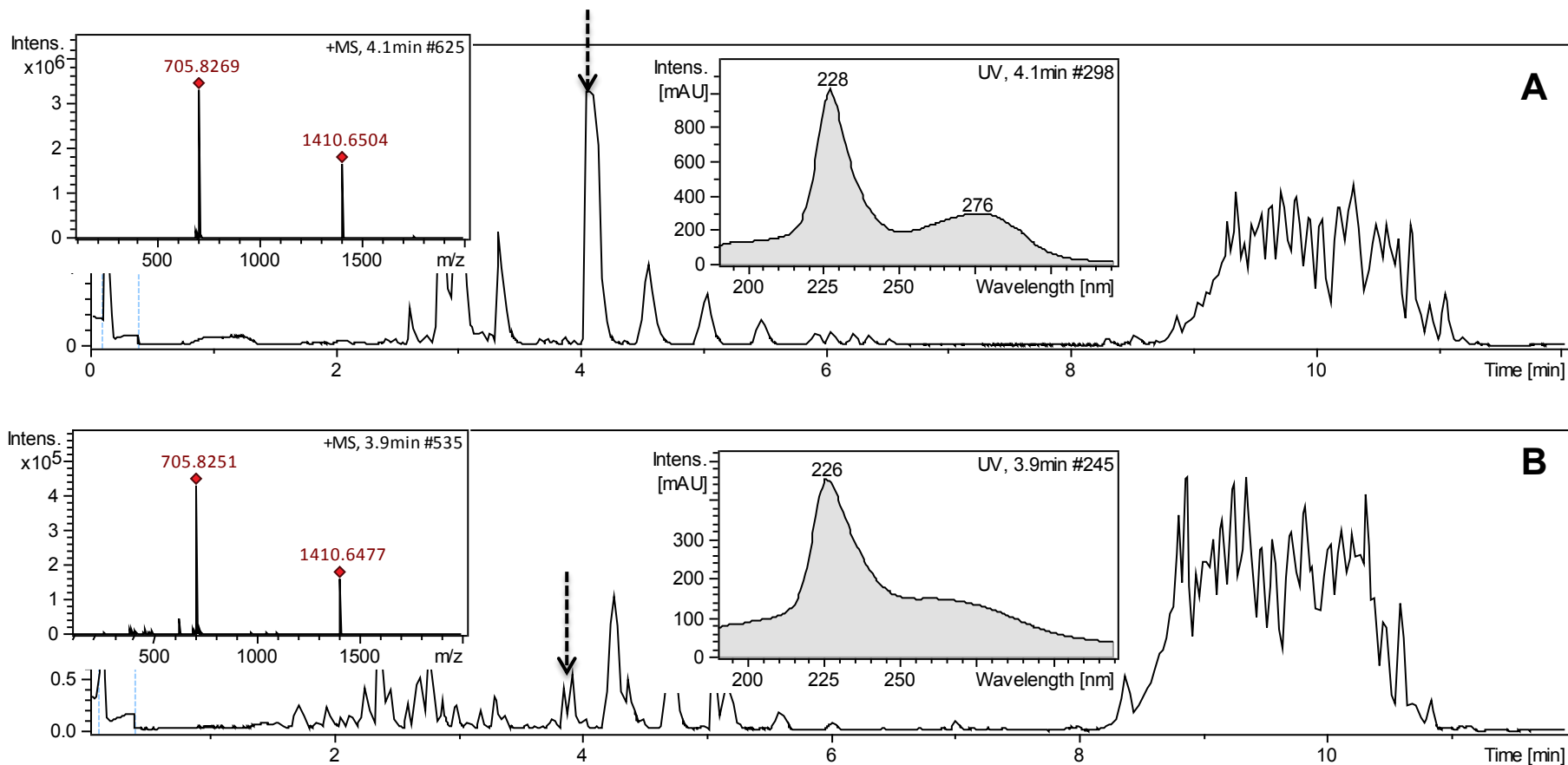


**Figure 19. High-resolution mass spectra for *Streptomyces huasconensis* HST28<sup>T</sup> small-scale culture extracts.** The base peak chromatograms for (A) SPM and (B) GYM culture extracts (main spectra), showed two peaks at retention times of 3.9 and 4.1 min respectively; which showed major peaks of absorbance at 228 and 226 nm respectively; and contained the  $m/z$  1410.6 [M+H]<sup>+</sup> and  $m/z$  705.8 [M+2H]<sup>2+</sup> corresponding to huascopeptin 1 (small spectra).

The HRESIMS spectra of purified huascopeptin 1 (Fig. 20A) allowed to establish its molecular formula  $C_{65}H_{88}N_{17}O_{19}$ , based on the  $[M+H]^+$  and  $[M+2H]^{2+}$  ions, which was consistent with  $C_{65}H_{90}N_{17}O_{20}$  previously predicted for unprocessed core sequence.

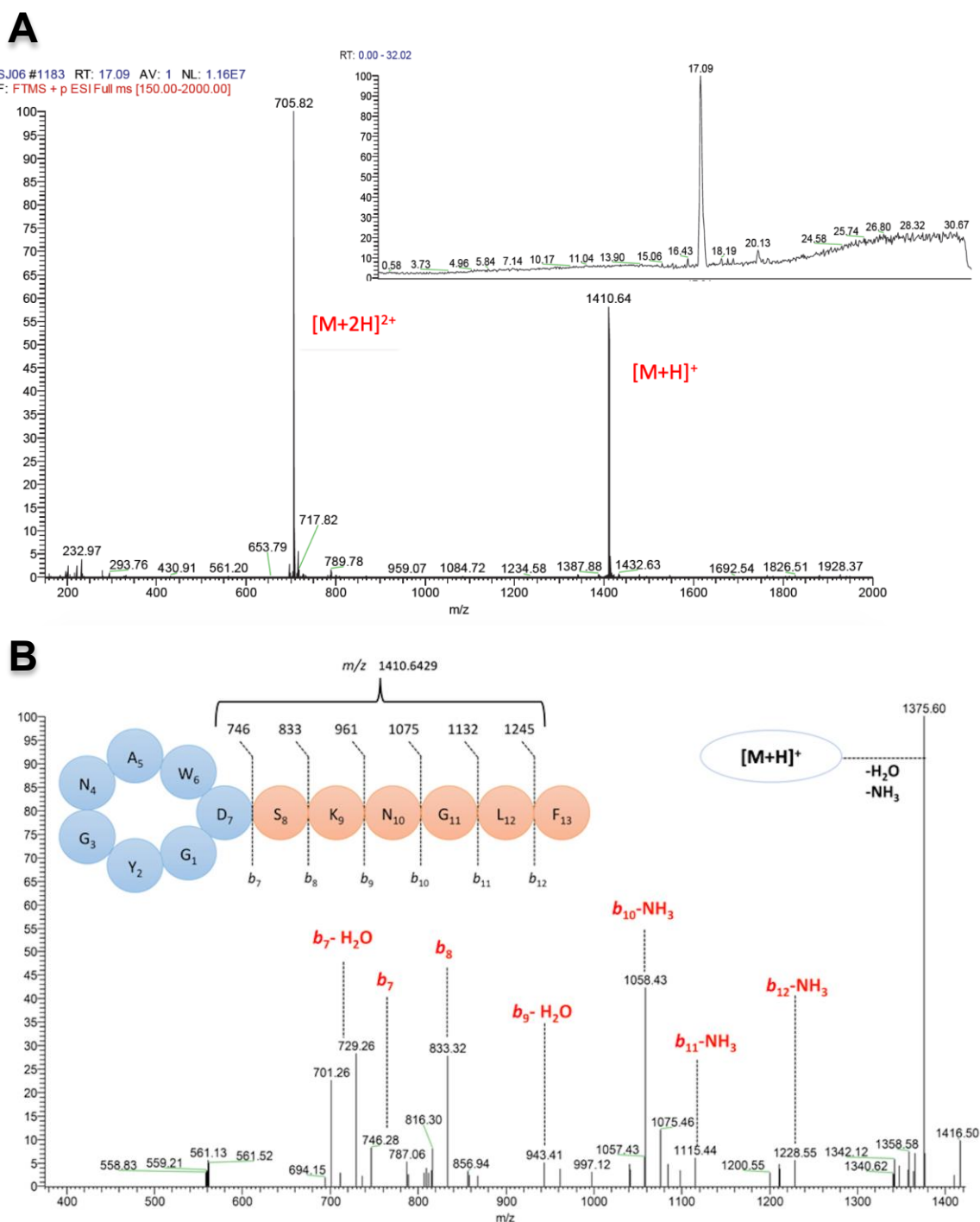


**Figure 20. High-resolution tandem mass spectrum (HRESIMS/MS) for purified huascopeptin 1. (A)** The small spectrum corresponds to the base peak chromatogram, showing only a single peak for huascopeptin 1, at a retention time of 17.09 min; and main spectrum, shows its  $[M+H]^+$  and  $[M+2H]^{2+}$  ions. **(B)**  $MS^2$  spectrum for  $m/z$  705.82  $[M+2H]^{2+}$  showing the  $b$ -fragment ions of the peptide tail in accordance with those predicted in silico from the core peptide sequence.

HRESIMS/MS data of purified **1**, allowed verifying the sequence of tail residues through the *b*-fragment ions obtained in the spectra (Figure 20B). The tail fragmented sequentially under Collision-induced dissociation (CID), as it is typically observed in most peptides. In contrast, the sequence of the remaining amino acid residues within the macrocycle could not be established using MS<sup>2</sup> due to high stability of the macrocycle and the low ionization voltages associated with CID.

<sup>1</sup>H, <sup>13</sup>C and <sup>15</sup>N NMR data were all in agreement with in silico and MS predictions. Along with one-dimensional experiments, two-dimensional <sup>1</sup>H-<sup>13</sup>C heteronuclear single-quantum correlation (HSQC), <sup>1</sup>H-<sup>15</sup>N HSQC, <sup>1</sup>H-<sup>13</sup>C heteronuclear multiple bond correlation (HMBC), <sup>1</sup>H-<sup>1</sup>H total correlation spectroscopy (TOCSY), <sup>1</sup>H-<sup>13</sup>C HSQC-TOCSY, and <sup>1</sup>H-<sup>1</sup>H Nuclear Overhauser enhancement spectroscopy (NOESY) allowed for almost all signals (Appx. 5) in the 13-residue peptide to be assigned, including three glycines (Gly), two asparagines (Asn), one tyrosine (Tyr), one tryptophan (Trp), one alanine (Ala), one aspartic acid (Asp), one serine (Ser), one lysine (Lys), one leucine (Leu), and one phenylalanine (Phe) (Appx. 6-12a).

Using a combination of HRESI-MS/MS and NMR data, the planar structure of **1** was defined as a seven-membered amino acid cyclic isopeptide with a six-membered amino acid side chain (Fig. 21), confirming the previous structure predicted in silico (Fig. 18C).

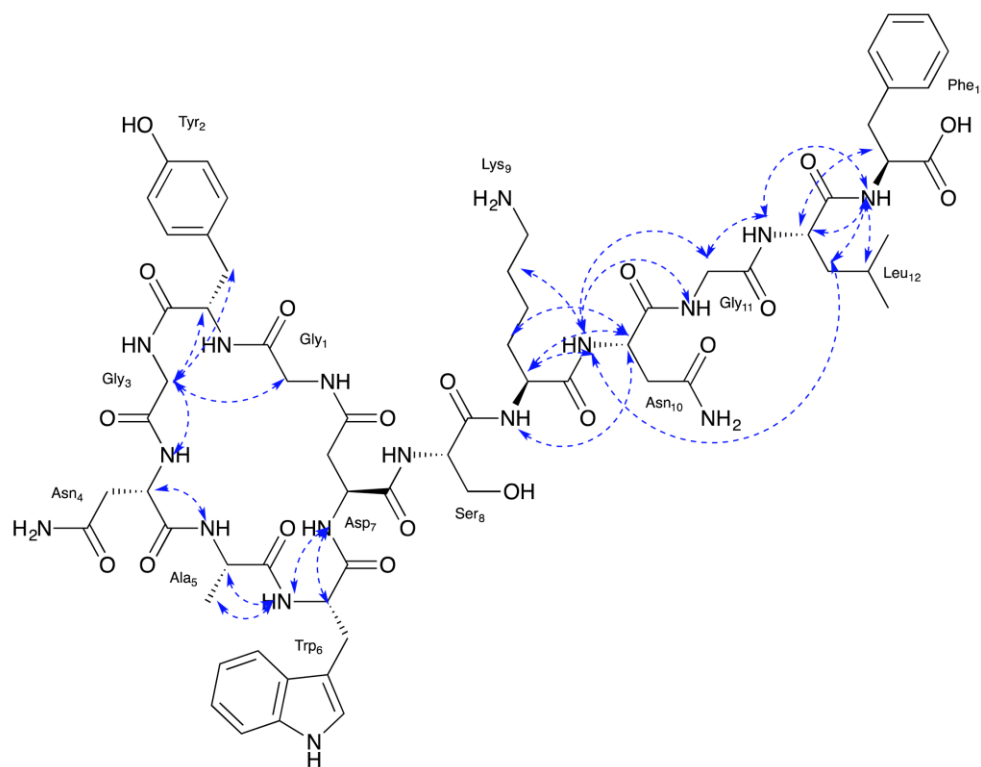


**Figure 21.** Key Nuclear Overhauser enhancement spectroscopy (NOESY) correlations (blue) confirming the majority of the connectivities for huascopeptin **1** peptide sequence.

Sequence connectivity of the lasso peptide tail was confirmed using NOESY correlations (Figure 21). The connection between Leu12-Phe13 was established using correlations between Leu12-H $\alpha$  to Phe13-H $\alpha$  and Leu12-NH to Leu12-H $\alpha$ , Leu12-H $\beta$ , and Leu12-H $\gamma$  all to Phe13-NH. The connection between Gly11-Leu12 was determined with correlations between Gly11-H $\alpha$  ( $\delta$ 3.99 and  $\delta$ 2.99) and Leu12-NH. Furthermore, connection between Asn10-Gly11 was established with correlations between Asn10-NH to Gly11-NH and Gly11-H $\alpha$  ( $\delta$ 3.99). The connection between Lys9-Asn10 was established using correlations between Lys9-NH to Asn10-H $\alpha$ , Lys9-H $\alpha$  to Asn10-NH and to Asn10-H $\alpha$ , Lys9-H $\beta$  ( $\delta$ 2.06 and  $\delta$ 1.68) to Asn10-H $\alpha$ , and lastly, Lys9-H $\delta$  ( $\delta$ 1.69) to Asn10-NH. Connectivity between Ser8-Lys9 and Asp7-Ser8 was established with MS2 data due to a lack of NMR evidence.

Sequence connectivity of the macrocycle was also confirmed using NOESY correlations (Figure 21). The connection between Tyr2-Gly3 was established using NOESY correlations between Tyr2-H $\alpha$  and Gly3-H $\alpha\alpha$  and Tyr2-H $\beta$  and Gly3-H $\alpha\alpha$ . Additionally, the connection between Gly3-Asn4 was established using the correlations between Gly3-H $\alpha\alpha$  and Asn4-NH. The connection between Gly1-Tyr2 was established through the link between Gly1-H $\alpha$  and Gly3-H $\alpha$ . The connection between Asn4-Ala5 was determined using the correlation between Asn4-H $\alpha$  and Ala5-NH. Furthermore, connection between Ala5-Trp6 was determined using correlations between Ala5-H $\alpha$  and Ala5-H $\beta$  to Trp6-NH. The connection between Trp6-Asp7 was established based on the correlations between Trp6-NH and Trp6-H $\alpha$  to Asp7-NH. Finally, while there is no NMR evidence that Asp7 and Gly1 form the macrolactam ring, MS<sup>2</sup> data confirms that the unfragmented ring is missing the predicted aspartic acid residue.

Due to the limited amount of sample available, was not possible to determine the absolute stereochemistry using Marfey's reagent. With the exception of rare epimerisation occurring at the C-terminus (Feng et al., 2018; Kaweewan et al., 2018), all remaining lasso peptides characterised thus far only contain L amino acids (Elsayed et al., 2015; Hegemann et al., 2015) and additionally there was no epimerase encoding gene in the *hpt* cluster (Fig. 18A), therefore L amino acids were used for planar structure.

The overall 3D structure of **1** was established by analysing NOESY spectra, which displayed a total of 33 sequential and 9 long-range interactions ( $\geq i+3$ ). Obtained distance restraints could confirm the ring structure of the peptide but were not sufficient to locate the position of tail relative to the ring. However, due to the presence of tail to ring NOE correlations as well as a wide range of amide NH chemical shifts (9.22-7.53) characteristic of the lasso topology (Xie et al., 2012), we used a lasso motif instead of a branched-cycle for models (Appx. 13). Hence, YASARA was used to model the structure of huascopeptin with chaxapeptin as a template; a typical class II lasso peptide for which the structure was calculated by NMR (Elsayed et al., 2015). The ring structure was realised by inserting a single *in trans* bond between the nitrogen of Gly1 and the side chain C $\gamma$  of Asp7. Subsequently, an energy minimisation step was performed with a YASARA2 force field to reduce any remaining tension after modelling. Following this, three models of huascopeptin were designed with various lengths of the loop region

(Fig. 22A-C). To explore their dynamics, molecular dynamic simulations were performed with an AMBER03 force field over 100 ns. During this time, model A (loop: Ser8 only) was unstable and lost the typical lasso peptide structure which is not in agreement with the high stability of lasso peptides under experimental conditions (Hegemann et al., 2015). Therefore, this model was discarded. After comparing energies between model B (loop: Ser8 and Lys9) and model C (loop: Ser8, Lys9 and Asn10), the latter showed lower energies of bonds, angles, dihedrals, planarity and van der Waals energies (Appx. 14). Further evidence for model C is the lasso motif established with the xanthomonins (Hegemann et al., 2014), which consists of a threaded glycine through the ring, as well as NOEs from the plug residues Asn10 and Leu12 (Appx. 13).

Thus, the 3D structure of compound **1** comprises a seven-residue ring with a short two-residue tail below the macrolactam ring (Fig. 22D). Asn10 and Leu12 are assumed to operate as the plug amino acids located above and below the ring (Fig. 22E). Additionally, huascopeptin possesses hydrogen bonds in the loop region (Asp7-Ser8 and Asp7-Lys9) and between residues in the tail and the ring (Gly1-Asn10, Gly3-Gly11, Gly3-Asn10), which results in a characteristic short  $\beta$ -sheet known to promote the observed high stabilities of lasso peptides (Iwatsuki et al., 2006). Furthermore, the structure of huascopeptin does not show any flexible regions, which is probably due to the short tail in comparison to other lasso peptides with longer tails (Fig. 22F) (Knappe et al., 2009; Arnison et al., 2013). Lastly, 400 $\mu$ g of compound **1** was evaluated for antimicrobial activity against MRSA and *P. aeruginosa* and cytotoxicity against MRC5 cells but was found inactive for all the tests.

A seven-membered macrocycle has only been described one other time for xanthomonins I-III (Hegemann et al., 2014). In the previous study, 25 xanthomonin II site-directed mutants were generated to evaluate the biosynthetic machinery of this group of lasso peptides. Multiple mutants were generated to determine if Asp could replace Glu in position 7 of the macrocycle, but the mutants were unable to produce a mature peptide. Nevertheless, the authors did foresee the possibility of a seven-membered macrocycle with Asp7, which is first described here. Huascopeptin not only represents a novel macrocycle linkage but also represents the smallest macrocycle opening as 22 atoms, one less than the xanthomonins.



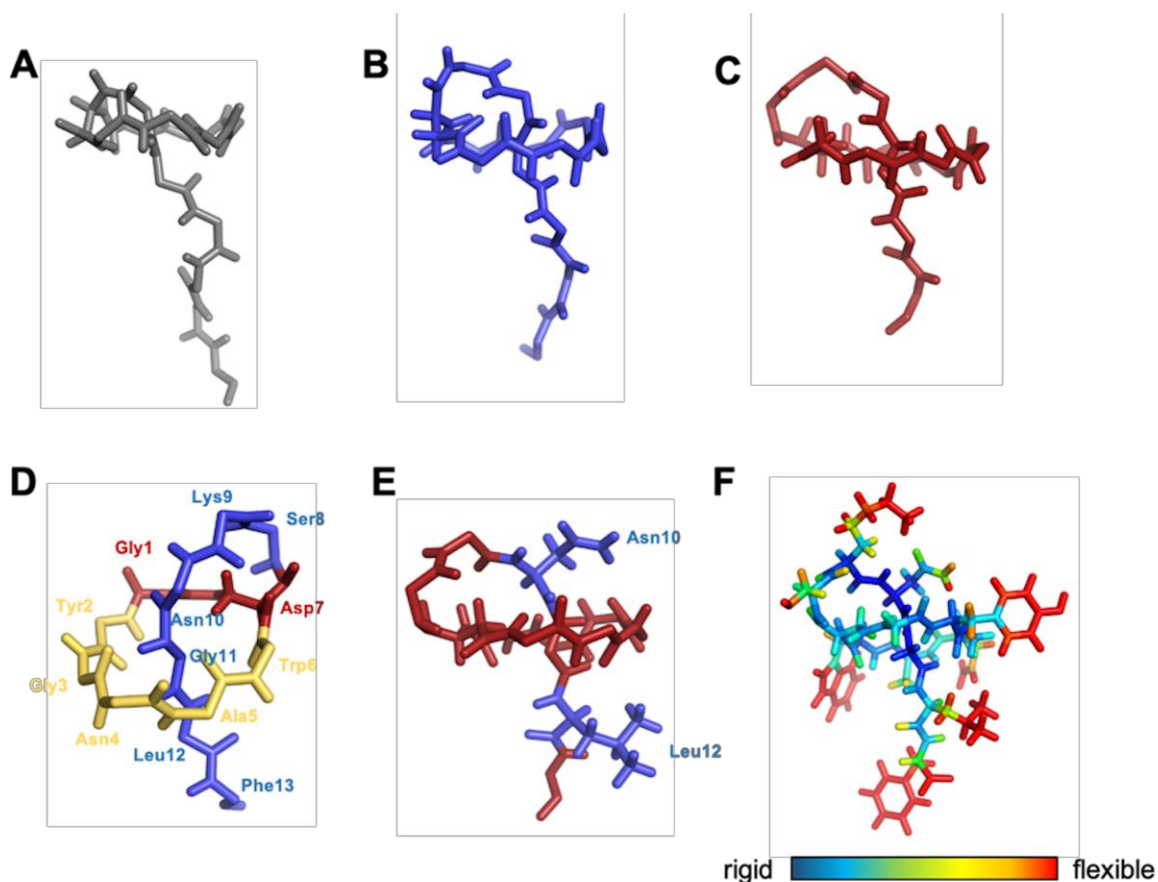


**Figure 22. In silico structural model for huascopeptin.** (A) Huascopeptin with a typical lasso peptide motif with a short loop (Ser8 only) and a long tail. (B) Huascopeptin with a lasso fold with Ser8 and Lys9 building the loop. (C) Huascopeptin with a lasso structure with a long loop comprising Ser8, Lys9 as well as Asn10 and a short tail. (D) Model C is energetically most favourable and likely to reflect the solution conformation of huascopeptin. It consists of a seven-residue ring, a three-residue loop and a two-residue tail below the ring. (E) The plug amino acids in huascopeptin are Asn10 above and Leu12 below the macrolactam ring pointing to the same direction. (F) Flexibility map (blue: rigid, red: flexible) of huascopeptin over a period of 100 ns during molecular dynamic simulations shows a rigid core structure typical for lasso peptides.

## 5.5 Conclusion

Peptidogenomics and genome mining continues to be a viable approach for the discovery of new chemistry. In addition to this, the previously unexplored source of Salar de Huasco and in a wider context, the Atacama Desert, have proven to be rich sources for specialised metabolites. Genome mining has led to the discovery of huascopeptin **1**, a novel class II lasso peptide containing a Gly-Asp seven-membered macrolactam ring, adding to the already structurally diverse group of RiPPs. This study also represents the first biosynthetic example of this lasso peptide structural chemotype.

# General conclusions

The poly-extreme ecosystems in Atacama Desert such as Salar de Huasco remain like the “treasure islands” for bioprospecting of a novel diversity of microorganisms, among them *Streptomyces*. The novel *Streptomyces* diversity obtained from this ecosystem, mainly the strains presenting greater taxonomic divergence, were mostly recovered from the soil samples with the most unfavourable physicochemical conditions (site H6). Therefore, these strains need to survive these predominant environmental conditions, developing specific adaptative strategies, which can be seen reflected on the production of specialized metabolites.

These *Streptomyces* strains presented a huge potential for the production of a new chemodiversity of natural products evidenced by the novelty of the metabolic profiles obtained from their crude extracts and an important spectra of bioactivities such as anti Gram-positive and –negative against human and phyto-pathogens and/or cytotoxicity against human cancer cell lines. These features make them interesting microorganisms for futures studies focused on the discovery of novel molecules directed to pharmaceutical applications.

Two of the most taxonomically divergent strains HST28 and HST21 showed phenotypic, genetic and genomic features that differentiate them from their closest phylogenetic relatives, therefore they merited description as the new alkalitolerant species *Streptomyces huasconensis* HST28<sup>T</sup> and *Streptomyces altiplanensis* HST21<sup>T</sup>, which contribute to increase the new diversity of Atacama Desert *Streptomyces* with high biotechnological potential. In parallel, two of the phylogenetic neighbours of *S. altiplanensis* HST21<sup>T</sup>, *Streptomyces chryseus* and *Streptomyces helveticus* shared common phenotypic, genetic and genomic features, which allowed to emend the later one as a heterotypic synonym of *S. chryseus*.

The large genomes of these two novel *Streptomyces* species and large number of new biosynthetic gene clusters (BGCs) for diverse peptidic natural products (PNPs), including many Ribosomally synthesized and Posttranslationally modified peptides (RiPPs), allowed to increase the probabilities of accessing novel peptidic natural products as huascopeptin in bacterial culture extracts and fermentations.

Discovery of huascopeptin, a novel class II lasso peptide containing a Gly-Asp seven-membered macrolactam ring, which is the smallest chemotype currently described; a new second lasso peptide class II, partially purified and in process of description; in addition to 8 new RiPPs precursors detected in the genomes of *S. huasconensis* HST28<sup>T</sup> and *S. altiplanensis* HST21<sup>T</sup>, confirmed the presence of a new chemodiversity of RiPPs in novel *Streptomyces* species from Salar de Huasco.

The protein-centric peptidogenomic approach applied in this study, guided by the genomic information of the conserved maturation enzymes and peptidic precursors proved to be a faster and more efficient strategy for the search and discovery of these peptides, allowing to know in advance its novelty and direct the search to specific targets.

# Future perspectives

The new species *Streptomyces huasconensis* HST28<sup>T</sup> and *Streptomyces altiplanenensis* HST21<sup>T</sup> have demonstrated great bioactive potential unveiled by their antimicrobial and cytotoxic activities and the large number of novel biosynthetic gene clusters (BGCs) for specialized metabolites encoded in their genomes. Strain HST28<sup>T</sup>, in addition to the production of huascopeptin and the second lasso peptide currently under characterization, presented 2 BGCs for novel lasso peptides (class II and IV), and 1 BGC for a novel lanthipeptide (class III); while strain HST21<sup>T</sup> presented 4 BGCs for novel lanthipeptides (3 class III and 1 class I) and 1 BGC for a novel lasso peptide (class II), all of them completely mapped and in process of publication.

Further studies should be focused on the detection and production of these novel peptides in order to exploit their bioactive potential. These novel BGCs can be expressed through biosynthetic pathways activation, exploring multiple fermentation media or modification of growth conditions, including certain types of stress or chemicals added to fermentations (e.g., heat, ethanol, rare earth elements, glucosamine, antibiotics and others). On the other hand, heterologous expression can also be a very useful tool for the expression of these BGCs, providing advantages mainly in the detection of these peptides through comparatively straightforward differential metabolic profiles of the wild and transformed host; or the use of so-called super hosts, which have been depleted of their own BGCs providing clean metabolic profiles that makes easier the detection of these heterologously produced peptidic products.

# Bibliography

- [1] Abdelkader MSA, Philippon T, Asenjo JA, Bull AT, Goodfellow M, Ebel R, Jaspars M, Rateb ME. Asenjonamides A-C, antibacterial metabolites isolated from *Streptomyces asenjonii* strain KNN 42.f from an extreme-hyper arid Atacama Desert soil. *J Antibiot* 2018; 71:425-431.
- [2] Angert ER. Alternatives to binary fission in bacteria. *Nat Rev Microbiol* 2005; 3:214-224.
- [3] Antony-Babu S, Goodfellow M. Biosystematics of alkaliphilic Streptomycetes isolated from seven locations across a beach and dune sand system. *Antonie Leeuwenhoek* 2008; 94, 581-591.
- [4] Arnison PG, Bibb MJ, Bierbaum G, Bowers A, Bugni TS, Bulaj G, Camarero JA, Campopiano DJ, Challis GL, Clardy J, Cotter PD, Craik DJ, Dawson M, Dittmann E, Donadio S, Dorrestein PC, Entian KD, Fischbach MA, Garavelli JS, Goransson U, Gruber CW, Haft DH, Hem-scheidt TK, Hertweck C, Hill C, Horswill AR, Jaspars M, Kelly WL, Klinman JP, Kuipers OP, Link AJ, Liu W, Marahiel MA, Mitchell DA, Moll GN, Moore BS, Muller R, Nair SK, Nes IF, Norris GE, Olivera BM, Onaka H, Patchett ML, Piel J, Reaney MJ, Rebuffat S, Ross RP, Sahl HG, Schmidt EW, Selsted ME, Severinov K, Shen B, Sivo-nen K, Smith L, Stein T, Sussmuth RD, Tagg JR, Tang GL, Truman AW, Vederas JC, Walsh CT, Walton JD, Wen-zel SC, Willey JM, van der Donk WA. Ribosomally synthesized and Posttranslationally modified peptide natural products: overview and recommendations for a universal nomenclature. *Nat. Prod. Rep.* 2013; 1, 108-160.
- [5] Ayuso-Sacido A, Genilloud O. New PCR primers for the screening of NRPS and PKS-I systems in Actinomycetes: Detection and distribution of these biosynthetic gene sequences in major taxonomic groups. *Microb. Ecol.* 2005; 49, 10-24.
- [6] Aziz RK, Bartels D, Best AA, Dejongh M, Disz T, Edwards RA, Formsma K, Gerdes S, Glass EM, Kubal M, Meyer F, Olsen GJ, Olson R, Osterman AL, Overbeek RA, McNeil LK, Paarmann D, Paczian T, Parrello B, Pusch GD, Reich C, Stevens R, Vassieva O, Vonstein V, Wilke A, Zagnitko O. The RAST Server: rapid annotations using subsystems technology. *BMC Genomics.* 2008; 9:75.
- [7] Bachmann BO, Van Lanen SG and Baltz RH. Microbial genome mining for accelerated natural products discovery: is a renaissance in the making? *J Ind Microbiol Biotechnol.* 2014; 41:175-184
- [8] Balows, A. *The Prokaryotes: a handbook on the biology of bacteria: ecophysiology, isolation, identification and applications.* 1992; 10.1007/978-1-4757-2191-121.
- [9] Baltz RH. Gifted microbes for genome mining and natural product discovery *J Ind Microbiol Biotechnol.* 2017; 44:573-588.
- [10] Bankevich A, Nurk S, Antipov D, Gurevich AA, Dvorkin M, Kulikov AS, Lesin VM, Nikolenko SI, Pham S, Pribelski AD, Pyshkin AV, Sirotkin AV, Vyahhi N, Tesler G, Alekseyev MA and Pevzner PA. SPAdes: a new genome assembly algorithm and its applications to single-cell sequencing. *J Comput Biol.* 2012; 19:455-477.
- [11] Bentley SD, Chater KF, Cerdeño-Tárraga AM, Challis GL, Thomson NR, James KD, Harris DE, Quail MA, Kieser H, Harper D, Bateman A, Brown S, Chandra G, Chen CW, Collins M, Cronin A, Fraser A, Goble A, Hidalgo J, Hornsby T, Howarth S, Huang CH, Kieser T, Larke L, Murphy L, Oliver K, O'Neil S, Rabinowitsch E, Rajandream MA, Rutherford K, Rutter S, Seeger K, Saunders D, Sharp S, Squares R,

- Squares S, Taylor K, Warren T, Wietzorrek A, Woodward J, Barrell BG, Parkhill J, Hopwood DA. Complete genome sequence of the model actinomycete *Streptomyces coelicolor* A3(2). *Nature* 2002; 417:141-147
- [12] Bérday J. Bioactive microbial metabolites. *J. Antibiot.* 2005, 58, 1–26.
- [13] Bowers KJ, Mesbah NM, Wiegel J. Biodiversity of poly-extremophilic Bacteria: Does combining the extremes of high salt, alkaline pH and elevated temperature approach a physico-chemical boundary for life? *Saline Syst.* 2009; 5, 9.
- [14] Buckingham, J. Dictionary of Natural Products on DVD, version 21:1; CRC Press Taylor and Francis Group: London, UK, 2012.
- [15] Burkhart BJ, Hudson GA, Dunbar KL, Mitchell DA. A prevalent peptide-binding domain guides ribosomal natural product biosynthesis. *Nat. Chem. Biol.* 2015; 8, 564-570.
- [16] Bull AT, Asenjo JA. Microbiology of hyper-arid environments: recent insights from the Atacama Desert, Chile. *Antonie van Leeuwenhoek* 2013; 103:1173-1179.
- [17] Bull AT and Goodfellow M. Dark, rare and inspirational microbial matter in the extremobiosphere: 16 000 m of bioprospecting campaigns. *Microbiology* 2019; 11, [Epub ahead of print].
- [18] Bull AT, Stach JE, Ward AC, Goodfellow M. Marine actinobacteria: Perspectives, challenges, future directions. *Antonie Leeuwenhoek* 2005; 87, 65-79.
- [19] Bull AT, Ward AC and Goodfellow M. Search and Discovery Strategies for Biotechnology: The Paradigm Shift. 2000; 64, 573-606.
- [20] Busarakam K, Bull AT, Girard G, Labeda DP, VanWezel GP, Goodfellow M. *Streptomyces leeuwenhoekii* sp. nov., the producer of chaxalactins and chaxamycins, forms a distinct branch in *Streptomyces* gene trees. *Antonie Leeuwenhoek* 2014; 105, 849-861.
- [21] Carver T, Harris SR, Berriman M, Parkhill J and McQuillan JA. Artemis: an integrated platform for visualization and analysis of high-throughput sequence-based experimental data. *Bioinformatics* 2012; 28, 464-469.
- [22] Chalkley RJ, Baker PR, Huang L, Hansen KC, Allen NP, Rexach M, Burlingame AL. Comprehensive analysis of a multidimensional liquid chromatography mass spectrometry dataset acquired on a quadrupole selecting, quadrupole collision cell, time-of-flight mass spectrometer: II. New developments in Protein Prospector allow for reliable and comprehensive automatic analysis of large datasets. *Mol. Cell. Proteomics* 2005; 8, 1194-1204.
- [23] Challis GL. Mining microbial genomes for new natural products and biosynthetic pathways. *Microbiology.* 2018; 154, 1555-1569.
- [24] Challis GL, Ravel J and Townsend C. Predictive, structure-based model of amino acid recognition by nonribosomal peptide synthetase adenylation domains. *Chem. Biol.* 2000; 7, 211-24.
- [25] Chater KF and Horinouchi S. Signalling early developmental events in two highly diverged *Streptomyces* species. *Mol. Microbiol.* 2003; 48, 9-15.
- [26] Choi S-S, Kim H-J, Lee H-S, Kim P and Kim E-S. Genome mining of rare actinomycetes and cryptic pathway awakening. *Process Biochemistry* 2015; 50, 1184-1193.
- [27] Choekijchai S, Kojima E, Anderson S, Nomizu M, Tanaka M, Machida M, Date T, Toyota K, Ishida S, Watanabe K. NP-06: a novel anti-human immunodeficiency virus polypeptide produced by a *Streptomyces* species. *Antimicrob. Agents Chemother.* 1995; 10, 2345-2347.

- [28] Chun J, Oren A, Ventosa A, Christensen H, Arahal DR, da Costa MS, Rooney AP, Yi H, Xu XW, De Meyer S, Trujillo ME. Proposed minimal standards for the use of genome data for the taxonomy of prokaryotes. *Int. J. Syst. Evol. Microbiol.* 2018; 68, 461-466.
- [29] Chun J, Rainey FA. Integrating genomics into the taxonomy and systematics of the bacteria and archaea. *Int J Syst Evol Microbiol* 2014; 64:316–324.
- [30] Corre C and Challis GL. New natural product biosynthetic chemistry discovered by genome mining. *Natural Product Reports* 2009; 26, 977.
- [31] Cortés-Albayay C, Dorador C, Schumann P, Andrews BA, Asenjo J, Nouioui I. *Streptomyces huasconensis* sp. nov., an haloalkalitolerant actinobacteria isolated from a high altitude saline wetland at the Chilean Altiplano. *Int J Syst Evol Microbiol* 2019; 69(8): 2315-2322.
- [32] Cortés-Albayay C, Dorador C, Schumann P, Schniete JK, Herron P, Andrews B, Asenjo J, Nouioui I. *Streptomyces altiplanensis* sp. nov., an alkalitolerant species isolated from Chilean Altiplano soil, and emended description of *Streptomyces chryseus* (Krasil'nikov et al. 1965) Pridham 1970. *Int J Syst Evol Microbiol* 2019; 69(8): 2498-2505.
- [33] Cortés-Albayay C, Silber J, Imhoff JF, Asenjo JA, Andrews B, Nouioui I and Dorador C. The polyextreme ecosystem, Salar de Huasco at the Chilean Altiplano of the Atacama Desert houses diverse *Streptomyces* spp. with promising pharmaceutical potentials. *Diversity* 2019; 11, 69.
- [34] Craik DJ, Fairlie DP, Liras S and Price D. The Future of Peptide-based Drugs. *Chem. Biol. Drug Des.* 2013; 81, 136-147.
- [35] Daffre S, Bulet P, Spisni A, Ehret-Sabatier L, Rodrigues EG and Travassos LR. Bioactive natural peptides. *Stud. Nat. Prod. Chem.* 2008; 35, 597-691.
- [36] De Querioz, VM, Albert CA. *Streptomyces iakyrus* nov. sp., produtor dos antibióticos laquirina I, II, III. *Rev. Inst. Antibiot. Univ. Recife* 1962; 4, 33-46.
- [37] Detlefsen DJ, Hill SE, Volk KJ, Klohr SE, Tsunakawa M, Furumai T, Lin PF, Nishio M, Kawano K, Oki T and Lee MS. Siamycins I and II, new anti-HIV-1 peptides. II. Sequence analysis and structure determination of siamycin I. *J. Antibiot.* 1995; 48:1515-1517.
- [38] Demergasso C, Casamayor EO, Chong G, Galleguillos P, Escudero L and Pedrós-Alió C. Distribution of prokaryotic genetic diversity in athalassohaline lakes of the Atacama Desert, Northern Chile. *FEMS Microbiol. Ecol.* 2004; 48, 57-69.
- [39] Dharmaraj S. Marine *Streptomyces* as a novel source of bioactive substances. *World J. Microbiol. Biotechnol.* 2010; 26, 2123-2139.
- [40] Donadio S, Monciardini P and Sosio M. Polyketide synthases and nonribosomal peptide synthetases: the emerging view from bacterial genomics. *Nat. Prod. Rep.* 2007; 24, 1073-1109.
- [41] Donia MS, Ravel J and Schmidt EW. A global assembly line for cyanobactins. *Nat. Chem. Biol.* 2008; 4, 341-3.
- [42] Dorador C, Meneses D, Urtuvia V, Demergasso C, Vila I, Witzel K.P, Imhoff JF. Diversity of Bacteroidetes in high-altitude saline evaporitic basins in northern Chile. *J. Geophys. Res.* 2009; 114, G00D05.
- [43] Dorador C, Vila I, Witzel K-P, Imhoff JF. Bacterial and archaeal diversity in high altitude wetlands of the Chilean Altiplano. *Fundam. Appl. Limnol.* 2013; 182, 135-159.
- [44] Dorador C, Vila I, Remonsellez F, Imhoff JF, Witzel K-P. Unique clusters of Archaea in Salar de Huasco, an athalassohaline evaporitic basin of the Chilean Altiplano. *FEMS Microbiol. Ecol.* 2010; 73, 291-302.

- [45] Dorador C, Vila I, Imhoff JF, Witzel K-P. Cyanobacterial diversity in Salar de Huasco, a high altitude saline wetland in northern Chile: An example of geographical dispersion? *FEMS Microbiol. Ecol.* 2008; 64, 419-432.
- [46] Duquesne S, Petit V, Peduzzi J and Rebuffat S. Structural and functional diversity of microcins, gene-encoded antibacterial peptides from Enterobacteria. *J. Mol. Microbiol. Biotechnol.* 2007; 13, 200-209.
- [47] Edgar RC. MUSCLE: Multiple sequence alignment with high accuracy and high throughput. *Nucleic Acids Res.* 2004; 32, 1792-1797.
- [48] Elsayed SS, Trusch F, Deng H, Raab A, Prokes I, Busarakam K, Asenjo JA, Andrews BA, VanWest P, Bull AT, Goodfellow M, Yi Y, Ebel R, Jaspars M and Rateb ME. Chaxapeptin, a lasso peptide from extremotolerant *Streptomyces leeuwenhoekii* strain C58 from the hyperarid Atacama Desert. *J. Org. Chem.* 2015; 80, 10252-10260.
- [49] El-Shatoury SA, El-Shenawy NS and Abd El-Salam IM. Antimicrobial, antitumor and in vivo cytotoxicity of actinomycetes inhabiting marine shellfish. *World J. Microbiol. Biotechnol.* 2009; 25, 1547-1555.
- [50] Felsenstein J. Evolutionary trees from DNA sequences: A maximum likelihood approach. *J. Mol. Evol.* 1981; 17, 368-376.
- [51] Feng Z, Ogasawara Y, Nomura S, Dairi T. Biosynthetic Gene Cluster of a d-Tryptophan- Containing Lasso Peptide, MS-271. *ChemBioChem*, 2018; 19, 2045-2048.
- [52] Fiedler, H.P.; Bruntner, C.; Bull, A.T.; Ward, A.C.; Goodfellow, M.; Potterat, O.; Puder, C.; Mihm, G. Marine Actinomycetes as a source of novel secondary metabolites. *Antonie Leeuwenhoek* 2005; 87, 37-42.
- [53] Fitch WM. Toward defining the course of evolution: minimum change for a specific tree topology. *Syst Biol* 1971; 20:406-416.
- [54] Frechet D, Guitton JD, Herman F, Faucher D, Helynck G, Monegier du Sorbier B, Ridoux JP, James-Surcouf E and Vuilhorgne M. Solution structure of RP 71955, a new 21 amino acid tricyclic peptide active against HIV-1 virus. *Biochemistry*, 1994; 33, 42-50.
- [55] Fosgerau K and Hoffmann T. Peptide therapeutics: current status and future directions. *Drug Discov. Today*. 2015; 20, 122-128.
- [56] Gause GF, Preobrazhenskaya TP, Sveshnikova MA, Terekhova L.P, Maximova TS. A Guide for the Determination of Actinomycetes. Genera *Streptomyces*, *Streptoverticillium*, and *Chainia*; Nauka: Moscow, Russia; 1983.
- [57] Gauze GF, Preobrazhenskaya TP, Kudrina ES, Blinov NO, Ryabova ID and Sveshnikova MA. "Problems of classification of actinomycetes-antagonists." Government Publishing House of Medical Literature, Medgiz, Moscow 1957; pp. 1-398.
- [58] Gavrish E, Sit CS, Cao S, Kandror O, Spoering A, Peoples A, Ling L, Fetterman A, Hughes D, Bissell A, Torrey H, Akopian T, Mueller A, Epstein S, Goldberg A, Clardy J, Lewis K. Lassomycin, a ribosomally synthesized cyclic peptide, kills *mycobacterium tuberculosis* by targeting the ATP dependent protease ClpC1P1P2. *Chem. Biol.* 2014; 4, 509-518.
- [59] Goloboff PA, Farris JS, Nixon KC. TNT, a free program for phylogenetic analysis. *Cladistics* 2008; 24:774-786.
- [60] Gomez-Escribano JP, Castro JF, Razmilic V, Chandra G, Andrews B, Asenjo J and Bibb JM. The *Streptomyces leeuwenhoekii* genome: de novo sequencing and assembly in single contigs of the chromosome, circular plasmid pSLE1 and linear plasmid pSLE2. *BMC Genomics* 2015; 16, 485.



- [61] Goodfellow M, Busarakam K, Idris H, Labeda DP, Nouioui I, Brown R, Kim BY, Montero-Calasanz MC, Andrews B, Bull AT. *Streptomyces asenjonii* sp. nov., isolated from hyper-arid Atacama Desert soils and emended description of *Streptomyces viridosporus* Pridham et al. 1958. *Antonie van Leeuwenhoek* 2017; 110:1133-1148.
- [62] Goodfellow M, Nouioui I, Sanderson R, Xie F, Bull AT. Rare taxa and dark microbial matter: Novel bioactive actinobacteria abound in Atacama Desert soils. *Antonie Leeuwenhoek* 2018; 111, 1315–1332.
- [63] Goodfellow M, Williams ST, Alderson G. Transfer of *Kitasatoa purpurea* Matsuma and Hata to the genus *Streptomyces* as *Streptomyces purpurea* comb. nov. *Syst. Appl. Microbiol.* 1986; 8, 65–66.
- [64] Goris J, Konstantinidis KT, Klappenbach JA, Coenye T, Vandamme P, Tiedje JM. DNA-DNA hybridization values and their relationship to whole-genome sequence similarities. *Int J Syst Evol Microbiol* 2007; 57:81–91.
- [65] Hegemann JD, Zimmermann M, Xie X, Marahiel MA. Lasso peptides: an intriguing class of bacterial natural products. *Acc. Chem. Res.* 2015; 7, 1909-1919.
- [66] Hegemann JD, Zimmermann M, Zhu S, Steuber H, Harms K, Xie X, Marahiel MA. Xanthomonins I- III: a new class of lasso peptides with a seven-residue macrolactam ring. *Chem. Int. Ed Engl.* 2014; 8, 2230-2234.
- [67] Han L, Zhang G, Miao G, Zhang X, Feng J. *Streptomyces kanasensis* sp. nov., an Antiviral Glycoprotein Producing Actinomycete Isolated from Forest Soil Around Kanas Lake of China. *Curr. Microbiol.* 2015; 71, 627-631.
- [68] Hernandez KL, Yannicelli B, Olsen LM, Dorador C, Menschel EJ et al. Microbial activity response to solar radiation across contrasting environmental conditions in salar de huasco, Northern Chilean altiplano. *Front Microbiol* 2016; 7:7.
- [69] Hetrick KJ, van der Donk WA. Ribosomally synthesized and Posttranslationally modified peptide natural product discovery in the genomic era. *Current Opinion in Chemical Biology*, 2017; 38:36-44.
- [70] Hou Y-H, Qin S, Li Y-X, Li F-C, Xia H-Z and Zhao F-Q. Heterologous Expression and Purification of Recombinant Allophycocyanin in Marine *Streptomyces* sp. Isolate M097. *World J. Microbiol. Biotechnol.* 2006; 22, 525-529.
- [71] Hudson GA, Burkhart BJ, DiCaprio AJ, Schwalen C, Kille B, Pogorelov TV, Mitchell DA. “Bioinformatic mapping of radical SAM-dependent RIPPs identifies new C $\alpha$ , C $\beta$ , and C $\gamma$ -linked thioether-containing peptides.” *J. Am. Chem. Soc.*, 2019; 141, 8228-8238.
- [72] Idris H, Labeda DP, Nouioui I, Castro JF, Del Carmen Montero-Calasanz M, Bull AT, Asenjo JA, Goodfellow M. *Streptomyces aridus* sp. nov., isolated from a high altitude Atacama desert soil and emended description of *Streptomyces noboritoensis* Isono et al. 1957. *Antonie van Leeuwenhoek* 2017; 110:705-717.
- [73] Ingebrigtsen RA, Hansen E, Andersen JH, Eilertsen HCJ. Light and temperature effects on bioactivity in diatoms. *Appl. Phycol.* 2016; 939-950.
- [74] Iwatsuki M, Tomoda H, Uchida R, Gouda H, Hirono S, Omura SJ. Am. Lariatins, antimycobacterial peptides produced by *Rhodococcus* sp. K01-B0171, have a lasso structure. *Chem. Soc.* 2006; 23, 7486-7491.
- [75] Kampf P. Genus I. *Streptomyces*. In: Whitman W, Goodfellow M, Kampf P, Busse H-J, Trujillo M et al. (editors). *Bergey's Manual of Systematic Bacteriology*, 2nd ed, vol. 5. The Actinobacteria, Part B. New York: Springer; 2012; pp. 1455-1767.
- [76] Kampf P, Kroppenstedt RM and Dott W. A numerical classification of the genera *Streptomyces* and *Streptoverticillium* using miniaturized physiological tests. *J. Gen. Microbiol.* 1991; 137, 1831-1891.

- [77] Kaweewan I, Hemmi H, Komaki H, Harada S, Kodani S. Isolation and structure determination of a new lasso peptide specialicin based on genome mining. *Bioorganic & Medicinal Chemistry* 2018; 23, 6050-6055.
- [78] Kelly KL. Color Name Charts Illustrated with Centroid Colors; Supplement to NBS Circular 553. Inter-Society Color Council—National Bureau of Standards (ISCC-NBS); U. S. National Bureau of Standards: Washington, DC, USA, 1964.
- [79] Kersten RD, Yang Y-L, Xu Y, Cimermancic P, Nam S-J, Fenical W, Fischbach MA, Moore BS and Dorrestein PC. A mass spectrometry-guided genome mining approach for natural product peptidogenomics. *Nat. Chem. Biol.* 2011; 7, 794-802.
- [80] Kimura M. A simple method for estimating evolutionary rates of base substitutions through comparative studies of nucleotide sequences. *J Mol Evol* 1980; 16:111-120.
- [81] Kim OS, Cho YJ, Lee K, Yoon SH, Kim M, Na H, Park SC, Jeon YS, Lee JH, Yi H, Won S, Chun J. Introducing EzTaxon-e: A prokaryotic 16S rRNA gene sequence database with phylotypes that represent uncultured species. *Int. J. Syst. Evol. Microbiol.* 2012; 62, 716–721-
- [82] Knappe TA, Linne U, Robbel L, Marahiel MA. Insights into the biosynthesis and stability of the lasso peptide capistrain. *Chemistry & Biology* 2009; 12, 1290-1298.
- [83] Krasil'nikov NA, Korenyako AI, Nikitina NI. Actinomycetes of the yellow group. In: Krasil'nikov NA (editor). *Biology of selected groups of Actinomycetes (in Russian)*. Moscow: Publishing Firm Nauka 1965; pp. 1-372.
- [84] Kroppenstedt R. Fatty acid and menaquinone analysis of actinomycetes and related organisms. In: Goodfellow M and Minnikin DE (editors). *Chemical Methods in Bacterial Systematics*. London: Elsevier Science & Technology Books 1985; pp. 173-199.
- [85] Kudrina ES. In: Gauze G, Preobrazhenskaya TP and Kudrina ES (editors). *Problems of Classification of Actinomycetes-Antagonists*. Moscow: Publishing house of medical literature, Medgiz; 1957. pp. 1–398.
- [86] Kuester E, Williams ST. Selection of media for isolation of *Streptomyces*. *Nature* 1964; 202, 928-929.
- [87] Kumar S, Stecher G, Tamura K. MEGA7: Molecular Evolutionary Genetics Analysis Version 7.0 for Bigger Datasets. *Mol. Biol. Evol.* 2016; 33, 1870-1874.
- [88] Kuykendall LD, Roy MA, O'Neill JJ, Devine TE. Fatty acids, antibiotic resistance, and deoxyribonucleic acid homology groups of *Bradyrhizobium japonicum*. *Int J Syst Bacteriol* 1988; 38:358-361.
- [89] Labeda DP. Taxonomic evaluation of putative *Streptomyces scabiei* strains held in the ARS Culture Collection (NRRL) using multilocus sequence analysis. *Antonie van Leeuwenhoek* 2016; 109:349-356.
- [90] Labeda DP, Dunlap CA, Rong X, Huang Y, Doroghazi JR, Ju KS, Metcalf WW. Phylogenetic relationships in the family Streptomycetaceae using multi-locus sequence analysis. *Antonie van Leeuwenhoek* 2017; 110:563-583.
- [91] Labeda DP, Goodfellow M, Brown R, Ward AC, Lanoot B et al. Phylogenetic study of the species within the family Streptomycetaceae. *Antonie van Leeuwenhoek* 2012; 101:73–104.
- [92] Lautru S, Deeth RJ, Bailey LM and Challis GL. Discovery of a new peptide natural product by *Streptomyces coelicolor* genome mining. *Nature Chemical Biology*, 2005; 1, 265-269.
- [93] Lechevalier MP, Lechevalier H. Chemical composition as a criterion in the classification of aerobic actinomycetes. *Int J Syst Bacteriol* 1970; 20:435-443.

- [94] Lee I, Ouk Kim Y, Park SC, Chun J. OrthoANI: An improved algorithm and software for calculating average nucleotide identity. *Int J Syst Evol Microbiol* 2016; 66:1100–1103.
- [95] Le Roes-Hill M, Rohland J, Meyers PR, Cowan DA, Burton SG. *Streptomyces hypolithicus* sp. nov., isolated from an Antarctic hypolith community. *Int J Syst Evol Microbiol* 2009; 59:2032-2035.
- [96] Li C and Kelly WL. Recent advances in thiopeptideantibiotic biosynthesis. *Nat. Prod. Rep.* 2010; 27, 153-164.
- [97] Li MH, Ung PM, Zajkowski J, Garneau-Tsodikova S and Sherman DH. Automated genome mining for natural products. *BMC Bioinformatics*, 2009; 10, 185.
- [98] Li Y, Ducasse R, Zirah S, Blond A, Goulard C, Lescop E, Giraud C, Hartke A, Guittet E, Pernodet JL, Rebuffat S. Characterization of Svceucin from *Streptomyces* Provides Insight into Enzyme Exchangeability and Disulfide Bond Formation in Lasso Peptides. *ACS Chem. Biol.* 2015; 11, 2641-2649.
- [99] Lindenbein W. Über Einige Chemisch Interessante Aktinomycetenstämme Und Ihre Klassifizierung. *Arch. Mikrobiol.* 1952; 17, 361-383.
- [100] Liu W-T, Yang Y-L, Xu Y, Lamsa A, Haste NM, Yang JY, Ng J, Gonzalez D, Ellermeier CD, Straight PD, Pevzner PA, Pogliano J, Nizet V, Pogliano K and Dorrestein PC. Imaging mass spectrometry of intraspecies metabolic exchange revealed the cannibalistic factors of *Bacillus subtilis*. *Proc. Natl. Acad. Sci. U. S. A.* 2010; 107, 16286-16290.
- [101] Lyutskanova D, Ivanova, V, Stoilova-Disheva M, Kolarova M, Aleksieva K, Peltekova V. Isolation and characterization of a psychrotolerant *Streptomyces* strain from permafrost soil in Spitsbergen, producing phthalic acid ester. *Biotechnol. Biotechnol. Equip.* 2009; 23, 1220-1224.
- [102] McIntosh JA, Donia MS and Schmidt EW. Ribosomal Peptide Natural Products: Bridging the Ribosomal and Nonribosomal Worlds. *Nat. Prod. Rep* 2009; 26, 537-559.
- [103] Maksimov MO, Link AJ. Discovery and characterization of an isopeptidase that linearizes lasso peptides. *J. Am. Chem. Soc.* 2013; 135, 12038-12047.
- [104] Maksimov MO and Link AJ. Prospecting genomes for lasso peptides. *J Ind Microbiol Biotechnol.* 2014; 41, 333-344.
- [105] Maksimov MO, Pan SJ, James LA. Lasso peptides: structure, function, biosynthesis, and engineering. *Nat. Prod. Rep.* 2012; 9, 996-1006.
- [106] Manfio GP, Atalan E, Zakrzewska-Czerwinska J, Mordarski M, Rodríguez C et al. Classification of novel soil Streptomycetes as *Streptomyces aureus* sp. nov., *Streptomyces laceyi* sp. nov. And *Streptomyces sanglieri* sp. nov. *Antonie van Leeuwenhoek* 2003; 83: 245–255.
- [107] Marchler-Bauer A, Derbyshire MK, Gonzales NR, Lu S, Chitsaz F, Geer LY, Geer RC, He J, Gwadz, M, Hurwitz DI, Lanczycki CL, Lu F, Marchler GH, Song JS, Thanki N, Wang Z, Yamashita RA, Zhang D and Bryant SH. CDD: NCBI's conserved domain database. *Nucleic Acids Res.* 2015, 43, D222-D226.
- [108] Meier-Kolthoff JP, Auch AF, Klenk HP, Göker M. Genome sequence-based species delimitation with confidence intervals and improved distance functions. *BMC Bioinformatics* 2013; 14:60.
- [109] Meier-Kolthoff JP, Göker M, Spröer C, Klenk HP. When should a DDH experiment be mandatory in microbial taxonomy? *Arch Microbiol* 2013; 195:413-418.
- [110] Meier-Kolthoff JP, Hahnke RL, Petersen J, Scheuner C, Michael V, Fiebig A, Rohde C, Rohde M, Fartmann B, Goodwin LA, Chertkov O, Reddy T, Pati A, Ivanova NN, Markowitz V, Kyrpidis NC, Woyke T, Göker M, Klenk HP. Complete genome sequence of DSM 30083T, the type strain (U5/41T) of *Escherichia coli*, and a proposal for delineating subspecies in microbial taxonomy. *Stand Genomic Sci* 2014; 9:2.

- [111] Miller LT. Single derivatization method for routine analysis of bacterial whole-cell fatty acid methyl esters, including hydroxy acids. *J Clin Microbiol* 1982; 16:584-586.
- [112] Miller ED, Kauffman CA, Jensen PR and Fenical W. Piperazimycins: Cytotoxic Hexadepsipeptides from a Marine-Derived Bacterium of the Genus *Streptomyces*. *J. Org. Chem.* 2007; 72, 323-330.
- [113] Minnikin DE, O'Donnell AG, Goodfellow M, Alderson G, Athalye M, Schaal A, Parlett JH. An integrated procedure for the extraction of bacterial isoprenoid quinones and polar lipids. *J Microbiol Methods* 1984; 2: 233-241.
- [114] Mohimani H and Pevzner PA. Dereplication, sequencing and identification of peptidic natural products: from genome mining to peptidogenomics to spectral networks. *Nat. Prod. Rep.* 2016; 33, 73-86.
- [115] Molina V, Hernandez K, Dorador C, Hengst M, Pérez, V. Bacterial active community cycling in response to solar radiation and their influence on nutrient changes in a high-altitude wetland. *Front. Microbiol.* 2016; 7, 1823.
- [116] Moore BS. Extending the Biosynthetic Repertoire in Ribosomal Peptide Assembly. *Angew. Chemie Int. Ed.* 2008; 47, 9386-9388.
- [117] Morris LA, Jantina Kettenes van den Bosch J, Versluis K, Thompson GS and Jaspars M. Structure Determination and MSn Analysis of Two New Lissoclinamides Isolated from the Indo-Pacific Ascidian *Lissoclinum patella*: NOE Restrained Molecular Dynamics Confirms the Absolute Stereochemistry Derived by Degradative Methods. *Tetrahedron*, 2000; 56(42), 8345-8353.
- [118] Muyzer G, de Waal EC, Uitterlinden AG. Profiling of complex microbial populations by denaturing gradient gel electrophoresis analysis of polymerase chain reaction-amplified genes coding for 16S rRNA. *Appl. Environ. Microbiol.* 1993; 59:695-700.
- [119] Nachtigall J, Kulik A, Helaly S, Bull AT, Goodfellow M, Asenjo JA, Maier A, Wiese J, Imhoff JF, Sussmuth RD and Fiedler HP. Atacamycins A–C, 22-membered antitumor macrolactones produced by *Streptomyces* sp. C38. *J. Antibiot.* 2011; 64, 775-780.
- [120] Nagai A, Khan ST, Tamura T, Takagi M, Shin-Ya K. *Streptomyces aomiensis* sp. nov., isolated from a soil sample using the membrane-filter method. *Int J Syst Evol Microbiol* 2011; 61:947-950.
- [121] Nett M. Genome Mining: Concept and Strategies for Natural Product Discovery. *Progress in the Chemistry of Organic Natural Products* 2014, 199-245.
- [122] Nolan EM and Walsh CT. How Nature Morphs Peptide Scaffolds into Antibiotics. *ChemBioChem*, 2009, 10, 34-53.
- [123] Nouioui I, Carro L, García-López M, Meier-Kolthoff JP, Woyke T, Kyrpides NC, Pukall R, Klenk HP, Goodfellow M, Göker M. Genome-based taxonomic classification of the phylum Actinobacteria. *Front Microbiol* 2018; 9:9.
- [124] Okami Y and Umezawa H. Production and isolation of a new antibiotic, kanamycin. *J. Antibiot.* 1957, 10,181-189.
- [125] Okoro CK, Brown R, Jones AL, Andrews BA, Asenjo JA et al. Diversity of culturable actinomycetes in hyper-arid soils of the Atacama Desert, Chile. *Antonie van Leeuwenhoek* 2009; 95:121–133.
- [126] Onaka H. Biosynthesis of heterocyclic antibiotics in Actinomycetes and an approach to synthesize the natural compounds. *Actinomycetologica* 2006; 20, 62–71.
- [127] Overbeek R, Olson R, Pusch GD, Olsen GJ, Davis JJ, Disz T, Edwards RA, Gerdes S, Parrello B, Shukla M, Vonstein V, Wattam AR, Xia F and Stevens R. The SEED and the Rapid Annotation of microbial genomes using Subsystems Technology (RAST). *Nucleic Acids Res* 2014; 42:D206–D214.

- [128] Pan SJ, Rajniak J, Maksimov MO, Link AJ. The role of a conserved threonine residue in the leader peptide of lasso peptide precursors. *Chem. Commun. (Camb)* 2012; 13, 1880-1882.
- [129] Pandian TJ. *Microbial Diversity and Bioprospecting*. Alan T. Bull (ed.). American Society for Microbiology, ASM Press, Washington DC. 2004; 496 pp.
- [130] Pathom-aree W, Stach JEM, Ward AC, Horikoshi K, Bull AT, Goodfellow M. Diversity of Actinomycetes isolated from Challenger Deep sediment (10,898 m) from the Mariana Trench. *Extremophiles* 2006; 10, 181-189.
- [131] Pridham TG, Hesseltine CW, Benedict RG. A guide for the classification of Streptomyces according to selected groups; placement of strains in morphological sections. *Appl Microbiol* 1958; 6:52-79.
- [132] Pattengale ND, Alipour M, Bininda-Emonds OR, Moret BM, Stamatakis A. How many bootstrap replicates are necessary? *J Comput Biol.* 2010; 17:337-354.
- [133] Ping X, Takahashi Y, Seino A, Iwai Y, Omura S. *Streptomyces scabrisporus* sp. nov. *Int J Syst Evol Microbiol* 2004; 54:577–581.
- [134] Potterat O, Stephan H, Metzger JW, Gnau V, Zähler H, Jung G. Aborycin – A Tricyclic 21 Peptide Antibiotic Isolated from *Streptomyces griseoflavus*. *Liebigs Annalen der Chemie* 1994; 7, 741-743.
- [135] Preobrazhenskaya, TP, Kudrina ES, Blinov NO, Ryabova ID, Sveshnikova MA. Eds; Government Publishing House of Medical Literature: Medgiz, Moscow, Russia. 1957; 1-398.
- [136] Rateb ME, Ebel R, Jaspars M. Natural product diversity of actinobacteria in the Atacama Desert. *Antonie van Leeuwenhoek* 2018; 111:1467-1477.
- [137] Rateb ME.; Houssen WE, Harrison WTA, Deng H, Okoro CK, Asenjo JA, Andrews BA, Bull AT, Goodfellow M, Ebel R, Jaspars M. Diverse metabolic profiles of a *Streptomyces* strain isolated from a hyper-arid environment. *J. Nat. Prod.* 2011, 74, 1965–1971.
- [138] Rausch C, Weber T, Kohlbacher O, Wohlleben W and Huson DH. Specificity prediction of adenylation domains in nonribosomal peptide synthetases (NRPS) using transductive support vector machines (TSVMs). *Nucleic Acids Res.* 2005; 33, 5799-5808.
- [139] Rateb ME, Houssen WE, Arnold M, Abdelrahman MH, Deng H, Harrison WT, Okoro CK, Asenjo JA, Andrews BA, Ferguson G, Bull AT, Goodfellow M, Ebel R, Jaspars M. Chaxamycins A-D, bioactive ansamycins from a hyper-arid desert *Streptomyces* sp. *J. Nat. Prod.* 2011; 74, 1491–1499.
- [140] Richter M, Rosselló-Móra R. Shifting the genomic gold standard for the prokaryotic species definition. *Proc Natl Acad Sci USA.* 2009;106:19126–19131.
- [141] Rong X, Huang Y. Multi-locus sequence analysis. Taking prokaryotic systematics to the next level. *Methods Microbiol* 2014; 41:221–251.
- [142] Rong X, Huang Y. Taxonomic evaluation of the *Streptomyces hygroscopicus* clade using multilocus sequence analysis and DNA-DNA hybridization, validates the MLSA scheme for systematics of the whole genus. *Syst Appl Microbiol* 2012; 35:7–18.
- [143] Röttig M, Medema MH, Blin K, Weber T, Rausch C and Kohlbacher O. NRSPredictor2 - a web server for predicting NRPS adenylation domain specificity. *Nucleic Acids Research* 2011; 39, W362- W367.
- [144] Saitou N, Nei M. The neighbor-joining method: A new method for reconstructing phylogenetic trees. *Mol. Biol. Evol* 1987; 4, 406-425.

- [145] Sánchez C, Méndez C, Salas JA. Engineering biosynthetic pathways to generate antitumor indolocarbazole derivatives. *J. Ind. Microbiol. Biotechnol* 2006; 33, 560–568.
- [146] Santhanam R, Okoro CK, Rong X, Huang Y, Bull AT, Weon HY, Andrews BA, Asenjo JA, Goodfellow M. *Streptomyces atacamensis* sp. nov., isolated from an extreme hyper-arid soil of the Atacama Desert, Chile. *Int. J. Syst. Evol. Microbiol* 2012; 62, 2680–2684.
- [147] Santhanam R, Okoro CK, Rong X, Huang Y, Bull AT, Andrews BA, Asenjo JA, Weon HY, Goodfellow M. *Streptomyces deserti* sp. nov., isolated from hyper-arid Atacama Desert soil. *Antonie Leeuwenhoek* 2012; 101, 575–581.
- [148] Santhanam R, Rong X, Huang Y, Andrews BA, Asenjo JA, Goodfellow M. *Streptomyces bullii* sp. nov., isolated from a hyper-arid Atacama Desert soil. *Antonie Leeuwenhoek* 2013; 103, 367–373.
- [149] Sasser M. Identification of Bacteria by Gas Chromatography of Cellular Fatty Acids, Technical Note 101. Microbial ID. Newark, USA: Del Inc; 1990.
- [150] Savic M, Bratic I, Vasiljevic B. *Streptomyces durmitorensis* sp. nov., a producer of an FK506-like immunosuppressant. *Int J Syst Evol Microbiol* 2007; 57:2119–2124.
- [151] Schneemann I, Kajahn I, Ohlendorf B, Zinecker H, Erhard A, Nagel K, Wiese J, Imhoff JF. Mayamycin, a Cytotoxic Polyketide from a *Streptomyces* Strain Isolated from the Marine Sponge *Halichondria panicea*. *J. Nat. Prod.* 2010; 73, 1309–1312.
- [152] Schniete JK, Salih TS, Algora-Gallardo L, Santos T, Filgueira- Martinez S et al. Draft genome sequence of *Streptomyces phaeoluteigriseus* DSM41896. *Genome Announc* 2017; 5:e00371–17.
- [153] Schulz D, Beese P, Ohlendorf B, Erhard A, Zinecker H, Dorador C, Imhoff JF. Abenquines A–D: Aminoquinone derivatives produced by *Streptomyces* sp. strain DB634. *J. Antibiot.* 2011; 64, 763–768.
- [154] Severinov K, Semenova E, Kazakov A, Kazakov T and Gelfand MS. Low-molecular-weight post-translationally modified microcins. *Mol. Microbiol.* 2007; 65, 1380–1394.
- [155] Shirling EB, Gottlieb D. Methods for characterization of *Streptomyces* species. *Int. J. Syst. Bacteriol.* 1966, 16, 313–340.
- [156] Sikandar A, Koehnke J. The role of protein-protein interactions in the biosynthesis of ribosomally synthesized and Posttranslationally modified peptides. *Nat Prod Rep*, 2019.
- [157] Silber J, Ohlendorf B, Labes A, Erhard A, Imhoff J.F. Calcarides A–E, antibacterial macrocyclic and linear polyesters from a *calcarisporium* strain. *Mar. Drugs* 2013, 11, 3309–3323.
- [158] Skinnider MA, Merwin NJ, Johnston CW, Magarvey NA. PRISM 3: expanded prediction of natural product chemical structures from microbial genomes. *Nucleic Acids Res.* 2017; W1, W49–W54.
- [159] Skinnider MA, Dejong CA, Rees PN, Johnston CW, Li H, Webster ALH, Wyatt MA and Magarvey NA. Genomes to natural products Prediction Informatics for Secondary Metabolomes (PRISM). *Nucleic Acids Res.* 2015; 43, 9645–9662,
- [160] Stackebrandt E, Liesack W. Nucleic Acids and Classification. In: Goodfellow M and O'Donnell AG (editors). *Handbook of New Bacterial Systematics* Academic Press 1993; pp. 151–194.
- [161] Stackebrandt E, Rainey FA and Ward-Rainey NL. Proposal for a New Hierarchic Classification System, Actinobacteria classis nov. *Int. J. Syst. Bacteriol.* 1997; 47, 479–491.
- [162] Starcevic A, Zucko J, Simunkovic J, Long, PF, Cullum J and Hranueli D. ClustScan: An integrated program package for the semi-automatic annotation of modular biosynthetic gene clusters and in silico prediction of novel chemical structures. *Nucleic Acids Res.* 2008; 36, 6882–6892.

- [163] Stamatakis A. RAxML version 8: a tool for phylogenetic analysis and post-analysis of large phylogenies. *Bioinformatics* 2014; 30: 1312–1313.
- [164] Staneck JL, Roberts GD. Simplified approach to identification of aerobic actinomycetes by thin-layer chromatography. *Appl Microbiol* 1974; 28:226–231.
- [165] Steven B, Pollard WH, Greer CW, Whyte LG. Microbial diversity and activity through a permafrost/ground ice core profile from the Canadian high Arctic. *Environ. Microbiol.* 2008; 10, 3388– 3403.
- [166] Swofford DL. P. PAUP\*. Phylogenetic Analysis Using Parsimony (\*and Other Methods). Version 4. Sunderland: Sinauer Associates 2003.
- [167] Tamura T, Hayakawa M, Hatano K. A new genus of the order Actinomycetales, *Cryptosporangium* gen. nov., with descriptions of *Cryptosporangium arvum* sp. nov. and *Cryptosporangium japonicum* sp. nov. *Int J Syst Bacteriol* 1998; 48 Pt 3:995–1005.
- [168] Tietz JI, Schwalen CJ, Patel PS, Maxson T, Blair PM, Tai HC, Zakai UI, Mitchell DA. A new genome-mining tool redefines the lasso peptide biosynthetic landscape. *Nat. Chem. Biol.* 2017; 5, 470- 478.
- [169] Tindall BJ. Lipid composition of *Halobacterium lacusprofundi*. *FEMS Microbiol Lett* 1990; 66:199–202.
- [170] Tsunakawa M, Hu SL, Hoshino Y, Detlefson DJ, Hill SE, Furumai T, White RJ, Nishio M, Kawano K, Yamamoto S, Fukagawa Y, Oki T. Siamycins I and II, new anti-HIV peptides: I. Fermentation, isolation, biological activity and initial characterization. *J Antibiot (Tokyo)*, 1995; 48:433-4.
- [171] Umezawa H, Ueda M, Maeda K, Yagishita K, Kondo S, Okami Y, Utahara R, Osato Y, Nitta K, Takeuchi T. Production and isolation of a new antibiotic: kanamycin. *J Antibiot* 1957; 10:181–188.
- [172] Vaas LA, Sikorski J, Hofner B, Fiebig A, Buddruhs N, Klenk HP, Goker M. opm: an R package for analysing OmniLog(R) phenotype microarray data. *Bioinformatics* 2013; 29: 1823-1824.
- [173] Vaas LA, Sikorski J, Michael V, Göker M, Klenk HP. Visualization and curve-parameter estimation strategies for efficient exploration of phenotype microarray kinetics. *PLoS One* 2012; 7:e34846.
- [174] Velásquez JE and Van der Donk WA. Genome mining for ribosomally synthesized natural products. *Curr. Opin. Chem. Biol.* 2011, 15, 11-21.
- [175] Vickers JC, Williams ST, Ross GW. A taxonomic approach to selective isolation of Streptomycetes from soil. In *Biological and Biochemical Aspects of Actinomycetes*; Ortiz-Ortiz, L., Bojalil, L.F., Yakole, V., Eds.; Academic Press: Orlando, FL, USA, 1984; pp. 553–561.
- [176] Vriend G. WHAT IF: A molecular modeling and drug design program. *J. Mol. Graph.* 1990; 8, 52-56.
- [177] Waksman SA, Henrici AT. The Nomenclature and Classification of the Actinomycetes. *J Bacteriol* 1943; 46:4.
- [178] Waksman SA, Lechevalier HA. Guide to the Classification and Identification of the Actinomycetes and Their Antibiotics. Baltimore: Williams & Wilkins; 1953.
- [179] Wang Q, Garrity GM, Tiedje JM, Cole JR. Naive bayesian classifier for rapid assignment of rRNA sequences into the new bacterial taxonomy. *Appl. Environ. Microbiol.* 2007, 73, 5261–5267.
- [180] Watve M, Tickoo R, Jog M, Bhole B. How many antibiotics are produced by the genus *Streptomyces*? *Arch. Microbiol.* 2001; 176, 386–390.

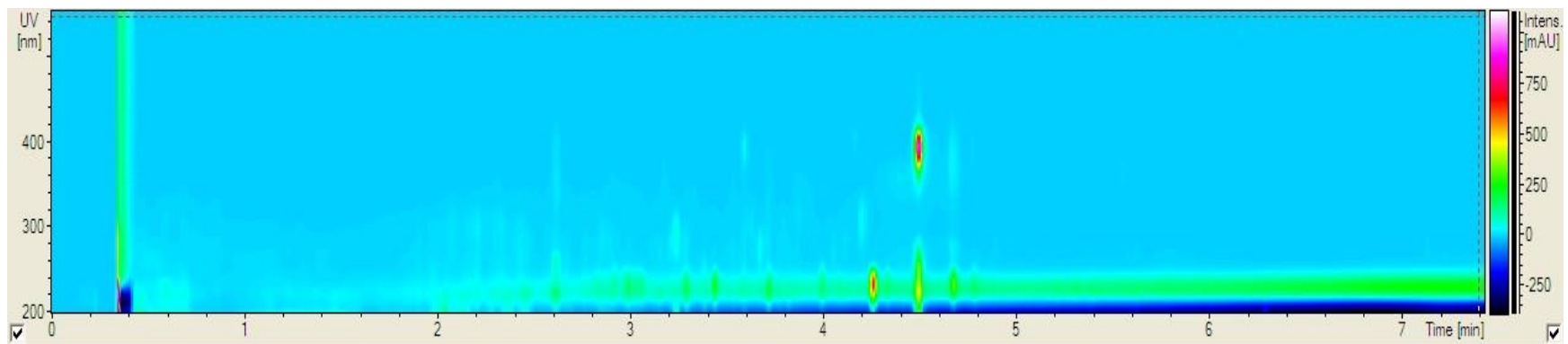
- [181] Wayne LG, Brenner DJ, Colwell RR, Grimont PAD, Kandler O, Krichevsky MI, Moore LH, Moore WEC, Murray RGE, Stackebrandt E, Starr MP, Truper HG. Report of the Ad Hoc Committee on Reconciliation of Approaches to Bacterial Systematics. *Int J Syst Evol Microbiol* 1987; 37, 463-464.
- [182] Weber W, Fischli W, Hochuli E, Kupfer E, Weibel EK. Anantin--a peptide antagonist of the atrial natriuretic factor (ANF). I. Producing organism, fermentation, isolation and biological activity. *J Antibiot*, 1991; 44(2): 164-71.
- [183] Weber T, Blin K, Duddela S, Krug D, Kim HU, Bruccoleri R, Lee SY, Fischbach MA, Muller R, Wohlleben W, Breitling R, Takano E and Medema MH. antiSMASH 3.0--a comprehensive resource for the genome mining of biosynthetic gene clusters. *Nucleic Acids Res.* 2015; 43, W237-43.
- [184] Williams ST, Goodfellow M, Wellington EM, Vickers JC, Alderson G, Sneath PH, Sackin MJ and Mortimer AM. A probability matrix for identification of some *Streptomyces*. *J. Gen. Microbiol.* 1983; 129, 1815-1830.
- [185] Wyss DF, Lahm HW, Manneberg M, Labhardt AM. Anantin--a peptide antagonist of the atrial natriuretic factor (ANF). II. Determination of the primary sequence by NMR on the basis of proton assignments. *J Antibiot (Tokyo)*. 1991; Feb;44(2):172-80.
- [186] Xie X, Marahiel MA. NMR as an effective tool for the structure determination of lasso peptides. *Chembiochem* 2012; 5, 621-625.
- [187] Xu LH, Jiang Y, Li WJ, Wen ML, Li MG, Jiang CL. *Streptomyces roseoalbus* sp. nov., an actinomycete isolated from soil in Yunnan, China. *Antonie Van Leeuwenhoek* 2005; 87:189-194.
- [188] Yano K, Toki S, Nakanishi S, Ochiai K, Ando K, Yoshida M, Matsuda Y, Yamasaki M. MS-271, a novel inhibitor of calmodulin-activated myosin light chain kinase from *Streptomyces* sp.--I. isolation, structural determination and biological properties of MS-271. *Bioorg. Med. Chem.* 1996; 1, 115.
- [189] Ye L, Zhou Q, Liu C, Luo X, Na G and Xi T. Identification and fermentation optimization of a marine-derived *Streptomyces griseorubens* with anti-tumor activity. *Indian J. Mar. Sci.* 2009; 38, 14-21.
- [190] Yoon SH, Ha SM, Kwon S, Lim J, Kim Y et al. Introducing EzBio- Cloud: a taxonomically united database of 16S rRNA gene sequences and whole-genome assemblies. *Int J Syst Evol Microbiol* 2017; 67:1613-1617.
- [191] Yoon SH, Ha SM, Lim J, Kwon S, Chun J. A large-scale evaluation of algorithms to calculate average nucleotide identity. *Antonie van Leeuwenhoek* 2017; 110:1281-1286.
- [192] Zhao P, Xue Y, Gao W, Li J, Zu X, Fu D, Feng S, Bai X, Zuo Y, Li P. Actinobacteria-Derived peptide antibiotics since 2000. *Peptides* 2018; 103:48-59
- [193] Zhu S, Fage CD, Hegemann JD, Mielcarek A, Yan D, Linne U, Marahiel MA. The B1 Protein Guides the Biosynthesis of a Lasso Peptide. *Sci. Rep.* 2016; 35604.
- [194] Ziemert N, Alanjary M and Weber T. Natural Product Reports The evolution of genome mining in microbes -- a review. *Nat. Prod. Rep.* 2016; 0, 1-18.



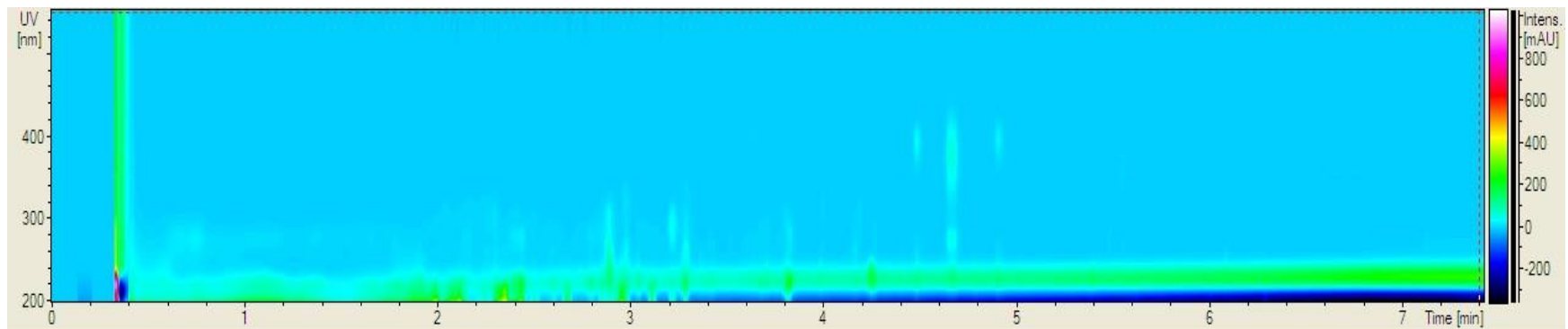
# Appendices

**Appendix 1.** HPLC-UV/Vis Chromatographic profiles obtained from culture metabolic extracts for analysed strains, which were grown in liquid media GYM4 **(A)** and SPM **(B)** both of them at 2% NaCl. To the left of the graphics it is the absorbance (nm) within UV spectrum, to the right, the intensity of the elution peaks (mAU), and at the bottom, the elution time.

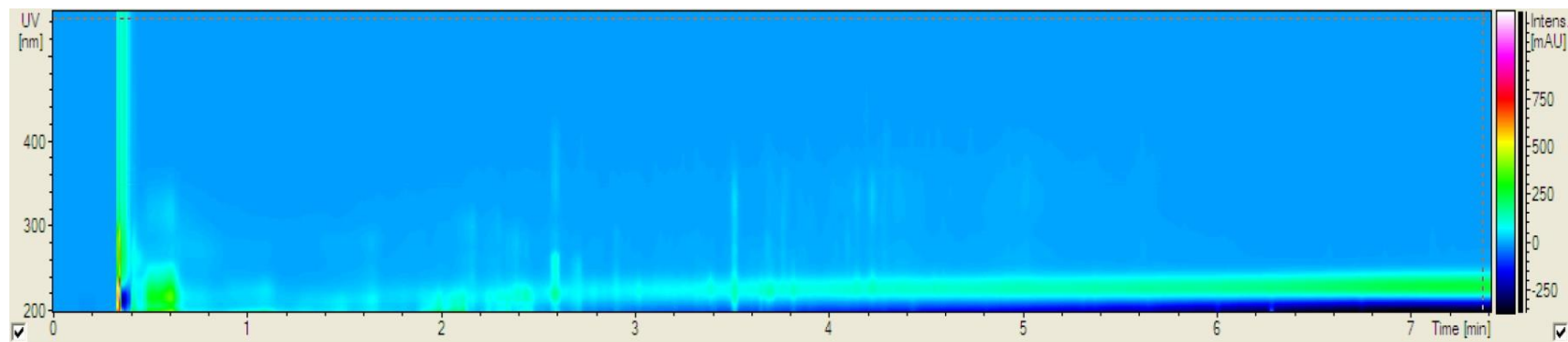
**(A) HST09-GYM**



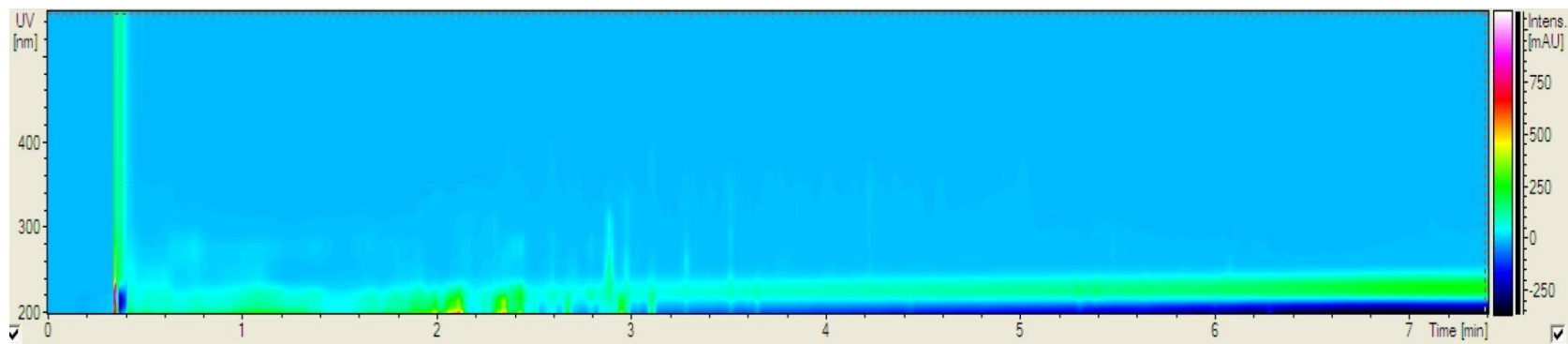
**(B) HST09-SPM**



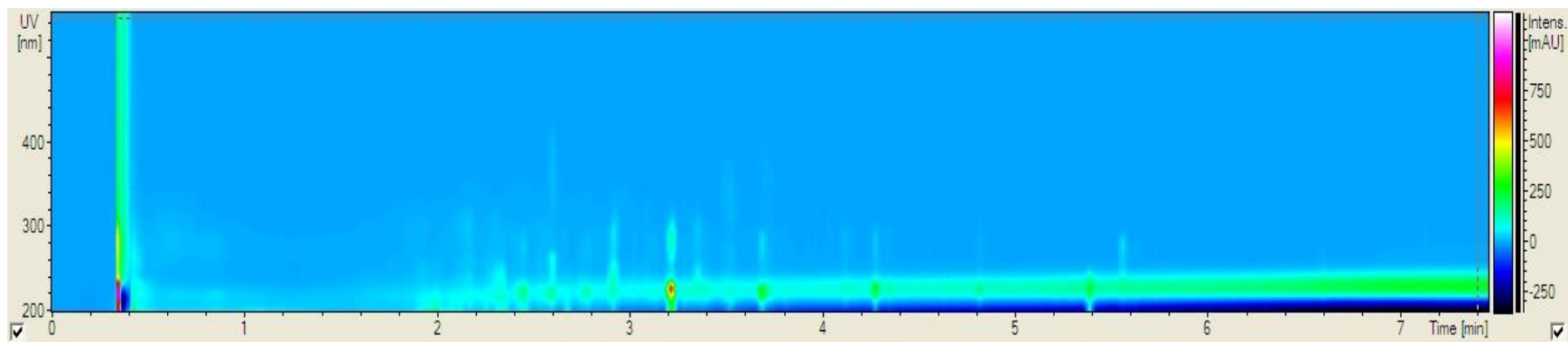
**(A) HST14-GYM**



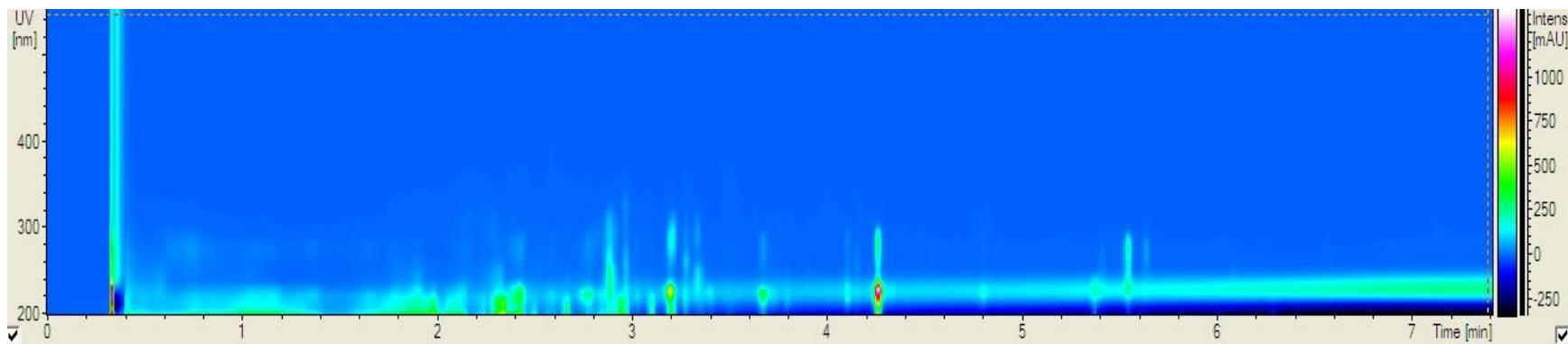
**(B) HST14-SPM**



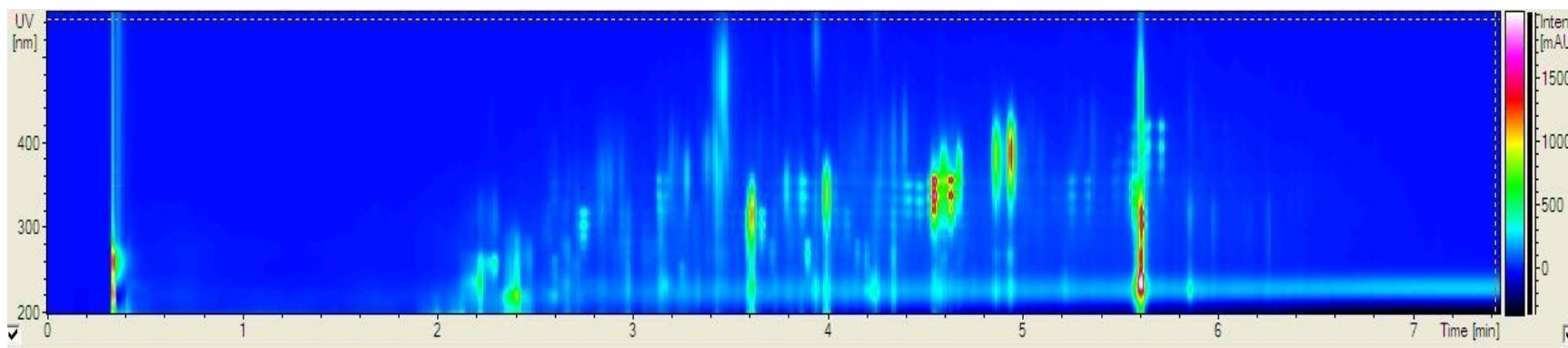
**(A) HST19-GYM**



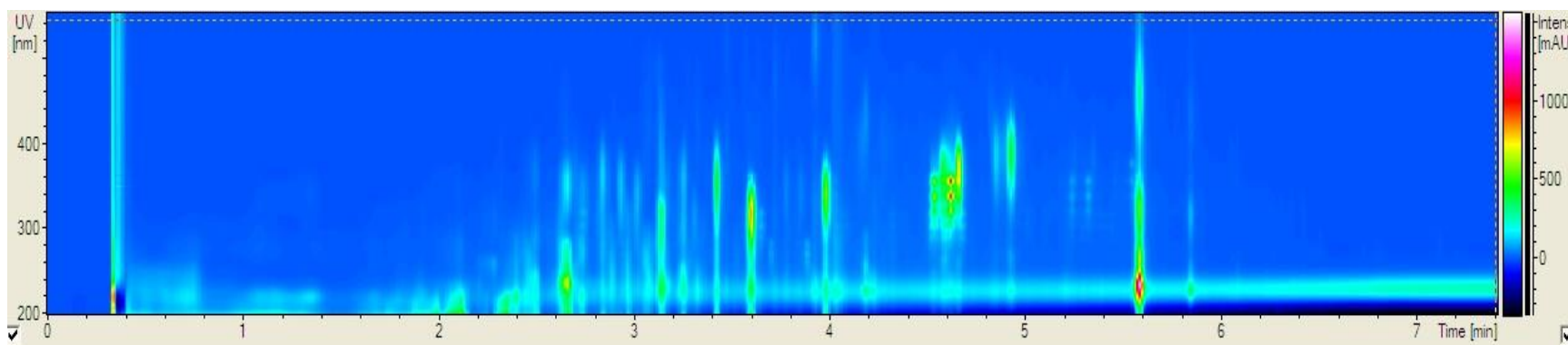
**(B) HST19-SPM**



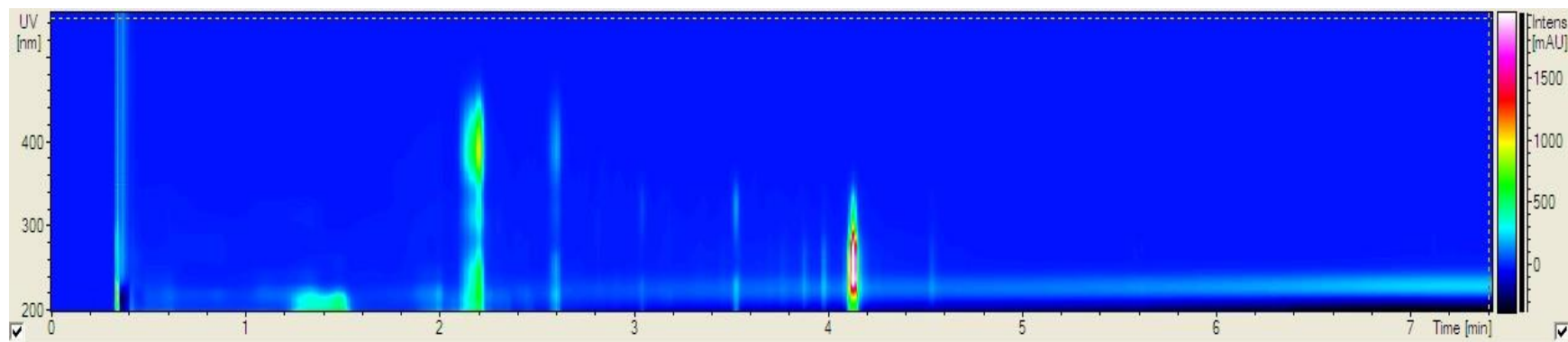
**(A) HST21-GYM**



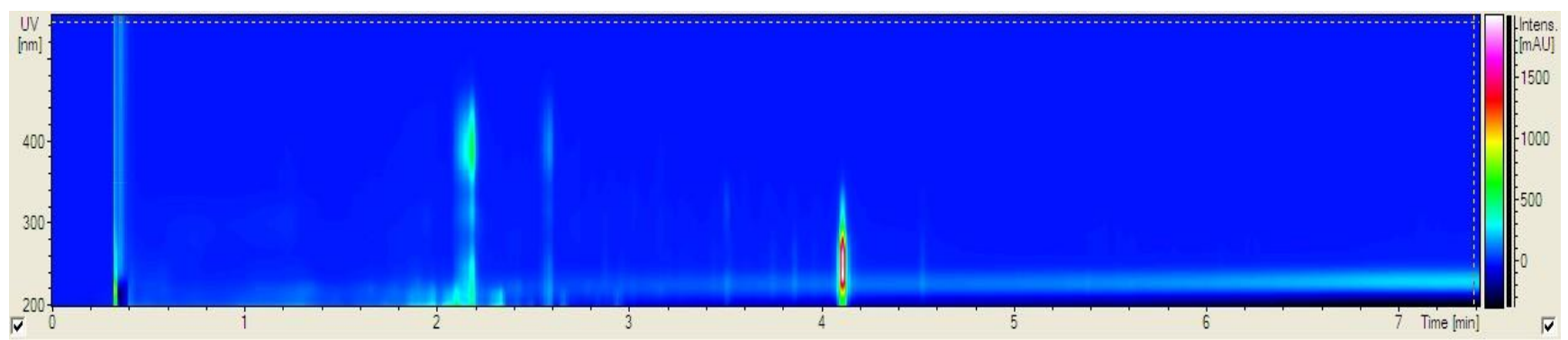
**(B) HST21-SPM**



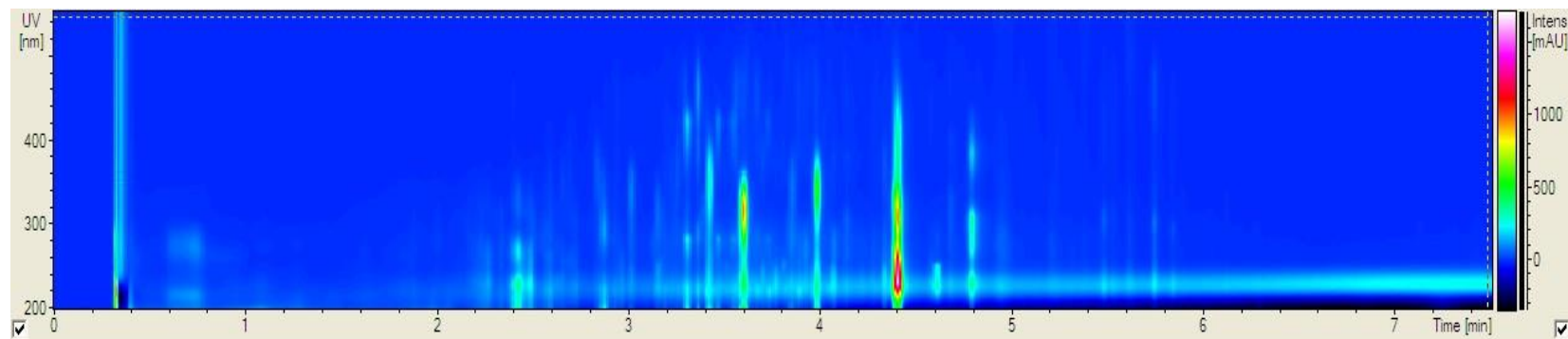
**(A) HST23-GYM**



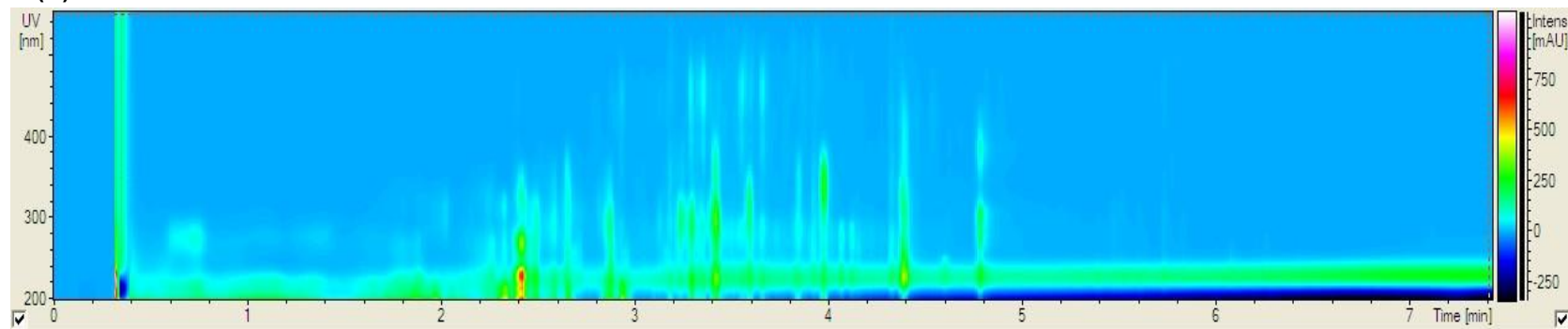
**(B) HST23-SPM**



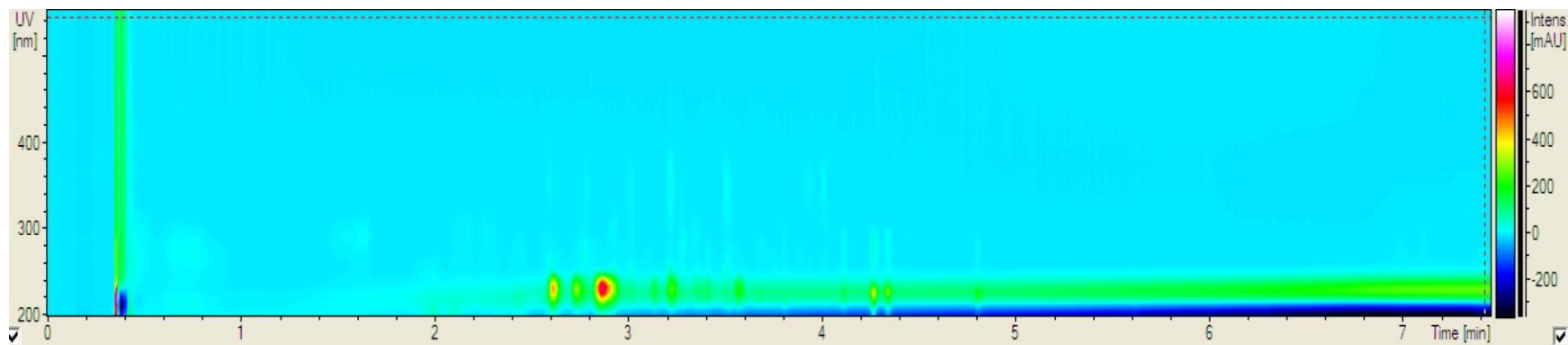
**(A) HST28-GYM**



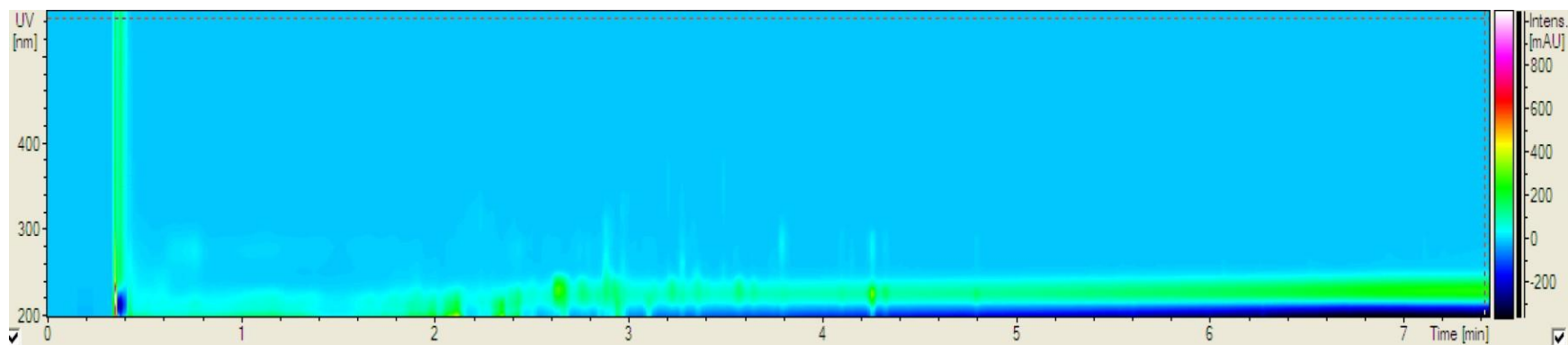
**(B) HST28-SPM**



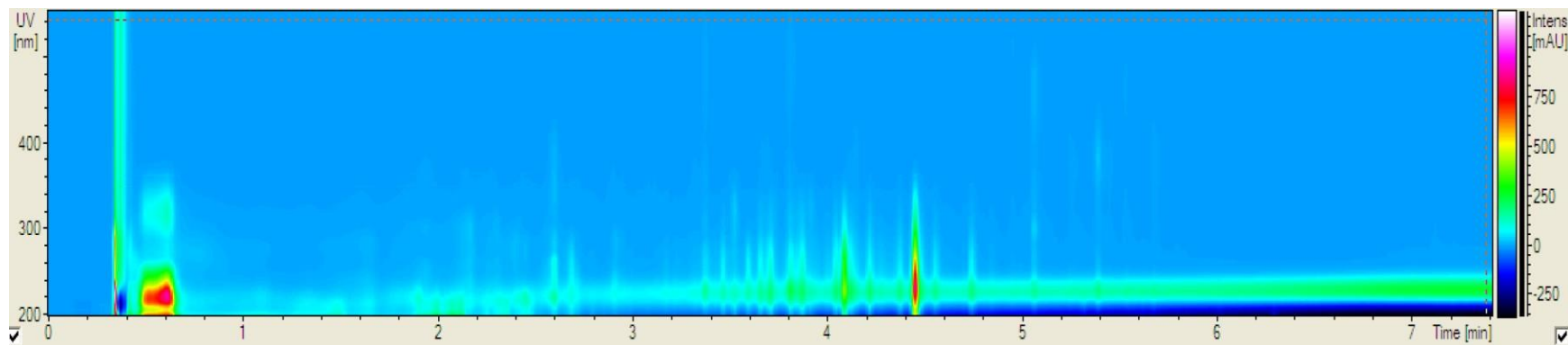
**(A) HST50-GYM**



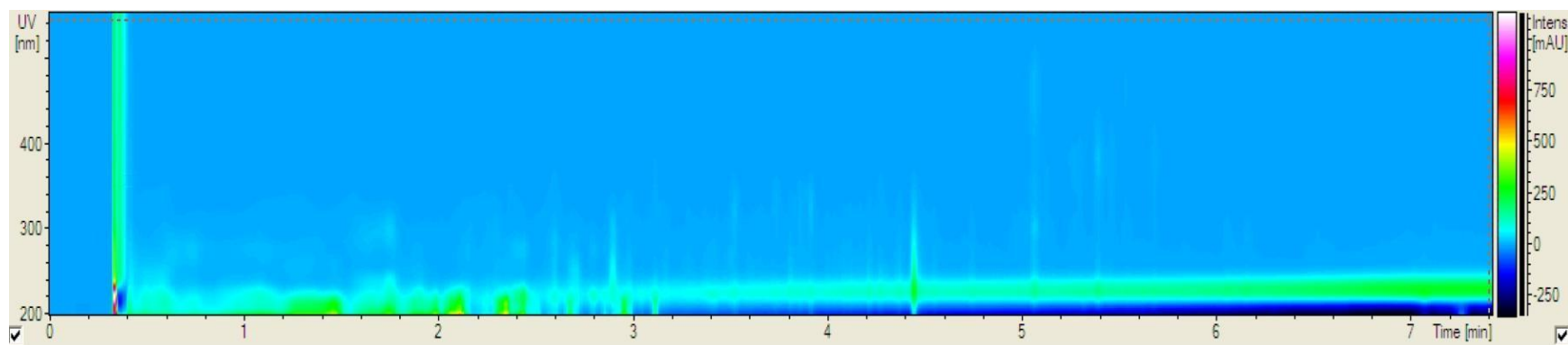
**(B) HST50-SPM**



**(A) HST54-GYM**

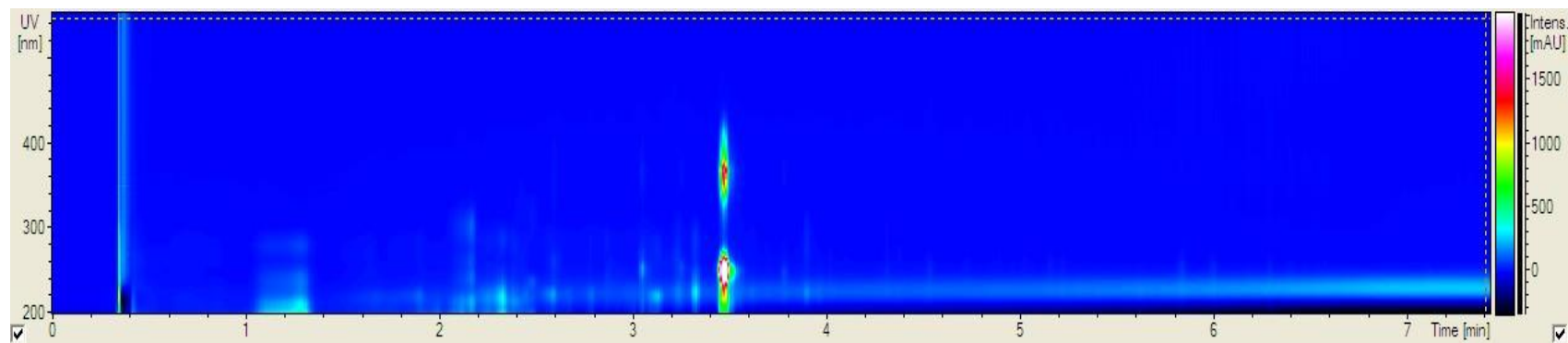


**(B) HST54-SPM**

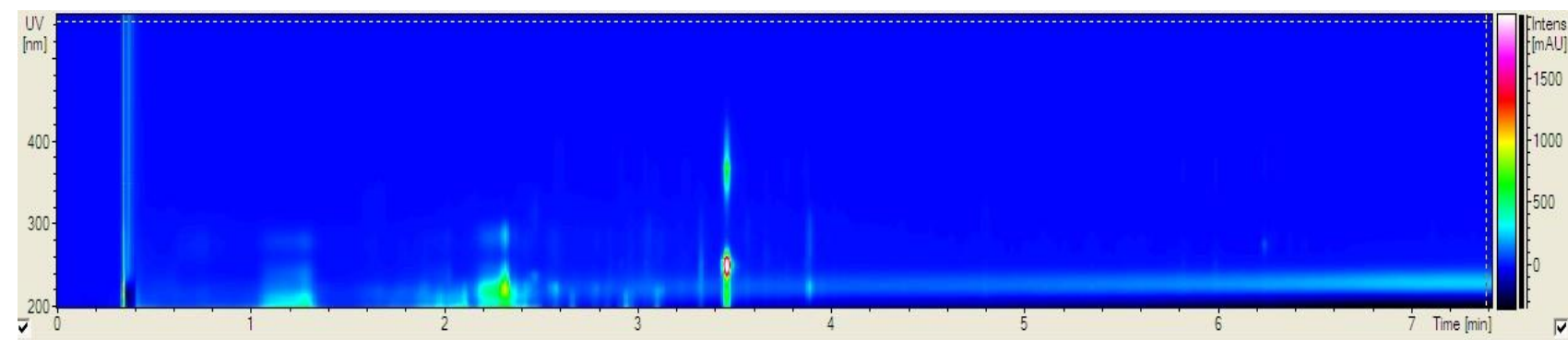




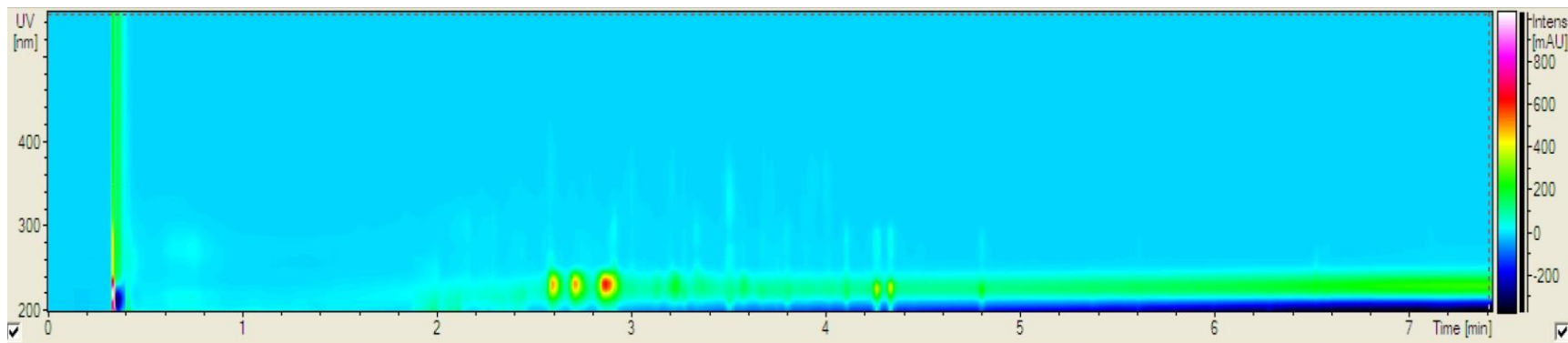
**(A) HST61-GYM**



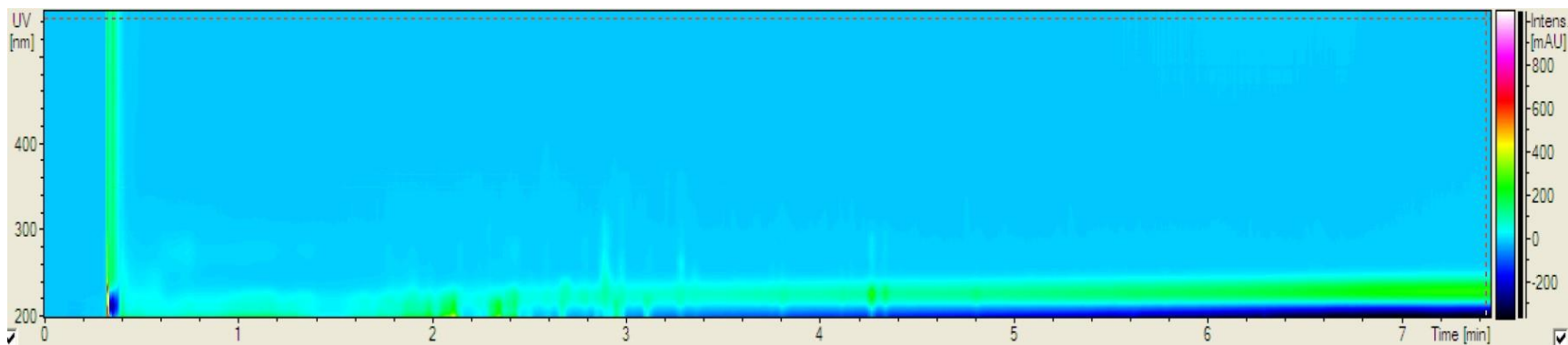
**(B) HST61-SPM**



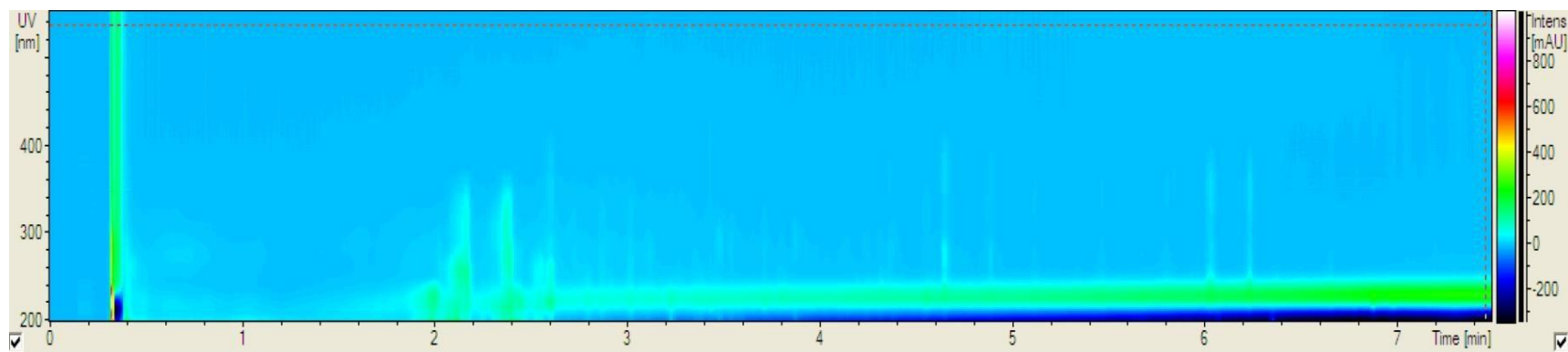
**(A) HST68-GYM**



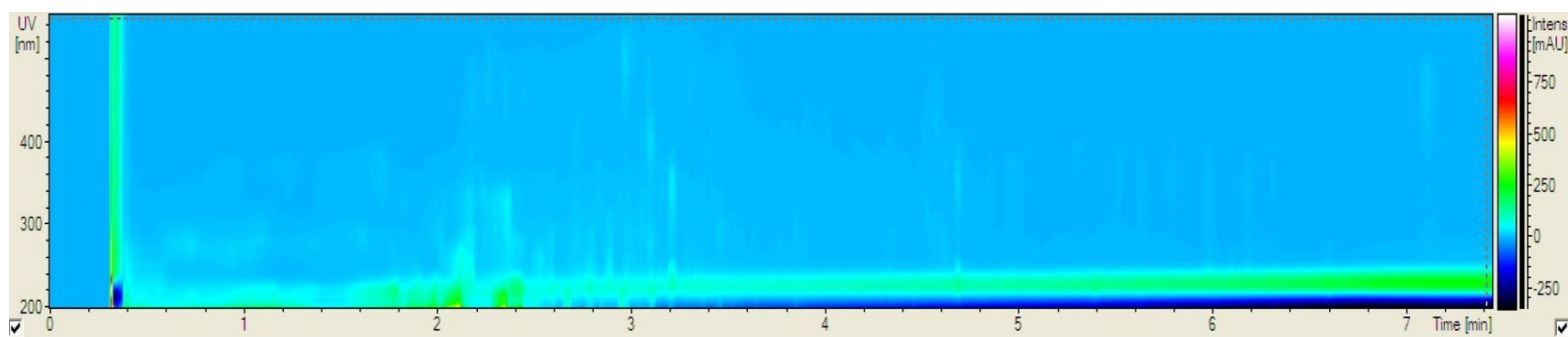
**(B) HST68-SPM**



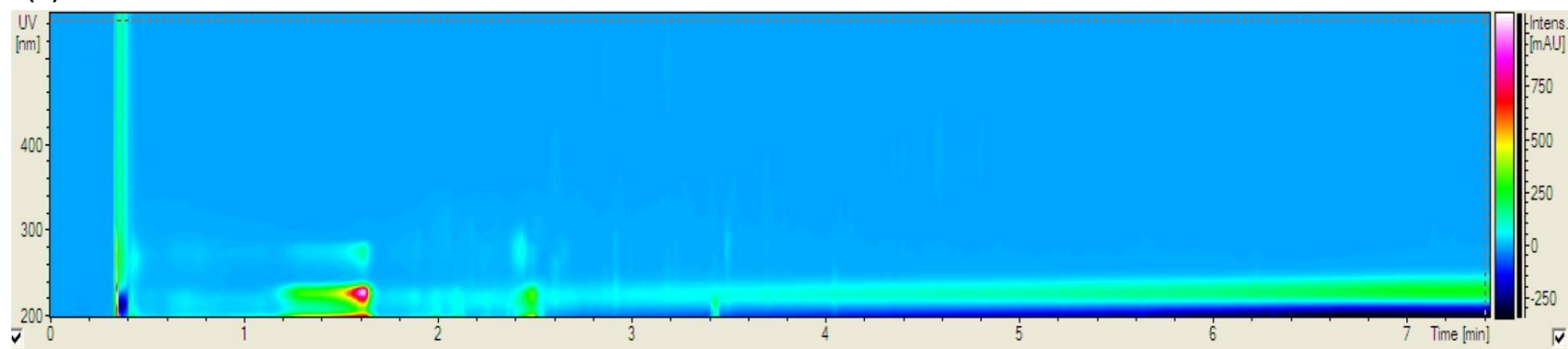
**(A) HST72-GYM**



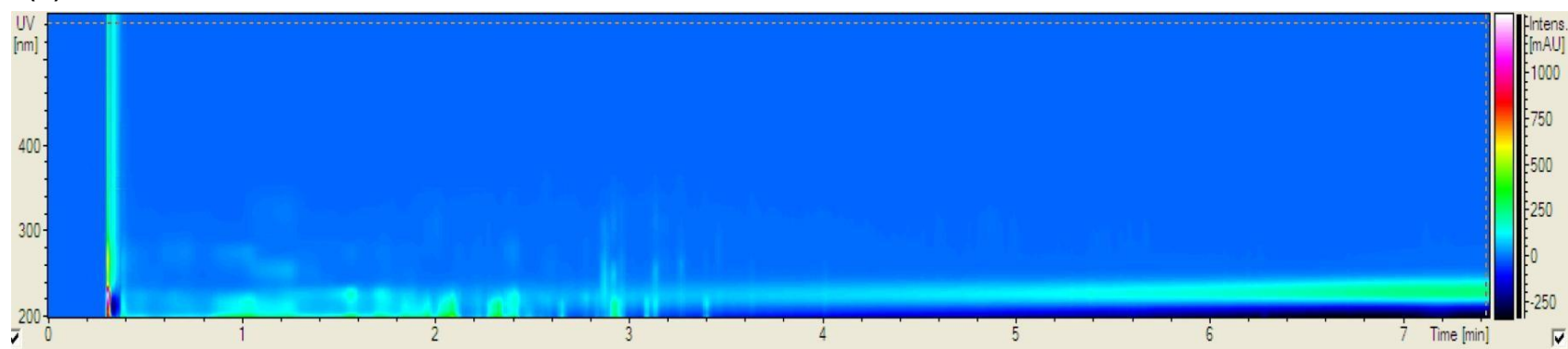
**(B) HST72-SPM**



**(A) HST82-GYM**



**(B) HST82-SPM**



**Appendix 2.** Genetic distance between strain HST28<sup>T</sup> and its phylogenetic relatives based on the concatenated partial sequences of the five housekeeping genes: *atpD*; *gyrB*; *recA*; *rpoB* and *trpB* using Kimura 2-parameter.

		1	2	3	4	5	6	7	8	9	10
1	<b>Strain HST28<sup>T</sup></b>	-									
2	<i>S. phaeochromogenes</i> NRRL B-1248 <sup>T</sup>	0.093	-								
3	<i>S. mirabilis</i> NRRL B-2400 <sup>T</sup>	0.095	0.069	-							
4	<i>S. rectiviolaceus</i> NRRL B-16374 <sup>T</sup>	0.086	0.104	0.108	-						
5	<i>S. bottropensis</i> ATCC 25435 <sup>T</sup>	0.111	0.097	0.084	0.118	-					
6	<i>S. kanamyceticus</i> NRRL B-2535 <sup>T</sup>	0.059	0.098	0.103	0.073	0.116	-				
7	<i>S. canus</i> DSM40017 <sup>T</sup>	0.092	0.082	0.076	0.112	0.064	0.102	-			
8	<i>S. olivochromogenes</i> DSM40451 <sup>T</sup>	0.102	0.096	0.062	0.111	0.083	0.104	0.080	-		
9	<i>S. griseorubiginosus</i> DSM40469 <sup>T</sup>	0.098	0.088	0.083	0.121	0.065	0.106	0.051	0.085	-	
10	<i>S. aureus</i> CGMCC 4.1833 <sup>T</sup>	0.081	0.107	0.101	0.107	0.097	0.100	0.091	0.102	0.106	-

**Appendix 3.** Evolutionary distances between strain HST21<sup>T</sup> and its phylogenetic relatives based on the concatenated partial sequences of the five housekeeping genes: *atpD*, *gyrB*, *recA*, *rpoB* and *trpB* using Kimura 2-parameter.

	1	2	3	4	5	6	7	8	9	10	11	12	13	14	15	16
1 <b>Strain HST21<sup>T</sup></b>	-															
2 <i>Streptomyces flavidovirens</i> DSM 40150 <sup>T</sup>	0,059	-														
3 <i>Streptomyces albidochromogenes</i> DSM 41800 <sup>T</sup>	0,063	0,052	-													
4 <i>Streptomyces helveticus</i> DSM 40431 <sup>T</sup>	0,086	0,068	0,041	-												
5 <i>Streptomyces chryseus</i> DSM 40420 <sup>T</sup>	0,085	0,068	0,041	0,000	-											
6 <i>Streptomyces violaceorectus</i> NRRL B-12181 <sup>T</sup>	0,101	0,110	0,106	0,121	0,120	-										
7 <i>Streptomyces xanthochromogenes</i> NRRL B-5410 <sup>T</sup>	0,111	0,120	0,117	0,118	0,118	0,103	-									
8 <i>Streptomyces cyaneofuscatus</i> CGMCC 4.1612 <sup>T</sup>	0,110	0,099	0,100	0,108	0,108	0,109	0,112	-								
9 <i>Streptomyces anulatus</i> NRRL B-2000 <sup>T</sup>	0,113	0,101	0,101	0,112	0,111	0,107	0,109	0,032	-							
10 <i>Streptomyces mauvecolor</i> NRRL B-24302 <sup>T</sup>	0,103	0,114	0,109	0,115	0,115	0,100	0,045	0,106	0,103	-						
11 <i>Streptomyces hypolithicus</i> NRRL B-24669 <sup>T</sup>	0,093	0,110	0,118	0,116	0,116	0,119	0,104	0,128	0,130	0,098	-					
12 <i>Streptomyces litmocidini</i> NRRL B-3635 <sup>T</sup>	0,101	0,108	0,106	0,117	0,117	0,063	0,108	0,104	0,109	0,101	0,118	-				
13 <i>Streptomyces puniceus</i> NRRL ISP-5083 <sup>T</sup>	0,115	0,106	0,103	0,117	0,117	0,114	0,118	0,045	0,032	0,108	0,133	0,110	-			
14 <i>Streptomyces hundertgensis</i> BH38 <sup>T</sup>	0,106	0,121	0,114	0,120	0,119	0,100	0,044	0,106	0,103	0,037	0,107	0,103	0,106	-		
15 <i>Streptomyces laurentii</i> ATCC 31255 <sup>T</sup>	0,111	0,109	0,109	0,114	0,114	0,073	0,102	0,094	0,100	0,100	0,119	0,069	0,102	0,102	-	
16 <i>Streptomyces gelaticus</i> CGMCC 4.1444 <sup>T</sup>	0,151	0,176	0,178	0,185	0,185	0,155	0,151	0,146	0,148	0,145	0,160	0,165	0,151	0,147	0,161	-
17 <i>Streptomyces albus</i> subsp. <i>albus</i> NRRL B-1811 <sup>T</sup>	0,145	0,134	0,133	0,134	0,133	0,139	0,145	0,128	0,130	0,136	0,148	0,144	0,140	0,141	0,141	0,187

**Appendix 4.** Theoretical ion fragments calculated for huascopeptin core sequence.

Fragment ion	m/z	Fragment ion	m/z	Fragment ion	m/z	Fragment ion	m/z
y <sub>1</sub>	148.0863	y <sub>6</sub> -NH <sub>3</sub>	630.3352	b <sub>9</sub> -NH <sub>3</sub>	944.4003	b <sub>11</sub> +H <sub>2</sub> O	1150.5018
b <sub>2</sub>	203.0921	b <sub>6</sub>	631.2729	y <sub>8</sub>	948.4680	y <sub>11</sub> -H <sub>2</sub> O	1172.5589
b <sub>3</sub>	260.1135	y <sub>6</sub>	647.3617	b <sub>9</sub>	961.4268	y <sub>11</sub> -NH <sub>3</sub>	1173.5429
y <sub>2</sub>	261.1703	b <sub>7</sub> -H <sub>2</sub> O	728.2893	y <sub>9</sub> -H <sub>2</sub> O	1001.4945	y <sub>11</sub>	1190.5695
y <sub>3</sub>	318.1918	b <sub>7</sub> -NH <sub>3</sub>	729.2733	y <sub>9</sub> -NH <sub>3</sub>	1002.4785	b <sub>12</sub> -H <sub>2</sub> O	1227.5647
b <sub>4</sub> -NH <sub>3</sub>	357.1299	y <sub>7</sub> -H <sub>2</sub> O	744.3781	y <sub>9</sub>	1019.5051	b <sub>12</sub> -NH <sub>3</sub>	1228.5487
b <sub>4</sub>	374.1565	y <sub>7</sub> -NH <sub>3</sub>	745.3621	b <sub>10</sub> -H <sub>2</sub> O	1057.4592	b <sub>12</sub>	1245.5753
y <sub>4</sub> -NH <sub>3</sub>	415.2082	b <sub>7</sub>	746.2998	b <sub>10</sub> -NH <sub>3</sub>	1058.4432	b <sub>12</sub> +H <sub>2</sub> O	1263.5858
b <sub>5</sub> -NH <sub>3</sub>	428.1670	y <sub>7</sub>	762.3886	b <sub>10</sub>	1075.4697	y <sub>12</sub> -H <sub>2</sub> O	1335.6222
y <sub>4</sub>	432.2347	b <sub>8</sub> -H <sub>2</sub> O	815.3213	b <sub>11</sub> -H <sub>2</sub> O	1114.4806	y <sub>12</sub> -NH <sub>3</sub>	1336.6062
b <sub>5</sub>	445.1936	b <sub>8</sub> -NH <sub>3</sub>	816.3053	b <sub>11</sub> -NH <sub>3</sub>	1115.4647	y <sub>12</sub>	1353.6328
y <sub>5</sub> -NH <sub>3</sub>	543.3031	b <sub>8</sub>	833.3319	y <sub>10</sub> -H <sub>2</sub> O	1115.5374	MH-H <sub>2</sub> O	1392.6437
y <sub>5</sub>	560.3297	y <sub>8</sub> -H <sub>2</sub> O	930.4574	y <sub>10</sub> -NH <sub>3</sub>	1116.5214	MH-NH <sub>3</sub>	1393.6277
b <sub>6</sub> -NH <sub>3</sub>	614.2463	y <sub>8</sub> -NH <sub>3</sub>	931.4414	b <sub>11</sub>	1132.4912	MH	1410.6543
y <sub>6</sub> -H <sub>2</sub> O	629.3511	b <sub>9</sub> -H <sub>2</sub> O	943.4163	y <sub>10</sub>	1133.5480		

**Appendix 5.** NMR Data for huascopeptin **1** (2.5 mM, CD<sub>3</sub>OH, 600/800 MHz, 298K) <sup>a</sup>

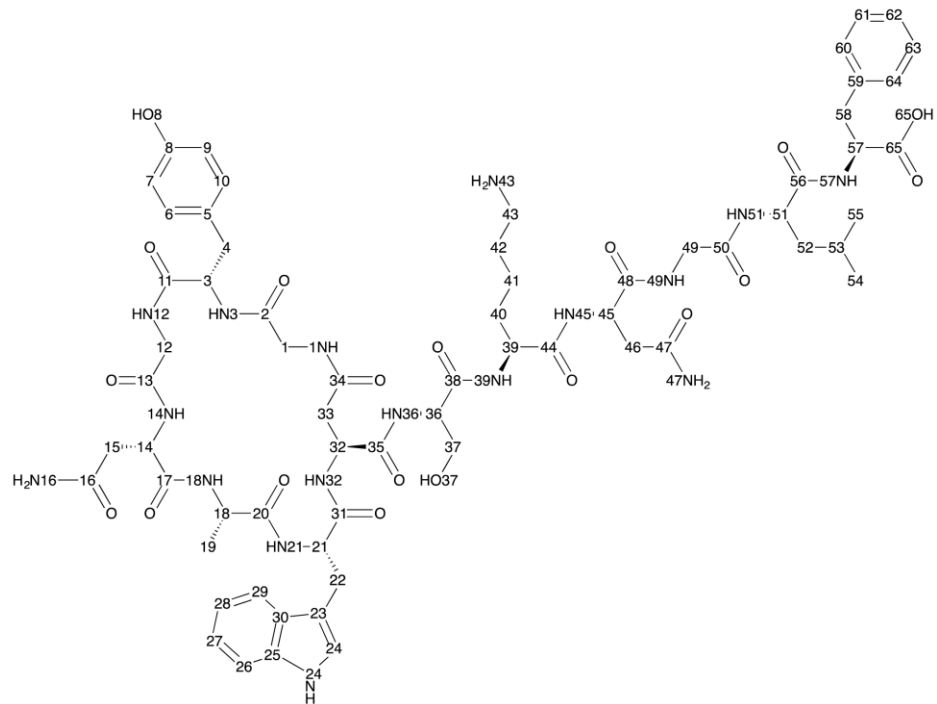
Residue	Atom number	Position	Type δC/δN	δH, mult. [J (Hz)]	Residue	Atom number	Position	Type δC/δN	δH, mult. [J (Hz)] 6
Gly1	1	α	43.1, CH <sub>2</sub>	a: 4.30, m b: 3.34, m	Ser8	36	α	61.1, CH	4.05, m
	2	CO				37	β	61.2, CH <sub>2</sub>	a: 3.98, m b: 3.89, m
Tyr2	1NH	NH	119.64	8.96, m	Lys9	38	CO		
	3	α	48.7, CH	4.43, m		36NH	NH	121.1	8.25, br s
	4	β	37.4, CH <sub>2</sub>	3.18, m		39	α	53.1, CH	4.48, m
	5	γ	128.6, C			40	β	30.5, CH <sub>2</sub>	a: 2.06, m b: 1.68, m
	6,10	δ/δ'	131.0, CH	7.06, m		41	γ	22.6, CH <sub>2</sub>	a: 1.42, m b: 1.36, m
	7,9	ε/ε'	116.0, CH	6.69, d (7.4)		42	δ	27.4, CH <sub>2</sub>	a: 1.69, m b: 1.58, m
	8	ζ	157.1, C			43	ε	40.2, CH <sub>2</sub>	2.91, m
	11	CO				44	CO		
	3NH	NH	115.7	8.81, m		39NH	NH	118.7	8.07, d (9.3)
	8OH	ζ-OH	-	-		43NH <sub>2</sub>	ε-NH <sub>2</sub>	-	8.22, d (9.4)
Gly3	12	α	42.6, CH <sub>2</sub>	a: 4.25, m b: 3.37, m	Asn10	45	α	53.6, CH	4.52, m
	13	CO				46	β	35.8, CH <sub>2</sub>	a: 3.11, m b: 2.84, m
Asn4	12NH	NH	-	8.79, m	Gly11	47	γ		
	14	α	51.1, CH	5.33, m		48	CO		
	15	β	38.3, CH <sub>2</sub>	a: 2.63, m b: 2.45, m		45NH	NH	113.7	8.43, d (6.5)
	16	γ				47NH <sub>2</sub>	γ-NH <sub>2</sub>	107.3/107.1	a:7.55/7.54, br s b:6.65/6.76, br s
	17	CO				49	α	42.8, CH <sub>2</sub>	a: 3.99, m b: 2.99, br s
	14NH	NH	121.5	8.38, m		50	CO		
16NH <sub>2</sub>	γ-NH <sub>2</sub>	107.1/107.3	a:7.54/7.55, br s b:6.76/6.65, br s						
Ala5	18	α	52.1, CH	3.63, d (7.1)					



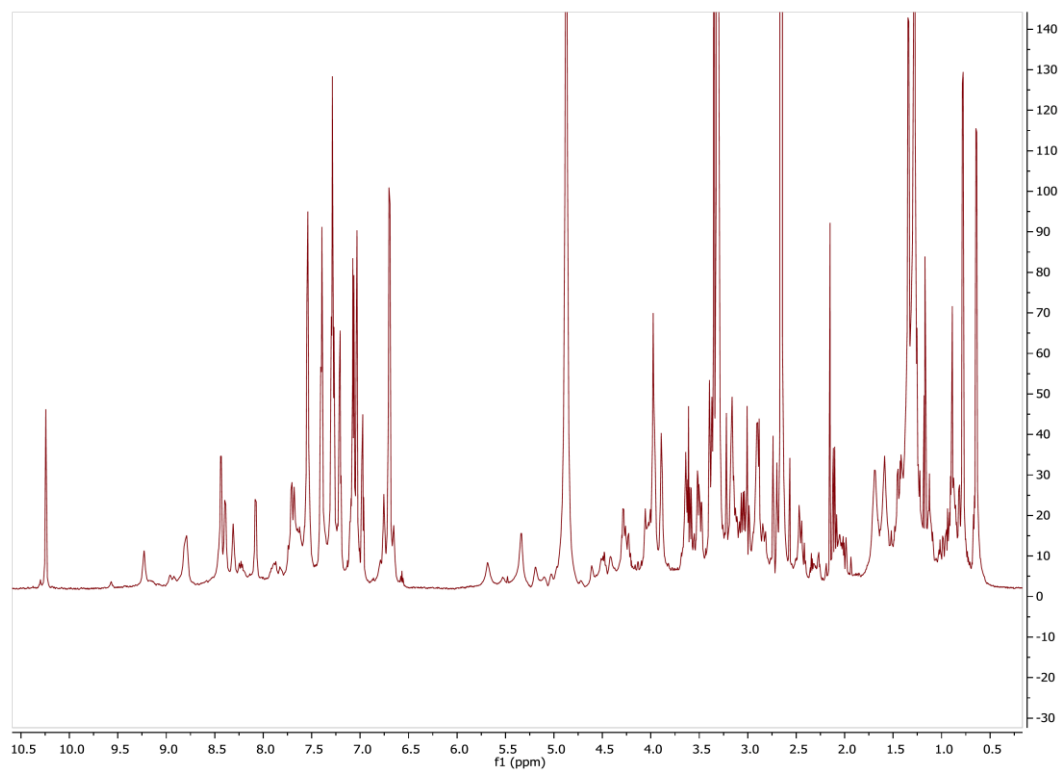
Appendix 5. Continued

Residue	Atom number	Position	Type $\delta C/\delta N$	$\delta H$ , mult. [J (Hz)]	Residue	Atom number	Position	Type $\delta C/\delta N$	$\delta H$ , mult. [J (Hz)] 6	
Trp6	19	$\beta$	14.7, CH <sub>3</sub>	1.34, d (7.1)	Leu12	49NH	NH	122.1	7.53, m	
	20	CO	173.0, C	-		51	$\alpha$	52.9, CH	4.29, m	
	18NH	NH	106.6	7.68, m		52	$\beta$	42.8, CH <sub>2</sub>	a: 1.41, m b: 1.27, m	
	21	$\alpha$	55.7, CH	5.22, m		53	$\gamma$	25.4, CH	1.12, m	
	22	$\beta$	27.9, CH <sub>2</sub>	a: 3.49, m b: 3.06, dd (15.8, 9.3)		54	$\delta$	22.1, CH <sub>3</sub>	0.8, d (6.9)	
	23	$\gamma$	110.8, C	-		55	$\delta'$	23.4, CH <sub>3</sub>	0.64, d (6.9)	
	24	$\delta$	124.3, CH	7.03, m		56	CO	-	-	
	25	$\epsilon$	137.6, C	-		Phe13	51NH	NH	-	7.89, m
	26	$\zeta$	112.0, CH	7.27, m			57	$\alpha$	54.9, CH	4.61, m
	27	$\eta$	122.1, CH	7.04, m			58	$\beta$	38.5, CH <sub>2</sub>	a: 3.38, m b: 3.15, m
	28	$\theta$	119.4, CH	6.97, t (7.4)			59	$\gamma$	139.1, C	-
	29	$\iota$	119.1, CH	7.55, d (7.9)			60,64	$\delta/\delta'$	130.0, CH	7.40, d (7.7)
	30	$\kappa$	128.6, C	-			61,63	$\epsilon/\epsilon'$	129.2, CH	7.29, m
31	CO	-	-	62	$\xi$		127.5, CH	7.21, m		
Asp7	21NH	NH	118.9	7.73, m	65	CO	-	-		
	24NH	Indole NH	127.3	10.2, br s	57NH	NH	-	8.31, br s		
	32	$\alpha$	50.8, CH	4.61 m						
	33	$\beta$	35.8, CH <sub>2</sub>	a: 3.34, m b: 2.72, m						
	35	$\gamma$	-	-						
34	CO	-	-							
32NH	NH	119.6	9.22, br s							

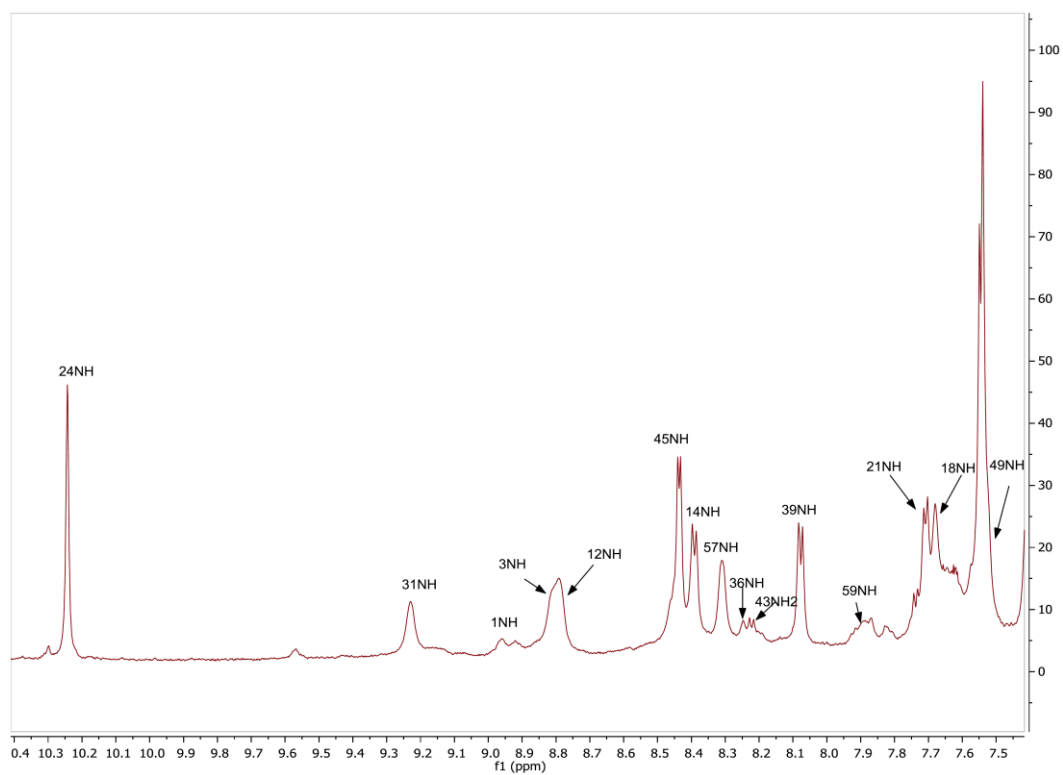
a: Assignments based on COSY, TOCSY, HSQC, HSQC-TOCSY, NOESY, and HMBC experiments.



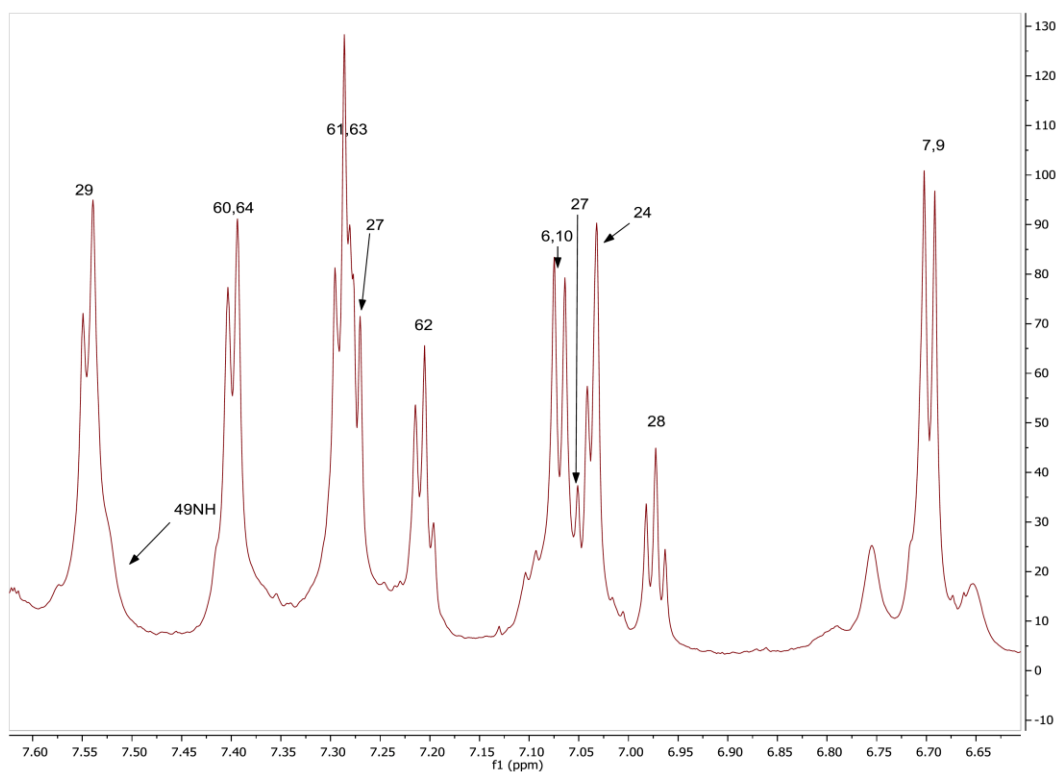
**Appendix 6.** Numbered planar structure of huascopeptin **1**.



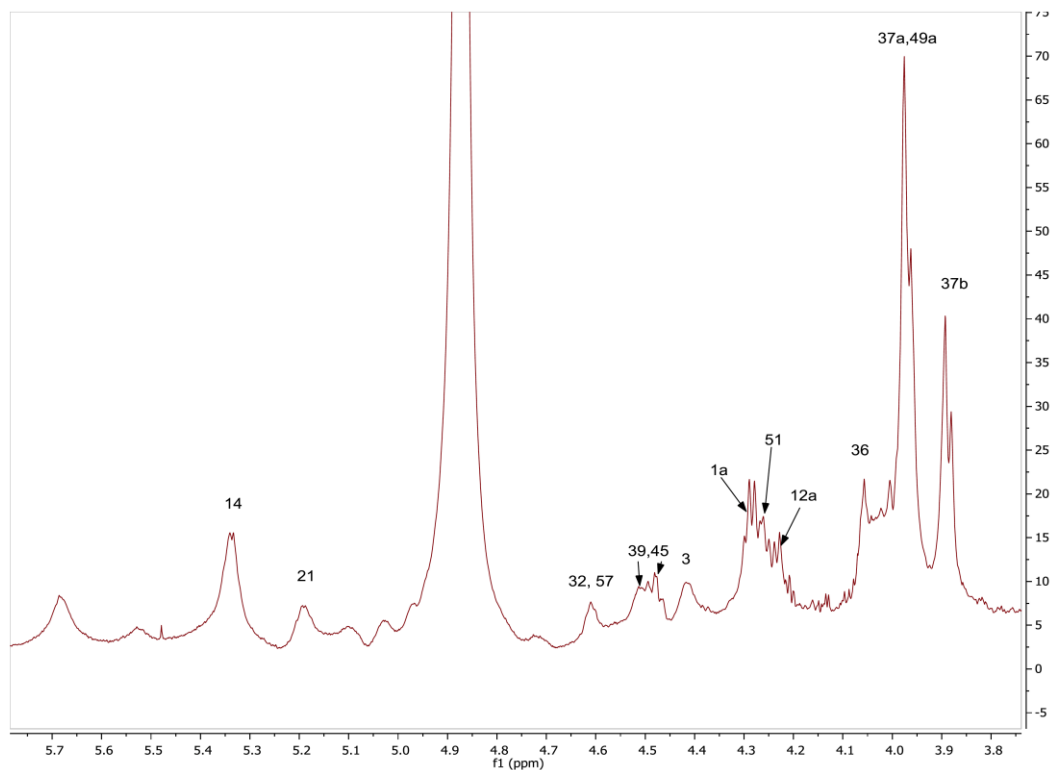
**Appendix 7.**  $^1\text{H}$  NMR of huascopeptin **1** (2.5 mM,  $\text{CD}_3\text{OH}$ , 800 MHz, 298K).



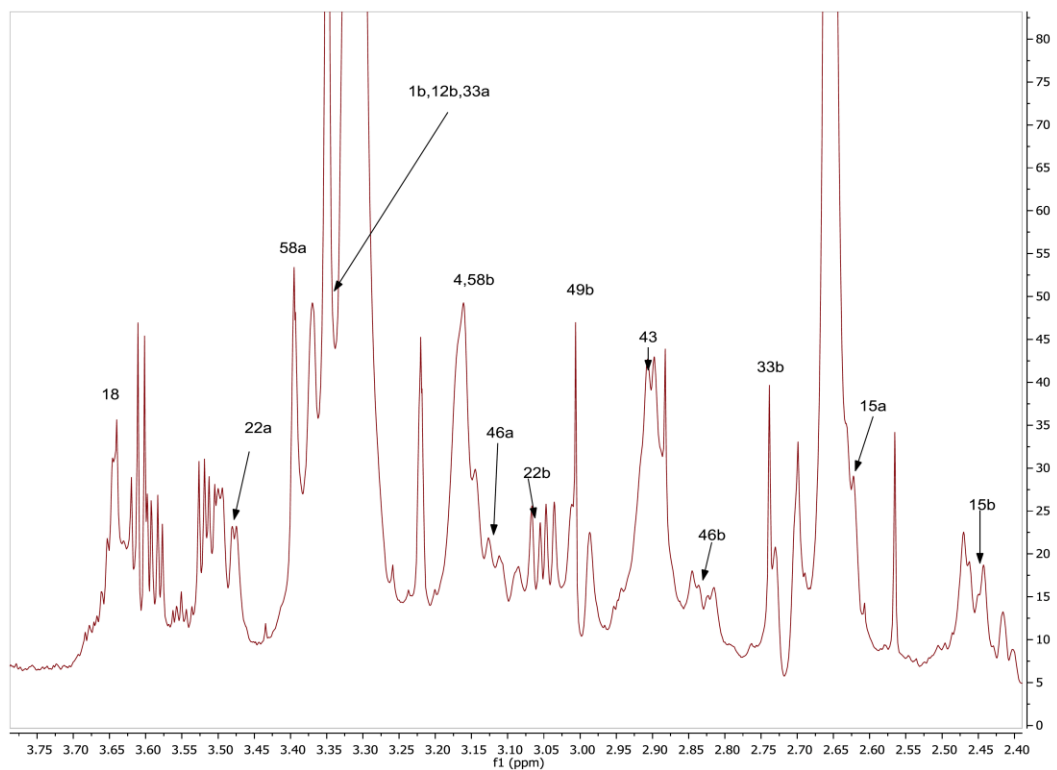
**Appendix 7a.** Expanded  $^1\text{H}$  NMR of huascopeptin **1** ( $\delta\text{H}$  10.40 – 7.50) (2.5 mM,  $\text{CD}_3\text{OH}$ , 800 MHz, 298K).



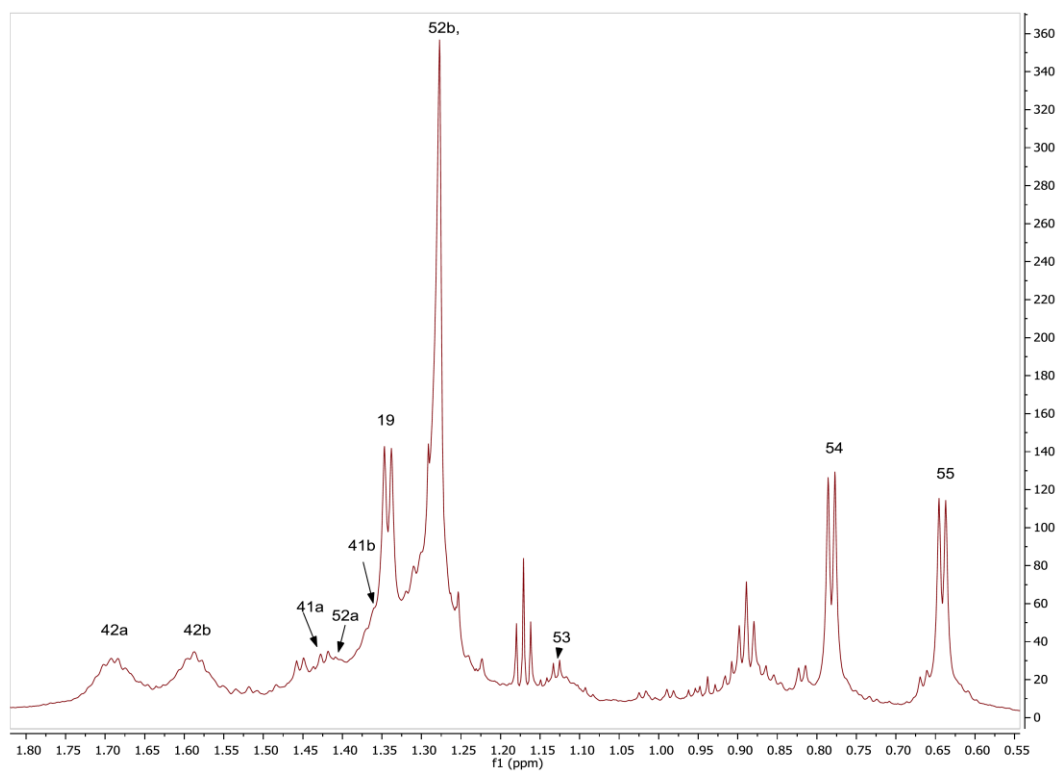
**Appendix 7b.** Expanded  $^1\text{H}$  NMR of huascopeptin **1** ( $\delta\text{H}$  7.50 – 6.65) (2.5 mM,  $\text{CD}_3\text{OH}$ , 800 MHz, 298K).



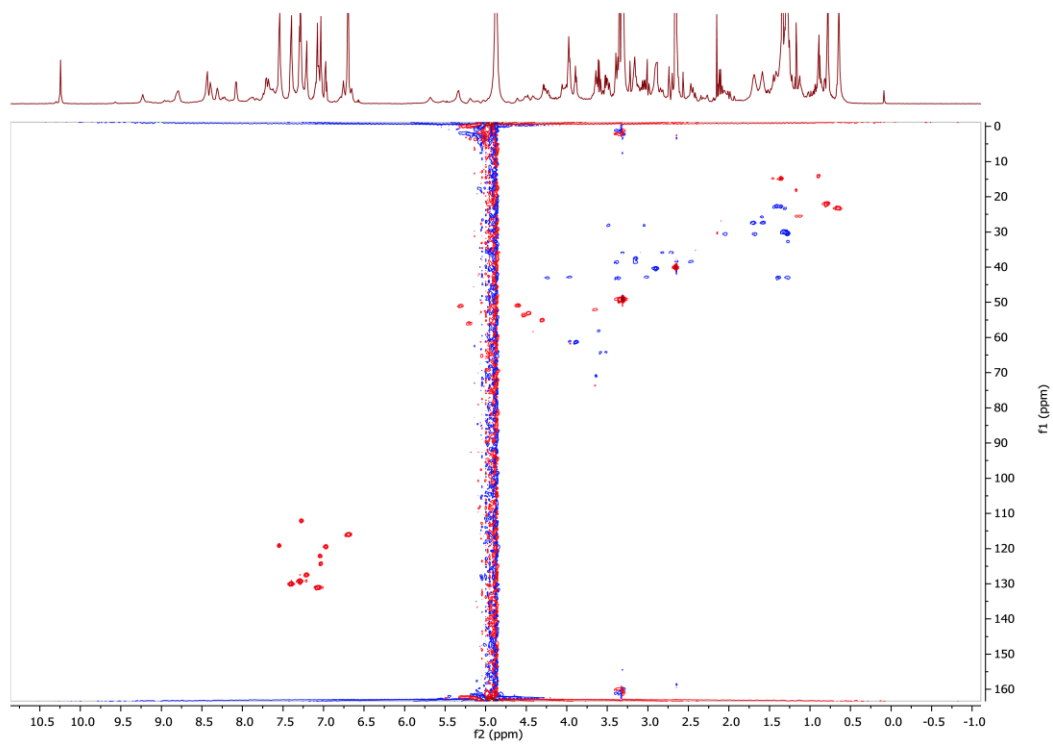
**Appendix 7c.** Expanded  $^1\text{H}$  NMR of huascopeptin **1** ( $\delta\text{H}$  5.80- 3.80) (2.5 mM,  $\text{CD}_3\text{OH}$ , 800 MHz, 298K).



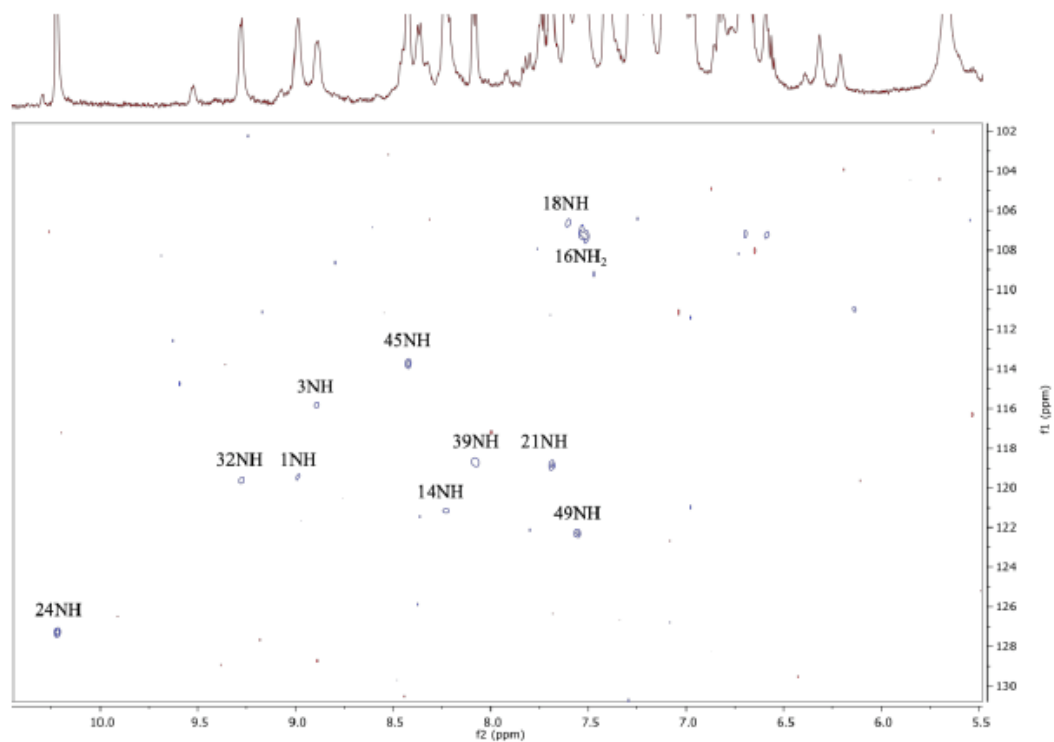
**Appendix 7d.** Expanded  $^1\text{H}$  NMR of huascopeptin **1** ( $\delta\text{H}$  3.80 - 2.40) (2.5 mM,  $\text{CD}_3\text{OH}$ , 800 MHz, 298K).



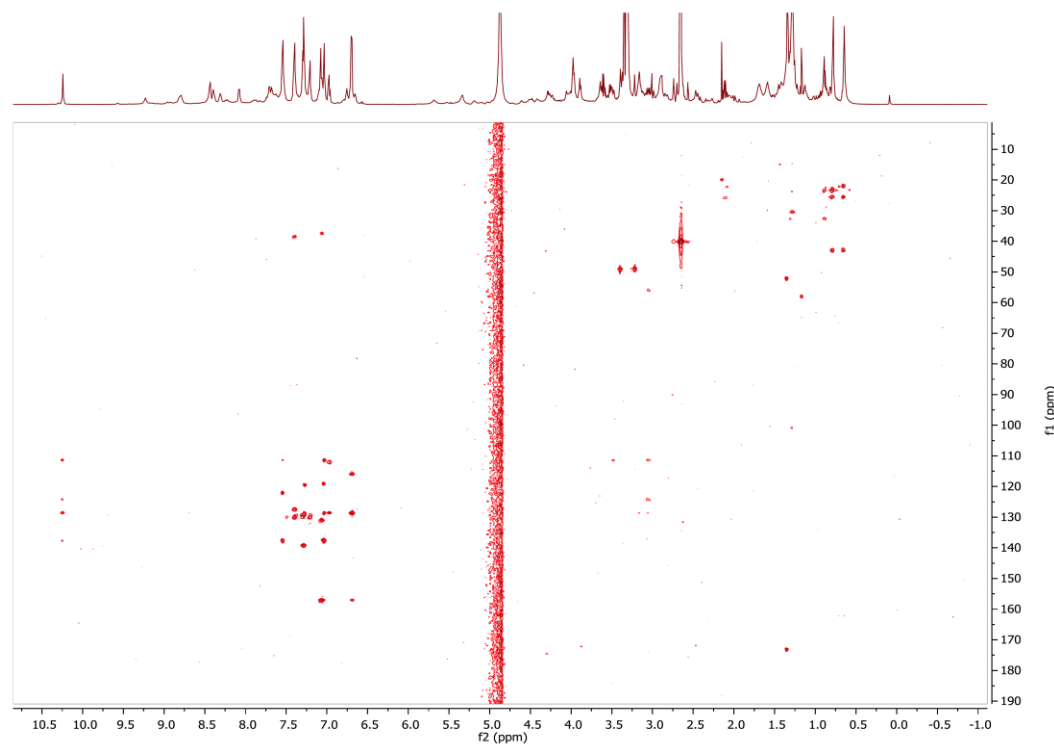
**Appendix 7e.** Expanded  $^1\text{H}$  NMR of huascopeptin **1** ( $\delta\text{H}$  1.80 – 0.60) (2.5 mM,  $\text{CD}_3\text{OH}$ , 800 MHz, 298K).



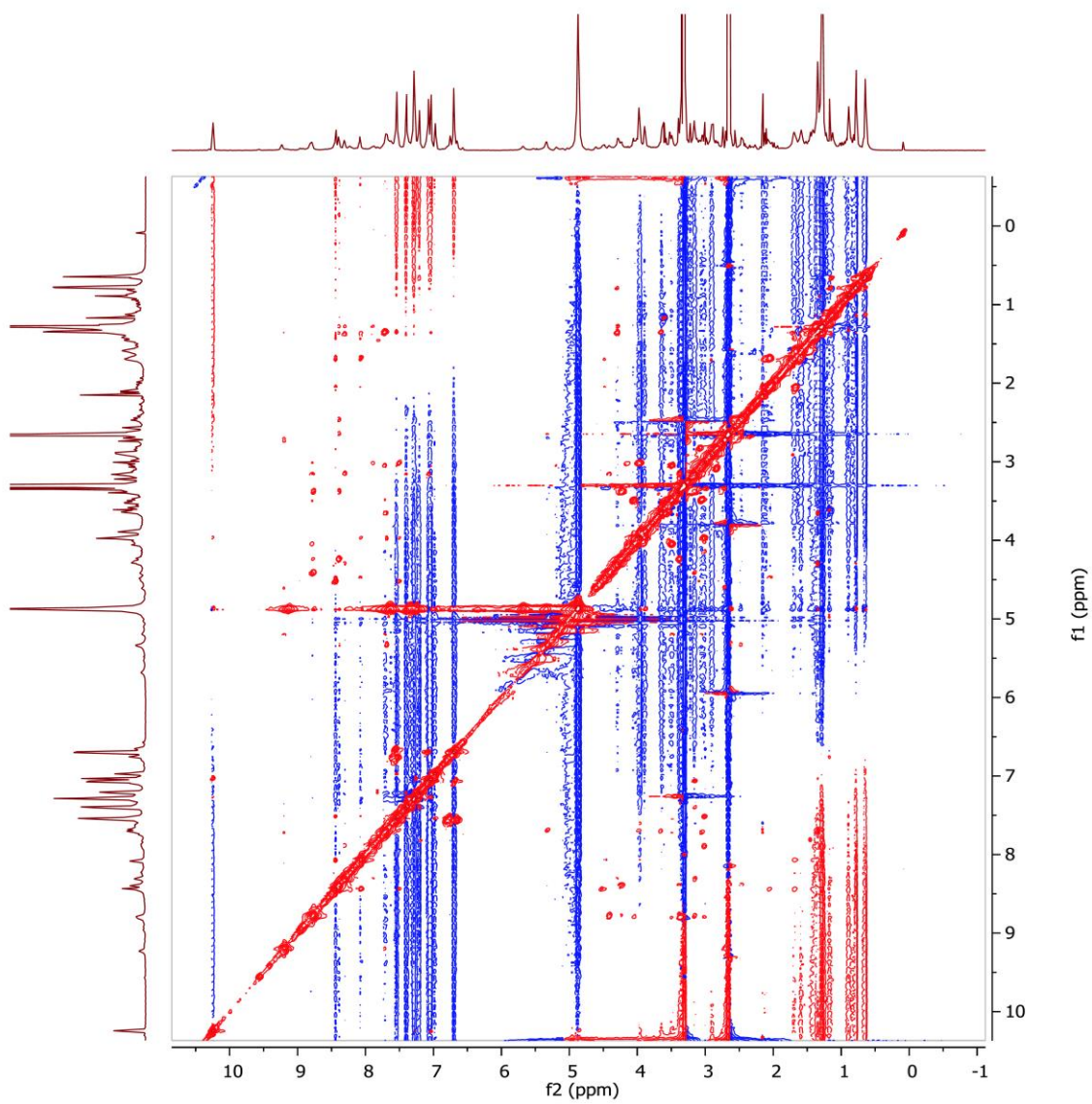
**Appendix 8.**  $^1\text{H}$ - $^{13}\text{C}$  HSQC spectrum of huascopeptin **1** (2.5 mM,  $\text{CD}_3\text{OH}$ , 800 MHz, 298K).



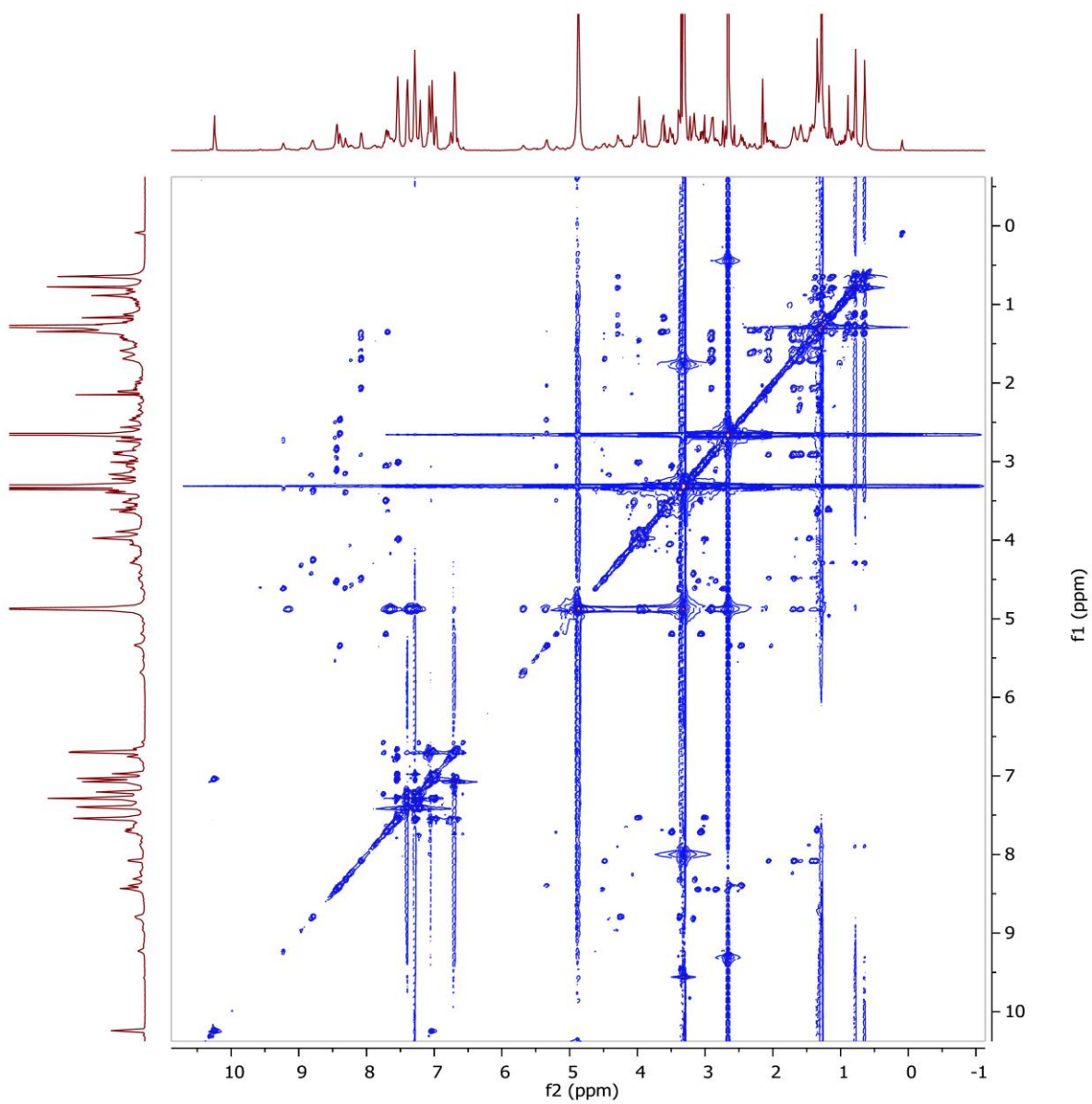
**Appendix 9.**  $^1\text{H}$ - $^{15}\text{N}$  HSQC spectrum of huascopeptin **1** (2.5 mM,  $\text{CD}_3\text{OH}$ , 600 MHz, 298K).



**Appendix 10.**  $^1\text{H}$ - $^{13}\text{C}$  HMBC spectrum of huascopeptin **1** (2.5 mM,  $\text{CD}_3\text{OH}$ , 800 MHz, 298K).

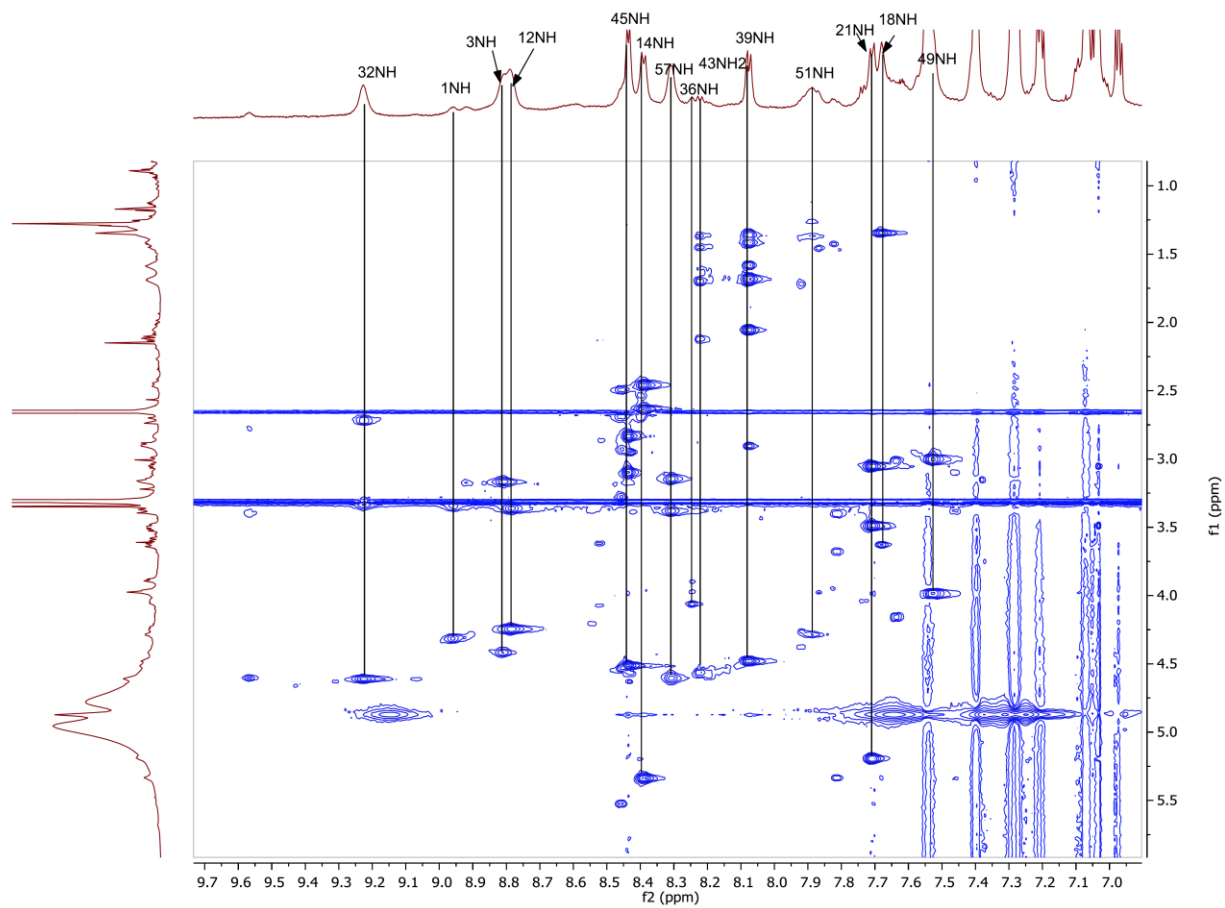


**Appendix 11.**  $^1\text{H}$ - $^1\text{H}$  NOESY spectrum of huascopeptin **1** (2.5 mM,  $\text{CD}_3\text{OH}$ , 800 MHz, 298K).

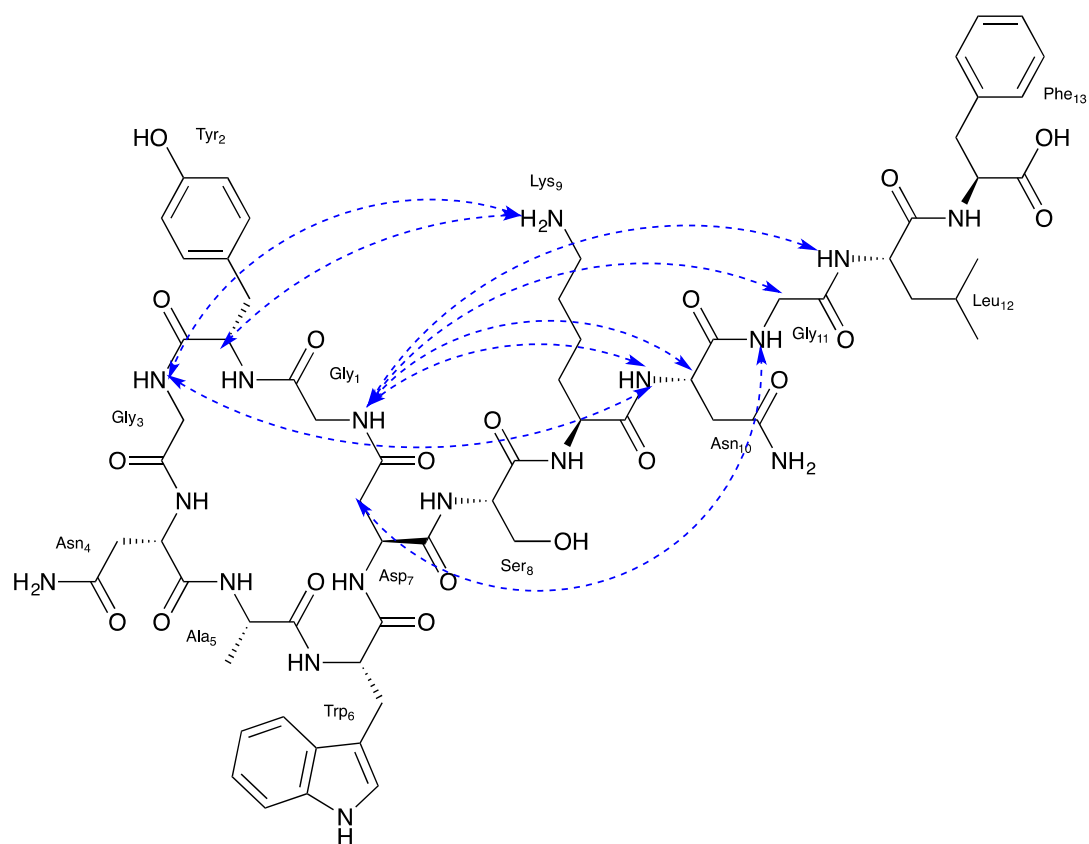


**Appendix 12.**  $^1\text{H}$ - $^1\text{H}$  TOCSY spectrum of huascopeptin **1** (2.5 mM,  $\text{CD}_3\text{OH}$ , 800 MHz, 298K).





**Appendix 12a.** Expanded  $^1\text{H}$ - $^1\text{H}$  TOCSY spectrum of huascopeptin **1** amino acid spin systems ( $\delta\text{H}$  9.70-7.40) (2.5 mM,  $\text{CD}_3\text{OH}$ , 800 MHz, 298K).



**Appendix 13.** Tail-to-ring NOE correlations of huascopeptin **1**, providing further evidence for the lasso conformation over a branched-cycle.



**Appendix 14.** Energies (kJ/mol) of model B and C during MD simulation over 100 ns.

	Bonds	Angle	Dihedral	Planarity	van der Waals
<b>model B</b>	3207.9	1542.7	4276.7	24.1	4392.2
<b>model C</b>	2777.1	1341.2	4265.0	22.5	3682.0

## **Papers currently published**

Article

# The Polyextreme Ecosystem, Salar de Huasco at the Chilean Altiplano of the Atacama Desert Houses Diverse *Streptomyces* spp. with Promising Pharmaceutical Potentials

Carlos Cortés-Albayay<sup>1,2,3,4</sup>, Johanna Silber<sup>5</sup>, Johannes F. Imhoff<sup>5</sup> , Juan A. Asenjo<sup>3</sup>, Barbara Andrews<sup>3</sup>, Imen Nouioui<sup>4,\*</sup> and Cristina Dorador<sup>1,2,\*</sup> 

<sup>1</sup> Laboratory of Microbial Complexity and Functional Ecology, Centre for Biotechnology and Bioengineering-CeBiB, University of Antofagasta, Av. Angamos, Antofagasta 601, Chile; c.j.cortesbt@gmail.com

<sup>2</sup> Department of Biotechnology, Faculty of Marine Science and Biological Resources, University of Antofagasta, Av. Angamos, Antofagasta 601, Chile

<sup>3</sup> Centre for Biotechnology and Bioengineering—CeBiB, Department of Chemical Engineering and Biotechnology, University of Chile, Beauchef, Santiago 851, Chile; juasenjo@ing.uchile.cl (J.A.A.); bandrews@ing.uchile.cl (B.A.)

<sup>4</sup> School of Natural and Environmental Sciences, Newcastle University, Newcastle upon Tyne NE1 7RU, UK

<sup>5</sup> GEOMAR Helmholtz-Zentrum für Ozeanforschung Kiel, Düsternbrooker Weg 20, D-24105 Kiel, Germany; jsilber@geomar.de (J.S.); jimhoff@geomar.de (J.F.I.)

\* Correspondence: imen.nouioui@newcastle.ac.uk (I.N.); cristina.dorador@uantof.cl (C.D.)

Received: 18 February 2019; Accepted: 24 April 2019; Published: 28 April 2019



**Abstract:** Salar de Huasco at the Chilean Altiplano of the Atacama Desert is considered a polyextreme environment, where solar radiation, salinity and aridity are extremely high and occur simultaneously. In this study, a total of 76 bacterial isolates were discovered from soil samples collected at two different sites in the east shoreline of Salar de Huasco, including H0 (base camp next to freshwater stream in the north part) and H6 (saline soils in the south part). All isolated bacteria were preliminarily identified using some of their phenotypic and genotypic data into the genera *Streptomyces* (86%), *Nocardioopsis* (9%), *Micromonospora* (3%), *Bacillus* (1%), and *Pseudomonas* (1%). *Streptomyces* was found dominantly in both sites (H0 = 19 isolates and H6 = 46 isolates), while the other genera were found only in site H0 (11 isolates). Based on the genotypic and phylogenetic analyses using the 16S rRNA gene sequences of all *Streptomyces* isolates, 18% (12 isolates) revealed <98.7% identity of the gene sequences compared to those in the publicly available databases and were determined as highly possibly novel species. Further studies suggested that many *Streptomyces* isolates possess the nonribosomal peptide synthetases-coding gene, and some of which could inhibit growth of at least two test microbes (i.e., Gram-positive and Gram-negative bacteria and fungi) and showed also the cytotoxicity against hepatocellular carcinoma and or mouse fibroblast cell lines. The antimicrobial activity and cytotoxicity of these *Streptomyces* isolates were highly dependent upon the nutrients used for their cultivation. Moreover, the HPLC-UV-MS profiles of metabolites produced by the selected *Streptomyces* isolates unveiled apparent differences when compared to the public database of existing natural products. With our findings, the polyextreme environments like Salar de Huasco are promising sources for exploring novel and valuable bacteria with pharmaceutical potentials.

**Keywords:** bioactive compounds; actinobacteria; Atacama; bioprospecting; Chilean Altiplano

## 1. Introduction

Actinomycetes are the most important bacteria that are capable of producing bioactive compounds. The majority of natural products for new pharmaceutical applications are derived from actinomycetes [1], while the notable member of actinomycetes, the genus *Streptomyces* is the major producer [2]. Many of these specialized metabolites biosynthesized by actinomycetes correspond to polyketides and nonribosomal peptides, which may act as antibiotics, immunosuppressants, anticancer/antitumor agents, toxins, and siderophores [3]. The members of the genus *Streptomyces* are widely distributed across various habitats and geographical locations [4]. *Streptomyces* produces spores that are characteristically resistant, allowing this bacterium to persist in the extreme environments and to maintain its viability for many years [5]. Previous studies showed that bacteria isolated from the extreme environments, such as the Mariana Trench [6], the polar and permafrost soils in the Arctic [7,8], and the extremely dry and saline soils of the Atacama Desert [9] are unique sources for the discovery of new bioactive compounds and many of them are possibly novel species [5,10,11].

The Atacama Desert is the driest place in the world located in South America, precisely in Chile, covering a 1000-km strip of land on the Pacific coast, west of the Andes Mountains. It is bordering Peru in the north and extending to the Copiapó River in the south. Nowadays, four novel *Streptomyces* species derive from this extreme desert, including *Streptomyces atacamensis* [12], *Streptomyces desertii* [13], *Streptomyces bulli* [14], and *Streptomyces leeuwenhoekii* [15]. *S. leeuwenhoekii* is the producer of two newly bioactive compounds comprised of (i) chaxamycins, showing antagonism against *Staphylococcus aureus* ATCC 25923, inhibiting the heat shock protein 90, and degrading proteins involved in cell proliferation [9] and (ii) chaxalactins, the anti-Gram-positive bacterial agents [16]. Two more novel compounds, atacamycins and chaxapeptin, each derive respectively from *Streptomyces* sp., C38 [17] and C58 [18] isolated from hyper-arid soil of the Laguna de Chaxa of Salar de Atacama in the north of Chile (a lagoon located in the commune of San Pedro de Atacama, province of El Loa). These two compounds are novel lasso-peptides produced by nonribosomal biosynthesis with post-translational modification and capable of inhibiting human lung cancer cell line A549. Another group of new compounds with antimicrobial activity, the abenquines A–D, was obtained from *Streptomyces* sp. DB634 isolated from the Salar de Tara in the Chilean Altiplano (>4000 m.a.s.l.) [19].

In Chile, the Chilean Altiplano of the Atacama Desert, is considered the highest plateau of the Andes Mountains (>3000 m.a.s.l.) with 14° to 22° S of latitude, in addition, it is subjected to strong climatic variation over different temporal scales [19]. This site offers a unique ecosystem with highly extreme conditions, such as changes in daily temperature from –10 to +25 °C [19] and it divides into different sites, for instance, Salar de Tara (at 150 km east of the town of San Pedro de Atacama, in the Province of El Loa, region Antofagasta) and Salar de Huasco (in the south of the town of Parinacota in the Arica and Parinacota regions). The Salar de Huasco is known by its polyextreme conditions, i.e., salinity gradient (from freshwater to saturation), elevated levels of solar radiation (<1100 W/m<sup>2</sup>), and negative water balance, which differs from the other locations previously studied in the Atacama Desert. Some areas of the Salar de Huasco have been found to house diverse microbes [20,21]. However, there is no study regarding the cultivable actinomycetes from this polyextreme ecosystem and their pharmaceutical potentials. Here, we aim to isolate bacteria with a focus on actinomycetes from different sites of the Salar de Huasco and to assess their pharmaceutical potentials in possession of nonribosomal peptide synthases (NRPS)-coding gene, antimicrobial activity, and cytotoxicity.

## 2. Materials and Methods

### 2.1. Isolation of Actinomycetes

Six soil samples were collected from sites H0 (base camp; freshwater stream) and H6 (saline soils) located in the northern and southern parts of the eastern shoreline of the Salar de Huasco, respectively [22] (Figure 1). Sites H0 and H6 were characterized as meso-saline and hyper saline sites with pH 7.6 and pH 8.6, respectively [23]. The samples were taken at 5 cm depth from the ground

surface using sterile polypropylene tubes and transferred to the laboratory. These samples were stored at ambient temperature for a period not exceeding 5 days. One g of soil sample was suspended in 9 mL of  $\frac{1}{4}$  strength Ringer's solution, and 1 mL of the soil suspension was diluted 100-fold and mixed in an orbital shaker at 150 rpm for 1 h. The diluted soil suspension was pretreated by heating at 55 °C for 6 min in a thermo-regulated bath [4]. The heated aliquot (0.1 mL) was spread over the surface of starch casein agar medium (SCA), supplemented with 50 µg/mL nystatin and 50 µg/mL cycloheximide to prevent fungal contamination [24]. All seeded agar plates were prepared in triplicate and incubated at 28 °C for 14–21 days [25]. Colonies with rough appearance, powdery or tough texture and branching filaments with and without aerial mycelia were subcultured on SCA plates and incubated at 28 °C for 14 days. A subculture of each isolate was prepared on International *Streptomyces* Project III (ISP3) medium [26] under the same condition cited above. The purity of the each isolates was checked using light microscope.

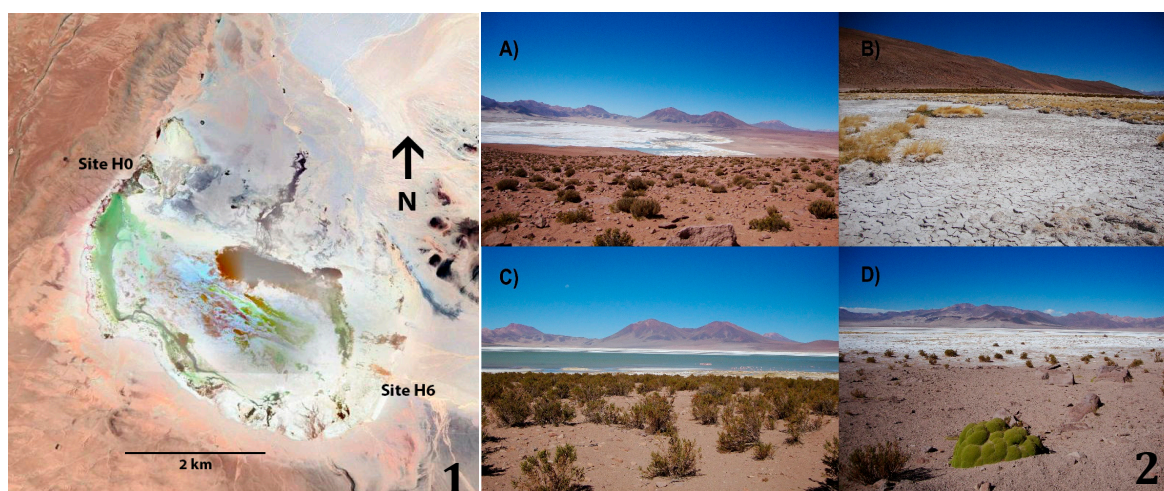


**Figure 1.** 1: Satellite image of Salar de Huasco indicating sampling sites. Image Google Earth V 7.3.2.5776. (3 March 2019). Salar de Huasco, Chile. 20°16′22.68″ S, 68°52′54.08′ W, Eye alt 14.35 mi. CNES/Airbus 2019 [30 March 2019]. <https://earth.google.com/web/@-20.29749527,-68.84083051,3780.51679815a,17347.67437889d,35y,360h,0t,0r>. 2: Sampling sites at Salar de Huasco, Northern Chile. (A) Panoramic view of Salar de Huasco, Chilean Altiplano; (B) Site H0, saline crusts; (C) Site H6, soils; (D) Site H6, saline soils.

## 2.2. Identification of Bacterial Isolates

### 2.2.1. Morphological Characterization Based on Color Grouping

The morphological characteristics of all bacterial isolates grown on ISP3 medium, such as aerial spore mass color, pigmentation of vegetative or substrate mycelium, and the production of diffusible pigment were examined. The color of the aerial and substrate mycelium of the isolates were described referring to the National Bureau of Standards (NBS) Color Name Charts [27]. Each isolate was maintained on glucose yeast extract and malt extract (GYM) medium and stored as spore suspensions and hyphae in 25% (*v/v*) glycerol at −80 °C.

### 2.2.2. 16S rRNA Gene-Based Phylogenetic Analysis

Bacterial cultures were prepared in tryptone yeast extract (ISP1) broth at 28 °C for 7 days, in which 2 mL was transferred to vials containing 0.5 mm glass beads (BioSpec Products Inc, Bartlesville, OK, USA) to breakdown mechanically the bacterial cells (Mini Bead Beater, Bead Homogenizer, BioSpec Products Inc, Bartlesville, OK, USA). Total genomic DNA was extracted from the homogenized bacterial suspension using the AxyPrep Bacterial Genomic DNA Miniprep kit (Axygen Biosciences, Union City, NJ, USA) as recommended by the manufacturer.

The 16S rRNA gene was amplified by PCR using the universal primers for bacteria, Eub9-27F and Eub1542R [28]. Every reaction was performed in a final volume of 50  $\mu$ L, containing 50–100 ng of genomic DNA, 2.0  $\mu$ M of each primer, 19  $\mu$ L of nuclease-free MilliQ-H<sub>2</sub>O (Merck Millipore, Burlington, MA, USA), and 25  $\mu$ L of SapphireAmp<sup>®</sup> Fast PCR Master Mix (TaKaRa, Japan). PCR was carried out in a thermocycler under the following conditions: Initial denaturation at 94 °C for 5 min, 30 cycles of denaturation at 94 °C for 45 s, annealing at 54 °C for 45 s, and extension at 72 °C for 1.5 min, and a final extension at 72 °C for 5 min. The PCR (Polymerase Chain Reaction) products were checked by 1% (*w/v*) agarose gel electrophoresis and subsequently sequenced by capillary sequencing using an ABI Prism 3730XL automated DNA sequencer (Applied Biosystems, Macrogen Inc., Seoul, Korea).

The 16S rRNA gene sequences were analyzed and edited using the software DNA Baser Sequence Assembler version 3.5 (Heracle BioSoft SRL, 2014). The partial 16S rRNA gene sequences of the isolates were aligned using RDP II [29]. EzTaxon [30] was used to retrieve the nearest phylogenetic neighbors of all bacterial isolates. The nearly completed 16S rRNA gene sequences (>1300 nt) of the isolates were deposited in the GenBank database with the accession numbers KX130868-KX130886.

The phylogenetic tree was constructed using Neighbor-Joining algorithms [31] with a Tamura-Nei substitution model using MEGA 7.0 software [32]. The multiple alignments of all the 16S rRNA gene sequences were performed using MUSCLE (MUltiple Sequence Comparison by Log- Expectation) algorithm [33]. The robustness of the tree was evaluated using 1000 Bootstrap [34].

### 2.3. Evaluations of Pharmaceutical Potentials

#### 2.3.1. Genotyping of Nonribosomal Peptide Synthetase (NRPS)

*Streptomyces* isolates with nearly complete 16S rRNA gene sequences were screened for the presence of nonribosomal peptide synthetase (NRPS) domains using the primers A3F (5'-GCSTACSYSATS TACACSTCSGG-3') and A7R (5'-SASGTCVCCSGTSCGGTAS-3') following a method described by Ayuso-Sacido and Genilloud [35].

#### 2.3.2. Preparation of Crude Extracts and Bioactivity Assessments

The secondary metabolites were extracted from *Streptomyces* isolates possessing NRPS domains following a protocol described by Schneemann et al. [36] with some modifications. Each isolate was grown in 100 mL of GYM (pH 7.2), and in starch-soy peptone (SPM, pH 7.0) liquid media supplemented with 2% NaCl and incubated at 28 °C for one week, with shaking at 135 rpm, in an orbital shaking incubator (MaxQ 4000, Thermo Fisher Scientific, Waltham, MA, USA). Extraction of metabolites from the whole culture broths started with the addition of 150 mL of ethyl acetate to each flask, followed by stirring and sonication cycles and kept at 4 °C overnight for effective phase separation. The lower aqueous phase was discarded, and the ethyl acetate phase (supernatant) was dried in a rotary evaporator (Büchi, Flawil, Switzerland) at ambient temperature.

The antimicrobial activity of the crude extracts was evaluated by bioassays using stocks solutions with a concentration of 1% *w/v* (equivalent to 10 mg/mL in methanol). The bioassays of antibacterial and antifungal activities were performed following a procedure described by Schneemann et al. [36]. Aliquot of 5  $\mu$ L of each crude extract was added in each well of the 96-well microtiter plate and then the solvent was evaporated using vacuum centrifuge (Biotage SPE Dry, Uppsala, Sweden) before append 195  $\mu$ L of the test microbial suspension. The final concentration of each crude extract in the bioassays was 250  $\mu$ g/mL. The test organisms comprised of gram-positive bacteria: *Staphylococcus epidermidis* DSM 20044<sup>T</sup>, methicillin-resistant *Staphylococcus aureus* DSM 18827, *Pseudomonas aeruginosa* DSM 50071<sup>T</sup>, and *Propionibacterium acnes* DSM 1897<sup>T</sup>, gram-negative bacteria: *Xanthomonas campestris* DSM 2405 and *Erwinia amylovora* DSM 50901, and fungi: *Candida albicans* DSM 1386, *Trichophyton rubrum*, *Septoria tritici*, and *Phytophthora infestans*. *Trichophyton rubrum* was obtained from F. Horter (Department of Dermatology, Allergology, and Venerology, University Hospital Schleswig-Holstein, Kiel, Germany while *Septoria tritici* and *Phytophthora infestans* were obtained from Dr. J. B. Speakman

(BASF, Ludwigshafen, Germany). The positive control for the test bacteria was 100 µg/well of chloramphenicol and that for the test fungi was 200 µg/well of cycloheximide, while the negative control was no compound applied.

The cytotoxicity test was performed following a method described by Schulz et al. [19]. Aliquot (1 µL) of each crude extract was added in a final assay volume of 100 µL of the mouse fibroblasts (NIH-3T3) and hepatocellular carcinoma (HepG2 ACC 180) cell lines. NIH-3T3 cell line was provided by G. Rimbach, University of Kiel, Germany while HepG2 ACC 180 was obtained from Leibniz Institute DSMZ-German collection of microorganisms and cell cultures, Braunschweig, Germany. The final concentration of each crude extract in the bioassays was 100 µg/mL. The positive control for these assays was tamoxifen with a final concentration of 40 µM. No compound was added for the negative control.

### 2.3.3. Profiling of Metabolites in Crude Extracts

The crude extracts dissolved in methanol were elucidated by analytical reversed-phase HPLC-UV-MS (High-Performance Liquid Chromatography with UV detector coupled to Mass Spectrometry), in a VWR-Hitachi La-Chrom Elite System, coupled to a diode array detector and a Phenomenex Onyx Monolithic column (C18, 100 × 3.00 mm) according to the conditions described by Silber et al. [37]. For the mass detection, the HPLC system was coupled to an ion trap detector (Esquire4000, Bruker Daltonics, Billerica, MA, USA). The UV-Vis spectra of peaks obtained from each bacterial crude extract were compared with the Dictionary of Natural Products 2012 [38].

## 3. Results and Discussion

### 3.1. Selective Isolation and Identification of the Isolates

A number of 30 and 46 isolates were obtained from soils samples of sites H0 and H6, respectively. These isolates were obtained from plates with 10 fold dilutions, and 97% (74 isolates) of them were found to be affiliated with the phylum *Actinobacteria* based on the 16S rRNA gene sequence similarity. Two isolates were classified as *Bacillus* and *Pseudomonas*, while the others belong to *Nocardiopsis* (7 isolates), *Micromonospora* (2 isolates), and *Streptomyces* (65 isolates) (Table 1).

**Table 1.** 16S rRNA gene-based identification of all bacteria isolated from Salar de Huasco.

Class	Family	Genus	Number of Isolate (%)	Site of Isolation
<i>Actinobacteria</i>	<i>Streptomycetaceae</i>	<i>Streptomyces</i>	65 (86%)	H0 and H6
	<i>Nocardiopsaceae</i>	<i>Nocardiopsis</i>	7 (9%)	H0
	<i>Micromonosporaceae</i>	<i>Micromonospora</i>	2 (3%)	H0
<i>Bacilli</i>	<i>Bacillaceae</i>	<i>Bacillus</i>	1 (1%)	H0
<i>Gammaproteobacteria</i>	<i>Pseudomonadaceae</i>	<i>Pseudomonas</i>	1 (1%)	H0

The eleven non-*Streptomyces* isolates were found only in the soil sample with neutral pH 7.6 collected from site H0, while the majority of the *Streptomyces* isolates (40) were obtained from the hypersaline site H6 with pH 8.6. All 65 *Streptomyces* isolates were subdivided into three color grouping after incubation on ISP3 agar medium at 28 °C for 14 days (Table 2). They showed the typical morphology of the genus *Streptomyces* in formation of aerial mycelium and spore chains. Most of these isolates produced diffusible pigments and excreted colored aqueous droplets on the hydrophobic surface of their colonies.



**Table 2.** Morphological and molecular characteristics of some *Streptomyces* spp. <sup>a</sup> isolated from Salar de Huasco.

Isolate Code	Site of Isolation	Morphological Characteristics <sup>b</sup>			Molecular Characteristics			
		Aerial Spore Mass	Substrate Mycelium	Diffusible Pigments	Closest Type Strain	16 rRNA Gene Accession Number	Similarity (%)	NRPS (Adenylation Domain)
HST05	H6	White	Light yellowish pink	-	<i>Streptomyces canus</i> DSM 40017 <sup>T</sup>	KQ948708	96.8	+
HST09	H6	Dark greyish blue	Deep purplish red	-	<i>Streptomyces lienomycini</i> LMG 20091 <sup>T</sup>	AJ781353	99.6	+
HST14	H6	White	Pale violet	Light greyish brown	<i>Streptomyces atroolivaceus</i> NRRL ISP-5137 <sup>T</sup>	JNXG01000049	96.0	-
HST18	H6	-	Dark olive green	Moderate yellow green	<i>Streptomyces alboniger</i> NRRL B-1832 <sup>T</sup>	LIQN01000245	96.7	+
HST19	H6	Dark greyish blue	Dark greenish yellowish green	Dark greyish yellowish brown	<i>Streptomyces collinus</i> NBRC 12759 <sup>T</sup>	AB184123	99.2	+
HST21	H6	White	Greyish yellow	Moderate olive brown	<i>Streptomyces albidochromogenes</i> NBRC 101003 <sup>T</sup>	AB249953	99.1	+
HST22	H6	White	Deep orange yellow	Moderate olive brown	<i>Streptomyces albidochromogenes</i> NBRC 101003 <sup>T</sup>	AB249953	99.0	+
HST23	H6	Light pink	Light orange yellow	Dark yellow	<i>Streptomyces purpureus</i> NBRC 13927 <sup>T</sup>	AB184547	98.8	-
HST28	H6	White	Light olive brown	Dark brown	<i>Streptomyces kanamyceticus</i> NBRC 13414 <sup>T</sup>	AB184388	98.8	+
HST50	H6	White	Greyish reddish brown	-	<i>Streptomyces ambofaciens</i> ATCC 23877 <sup>T</sup>	CP012382	96.0	-
HST51	H6	Light pink	Strong yellowish brown	-	<i>Streptomyces alboniger</i> NRRL B-1832 <sup>T</sup>	LIQN01000245	98.6	+
HST54	H6	White	Deep red	Light greyish brown	<i>Streptomyces griseolus</i> NRRL B-2925 <sup>T</sup>	JOFC01000069	97.6	-
HST61	H6	Pale yellowish pink	Pale orange yellow	-	<i>Streptomyces kansasensis</i> ZX01 <sup>T</sup>	JN572690	99.6	-
HST66	H6	White	Deep greenish yellow	-	<i>Streptomyces funanus</i> NBRC 13042 <sup>T</sup>	AB184273	96.9	+
HST68	H6	Greyish blue	Pinkish grey	-	<i>Streptomyces ambofaciens</i> ATCC 23877 <sup>T</sup>	CP012382	96.0	+
HST69	H0	White	Brilliant yellow	-	<i>Streptomyces chlorus</i> BK125 <sup>T</sup>	LIQN01000245	98.1	+
HST72	H0	White	Strong yellowish brown	Strong brown	<i>Streptomyces microflavus</i> NBRC 13062 <sup>T</sup>	AB184284	97.9	-
HST82	H0	White	Pale yellowish pink	-	<i>Streptomyces cyaneofuscatus</i> NRRL B-2570 <sup>T</sup>	JOEM01000050	95.6	-
HST83	H0	White	Strong yellowish brown	Strong brown	<i>Streptomyces pratensis</i> ch24 <sup>T</sup>	JQ806215	97.8	+

<sup>a</sup> These *Streptomyces* isolates were selected based on the quality of their 16S rRNA gene sequences (>1300 nt). <sup>b</sup> The morphological characteristics were observed after growing *Streptomyces* isolates on ISP3 agar medium at 28 °C for 14 days.

Nineteen out of 65 *Streptomyces* isolates were selected for further study based on their nearly complete 16S rRNA gene sequences (>1300 bp). These 19 isolates widely distributed across the phylogenetic tree of the genus *Streptomyces* supported by high bootstrap values as shown in Figure 2. A total of 12 isolates showed a 16S rRNA gene sequence similarity below the 98.7% threshold for proposing as novel species [39] (Table 2), while the other seven (HST09, HST19, HST21, HST22, HST23, HST28, and HST61) found to occupy distinct phylogenetic positions from their closest relatives with no close relationship with any species and type strains of the genus *Streptomyces* from the Atacama Desert described so far [11–15] (Figure 2).

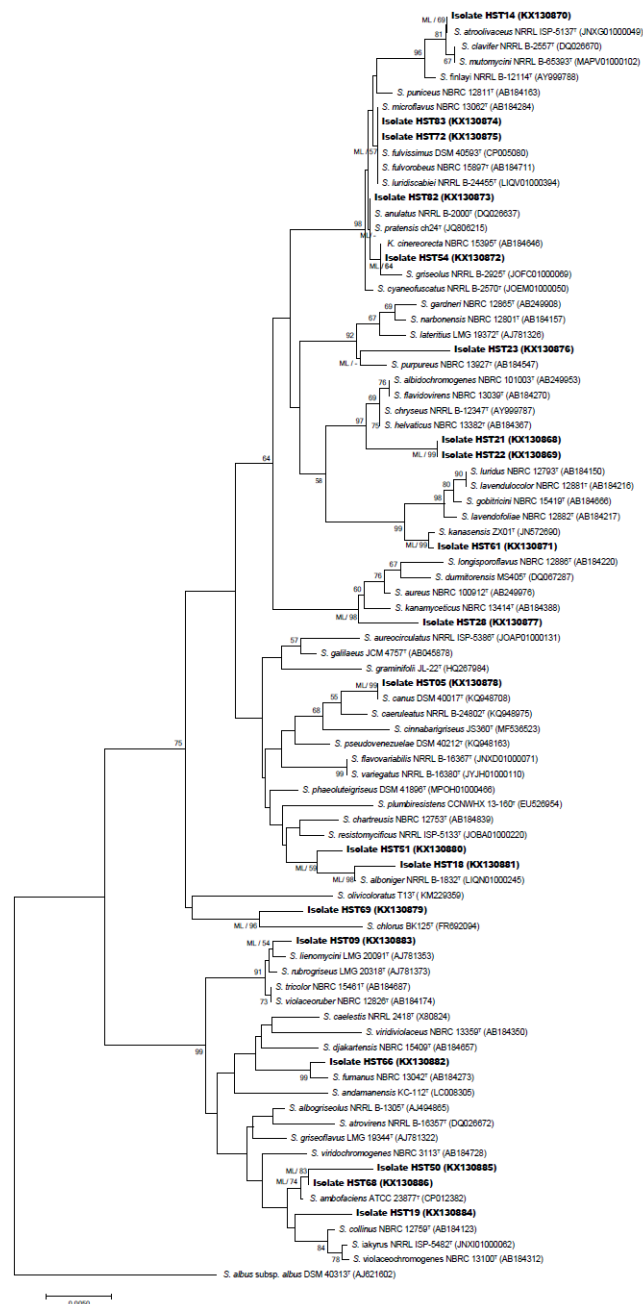


**Figure 2.** Neighbor-joining phylogenetic tree based on almost complete 16S RNA sequences (>1300 nt) of the 19 *Streptomyces* isolates derived from Salar de Huasco and their closely related species. The tree was constructed using the Neighbor-Joining algorithm and the Jukes–Cantor substitution model. The scale bar indicates 0.005 substitutions per nucleotide, and *Streptomyces albus* subsp. *albus* DSM 40313<sup>T</sup> was used as an out-group. Bootstrap values above 50% are present.

Isolate HST19 forms a distinct branch closely related to the type strain of *Streptomyces collinus* NBRC 12759<sup>T</sup> (99.2%) [40], *Streptomyces iakyrus* NRRL ISP-5482<sup>T</sup> (98.8%) [41], and *Streptomyces violaceochromogenes* NBRC 13100<sup>T</sup> (99.3%) [42]. Isolates HST21 and HST22 form a well-supported sub-clade closely associated to *Streptomyces albidochromogenes* NBRC 101003<sup>T</sup> (99.0%) [43]. Strain HST61 occupied a phylogenetic position close to “*Streptomyces kanasensis*” ZX01 (99.6%) which is a producer of a novel antiviral glycoprotein [44]. Isolate HST28 showed close phylogenetic relationship with *Streptomyces kanamyceticus* NBRC 13414<sup>T</sup> (98.8%) [45], while isolate HST23 had close relatedness to *Streptomyces purpureus* NBRC 13927<sup>T</sup> (98.8%) [46]. Isolates HST09 occupied distant subclade closely related to *Streptomyces lienomycini* LMG 20091<sup>T</sup> (99.6%) [43].

The length of the branch of all *Streptomyces* isolates in the phylogenetic tree and the assignment to these isolates to completely different clades from each other, except for isolates HST21 and HST22, highlight the divergence of them from their closely related neighbors. Further studies need to be performed to confirm the right affiliations of these isolates to the novel species within the evolutionary radiation of the genus *Streptomyces*.

Most isolates (except for isolates HST83, HST72, HST21, and HST22) showed divergent phylogenetic positions compared to the type species of the genus *Streptomyces* (Figure 2). Therefore, these strains should be designed for further taxonomic and analytical chemistry analyses to confirm their novelty at species rank and as a source of novel chemical entities (Table 3).

**Table 3.** Bioactivities of crude extracts derived from *Streptomyces* spp. of Salar de Huasco.

Crude Extract Derived From <i>Streptomyces</i> Isolate Grown in Different Media	Growth Inhibition (%) <sup>a</sup>										
	Antibacterial Activity					Antifungal Activity				Cytotoxicity	
	Gram-Positive Bacteria			Gram-Negative Bacteria		Ca	Tru	Sep	PhA	NIH-3T3	HepG2
	Se	MRSA	Pa	Xc	Ea	Ca	Tru	Sep	PhA	NIH-3T3	HepG2
HST09-GYM	96	92	-	27	-	-	72	-	-	99	79
HST09-SPM	28	28	-	-	-	-	-	-	-	36	-
HST14-GYM	-	-	-	-	-	-	33	-	-	50	40
HST14-SPM	-	-	-	-	-	-	30	-	-	51	42
HST19-GYM	-	-	57	55	-	-	58	-	-	57	34
HST19-SPM	61	60	53	76	-	-	-	-	-	20	-
HST21-GYM	99	98	-	84	91	-	86	22	50	99	99
HST21-SPM	97	95	-	79	96	-	100	-	53	99	99
HST23-GYM	93	92	100	97	71	77	100	100	49	99	99
HST23-SPM	98	97	97	99	97	76	100	100	49	99	99
HST28-GYM	97	98	100	100	22	45	37	94	27	100	100
HST28-SPM	100	100	100	100	-	39	29	89	25	97	100
HST50-GYM	96	-	90	97	92	-	41	29	-	43	38
HST50-SPM	93	41	97	98	-	-	57	30	-	-	-
HST54-GYM	96	95	96	78	-	-	48	-	39	53	24
HST54-SPM	95	92	93	71	-	-	47	-	35	52	25
HST61-GYM	73	-	-	76	63	-	59	59	22	-	-
HST61-SPM	81	41	-	62	68	-	43	62	26	-	-
HST68-GYM	93	-	90	97	91	-	30	21	-	-	21
HST68-SPM	38	-	50	24	-	-	45	-	-	-	-
HST72-GYM	95	97	98	35	-	28	60	100	47	97	69
HST72-SPM	97	97	99	56	-	-	50	96	28	86	59
HST82-GYM	100	97	90	92	-	-	41	-	-	50	40
HST82-SPM	-	47	-	-	-	-	26	-	-	39	38

<sup>a</sup> The average results derived from triplicate assays are shown with inhibition percentage (%) of growth of Se (*Staphylococcus epidermis*), MRSA (methicillin-resistant *Staphylococcus aureus*), Pa (*Propionibacterium acnes*), Xc (*Xanthomonas campestris*), Ea (*Erwinia amylovora*), Ca (*Candida albicans*), Tru (*Trichophyton rubrum*), Sep (*Septoria tritici*), Pha (*Phytophthora infestans*), NIH-3T3 (mouse fibroblasts), and HepG2 (hepatocellular carcinoma). GYM and SPM refer respectively to glucose yeast extract plus malt extract medium and starch-soy peptone medium, in which the *Streptomyces* isolates were grown before the preparation of their crude extracts. The negative results are shown with (-).

### 3.2. Secondary Metabolite Analysis

The NRPSs are multimodular enzymatic complexes constituted by three main catalytic domains: The adenylation (A) domain, responsible for the recognition and activation of a specific amino acid, the condensation (C) domain catalyses the formation of the peptidic bond (C-N) between different modules, and the peptidyl-carrier (T) domain which transfers the activated amino acids from the A domain to the C domain of the same module [6]. The presence of A domain in actinobacterial genomes reflects the biosynthesis of secondary metabolites. The products of the NRPS biosynthetic pathway are diverse secondary metabolites including several antitumor compounds [47,48]. A total of 12 *Streptomyces* isolates (63%) (Table 2) revealed the possession of NRPS A domain. A correlation has been previously observed between the numbers of isolates with the positive NRPS-PCR reaction and the production of bioactive compounds [36]. The 12 NRPS-holding isolates were tested further for their bioactivities. Isolates HST05, HST14, HST18 and HST51 were discarded from this analysis due to their low growth rate on the test media. From the pairs of isolates HST83-HST72 and HST21-HST22 that occupied the same phylogenetic position (Figure 2), we only included isolates HST21 and HST72 for the bioactivity tests.

The crude extracts obtained from *Streptomyces* isolates grown previously in GYM or SPM broth demonstrated the different HPLC profiles (Figure S1). These isolates have a wide range of metabolites in their chromatograms (Figure S1). The UV-Vis and MS data of the crude extracts in comparison with the Dictionary of Natural Products Database exhibited a low similarity to the known compounds, which highlights the novelty of these natural entities. The majority of the isolates showed high antifungal, antibacterial and cytotoxic activities (Table 3), supported by the high levels of growth inhibition (>90%) against several pathogens, such as, MRSA (HST09, HST21, HST23, HST28, HST72, HST82, HST50, HST54, and HST68), *P. acnes* (HST23, HST23, HST28, HST50, HST54, and HST72), *X. campestris* (HST23, HST28, HST50, and HST68), and *Trichophyton rubrum* (HST21 and HST23). The crude extracts at a final extract concentration of 100 µg/mL from isolates HST09, HST21, HST23, HST28, HST66, and HST72 also showed the high levels of cytotoxicity (~99%) against the tumor cell lines of HepG2 and NIH-3T3. Based on the overall bioactivities, isolates HST21, HST23, and HST28 were the producers of broad-spectrum antibiotics. These results are coherent with those described *Streptomyces* spp. isolated from the other Salar sites of the Atacama Desert, e.g., *Streptomyces* sp. C38 from Salar de Atacama that produces atacamycins A–C [17] and *Streptomyces* sp. DB634 from Salar de Tara that produces abenquines A–D [19].

The polyextreme ecosystem of Salar de Huasco forces the microorganisms to adapt to it [49], which led to the development of unique *Streptomyces* taxa that are clearly different from the other sites in the Atacama Desert and the Altiplano [9] and probably vary due to the spatial heterogeneity within the same area [50].

## 4. Conclusions

*Streptomyces* spp. isolated from the Salar de Huasco at the Chilean Altiplano showed taxonomic divergences from the species with validly published names and capabilities to produce novel secondary metabolites with interesting pharmaceutical potentials. These findings open up the prospect for novel drug discovery. Further analytical and chemical analyses should be carried out to elucidate these microbial products in order to be exploited for future biotechnological applications.

**Supplementary Materials:** The following are available online at <http://www.mdpi.com/1424-2818/11/5/69/s1>, Figure S1: HPLC-UV/Vis Chromatographic profiles of extracts obtained from culture metabolic extracts for analyzed strains, which were grown in liquid media GYM (A) and SPM (B) both of them at 2% NaCl.

**Author Contributions:** C.C.-A. carried out the experiments, analyzed the data and wrote the manuscript with support from I.N., C.D., J.A.A. and B.A. I.N. contributed to the interpretation of the results and helped in writing the manuscript. C.D. designed the experiments and supervised the work. J.S. and J.F.I. performed the bioassays tests and the mass spectrometry analyses. All the authors discussed the results and contributed to the final version of the manuscript.

**Funding:** This study was supported by grants from DAAD-CONICYT Project 698, FONDECYT 1110953; 1140179 and by CONICYT with the PFCHA/DOCTORADO BECAS CHILE/2016—21160585 and the Basal Centre Grant for CeBiB (FB0001).

**Acknowledgments:** We acknowledge to Jaime Guerrero for his help in the field, Pablo Aguilar for sampling support, Diego Cornejo for technical support and the whole team of the Laboratory of Functional Ecology and Microbial Complexity of Antofagasta Institute, University of Antofagasta (Antofagasta, Chile).

**Conflicts of Interest:** The authors declare that the research was conducted in the absence of any commercial or financial relationships that could be construed as a potential conflict of interest.

## References

1. Bérdy, J. Bioactive microbial metabolites. *J. Antibiot.* **2005**, *58*, 1–26. [[CrossRef](#)]
2. Watve, M.; Tickoo, R.; Jog, M.; Bhole, B. How many antibiotics are produced by the genus *Streptomyces*? *Arch. Microbiol.* **2001**, *176*, 386–390. [[CrossRef](#)]
3. Amoutzias, G.D.; Anargyros Chaliotis, A.; Mossialos, D. Discovery Strategies of Bioactive Compounds Synthesized by Nonribosomal Peptide Synthetases and Type-I Polyketide Synthases Derived from Marine Microbiomes. *Mar. Drugs* **2016**, *14*, 80. [[CrossRef](#)]
4. Antony-Babu, S.; Goodfellow, M. Biosystematics of alkaliphilic *Streptomyces* isolated from seven locations across a beach and dune sand system. *Antonie Leeuwenhoek* **2008**, *94*, 581–591. [[CrossRef](#)] [[PubMed](#)]
5. Bull, A.T.; Stach, J.E.; Ward, A.C.; Goodfellow, M. Marine actinobacteria: Perspectives, challenges, future directions. *Antonie Leeuwenhoek* **2005**, *87*, 65–79. [[CrossRef](#)]
6. Pathom-aree, W.; Stach, J.E.M.; Ward, A.C.; Horikoshi, K.; Bull, A.T.; Goodfellow, M. Diversity of Actinomycetes isolated from Challenger Deep sediment (10,898 m) from the Mariana Trench. *Extremophiles* **2006**, *10*, 181–189. [[CrossRef](#)]
7. Lyutskanova, D.; Ivanova, V.; Stoilova-Disheva, M.; Kolarova, M.; Aleksieva, K.; Peltekova, V. Isolation and characterization of a psychrotolerant *Streptomyces* strain from permafrost soil in Spitsbergen, producing phthalic acid ester. *Biotechnol. Biotechnol. Equip.* **2009**, *23*, 1220–1224. [[CrossRef](#)]
8. Steven, B.; Pollard, W.H.; Greer, C.W.; Whyte, L.G. Microbial diversity and activity through a permafrost/ground ice core profile from the Canadian high Arctic. *Environ. Microbiol.* **2008**, *10*, 3388–3403. [[CrossRef](#)]
9. Okoro, C.K.; Asenjo, J.A.; Andrews, B.A.; Ferguson, G.; Bull, A.T.; Goodfellow, M.; Ebel, R.; Jaspars, M. Chaxamycins A–D, bioactive ansamycins from a hyper-arid desert *Streptomyces* sp. *J. Nat. Prod.* **2011**, *74*, 1491–1499. [[CrossRef](#)]
10. Fiedler, H.P.; Bruntner, C.; Bull, A.T.; Ward, A.C.; Goodfellow, M.; Potterat, O.; Puder, C.; Mihm, G. Marine Actinomycetes as a source of novel secondary metabolites. *Antonie Leeuwenhoek* **2005**, *87*, 37–42. [[CrossRef](#)]
11. Goodfellow, M.; Nouioui, I.; Sanderson, R.; Xie, F.; Bull, A.T. Rare taxa and dark microbial matter: Novel bioactive actinobacteria abound in Atacama Desert soils. *Antonie Leeuwenhoek* **2018**, *111*, 1315–1332. [[CrossRef](#)]
12. Santhanam, R.; Okoro, C.K.; Rong, X.; Huang, Y.; Bull, A.T.; Weon, H.Y.; Andrews, B.A.; Asenjo, J.A.; Goodfellow, M. *Streptomyces atacamensis* sp. nov., isolated from an extreme hyper-arid soil of the Atacama Desert, Chile. *Int. J. Syst. Evol. Microbiol.* **2012**, *62*, 2680–2684. [[CrossRef](#)]
13. Santhanam, R.; Okoro, C.K.; Rong, X.; Huang, Y.; Bull, A.T.; Andrews, B.A.; Asenjo, J.A.; Weon, H.Y.; Goodfellow, M. *Streptomyces deserti* sp. nov., isolated from hyper-arid Atacama Desert soil. *Antonie Leeuwenhoek* **2012**, *101*, 575–581. [[CrossRef](#)] [[PubMed](#)]
14. Santhanam, R.; Rong, X.; Huang, Y.; Andrews, B.A.; Asenjo, J.A.; Goodfellow, M. *Streptomyces bullii* sp. nov., isolated from a hyper-arid Atacama Desert soil. *Antonie Leeuwenhoek* **2013**, *103*, 367–373. [[CrossRef](#)]
15. Busarakam, K.; Bull, A.T.; Girard, G.; Labeda, D.P.; Van Wezel, G.P.; Goodfellow, M. *Streptomyces leeuwenhoekii* sp. nov., the producer of chaxalactins and chaxamycins, forms a distinct branch in *Streptomyces* gene trees. *Antonie Leeuwenhoek* **2014**, *105*, 849–861. [[CrossRef](#)]
16. Rateb, M.E.; Houssen, W.E.; Harrison, W.T.A.; Deng, H.; Okoro, C.K.; Asenjo, J.A.; Andrews, B.A.; Bull, A.T.; Goodfellow, M.; Ebel, R.; et al. Diverse metabolic profiles of a *Streptomyces* strain isolated from a hyper-arid environment. *J. Nat. Prod.* **2011**, *74*, 1965–1971. [[CrossRef](#)]
17. Nachtigall, J.; Kulik, A.; Helaly, S.; Bull, A.T.; Goodfellow, M.; Asenjo, J.A.; Maier, A.; Wiese, J.; Imhoff, J.F.; Sussmuth, R.D.; et al. Atacamycins A–C, 22-membered antitumor macrolactones produced by *Streptomyces* sp. C38. *J. Antibiot.* **2011**, *64*, 775–780. [[CrossRef](#)]

18. Elsayed, S.S.; Trusch, F.; Deng, H.; Raab, A.; Prokes, I.; Busarakam, K.; Asenjo, J.A.; Andrews, B.A.; Van West, P.; Bull, A.T.; et al. Chaxapeptin, a lasso peptide from extremotolerant *Streptomyces leeuwenhoekii* strain C58 from the hyperarid Atacama Desert. *J. Org. Chem.* **2015**, *80*, 10252–10260. [[CrossRef](#)] [[PubMed](#)]
19. Schulz, D.; Beese, P.; Ohlendorf, B.; Erhard, A.; Zinecker, H.; Dorador, C.; Imhoff, J.F. Abenquines A–D: Aminoquinone derivatives produced by *Streptomyces* sp. strain DB634. *J. Antibiot.* **2011**, *64*, 763–768. [[CrossRef](#)] [[PubMed](#)]
20. Dorador, C.; Vila, I.; Witzel, K.-P.; Imhoff, J.F. Bacterial and archaeal diversity in high altitude wetlands of the Chilean Altiplano. *Fundam. Appl. Limnol.* **2013**, *182*, 135–159. [[CrossRef](#)]
21. Molina, V.; Hernandez, K.; Dorador, C.; Hengst, M.; Pérez, V. Bacterial active community cycling in response to solar radiation and their influence on nutrient changes in a high-altitude wetland. *Front. Microbiol.* **2016**, *7*, 1823. [[CrossRef](#)]
22. Dorador, C.; Vila, I.; Remonsellez, F.; Imhoff, J.F.; Witzel, K.-P. Unique clusters of Archaea in Salar de Huasco, an athalassohaline evaporitic basin of the Chilean Altiplano. *FEMS Microbiol. Ecol.* **2010**, *73*, 291–302. [[CrossRef](#)]
23. Dorador, C.; Meneses, D.; Urtuvia, V.; Demergasso, C.; Vila, I.; Witzel, K.P.; Imhoff, J.F. Diversity of Bacteroidetes in high-altitude saline evaporitic basins in northern Chile. *J. Geophys. Res.* **2009**, *114*, G00D05. [[CrossRef](#)]
24. Kuester, E.; Williams, S.T. Selection of media for isolation of *Streptomyces*. *Nature* **1964**, *202*, 928–929. [[CrossRef](#)]
25. Vickers, J.C.; Williams, S.T.; Ross, G.W. A taxonomic approach to selective isolation of *Streptomyces* from soil. In *Biological and Biochemical Aspects of Actinomycetes*; Ortiz-Ortiz, L., Bojalil, L.F., Yakoleff, V., Eds.; Academic Press: Orlando, FL, USA, 1984; pp. 553–561.
26. Shirling, E.B.; Gottlieb, D. Methods for characterization of *Streptomyces* species. *Int. J. Syst. Bacteriol.* **1966**, *16*, 313–340. [[CrossRef](#)]
27. Kelly, K.L. *Color Name Charts Illustrated with Centroid Colors*; Supplement to NBS Circular 553. Inter-Society Color Council—National Bureau of Standards (ISCC-NBS); U. S. National Bureau of Standards: Washington, DC, USA, 1964.
28. Stackebrandt, E.; Liesack, W. Nucleic Acids and Classification. In *Handbook of New Bacterial Systematics*; Goodfellow, M., O'Donnell, A.G., Eds.; Academic Press: London, UK, 1993; pp. 151–194.
29. Wang, Q.; Garrity, G.M.; Tiedje, J.M. Cole JR (2007) Naive bayesian classifier for rapid assignment of rRNA sequences into the new bacterial taxonomy. *Appl. Environ. Microbiol.* **1984**, *73*, 5261–5267. [[CrossRef](#)] [[PubMed](#)]
30. Kim, O.S.; Cho, Y.J.; Lee, K.; Yoon, S.H.; Kim, M.; Na, H.; Park, S.C.; Jeon, Y.S.; Lee, J.H.; Yi, H.; et al. Introducing EzTaxon-e: A prokaryotic 16S rRNA gene sequence database with phylotypes that represent uncultured species. *Int. J. Syst. Evol. Microbiol.* **2012**, *62*, 716–721. [[CrossRef](#)] [[PubMed](#)]
31. Saitou, N.; Nei, M. The neighbor-joining method: A new method for reconstructing phylogenetic trees. *Mol. Biol. Evol.* **1987**, *4*, 406–425. [[CrossRef](#)]
32. Kumar, S.; Stecher, G.; Tamura, K. MEGA7: Molecular Evolutionary Genetics Analysis Version 7.0 for Bigger Datasets. *Mol. Biol. Evol.* **2016**, *33*, 1870–1874. [[CrossRef](#)]
33. Edgar, R.C. MUSCLE: Multiple sequence alignment with high accuracy and high throughput. *Nucleic Acids Res.* **2004**, *32*, 1792–1797. [[CrossRef](#)]
34. Felsenstein, J. Evolutionary trees from DNA sequences: A maximum likelihood approach. *J. Mol. Evol.* **1981**, *17*, 368–376. [[CrossRef](#)]
35. Ayuso-Sacido, A.; Genilloud, O. New PCR primers for the screening of NRPS and PKS-I systems in Actinomycetes: Detection and distribution of these biosynthetic gene sequences in major taxonomic groups. *Microb. Ecol.* **2005**, *49*, 10–24. [[CrossRef](#)]
36. Schneemann, I.; Kajahn, I.; Ohlendorf, B.; Zinecker, H.; Erhard, A.; Nagel, K.; Wiese, J.; Imhoff, J.F. Mayamycin, a Cytotoxic Polyketide from a *Streptomyces* Strain Isolated from the Marine Sponge *Halichondria panicea*. *J. Nat. Prod.* **2010**, *73*, 1309–1312. [[CrossRef](#)] [[PubMed](#)]
37. Silber, J.; Ohlendorf, B.; Labes, A.; Erhard, A.; Imhoff, J.F. Calcarides A–E, antibacterial macrocyclic and linear polyesters from a calcarisporium strain. *Mar. Drugs* **2013**, *11*, 3309–3323. [[CrossRef](#)]
38. Buckingham, J. *Dictionary of Natural Products on DVD*, version 21:1; CRC Press Taylor and Francis Group: London, UK, 2012.

39. Chun, J.; Oren, A.; Ventosa, A.; Christensen, H.; Arahal, D.R.; da Costa, M.S.; Rooney, A.P.; Yi, H.; Xu, X.W.; De Meyer, S.; et al. Proposed minimal standards for the use of genome data for the taxonomy of prokaryotes. *Int. J. Syst. Evol. Microbiol.* **2018**, *68*, 461–466. [[CrossRef](#)]
40. Lindenbein, W. Über Einige Chemisch Interessante Aktinomycetenstämme Und Ihre Klassifizierung. *Arch. Mikrobiol.* **1952**, *17*, 361–383. [[CrossRef](#)]
41. De Querioz, V.M.; Albert, C.A. *Streptomyces iakyrus* nov. sp., produtor dos antibióticos Iaquirina I, IIe, III. *Rev. Inst. Antibiot. Univ. Recife* **1962**, *4*, 33–46.
42. Ryabova, I.D.; Preobrazhenskaya, T.P. *Problems of Classification of Actinomycetes-Antagonists*; Gauze, G.F., Preobrazhenskaya, T.P., Kudrina, E.S., Blinov, N.O., Ryabova, I.D., Sveshnikova, M.A., Eds.; Government Publishing House of Medical Literature: Medgiz, Moscow, Russia, 1957; pp. 1–398.
43. Gause, G.F.; Preobrazhenskaya, T.P.; Sveshnikova, M.A.; Terekhova, L.P.; Maximova, T.S. *A Guide for the Determination of Actinomycetes. Genera Streptomyces, Streptovercillium, and Chainia*; Nauka: Moscow, Russia, 1983.
44. Han, L.; Zhang, G.; Miao, G.; Zhang, X.; Feng, J. *Streptomyces kanasensis* sp. nov., an Antiviral Glycoprotein Producing Actinomycete Isolated from Forest Soil Around Kanas Lake of China. *Curr. Microbiol.* **2015**, *71*, 627–631. [[CrossRef](#)] [[PubMed](#)]
45. Okami, Y.; Umezawa, H. Production and isolation of a new antibiotic, kanamycin. *J. Antibiot.* **1957**, *10*, 181–189.
46. Goodfellow, M.; Williams, S.T.; Alderson, G. Transfer of *Kitasatoa purpurea* Matsuma and Hata to the genus *Streptomyces* as *Streptomyces purpurea* comb. nov. *Syst. Appl. Microbiol.* **1986**, *8*, 65–66. [[CrossRef](#)]
47. Onaka, H. Biosynthesis of heterocyclic antibiotics in Actinomycetes and an approach to synthesize the natural compounds. *Actinomycetologica* **2006**, *20*, 62–71. [[CrossRef](#)]
48. Sánchez, C.; Méndez, C.; Salas, J.A. Engineering biosynthetic pathways to generate antitumor indolocarbazole derivatives. *J. Ind. Microbiol. Biotechnol.* **2006**, *33*, 560–568. [[CrossRef](#)]
49. Bowers, K.J.; Mesbah, N.M.; Wiegel, J. Biodiversity of poly-extremophilic Bacteria: Does combining the extremes of high salt, alkaline pH and elevated temperature approach a physico-chemical boundary for life? *Saline Syst.* **2009**, *5*, 9. [[CrossRef](#)]
50. Dorador, C.; Vila, I.; Imhoff, J.F.; Witzel, K.-P. Cyanobacterial diversity in Salar de Huasco, a high altitude saline wetland in northern Chile: An example of geographical dispersion? *FEMS Microbiol. Ecol.* **2008**, *64*, 419–432. [[CrossRef](#)] [[PubMed](#)]



© 2019 by the authors. Licensee MDPI, Basel, Switzerland. This article is an open access article distributed under the terms and conditions of the Creative Commons Attribution (CC BY) license (<http://creativecommons.org/licenses/by/4.0/>).

# *Streptomyces huasconensis* sp. nov., an haloalkalitolerant actinobacterium isolated from a high altitude saline wetland at the Chilean Altiplano

Carlos Cortés-Albayay,<sup>1,2</sup> Cristina Dorador,<sup>3</sup> Peter Schumann,<sup>4</sup> Barbara Andrews,<sup>2</sup> Juan Asenjo<sup>2</sup> and Imen Nouioui<sup>1,\*</sup>

## Abstract

*Streptomyces* strain HST28<sup>T</sup> isolated from the Salar de Huasco, an athalassohaline and poly-extreme high altitude saline wetland located in northern Chile, was the subject of a polyphasic taxonomic study. Strain HST28<sup>T</sup> showed morphological and chemotaxonomic features in line with its classification in the genus *Streptomyces*. Optimal growth of strain HST28<sup>T</sup> was obtained at 28 °C, pH 8–9 and up to 10 % (w/v) NaCl. Single (16S rRNA) and multi-locus gene sequence analyses showed that strain HST28<sup>T</sup> had a distinct phylogenetic position from its closest relatives, the type strains of *Streptomyces aureus* and *Streptomyces kanamyceticus*. Digital DNA–DNA hybridization (23.3 and 31.0 %) and average nucleotide identity (79.3 and 85.6 %) values between strain HST28<sup>T</sup> and its corresponding relatives mentioned above were below the threshold of 70 and 96 %, respectively, defined for assigning a prokaryotic strains to the same species. Strain HST28<sup>T</sup> was characterised by the presence of L-diaminopimelic acid in its peptidoglycan layer; galactose, glucose, ribose and traces of arabinose and mannose as whole-cell sugars; phosphatidylmethylethanolamine, phosphatidylinositol, aminolipid, glycopospholipid and an unidentified lipid as polar lipids; and the predominating menaquinones MK-9(H<sub>6</sub>), MK-9(H<sub>8</sub>) and MK-9(H<sub>4</sub>) (>20 %) as well as anteiso-C<sub>15:0</sub> and anteiso-C<sub>17:0</sub> as major fatty acids (>15 %). Based on the phenotypic and genetic results, strain HST28<sup>T</sup> (DSM 107268<sup>T</sup>=CECT 9648<sup>T</sup>) merits recognition as a new species named *Streptomyces huasconensis* sp. nov.

The genus *Streptomyces* encompasses more than 800 species with validly published names ([www.bacterio.net/streptomyces.html](http://www.bacterio.net/streptomyces.html)) which were grouped in different clusters based on single gene [1, 2], multi-locus sequence analysis [3] and genome sequence [4]. The monophyly of the genus *Streptomyces* was recently questioned and a taxonomic revision of this taxon was performed based on genome sequence and led to transfer the species *Streptomyces scabrissporus* [5] and *Streptomyces aomiensis* [6] to two novel genera, *Embleya* and *Yinghuangia* [4]. *Streptomyces* strains are aerobic, Gram-stain positive and heterotrophic micro-organisms characterized by extensive branched substrate and aerial mycelia which differentiate into spore chains [7];

peptidoglycan-rich mainly in L-diaminopimelic acid (A<sub>2</sub>pm), but meso-A<sub>2</sub>pm was also detected in certain species; major amounts of saturated iso- and anteiso-fatty acids; diphosphatidylglycerol, phosphatidylethanolamine; phosphatidylinositol and phosphatidylinositol mannosides as major polar lipids; hexa- and octa-hydrogenated menaquinones with nine isoprene units as predominant isoprenologues [1, 8]. Members of this taxon were abundant in soil including composts and some species are pathogenic for animal and human, and others are phytopathogens [1].

This taxon has been the main target of several bioprospecting strategies due to its significant ability to produce secondary metabolites compared to the other actinobacterium

**Author affiliations:** <sup>1</sup>School of Natural and Environmental Sciences, Newcastle University, Devonshire Building, Newcastle upon Tyne NE1 7RU, UK; <sup>2</sup>Centre for Biotechnology and Bioengineering, University of Chile, Beauchef 851, Santiago, Chile; <sup>3</sup>Laboratory of Microbial Complexity and Functional Ecology, Departamento de Biotecnología, Facultad de Ciencias del Mar y Recursos Biológicos and Centre for Biotechnology and Bioengineering, Universidad de Antofagasta, Chile; <sup>4</sup>Leibniz Institute DSMZ-German Collection of Microorganisms and Cell Cultures, Germany.

\*Correspondence: Imen Nouioui, [imen.nouioui@newcastle.ac.uk](mailto:imen.nouioui@newcastle.ac.uk)

**Keywords:** polyphasic taxonomy; systematic; phylogeny; phenotyping.

**Abbreviations:** *atpD*, ATP synthase F1, beta subunit; A<sub>2</sub>pm, diaminopimelic acid; AGPL, amino glycopospholipid; AL, aminolipid; ANI, average nucleotide identity; BLAST, basic local alignment search tool; BGCs, biosynthetic gene clusters; dDDH, digital DNA–DNA hybridization; DPG, diphosphatidylglycerol; *gyrB*, DNA gyrase B subunit; GGDC, Genome-to-Genome Distance Calculator; GL, glycolipid; GPL, glycopospholipid; GYM, glucose–yeast extract–malt extract; HPLC, high-performance liquid chromatography; ISP, International *Streptomyces* project; L, unknown lipid; MEGA, molecular evolutionary genetics analysis; MIDI, microbial identification; ML, maximum-likelihood; MLSA, multilocus sequence analysis; MP, maximum-parsimony; PAUP, phylogenetic analysis using parsimony; PE, phosphatidylethanolamine; PGM, personal genome machine; PI, phosphatidylinositol; PL, phospholipid; PME, phosphatidylmethyl-ethanolamine; PSU, practical salinity units; *recA*, recombinase A; *rpoB*, RNA polymerase beta subunit; RAXML, Randomized Axelerated Maximum Likelihood; RAST, rapid annotation using subsystems technology; *trpB*, tryptophane synthase beta chain; TLC, thin-layer chromatography; TNT, Tree analysis New Technology.

Two supplementary figures and two supplementary tables are available with the online version of this article.



taxa [9]. The genus *Streptomyces* is well known by its high G+C content (69–78 mol%) and a large genome size ( $\approx 8.0$  Mb), which contains a high number of biosynthetic gene clusters (BGCs). In this context, the hyper-arid soil of the Atacama Desert was the target for bioprospecting studies [10]. Forty-six natural products were obtained from diverse micro-organisms isolated from the Atacama Desert [11] including 14 compounds with novel chemical structures identified from *Streptomyces* species: (i) *Streptomyces leeuwenhoekii*, isolated from the Laguna Chaxa [12, 13], produces metabolites, Atacamycins A–C [14], Chaxalactins A–C [15], Chaxamycins A–D [16] and Chaxapeptin [17], with antibacterial and cytotoxic activities; (ii) *Streptomyces asenjonii*, isolated from the Salar de Atacama [18], produces novel natural compounds, Asenjonamides A–C [19], with antibiotic and anti-ageing activities. These findings have reinforced the continued search for novel *Streptomyces* species from these ecosystems, mainly from unexploited sites such as high altitude soils and salt lakes of the Atacama Desert located at the Altiplano (3000–5000 m.a.s.l.).

In this present study, *Streptomyces* strain HST28<sup>T</sup> isolated from the Salar de Huasco [20], an athalassohaline and poly-extreme high-altitude saline wetland (3800 m.a.s.l.) located in the Altiplano, the high plateau of the Andes [21], was the subject of a polyphasic taxonomic study. The resultant data showed that the isolate HST28<sup>T</sup> represents a new species within the evolutionary radiation of the genus *Streptomyces* for which the name *Streptomyces huasconensis* sp. nov. is proposed.

The isolate HST28<sup>T</sup> was recovered from arid soil samples, site H6 (–20.328611 S, –68.838611 W) [21], collected at a location in the Salar de Huasco [20] in complete absence of vegetation. This site has a wide range of salinity that reaches the maximum of 49.1 PSU (practical salinity units) above the oceanic average, high daily temperature changes (–10 to 25 °C) and one of the highest solar radiation levels registered worldwide ( $>1200$  W m<sup>–2</sup>) [22].

The soil sample and the isolation procedures were performed following Okoro *et al.* [12]. Strain HST28<sup>T</sup> was isolated as described by Cortés-Albayay *et al.* [20] and maintained together with its nearest phylogenetic neighbours, *Streptomyces aureus* DSM 41785<sup>T</sup> [23] and *Streptomyces kanamyceticus* DSM 40500<sup>T</sup> [24] [both strains were obtained from the German Collection of Microorganisms and Cell Cultures (DSMZ)], on GYM (medium 65, DSMZ) medium. All the strains were stored as spore suspensions and hyphae in 25 % v/v glycerol at –80 °C. *S. aureus* DSM 40500<sup>T</sup> and *S. kanamyceticus* DSM 41785<sup>T</sup> were originally deposited in DSMZ by Professor Michael Goodfellow and Dr Elwood B. Shirling, respectively.

Cultural features of the strain were determined on GYM, yeast extract–malt extract agar, tryptone–yeast extract, yeast extract–malt extract, oatmeal, inorganic salts–starch, glycerol–asparagine, peptone–yeast extract–iron and tyrosine agar plates (International *Streptomyces* Project [ISP 1–

**Table 1.** Growth and cultural features of strain HST28<sup>T</sup> after 7 days of incubation at 28 °C

Medium	Growth	Substrate mycelium colour	Aerial mycelium colour
Tryptone–yeast extract agar (ISP 1)	++	Strong yellow	Pale yellowish green
Yeast extract–malt extract agar (ISP 2)	+	Deep yellow	Pinkish white
Oatmeal agar (ISP 3)	++	Grayish green	Pale green
Inorganic salts–starch agar (ISP 4)	++	Strong yellowish brown	White
Glycerol–asparagine agar (ISP 5)	++	Moderate yellow	Yellowish white
Tyrosine agar (ISP 7)	++	Dark yellow	Greenish white
GYM (DSMZ 65)	+++	Dark brown	Pinkish white

7]; [25]). The ability of strain HST28<sup>T</sup> to grow at different temperatures, 4, 10, 15, 25, 28, 37 and 45 °C as well as in a wide range of pH (pH 5, 6, 7, 8, 9, 11 and 12) was examined on GYM medium after incubation for 7 days at 28 °C. The tolerance of the studied strain HST28<sup>T</sup> to salinity was evaluated after incubation on GYM medium supplemented with different concentrations of NaCl (2, 4, 8, 10, 12, 15 and 20 %) for 7 days at 28 °C. Strain HST28<sup>T</sup> was able to grow on all the media (Table 1) and in a temperature range between 25–37 °C as well as in a wide range of pH (pH 6–11) and up to 10 % (w/v) NaCl. Optimal growth of strain HST28<sup>T</sup> was observed on GYM medium at temperature 28 °C, pH 8–9 and up to 10 % (w/v) NaCl. The strain formed a pinkish white aerial mycelium with no diffusible pigment after incubation for 7 days at 28 °C.

The cell structures, including spore chain ornamentation and spore surface morphology, of the studied strain were recorded after incubation for 14 days on GYM medium at 28 °C, using a field-emission scanning electron microscope (Tescan Vega 3 LMU). Strain HST28<sup>T</sup> showed rectiflexible spore chains in section with hairy spore surfaces (Fig. S1, available in the online version of this article) while the nearest phylogenetic neighbours, *S. kanamyceticus* DSM 40500<sup>T</sup> and *S. aureus* DSM 41785<sup>T</sup>, were identified by their smooth spore surface [1].

The biomass of strain HST28<sup>T</sup> used for all the molecular and phenotypic tests was prepared on GYM agar plates after incubation for 7 days at 28 °C. Strain HST28<sup>T</sup> together with its nearest phylogenetic neighbours, type strains *S. aureus* and *S. kanamyceticus*, were examined for their ability to use a wide range of carbon and nitrogen sources as well as for their susceptibility to grow in the presence of different inhibitory compounds using GENIII MicroPlates in an Omnilog device (Biolog). The tests were carried out in duplicate and the resultant data were exported and analysed using the opm package for R [26, 27] version 1.06. Strain HST28<sup>T</sup> and its closest phylogenetic neighbour, *S. kanamyceticus* DSM 40500<sup>T</sup>, were able to metabolise D-fructose, D-fructose-6-phosphate and myo-inositol (carbon sources); L-

**Table 2.** Phenotypic features that distinguish strain HST28<sup>T</sup> from its nearest phylogenetic neighbours *S. aureus* DSM 41785<sup>T</sup> and *S. kanamyceticus* DSM 40500<sup>T</sup>

All the strains oxidised D-glucose, D-mannose, D-galactose, trehalose, cellobiose,  $\beta$ -gentiobiose, D-mannitol, glycerol, N-acetyl-D-glucosamine, Tween 40, dextrin and gelatin (carbon source); L-aspartic acid, L-glutamic acid and L-histidine (amino acids); acetic acid,  $\alpha$ -hydroxy-butyric acid,  $\alpha$ -keto-butyric acid,  $\alpha$ -keto-glutaric acid,  $\beta$ -hydroxy-butyric acid, D-gluconic acid, L-malic acid and propionic acid (organic acids); and growth in presence of aztreonam, lithium chloride, nalidixic acid, tetrazolium blue (inhibitory compounds) and NaCl (1–8 % w/v). In contrast none of the strains metabolised glucuronamide and L-galactonic acid- $\gamma$ -lactone, and grew in presence of fusidic acid, niaproof, tetrazolium violet, troleandomycin and vancomycin (inhibitory compounds).

	HST28 <sup>T</sup>	<i>S. aureus</i> DSM 41785 <sup>T</sup>	<i>S. kanamyceticus</i> DSM 40500 <sup>T</sup>
<b>Carbon source utilization</b>			
Lactose, D-galacturonic acid, maltose, D-salicin and N-acetyl-neuraminic acid	–	+	+
Methyl $\beta$ -D-glucoside, D-fucose, raffinose, D-sorbitol, D-glucose-6-phosphate, inosine, N-acetyl- $\beta$ -D-mannosamine, N-acetyl-D-galactosamine, pectin, sucrose, turanose, stachyose and 3-O-methyl-D-glucose	–	–	+
D-Arabitol, melibiose, L-fucose and L-rhamnose	–	w	+
D-Fructose, D-fructose-6-phosphate and myo-inositol	+	–	+
<b>Amino acids</b>			
D-Aspartic acid, D-serine #1, D-serine #2 and L-serine	–	–	+
Gly-Pro and L-pyroglutamic acid	–	w	+
L-Arginine and L-alanine	+	–	+
<b>Organic acids</b>			
Acetoacetic acid	+	–	+
Bromo-succinic acid	–	w	+
Butyric acid, citric acid, D-glucuronic acid, sodium formate, $\gamma$ -amino-n-butyric acid and mucic acid	–	+	+
D-Lactic acid methyl ester, D-malic acid, L-lactic acid, p-hydroxy-phenylacetic acid and quinic acid	–	–	+
D-Saccharic acid	–	w	+
Methyl pyruvate	+	w	w
<b>Inhibitory compounds</b>			
Guanidine hydrochloride	–	w	+
Lincomycin, rifamycin SV and sodium bromate	–	–	+
Minocycline and 1 % sodium lactate	–	+	+
Potassium tellurite	+	–	+

arginine and L-alanine (nitrogen sources); acetoacetic acid (organic acid); however, *S. kanamyceticus* DSM 40500<sup>T</sup> was able to oxidise a large number of carbon and nitrogen substrates in addition to its tolerance to several inhibitory compounds, unlike strain HST28<sup>T</sup> (Table 2).

Chemotaxonomic markers of strain HST28<sup>T</sup> and its closest neighbours, type strains of *S. aureus* and *S. kanamyceticus*, were identified using standard procedures. Cells were harvested from cultures after shaking at 250 r.p.m., washed twice with sterile distilled water and freeze-dried. TLC was used to determine A<sub>2</sub>pm isomers [28], whole-cell sugars [29] and polar lipid profiles [30]. Menaquinones were extracted as described by Tindall [31] and analysed by using an Agilent 1260 Infinity II HPLC system. The analytical column 125/2 Nucleosil 120–3 C18 column (length 125 mm, diameter 2 mm, particle size 3  $\mu$ m) was thermostatted at 35 °C. An isocratic solvent system (acetonitrile/isopropanol, 65:35, v/v; 0.4 ml min<sup>-1</sup>) was used. Fatty acid extraction was carried out for all the strains cited above following the protocol of Miller [32] and Kuykendall *et al.* [33]. The fatty acid extracts were analysed using gas chromatography (Agilent 6890 N instrument) and identified using the standard

microbial identification (MIDI) system version 4.5 and the ACTIN 6 database [34].

The chemotaxonomic features of strain HST28<sup>T</sup> were in line with those of the genus *Streptomyces*. Whole-cell hydrolysates of the isolate were rich in LL-A<sub>2</sub>pm and galactose, glucose, ribose and traces of arabinose and mannose as whole-cell sugars. However, the type strain of *S. kanamyceticus* contained traces of mannose and xylose while *S. aureus* DSM 41785<sup>T</sup> lacks galactose and had traces of mannose. The polar lipid pattern of strain HST28<sup>T</sup> contained phosphatidylmethylethanolamine (PME), phosphatidylinositol (PI), aminolipid (AL), glycopospholipid (GPL) and an unidentified lipid (L) (Fig. S2), while the type strains of *S. aureus* (DPG, PE, PME, AL, PI, GPL, L, PL) and *S. kanamyceticus* (DPG, PME, PI, GPL, AGPL, GL, L) have, in addition, diphosphatidylglycerol (DPG). The menaquinone profile of strain HST28<sup>T</sup> comprised the following components MK-9(H<sub>6</sub>) (45 %), MK-9(H<sub>8</sub>) (34 %), MK-9(H<sub>4</sub>) (11 %), MK-10 (6 %) and MK-8(H<sub>2</sub>) (4 %), while *S. kanamyceticus* DSM 40500<sup>T</sup> had MK-9(H<sub>8</sub>) (48 %), MK-9(H<sub>6</sub>) (29 %), MK-9(H<sub>4</sub>) (12 %), MK-9(H<sub>2</sub>) (4 %), MK-10(H<sub>2</sub>) (3 %), MK-10 (2 %), MK-8(H<sub>4</sub>) (1 %) and MK-9 (1 %). The

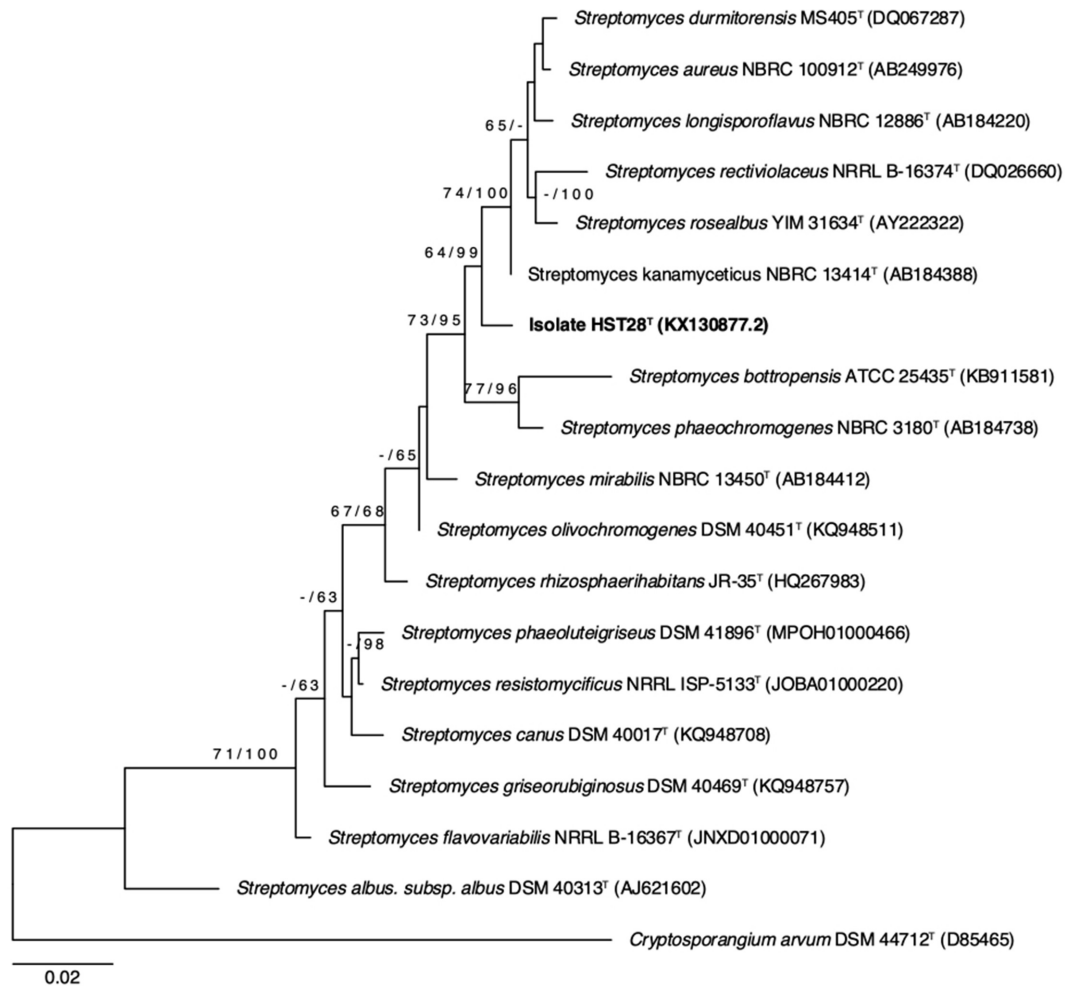


**Fig. 1.** Maximum-likelihood phylogenetic tree based on the 16S rRNA gene sequences showing the phylogenetic relationships between the isolate HST28<sup>T</sup> and its closest phylogenetic relatives. The tree was inferred using the GTR+GAMMA model and rooted using the 16S rRNA sequence of *Cryptosporangium arzum* DSM 44712<sup>T</sup>. The branches were scaled in terms of the expected number of substitutions per site and the numbers above the nodes correspond to the support values for maximum-likelihood (left) and maximum-parsimony (right).

type strain of *S. aureus* contained the following menaquinones: MK-9(H<sub>8</sub>) (54%), MK-9(H<sub>6</sub>) (20%), MK-9(H<sub>4</sub>) (9%), MK-10(H<sub>2</sub>) (7%), MK-9(H<sub>2</sub>) (4%), MK-9 (2%), MK-10 (2%) and MK-8(H<sub>4</sub>) (2%). The major fatty acids (>15%) in strain HST28<sup>T</sup> and its nearest neighbour, *S. kanamyceticus* DSM 40500<sup>T</sup>, had similar compositions [*anteiso*-C<sub>15:0</sub> (~31.8%) and *anteiso*-C<sub>17:0</sub> (~18.3%)], while the type strain of *S. aureus* DSM 41785<sup>T</sup> was characterized by the presence of *iso*-C<sub>16:0</sub> (26.5%) and *anteiso*-C<sub>15:0</sub> (20.8%) (Table S1).

The genomic DNA of strain HST28<sup>T</sup> was extracted using the UltraClean Microbial DNA isolation kit (MoBio Labs), following the instructions of the manufacturer. The 16S rRNA-PCR amplification was evaluated using the primers Eub9-27F and Eub1542R and according to the conditions cited by Stackebrandt and Liesack [35]. A BLAST of the

complete 16S rRNA gene sequence (1517 bp; accession number KX130877) of strain HST28<sup>T</sup> was performed using the EzTaxon server [36].

The pairwise sequence similarities were calculated based on the method recommended by Meier-Kolthoff *et al.* [37]. The multiple sequence alignments were performed using MUSCLE [38]. The maximum-likelihood (ML) [39] and maximum-parsimony (MP) phylogenetic trees [40] were reconstructed by using the DSMZ phylogenomics pipeline [41] available on the Genome-to-Genome Distance Calculator (GGDC) web server [42] (ggdc.dsmz.de/). ML and MP trees were inferred using RAxML [43] and TNT [44], respectively. The search for the best topology for the resultant ML tree was obtained from a rapid bootstrapping method in combination with the autoMRE bootstopping criterion [45], while a bootstrapping method of 1000 iterations, in

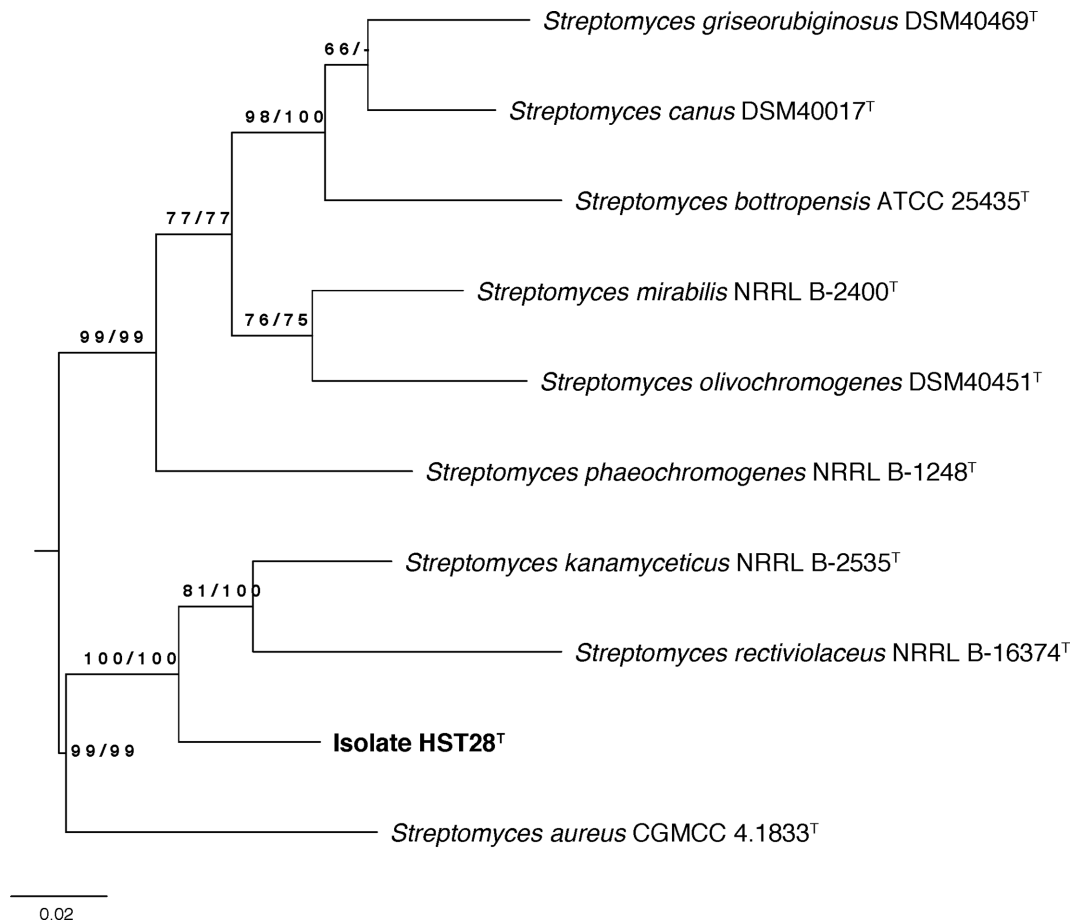


**Fig. 2.** Maximum-likelihood MLSA tree based on the concatenated partial sequences of five housekeeping genes: *atpD*, *gyrB*, *recA*, *rpoB* and *trpB*. The tree was inferred using the GTR+GAMMA model and rooted by midpoint-rooting. The branches were scaled in terms of the expected number of substitutions per site and the numbers above the nodes correspond to the support values for maximum-likelihood (left) and maximum-parsimony (right).

combination with a tree-bisection-and-reconnection branch swapping method with ten additional random sequence replicates, was used for the MP tree. The tree was rooted using *Cryptosporangium arvum* DSM 44712<sup>T</sup> [46] and the sequences were checked for a compositional bias using the  $X^2$  test as implemented in PAUP\* [47]. Multi-locus sequence analysis (MLSA) was performed based on five well-known housekeeping genes in refining the phylogeny of the genus *Streptomyces*: *atpD* (ATP synthase F1, beta subunit), *gyrB* (DNA gyrase B subunit), *rpoB* (RNA polymerase beta subunit), *recA* (recombinase A) and *trpB* (tryptophane synthase beta chain) gene sequences [3, 13, 48, 49]. All the partial housekeeping sequences of the nearest phylogenetic neighbours were retrieved from the GenBank database and the ARS Microbial Genome Sequence Database server (<http://199.133.98.43>); those of strain HST28<sup>T</sup> were extracted from the draft genome sequence (accession number RBWT00000000). The ML and MP algorithms were used to establish an MLSA phylogenetic tree based on the phylogenomic pipeline of DSMZ cited above. The genetic

distance between the loci of the studied strain and its closest phylogenetic neighbours was estimated with Kimura's two-parameter model [39] using MEGA 7.0 software [50].

BLAST results of the complete 16S rRNA gene sequence of strain HST28<sup>T</sup> showed values of 99.0% (14 nt difference) and 98.9% (16 nt) of similarity to *S. kanamyceticus* NRRL B-2535<sup>T</sup> and *S. aureus* NRRL B-2808<sup>T</sup>, respectively. These results are in line with the phylogenetic position of strain HST28<sup>T</sup> in the 16S rRNA gene tree (Fig. 1) where it formed a distinct branch loosely associated to a well-supported clade housing the type strains of *S. aureus*, *Streptomyces durmitorensis* [51], *S. kanamyceticus*, *Streptomyces longisporoflavus* [52], *Streptomyces rectiviolaceus* [53] and *Streptomyces rosealbus* [54]; the type strains of *S. aureus* and *S. kanamyceticus* appeared in the phylogenetic tree as the closest phylogenetic neighbours of strain HST28<sup>T</sup> (Fig. 1).

In the MLSA tree, strain HST28<sup>T</sup> formed a well-supported subclade closely related to the type strain of *S. kanamyceticus* and next to the *S. aureus* species (Fig. 2). The evolutionary

genetic distances, based on the concatenated sequences, between strain HST28<sup>T</sup> and its closest neighbours cited above were above the threshold of 0.007 (Table S2) for the conspecific assignment [55, 56].

For genome sequencing, the genomic DNA extraction for strain HST28<sup>T</sup> was performed according to Schniete *et al.* [57]. The draft genome was sequenced using an Ion Torrent PGM (Personal Genome Machine) sequencer, and the Ion PGM Hi-Q Sequencing Kit (Life Technologies) on a 318 v2 chip type (Life Technologies). The genome was assembled using the SPAdes software [58], annotated through the RAST server [59, 60] and deposited in the GenBank database under accession number RBWT00000000.

The resultant sequencing data showed a coverage of 78× with 468 contigs. Strain HST28<sup>T</sup> had a genome size of 8.6 Mb and 71.5 mol% as an *in silico* G+C content, 67 RNAs and 8211 coding sequences. Similarly, the type strains of *S. kanamyceticus* and *S. aureus* have genome sizes of 9.8 Mb and 7.9 Mb and *in silico* 71.0 and 71.8 mol% G+C content, respectively.

Digital DNA–DNA hybridization (dDDH) between the draft genome sequence of strain HST28<sup>T</sup> and its closest neighbours, *S. aureus* NRRL B-2808<sup>T</sup> (GenBank accession number LIPQ00000000) and *S. kanamyceticus* NRRL B-2535<sup>T</sup> (GenBank accession number LIQU00000000), were calculated using the GGDC server with the recommended formula 2 [42]. In addition, the ANI values between the strains cited above were also estimated using an OrthoANIu algorithm of the ANI calculator [61, 62].

The dDDH values between the draft genome sequences of strain HST28<sup>T</sup> and its closest relatives, *S. aureus* NRRL B-2808<sup>T</sup> (23.3% [21–25.8%]) and *S. kanamyceticus* NRRL B-2535<sup>T</sup> (31.0% [28.6–33.5%]), were well below the 70% cut-off point recommended for assigning prokaryotic strains to the same species [63]. These results are coherent with the corresponding ANI values of 79.3 and 85.6%, which are well below the threshold of 95–96% used to delineate prokaryotic species [64–66].

*In silico* genome analysis revealed the genetic potential of strain HST28<sup>T</sup> in producing new secondary metabolites well known by their antimicrobial and anticancer activities [20].

It is clear from the resultant phenotypic, genetic and genomic data that strain HST28<sup>T</sup> can be distinguished from its nearest phylogenetic neighbours and form a new taxonomic centre within the evolution of the genus *Streptomyces*. Therefore it merits the recognition as a new species, namely *Streptomyces huasconensis* sp. nov.

## DESCRIPTION OF *STREPTOMYCES HUASCONENSIS* SP. NOV.

*Streptomyces huasconensis* (hu.as.co.nen'sis. N.L. masc. adj. *huasconensis* referring to the site, Salar de Huasco, where the strain was isolated).

Aerobic, Gram-stain-positive actinobacterium producing a pinkish-white aerial mycelium on GYM agar plates after 7 days at 28 °C. Optimal growth of strain HST28<sup>T</sup> is obtained at 28 °C, pH 8–9 and up to 10% (w/v) NaCl. It was able to metabolise D-fructose, D-fructose-6-phosphate and myo-inositol (carbon sources); L-arginine and L-alanine (nitrogen sources); acetoacetic acid (organic acid) and to grow in the presence of aztreonam, lithium chloride, nalidixic acid and tetrazolium blue. It is characterised by LL-diaminopimelic acid in its peptidoglycan layer and galactose, glucose, ribose and traces of arabinose and mannose as whole-cell sugars; the polar lipid profile contains phosphatidylmethylethanolamine, phosphatidylinositol, aminolipid, glycerophospholipid and an unidentified lipid. MK-9(H<sub>6</sub>), MK-9(H<sub>8</sub>) and MK-9(H<sub>4</sub>) are the predominating menaquinones. The fatty acid profile contains major amounts of anteiso-C<sub>15:0</sub>, iso-C<sub>16:0</sub> and anteiso-C<sub>17:0</sub>. The genome size is 8.6 Mb with an *in silico* G+C content of 71.5 mol%. The type strain, HST28<sup>T</sup> (DSM 107268<sup>T</sup>=CECT 9648<sup>T</sup>), was isolated from hyper arid soil of Salar de Huasco in the Atacama Desert, Chile.

### Funding information

This project was supported by the School of Natural and Environmental Sciences at Newcastle University. I. N. is grateful to Newcastle University for a post-doctoral fellowship. C. C-A. is grateful to CONICYT for PFCHA/DOCTORADO BECAS CHILE/2016–21160585 fellowship and operational expenses. This work was also financially supported by the Basal Centres Programme of CONICYT (Chile) for funding the Centre for Biotechnology and Bioengineering, CeBiB (project FB0001) and FONDECYT 1110953; 1181773 grants.

### Acknowledgements

We thank Dr Paul Herron (Strathclyde Institute of Pharmacy and Biomedical Sciences, University of Strathclyde, Glasgow, United Kingdom) and Dr. Jana K. Schniete (Department of Physics, University of Strathclyde, Glasgow, United Kingdom) for providing the genome sequence.

### Conflicts of interest

The authors declare that there are no conflicts of interest.

### References

- Kämpfer P. Genus I. Streptomyces. In: Whitman W, Goodfellow M, Kämpfer P, Busse H-J, Trujillo M *et al.* (editors). *Bergey's Manual of Systematic Bacteriology*, 2nd ed, vol. 5. The Actinobacteria, Part B. New York: Springer; 2012. pp. 1455–1767.
- Labeda DP, Goodfellow M, Brown R, Ward AC, Lanoot B *et al.* Phylogenetic study of the species within the family Streptomycetaceae. *Antonie van Leeuwenhoek* 2012;101:73–104.
- Labeda DP, Dunlap CA, Rong X, Huang Y, Doroghazi JR *et al.* Phylogenetic relationships in the family Streptomycetaceae using multi-locus sequence analysis. *Antonie van Leeuwenhoek* 2017; 110:563–583.
- Nouioui I, Carro L, García-López M, Meier-Kolthoff JP, Woyke T *et al.* Genome-based taxonomic classification of the phylum Actinobacteria. *Front Microbiol* 2018;9:9.
- Ping X, Takahashi Y, Seino A, Iwai Y, Omura S. *Streptomyces scabrisporus* sp. nov. *Int J Syst Evol Microbiol* 2004;54:577–581.
- Nagai A, Khan ST, Tamura T, Takagi M, Shin-Ya K. *Streptomyces aomiensis* sp. nov., isolated from a soil sample using the membrane-filter method. *Int J Syst Evol Microbiol* 2011;61:947–950.
- Angert ER. Alternatives to binary fission in bacteria. *Nat Rev Microbiol* 2005;3:214–224.
- Kroppenstedt R. Fatty acid and menaquinone analysis of actinomycetes and related organisms. In: Goodfellow M and Minnikin DE

- (editors). *Chemical Methods in Bacterial Systematics*. London: Elsevier Science & Technology Books; 1985. pp. 173–199.
9. Watve MG, Tickoo R, Jog MM, Bhole BD. How many antibiotics are produced by the genus *Streptomyces*? *Arch Microbiol* 2001;176:386–390.
  10. Bull AT, Asenjo JA. Microbiology of hyper-arid environments: recent insights from the Atacama Desert, Chile. *Antonie van Leeuwenhoek* 2013;103:1173–1179.
  11. Rateb ME, Ebel R, Jaspars M. Natural product diversity of actinobacteria in the Atacama Desert. *Antonie van Leeuwenhoek* 2018;111:1467–1477.
  12. Okoro CK, Brown R, Jones AL, Andrews BA, Asenjo JA et al. Diversity of culturable actinomycetes in hyper-arid soils of the Atacama Desert, Chile. *Antonie van Leeuwenhoek* 2009;95:121–133.
  13. Busarakam K, Bull AT, Girard G, Labeda DP, van Wezel GP et al. *Streptomyces leeuwenhoekii* sp. nov., the producer of chaxalactins and chaxamycins, forms a distinct branch in *Streptomyces* gene trees. *Antonie van Leeuwenhoek* 2014;105:849–861.
  14. Nachtigall J, Kulik A, Helaly S, Bull AT, Goodfellow M et al. Atacamycins A-C, 22-membered antitumor macrolactones produced by *Streptomyces* sp. C38. *J Antibiot* 2011;64:775–780.
  15. Rateb ME, Houssen WE, Harrison WT, Deng H, Okoro CK et al. Diverse metabolic profiles of a *Streptomyces* strain isolated from a hyper-arid environment. *J Nat Prod* 2011;74:1965–1971.
  16. Rateb ME, Houssen WE, Arnold M, Abdelrahman MH, Deng H et al. Chaxamycins A-D, bioactive ansamycins from a hyper-arid desert *Streptomyces* sp. *J Nat Prod* 2011;74:1491–1499.
  17. Elsayed SS, Trusch F, Deng H, Raab A, Prokes I et al. Chaxapeptin, a Lasso Peptide from Extremotolerant *Streptomyces leeuwenhoekii* Strain C58 from the Hyperarid Atacama Desert. *J Org Chem* 2015;80:10252–10260.
  18. Goodfellow M, Busarakam K, Idris H, Labeda DP, Nouioui I et al. *Streptomyces asenjonii* sp. nov., isolated from hyper-arid Atacama Desert soils and emended description of *Streptomyces viridosporus* Pridham et al. 1958. *Antonie van Leeuwenhoek* 2017;110:1133–1148.
  19. Abdelkader MSA, Philippon T, Asenjo JA, Bull AT, Goodfellow M et al. Asenjonamides A-C, antibacterial metabolites isolated from *Streptomyces asenjonii* strain KNN 42.f from an extreme-hyper arid Atacama Desert soil. *J Antibiot* 2018;71:425–431.
  20. Cortés-Albayay C, Silber J, Imhoff JF, Asenjo JA, Andrews B et al. The polyextreme ecosystem, Salar de Huasco at the Chilean Altiplano of the Atacama Desert houses diverse *Streptomyces* spp. with promising pharmaceutical potentials. *Diversity* 2019; 11:69.
  21. Dorador C, Meneses D, Urtuvia V, Demergasso C, Vila I et al. Diversity of *Bacteroidetes* in high-altitude saline evaporitic basins in northern Chile. *J Geophys Res* 2009;114:n/a–11.
  22. Hernández KL, Yannicelli B, Olsen LM, Dorador C, Menschel EJ et al. Microbial activity response to solar radiation across contrasting environmental conditions in salar de huasco, Northern Chilean altiplano. *Front Microbiol* 2016;7:7.
  23. Manfio GP, Atalan E, Zakrzewska-Czerwinska J, Mordarski M, Rodríguez C et al. Classification of novel soil streptomycetes as *Streptomyces aureus* sp. nov., *Streptomyces laceyi* sp. nov. and *Streptomyces sanglieri* sp. nov. *Antonie van Leeuwenhoek* 2003;83:245–255.
  24. Umezawa H, Ueda M, Maeda K, Yagishita K, Kondo S et al. Production and isolation of a new antibiotic: kanamycin. *J Antibiot* 1957;10:181–188.
  25. Shirling EB, Gottlieb D. Methods for characterization of *Streptomyces* species. *Int J Syst Bacteriol* 1966;16:313–340.
  26. Vaas LA, Sikorski J, Michael V, Göker M, Klenk HP. Visualization and curve-parameter estimation strategies for efficient exploration of phenotype microarray kinetics. *PLoS One* 2012;7:e34846.
  27. Vaas LA, Sikorski J, Hofner B, Fiebig A, Buddruhs N et al. opm: an R package for analysing OmniLog(R) phenotype microarray data. *Bioinformatics* 2013;29:1823–1824.
  28. Stanek JL, Roberts GD. Simplified approach to identification of aerobic actinomycetes by thin-layer chromatography. *Appl Microbiol* 1974;28:226–231.
  29. Lechevalier MP, Lechevalier H. Chemical composition as a criterion in the classification of aerobic actinomycetes. *Int J Syst Bacteriol* 1970;20:435–443.
  30. Minnikin DE, O'Donnell AG, Goodfellow M, Alderson G, Athalye M et al. An integrated procedure for the extraction of bacterial isoprenoid quinones and polar lipids. *J Microbiol Methods* 1984;2:233–241.
  31. Tindall BJ. Lipid composition of *Halobacterium lacusprofundi*. *FEMS Microbiol Lett* 1990;66:199–202.
  32. Miller LT. Single derivatization method for routine analysis of bacterial whole-cell fatty acid methyl esters, including hydroxy acids. *J Clin Microbiol* 1982;16:584–586.
  33. Kuykendall LD, Roy MA, O'Neill JJ, Devine TE. Fatty acids, antibiotic resistance, and deoxyribonucleic acid homology groups of *Bradyrhizobium japonicum*. *Int J Syst Bacteriol* 1988;38:358–361.
  34. Sasser M. *Identification of Bacteria by Gas Chromatography of Cellular Fatty Acids*, Technical Note 101. Microbial ID. Newark, USA: Del Inc; 1990.
  35. Stackebrandt E, Liesack W. Nucleic Acids and Classification. In: Goodfellow M and O'Donnell AG (editors). *Handbook of New Bacterial Systematics* Academic Press; 1993. pp. 151–194.
  36. Yoon SH, Ha SM, Kwon S, Lim J, Kim Y et al. Introducing EzBioCloud: a taxonomically united database of 16S rRNA gene sequences and whole-genome assemblies. *Int J Syst Evol Microbiol* 2017; 67:1613–1617.
  37. Meier-Kolthoff JP, Göker M, Spröer C, Klenk HP. When should a DDH experiment be mandatory in microbial taxonomy? *Arch Microbiol* 2013;195:413–418.
  38. Edgar RC. MUSCLE: multiple sequence alignment with high accuracy and high throughput. *Nucleic Acids Res* 2004;32:1792–1797.
  39. Kimura M. A simple method for estimating evolutionary rates of base substitutions through comparative studies of nucleotide sequences. *J Mol Evol* 1980;16:111–120.
  40. Fitch WM. Toward defining the course of evolution: minimum change for a specific tree topology. *Syst Biol* 1971;20:406–416.
  41. Meier-Kolthoff JP, Hahnke RL, Petersen J, Scheuner C, Michael V et al. Complete genome sequence of DSM 30083<sup>T</sup>, the type strain (U5/41<sup>T</sup>) of *Escherichia coli*, and a proposal for delineating subspecies in microbial taxonomy. *Stand Genomic Sci* 2014;9:2.
  42. Meier-Kolthoff JP, Auch AF, Klenk HP, Göker M. Genome sequence-based species delimitation with confidence intervals and improved distance functions. *BMC Bioinformatics* 2013;14:60.
  43. Stamatakis A. RAxML version 8: a tool for phylogenetic analysis and post-analysis of large phylogenies. *Bioinformatics* 2014;30:1312–1313.
  44. Goloboff PA, Farris JS, Nixon KC. TNT, a free program for phylogenetic analysis. *Cladistics* 2008;24:774–786.
  45. Pattengale ND, Alipour M, Bininda-Emonds OR, Moret BM, Stamatakis A. How many bootstrap replicates are necessary? *J Comput Biol* 2010;17:337–354.
  46. Tamura T, Hayakawa M, Hatano K. A new genus of the order *Actinomycetales*, *Cryptosporangium* gen. nov., with descriptions of *Cryptosporangium arvum* sp. nov. and *Cryptosporangium japonicum* sp. nov. *Int J Syst Bacteriol* 1998;48:995–1005.
  47. Swofford DL. P. PAUP\*. Phylogenetic Analysis Using Parsimony (\*and Other Methods). Version 4. Sunderland: Sinauer Associates 2003.
  48. Idris H, Labeda DP, Nouioui I, Castro JF, Del Carmen Montero-Calasanz M et al. *Streptomyces aridus* sp. nov., isolated from a high altitude Atacama desert soil and emended description of

- Streptomyces noboritoensis* Isono et al. 1957. *Antonie van Leeuwenhoek* 2017;110:705–717.
49. Labeda DP. Taxonomic evaluation of putative *Streptomyces scabiei* strains held in the ARS Culture Collection (NRRL) using multi-locus sequence analysis. *Antonie van Leeuwenhoek* 2016;109:349–356.
  50. Kumar S, Stecher G, Tamura K. MEGA7: molecular evolutionary genetics analysis version 7.0 for bigger datasets. *Mol Biol Evol* 2016;33:1870–1874.
  51. Savic M, Bratic I, Vasiljevic B. *Streptomyces durmitorensis* sp. nov., a producer of an FK506-like immunosuppressant. *Int J Syst Evol Microbiol* 2007;57:2119–2124.
  52. Waksman SA, Lechevalier HA. *Guide to the Classification and Identification of the Actinomycetes and Their Antibiotics*. Baltimore: Williams & Wilkins; 1953.
  53. Gause GF, Preobrazhenskaya TP, Sveshnikova MA, Terekhova LP, Maximova TS et al. *A Guide for the Determination of Actinomycetes. Genera Streptomyces, Streptovercillium and Chainia*. Moscow: Nauka; 1983.
  54. Xu LH, Jiang Y, Li WJ, Wen ML, Li MG et al. *Streptomyces rosealbus* sp. nov., an actinomycete isolated from soil in Yunnan, PR China. *Antonie van Leeuwenhoek* 2005;87:189–194.
  55. Rong X, Huang Y. Multi-locus sequence analysis. Taking prokaryotic systematics to the next level. *Methods Microbiol* 2014;41:221–251.
  56. Rong X, Huang Y. Taxonomic evaluation of the *Streptomyces hygroscopicus* clade using multilocus sequence analysis and DNA-DNA hybridization, validating the MLSA scheme for systematics of the whole genus. *Syst Appl Microbiol* 2012;35:7–18.
  57. Schniete JK, Salih TS, Algora-Gallardo L, Santos T, Filgueira-Martinez S et al. Draft genome sequence of *Streptomyces phaeoluteigriseus* DSM41896. *Genome Announc* 2017;5:e00371–17.
  58. Bankevich A, Nurk S, Antipov D, Gurevich AA, Dvorkin M et al. SPAdes: a new genome assembly algorithm and its applications to single-cell sequencing. *J Comput Biol* 2012;19:455–477.
  59. Aziz RK, Bartels D, Best AA, Dejongh M, Disz T et al. The RAST Server: rapid annotations using subsystems technology. *BMC Genomics* 2008;9:75.
  60. Overbeek R, Olson R, Pusch GD, Olsen GJ, Davis JJ et al. The SEED and the Rapid Annotation of microbial genomes using Subsystems Technology (RAST). *Nucleic Acids Res* 2014;42:D206–D214.
  61. Yoon SH, Ha SM, Lim J, Kwon S, Chun J. A large-scale evaluation of algorithms to calculate average nucleotide identity. *Antonie van Leeuwenhoek* 2017;110:1281–1286.
  62. Lee I, Ouk Kim Y, Park SC, Chun J. OrthoANI: An improved algorithm and software for calculating average nucleotide identity. *Int J Syst Evol Microbiol* 2016;66:1100–1103.
  63. Wayne LG, Moore WEC, Stackebrandt E, Kandler O, Colwell RR et al. Report of the Ad Hoc Committee on Reconciliation of Approaches to Bacterial Systematics. *Int J Syst Evol Microbiol* 1987;37:463–464.
  64. Goris J, Konstantinidis KT, Klappenbach JA, Coenye T, Vandamme P et al. DNA-DNA hybridization values and their relationship to whole-genome sequence similarities. *Int J Syst Evol Microbiol* 2007;57:81–91.
  65. Richter M, Rosselló-Móra R. Shifting the genomic gold standard for the prokaryotic species definition. *Proc Natl Acad Sci USA* 2009;106:19126–19131.
  66. Chun J, Rainey FA. Integrating genomics into the taxonomy and systematics of the bacteria and archaea. *Int J Syst Evol Microbiol* 2014;64:316–324.

### Five reasons to publish your next article with a Microbiology Society journal

1. The Microbiology Society is a not-for-profit organization.
2. We offer fast and rigorous peer review – average time to first decision is 4–6 weeks.
3. Our journals have a global readership with subscriptions held in research institutions around the world.
4. 80% of our authors rate our submission process as 'excellent' or 'very good'.
5. Your article will be published on an interactive journal platform with advanced metrics.

Find out more and submit your article at [microbiologyresearch.org](http://microbiologyresearch.org).

# *Streptomyces altiplanensis* sp. nov., an alkalitolerant species isolated from Chilean Altiplano soil, and emended description of *Streptomyces chryseus* (Krasil'nikov *et al.* 1965) Pridham 1970

Carlos Cortés-Albayay,<sup>1,2</sup> Cristina Dorador,<sup>3</sup> Peter Schumann,<sup>4</sup> Jana K. Schniete,<sup>5</sup> Paul Herron,<sup>6</sup> Barbara Andrews,<sup>2</sup> Juan Asenjo<sup>2</sup> and Imen Nouioui<sup>1,\*</sup>

## Abstract

A polyphasic approach was used for evaluating the taxonomic status of strain HST21<sup>T</sup> isolated from Salar de Huasco in the Atacama Desert. The results of 16S rRNA gene and multilocus sequence phylogenetic analyses assigned strain HST21<sup>T</sup> to the genus *Streptomyces* with *Streptomyces albidochromogenes* DSM 41800<sup>T</sup> and *Streptomyces flavidovirens* DSM 40150<sup>T</sup> as its nearest neighbours. Digital DNA–DNA hybridization (dDDH) and average nucleotide identity (ANI) values between the genome sequences of strain HST21<sup>T</sup> and *S. albidochromogenes* DSM 41800<sup>T</sup> (35.6 and 88.2%) and *S. flavidovirens* DSM 40150<sup>T</sup> (47.2 and 88.8%) were below the thresholds of 70 and 95–96% for prokaryotic conspecific assignment. Phenotypic, chemotaxonomic and genetic results distinguished strain HST21<sup>T</sup> from its closest neighbours. Strain HST21<sup>T</sup> is characterized by the presence of LL-diaminopimelic acid in its peptidoglycan layer; glucose and ribose as whole cell sugars; diphosphatidylglycerol, phosphatidylmethylethanolamine, phosphatidylethanolamine, phosphatidylinositol, glycopospholipids, unknown lipids and phospholipids as polar lipids; and *anteiso*-C<sub>15:0</sub> (21.6%) and *anteiso*-C<sub>17:0</sub> (20.5%) as major fatty acids (>15%). Based on these results, strain HST21<sup>T</sup> merits recognition as a novel species, for which the name *Streptomyces altiplanensis* sp. nov. is proposed. The type strain is HST21<sup>T</sup>=DSM 107267<sup>T</sup>=CECT 9647<sup>T</sup>. While analysing the phylogenies of strain HST21<sup>T</sup>, *Streptomyces chryseus* DSM 40420<sup>T</sup> and *Streptomyces helveticus* DSM 40431<sup>T</sup> were found to have 100% 16S rRNA gene sequence similarity with digital DNA–DNA hybridization (dDDH) and average nucleotide identity (ANI) values of 95.3 and 99.4%, respectively. Therefore, *S. helveticus* is considered as a later heterotypic synonym of *S. chryseus* and, consequently, we emend the description of *S. chryseus*.

Members of the genus *Streptomyces* of the family *Streptomycetaceae* [1] are well known as a pre-eminent source of secondary metabolites and antibiotic production [2]. This taxon encompasses Gram-stain-positive, aerobic and heterotrophic micro-organisms with extensive branched substrate and aerial mycelia [3]. Over 800 *Streptomyces* species

have been validly named and characterized by the presence of LL-diaminopimelic acid (A<sub>2</sub>pm) in their peptidoglycan layer; diphosphatidylglycerol, phosphatidylethanolamine, phosphatidylinositol and phosphatidylinositol mannosides as major polar lipids; saturated *iso* and *anteiso* fatty acids as major fatty acids; hexa- and octa-hydrogenated

**Author affiliations:** <sup>1</sup>School of Natural and Environmental Sciences, Newcastle University, Devonshire Building, Newcastle upon Tyne NE1 7RU, UK; <sup>2</sup>Centre for Biotechnology and Bioengineering, University of Chile, Beauchef 851, Santiago, Chile; <sup>3</sup>Laboratory of Microbial Complexity and Functional Ecology, Departamento de Biotecnología, Facultad de Ciencias del Mar y Recursos Biológicos & Centre for Biotechnology and Bioengineering, Universidad de Antofagasta, Chile; <sup>4</sup>Leibniz Institute DSMZ-German Collection of Microorganisms and Cell Cultures, Germany; <sup>5</sup>Department of Physics, University of Strathclyde, 107 Rottenrow, Glasgow G4 0NG, UK; <sup>6</sup>Strathclyde Institute of Pharmacy and Biomedical Sciences, University of Strathclyde, 161 Cathedral Street, Glasgow G4 0RE, UK.

\*Correspondence: Imen Nouioui, imen.nouioui@newcastle.ac.uk

**Keywords:** Actinobacteria; taxonomy; genome sequence; Atacama Desert.

**Abbreviations:** atpD, ATP synthase F1, beta subunit; A<sub>2</sub>pm, diaminopimelic acid; AGLP, amino glycopospholipid; AL, aminolipid; ANI, average nucleotide identity; dDDH, digital DNA–DNA hybridization; DPG, diphosphatidylglycerol; gyrB, DNA gyrase B subunit; GGDC, Genome-to-Genome Distance Calculator; GL, glycolipid; GPL, glycopospholipid; GYM, glucose–yeast extract–malt extract; HPLC, high-performance liquid chromatography; ISP, International Streptomyces project; L, unknown lipid; MEGA, molecular evolutionary genetics analysis; MIDI, microbial identification; ML, maximum-likelihood; MLSA, multilocus sequence analysis; MP, maximum-parsimony; PAUP, phylogenetic analysis using parsimony; PE, phosphatidylethanolamine; PGM, personal genome machine; PI, phosphatidylinositol; PL, phospholipid; PME, phosphatidylmethyl-ethanolamine; recA, recombinase A; rpoB, RNA polymerase beta subunit; RAXML, Randomized Axelerated Maximum Likelihood; RAST, rapid annotation using subsystems technology; trpB, tryptophane synthase beta chain; TNT, Tree analysis New Technology.

The GenBank accession numbers of the 16S rRNA gene and genome sequences of strain HST21<sup>T</sup> are KX130868.2 and RHMC00000000, respectively. Three supplementary tables and three supplementary figures are available with the online version of this article.



**Table 1.** Growth and cultural features of strain HST21<sup>T</sup> after 10 days of incubation at 28 °C

+, Poor growth; ++, moderate growth; +++, good growth; –, absence.

Medium	Growth	Substrate mycelium colour	Aerial mycelium colour	Diffusible pigments
Tryptone–yeast extract agar (ISP1)	++	Deep reddish brown	Dark brown	Strong reddish brown
Yeast extract–malt extract agar (ISP2)	+	White	White	–
Oatmeal agar (ISP3)	+++	–	White	Deep reddish brown
Inorganic salts–starch agar (ISP4)	++	Dark greyish yellow	Light greyish olive	Vivid greenish yellow
Glycerol–asparagine agar (ISP5)	++	Light olive brown	Strong yellowish brown	Strong yellow
Tyrosine agar (ISP7)	++	Dark yellowish brown	Light olive brown	Dark yellow
GYM (DSMZ medium 65)	+++	Strong brown	White	Deep reddish brown

menaquinones with nine isoprene units as predominant isoprenologues [4, 5]; and a G+C content range between 69–78 mol%. The genus *Streptomyces* is widely distributed in various ecosystems, such as soil, fresh and marine waters, clinical samples, and extreme or poly-extreme environments.

During our investigation of *Streptomyces* biodiversity in the poly-extreme high altitude saline wetland (3800 m.a.s.l) of the Atacama Desert, strain HST21<sup>T</sup> was isolated based on polyphasic taxonomic approach. Strain HST21<sup>T</sup> was found to represent a new species within the evolutionary radiation of the genus *Streptomyces* for which the name *Streptomyces altiplanensis* sp. nov. is proposed.

Strain HST21<sup>T</sup> was isolated from arid soil samples (site H6) in the Salar de Huasco [6] of the Atacama Desert. The characteristics of site H6 and the isolation procedures are as described by Cortés-Albayay et al. [6]. Strain HST21<sup>T</sup> was maintained on GYM (Glucose–Yeast extract–Malt extract; DSMZ medium 65) agar plates, for 10 days of incubation at 28 °C, together with its closest phylogenetic relatives, *Streptomyces albidochromogenes* DSM 41800<sup>T</sup> [7], *Streptomyces flavidovirens* DSM 40150<sup>T</sup> [8, 9], *Streptomyces chryseus* DSM 40420<sup>T</sup> [9, 10] and *Streptomyces helveticus* DSM 40431<sup>T</sup> [9, 10], which were obtained from the German Collection of Microorganisms and Cell Cultures (DSMZ, www.dsmz.de/). All strains were preserved in 25 % v/v glycerol at –80 °C. *S. albidochromogenes* DSM 41800<sup>T</sup> and *S.*

*chryseus* DSM 40420<sup>T</sup>, *S. flavidovirens* DSM 40150<sup>T</sup>, and *S. helveticus* DSM 40431<sup>T</sup> were originally deposited in DSMZ by L. Evtushenko and Elwood B. Shirling, respectively.

Cultural properties of strain HST21<sup>T</sup> were examined using different agar media: International *Streptomyces* Project (ISP1–5 and ISP7) [11] and GYM (DSMZ medium 65). A range of temperatures of 4, 10, 15, 25, 28, 37 and 45 °C as well as pH ranges from 6 to 12 were tested on HST21<sup>T</sup> culture using GYM medium. Strain HST21<sup>T</sup> was able to grow in all the tested media but with poor growth on ISP2 (Table 1). Growth was detected after 10 days of incubation at 28 and 37 °C, and pH from 7 to 11.5. Optimal growth of the studied strain was observed on GYM and ISP3 media and between pH 9–11 at 28 °C; these results highlighted the alkaliphilic trait of strain HST21<sup>T</sup>. This later formed a white aerial mycelium and brownish substrate mycelia with diffusible pigment after 10 days of incubation at 28 °C on GYM medium. More details about the cultural characteristics of strain HST21<sup>T</sup> are given in Table 1.

A field-emission scanning electron microscope (Vega 3 LMU, Tescan) was used to describe the spore chain ornamentation and spore surface morphology of strain HST21<sup>T</sup> grown for 10 days on GYM media at 28 °C. It was characterized by the presence of rectiflexible spore chains in section with spiny spore surfaces (Fig. 1) while *S. albidochromogenes* DSM 41800<sup>T</sup> and *S. flavidovirens* DSM 40150<sup>T</sup>, the nearest phylogenetic neighbours, have spiral and

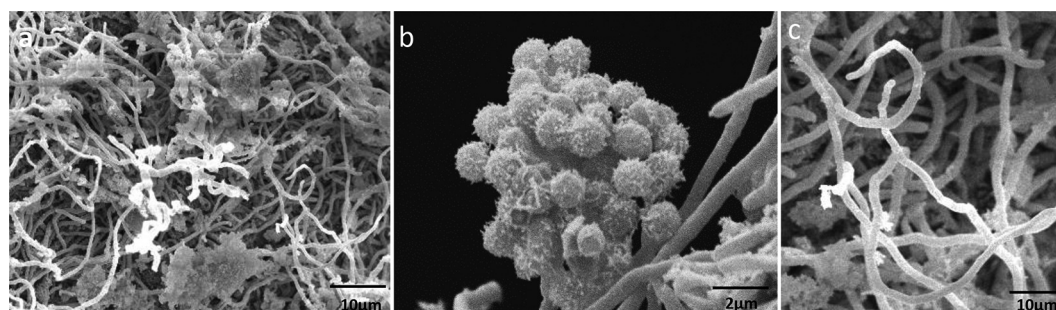


**Fig. 1.** Scanning electron micrograph of strain HST21<sup>T</sup> showing 'rectiflexible' spore chains sections (a, c) and spores with a spiny surface (b), after incubation for 10 days on GYM agar plates at 28 °C.

**Table 2.** Phenotypic features that distinguish strain HST21<sup>T</sup> from its nearest phylogenetic neighbours *Streptomyces albidochromogenes* DSM 41800<sup>T</sup> and *Streptomyces flavidovirens* DSM 40150<sup>T</sup>

+, Positive reaction; −, negative reaction. All strains were able to metabolize dextrin, maltose, L-fucose, trehalose, N-acetyl-β-D-mannosamine, cellobiose, β-gentobiose, methyl β-D-glucoside, D-salicin, N-acetyl-D-glucosamine, D-glucose, D-mannose, D-galactose, inosine, glycerol, D-glucose-6-phosphate, D-fructose-6-phosphate, gelatin and sucrose (carbon source); L-arginine, L-alanine, L-aspartic acid, L-glutamic acid and L-histidine (amino acids); butyric acid, β-hydroxy-butyric acid, D-gluconic acid, α-keto glutaric acid, L-malic acid, γ-amino-n-butyric acid, α-hydroxy-butyric acid, α-keto-butyric acid, acetoacetic acid, propionic acid and acetic acid (organic acids); to grow in presence of aztreonam, nalidixic acid, lithium chloride, potassium tellurite, sodium bromate and tween 40 (inhibitory compounds); and at 1–4% (w/v) NaCl and pH 6–8. In contrast, none of the strains used D-sorbitol, 3-O-methyl-D-glucose and glucuronamide (carbon source); D-aspartic acid and D-serine 1 (amino acids); D-glucuronic acid, D-galacturonic acid, p-hydroxy-phenylacetic acid, D-saccharic acid and mucic acid (organic acids); and were unable to grow in presence of guanidine hydrochloride, tetrazolum blue and violet, troleandomycin, vancomycin, minocycline, lincomycin, Niaproof, fusidic acid, and pH 5.

	Strain HST21 <sup>T</sup>	<i>S. albidochromogenes</i> DSM 41800 <sup>T</sup>	<i>S. flavidovirens</i> DSM 40150 <sup>T</sup>
<b>Carbon utilization</b>			
D-Arabitol, D-fructose, lactose, myo-inositol, D-mannitol, raffinose, pectin, stachyose and turanose	+	−	+
D-Fucose, N-acetyl-D-galactosamine and melibiose	−	−	+
L-Rhamnose	+	−	−
Methyl pyruvate	−	−	+
<b>Amino acids</b>			
D-Serine 2, L-Serine	−	+	−
Glycine proline	+	+	−
<b>Organic acids</b>			
Bromo-succinic acid, citric acid and L-pyroglytamic acid	+	−	+
D-Lactic acid methyl ester, L-galactonic acid-γ-lactone and L-lactic acid	−	−	+
D-Malic acid and sodium formate	+	+	−
N-acetyl-neuraminic acid	−	+	−
Quinic acid	+	−	−
<b>Inhibitory compounds</b>			
Rifamycin sv, 1% sodium lactate	+	+	−
8% NaCl	+	−	−
<b>Menaquinone patterns</b>			
	MK-9(H <sub>6</sub> ) 33%, MK-9(H <sub>8</sub> ) 32%, MK-9(H <sub>4</sub> ) 10%, MK-7(H <sub>2</sub> ) 10%, MK-8(H <sub>2</sub> ) 8%, MK-9(H <sub>2</sub> ) 4%, MK-10 3%	MK-9(H <sub>8</sub> ) 78%, MK-9(H <sub>6</sub> ) 7%, MK-9(H <sub>4</sub> ) 7%, MK-9(H <sub>2</sub> ) 7%, MK-10(H <sub>2</sub> ) 1%	MK-9(H <sub>8</sub> ) 52%, MK-9(H <sub>6</sub> ) 22%, MK-9(H <sub>4</sub> ) 11%, MK-9(H <sub>2</sub> ) 9%, MK-10(H <sub>2</sub> ) 3%, MK-8(H <sub>4</sub> ) 2%, MK-9 1%

rectiflexible spore chains with a smooth spore surface, respectively [4].

The ability of strain HST21<sup>T</sup> to use different carbon and nitrogen sources and to grow in the presence of inhibitory compounds was examined using GENIII MicroPlates in an OmniLog device (Biolog). The type strains of *S. albidochromogenes* and *S. flavidovirens* species were included in this test, which was carried out in duplicate. The Opm package for R version 1.06 was used to analyse the resultant data [12,13]. Strain HST21<sup>T</sup> could be distinguished from its relatives cited above by its ability to metabolize rhamnose (carbon source) and quinic acid (organic acid; Table 2) while strain DSM 40150<sup>T</sup> was able to oxidize D-fucose, N-acetyl-D-galactosamine, melibiose and methyl pyruvate (carbon sources), D-lactic acid methyl ester, L-galactonic acid-γ-lactone and L-lactic acid (organic acids). However

strain DSM 41800<sup>T</sup> could use N-acetyl-neuraminic acid (organic acid) and D-serine 2 and L-serine (Table 2).

Standard procedures for chemotaxonomic analyses were used to characterize strains HST21<sup>T</sup>, *S. albidochromogenes* DSM 41800<sup>T</sup> and *S. flavidovirens* DSM 40150<sup>T</sup>. Diaminopimelic acid isomers [14], whole-cell sugars [15], polar lipid profiles [16] and menaquinones [17] were determined using freeze-dried cells obtained following the same procedure of Cortés-Albayay et al. [18]. The menaquinones were analysed by using an Agilent 1260 Infinity II HPLC system with a 125/2 Nucleosil 120–3 C18 column and an isocratic solvent system (acetonitrile/isopropanol, 65:35, v/v; 0.4 ml min<sup>−1</sup>). Fatty acid analyses were performed for strain HST21<sup>T</sup> and all the reference strains cited above, following the protocols of Miller [19] and Kuykendall et al. [20] and using a gas chromatography (Agilent 6890 N) instrument.

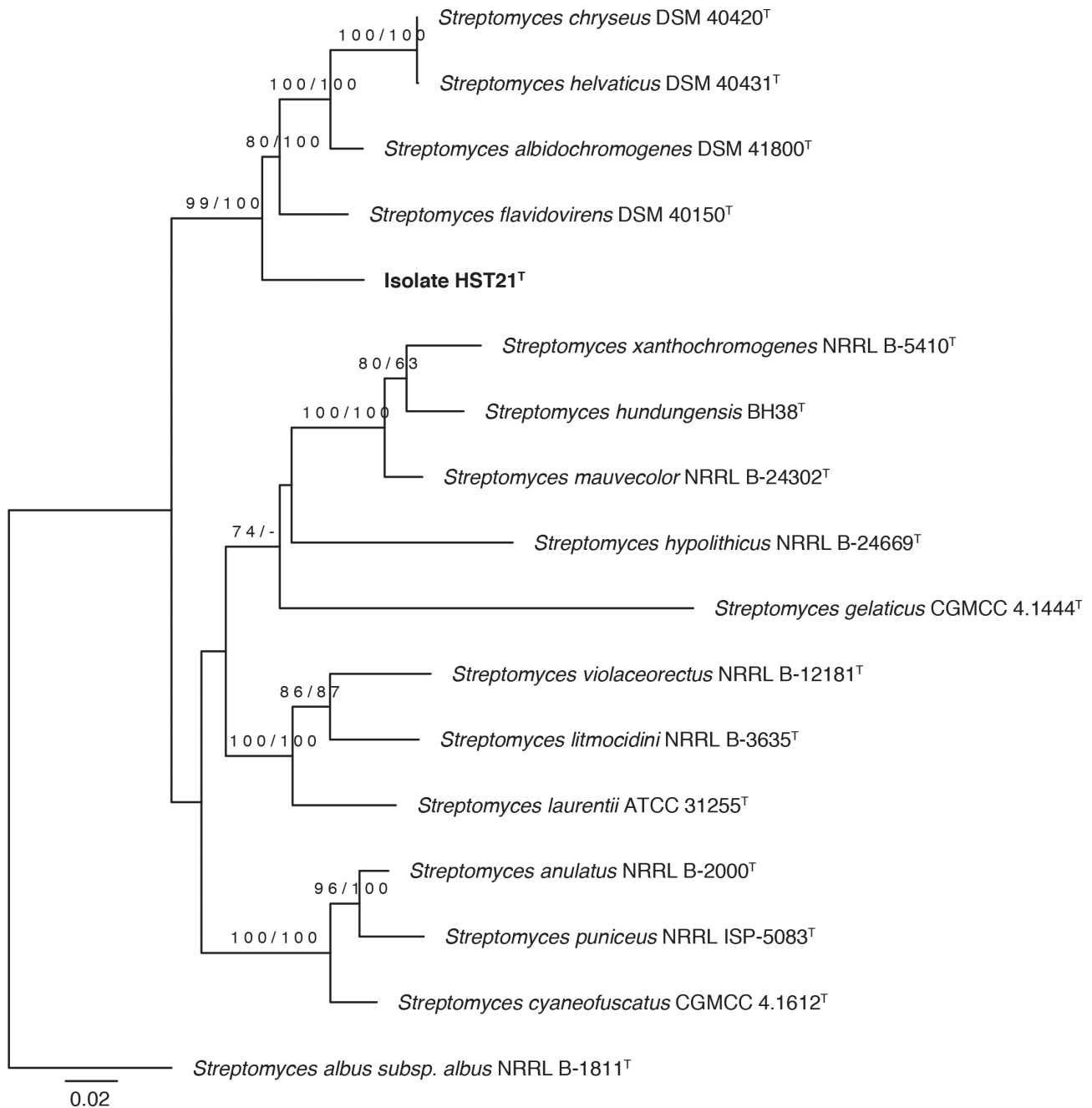


**Fig. 2.** Maximum-likelihood phylogenetic tree based on concatenated sequences of five genes, *atpD*, *gyrB*, *recA*, *rpoB* and *trpB*, showing the phylogenetic relationship between strain HST21<sup>T</sup> and its relatives within the genus *Streptomyces*. The numbers above the branches are bootstrap support values greater than 60% for maximum-likelihood (left) and Maximum-parsimony (right) analyses.

The extracts were identified using the standard Microbial Identification (MIDI) system version 4.5 and the ACTIN 6 database [21].

Whole-cell hydrolysates of strain HST21<sup>T</sup> were rich in LL-diaminopimelic acid, glucose and ribose as whole-cell sugars, while the type strains of *S. albidochromogenes* and *S. flavidovirens* also have mannose. Strain HST21<sup>T</sup> contained, in

its polar lipid profile, diphosphatidylglycerol (DPG), phosphatidylmethylethanolamine (PME), phosphatidylethanolamine (PE), phosphatidylinositol (PI), glycopospholipids (GPL1–2), unknown lipids (L1–2) and phospholipids (PL1–2). The same profile was obtained for *S. flavidovirens* DSM 40150<sup>T</sup> and *S. albidochromogenes* DSM 41800<sup>T</sup>, but devoid of PME (Fig. S1) and with unidentified aminolipids (AL1–2) and glycolipids (GL1–4) for strain DSM 41800<sup>T</sup>. Strain

HST21<sup>T</sup>, like its closest neighbour *S. flavidovirens* DSM 40150<sup>T</sup>, had MK-9(H<sub>6</sub>) and MK-9(H<sub>8</sub>) as predominant menaquinones (>20 %) while *S. albidochromogenes* DSM 41800<sup>T</sup> had MK-9(H<sub>8</sub>) (Table 2). Strain HST21<sup>T</sup> had *anteiso*-C<sub>15:0</sub> (21.6 %) and *anteiso*-C<sub>17:0</sub> (20.5 %) as major fatty acids (>15 %); however, its nearest relatives *S. flavidovirens* DSM 40150<sup>T</sup> and *S. albidochromogenes* DSM 41800<sup>T</sup> had *anteiso*-C<sub>15:0</sub> (38.7 %) and *anteiso*-C<sub>15:0</sub> (27.0 %) and C<sub>16:0</sub> (16.0 %), respectively (Table S1).

The genomic DNA extraction of strain HST21<sup>T</sup> and 16S rRNA gene PCR amplification were carried out as described by Cortés-Albayay *et al.* [18]. The retrieval of the nearest phylogenetic neighbours of strain HST21<sup>T</sup> was performed following the alignment of the complete 16S rRNA gene sequence (1517 bp; accession number KX130868.2) of isolate HST21<sup>T</sup> against those available in the EzBioCloud database [22].

The phylogenetic trees were inferred from the DSMZ phylogenomics pipeline [23] available at the Genome-to-Genome distance Calculator (GGDC) web server [24] (<http://ggdc.dsmz.de/>). Pairwise sequence similarities of 16S rRNA genes were estimated based on the method of Meier-Kolthoff *et al.* [25]. The MUSCLE program was used for multiple sequence alignments [26]. RAXML [27] and TNT [28] were used for reconstruction of the maximum-likelihood (ML) [29] and maximum-parsimony (MP) [30] phylogenetic trees, respectively. A rapid bootstrapping method together with the autoMRE bootstrapping criterion [31] were used for the resultant ML tree. However, the resultant best topology of the MP tree was obtained based on a combination of the bootstrapping method with 1000 iterations with a tree-bisection-and-reconnection branch swapping method in addition to the use of ten additional random sequence replicates. The X<sup>2</sup> test of the PAUP program [32] was used to check the sequences for a compositional bias. All the trees were rooted using the type species of the genus, *Cryptosporangium arvum* DSM 44712<sup>T</sup> [33].

Multilocus sequence analyses (MLSA) was carried out based on five partial housekeeping gene sequences, *atpD* (ATP synthase F1, beta subunit), *gyrB* (DNA gyrase subunit), *rpoB* (RNA polymerase beta subunit), *recA* (recombinase A) and *trpB* (tryptophane B, beta subunit) [34–37]. All the genes of strain HST21<sup>T</sup> were taken from the draft genome sequence (accession number RHMC00000000) and those of the reference strains were retrieved from the ARS Microbial Genome Sequence (<http://199.133.98.43>) and the GenBank databases (Table S2). An ML phylogenetic tree was inferred using the DSMZ phylogenomics pipeline cited above while the NJ tree was reconstructed by using MEGA software version 7. Kimura's two-parameter model [38] was used to estimate the genetic distance between the loci of strain HST21<sup>T</sup> and those of its closest phylogenetic neighbours.

Strain HST21<sup>T</sup> showed 16S rRNA gene sequence similarity values of 99.2 % to *S. albidochromogenes* NBRC 101003<sup>T</sup> (12 nt difference) and *S. flavidovirens* NBRC13039<sup>T</sup> (12 nt

difference) and 99.1 % to *S. chryseus* NRRL B-12347<sup>T</sup> (13 nt difference) and *S. helveticus* NBRC 13382<sup>T</sup> (13 nt difference). These results were reflected in the 16S rRNA gene phylogenetic tree (Fig. 2), where strain HST21<sup>T</sup> formed, together with all the strains cited above, a well-supported clade next to *Streptomyces hypolithicus* HSM10<sup>T</sup> (Fig. S2) [39]. The phylogenetic positions of *S. albidochromogenes* NBRC 101003<sup>T</sup>, *S. chryseus* NRRL B-12347<sup>T</sup>, *S. flavidovirens* NBRC13039<sup>T</sup> and *S. helveticus* NBRC 13382<sup>T</sup> (16S rRNA gene sequence similarities between 99.9 and 100 %) in the same branch are in line with the previous studies [4, 34, 40] and call for taxonomic revision of the status of these species based on MLSA and genomic analyses.

In the MLSA tree, strain HST21<sup>T</sup> formed a subclade with *S. flavidovirens* DSM 40150<sup>T</sup> next to the one that encompasses the representative strains of *S. albidochromogenes*, *S. chryseus* and *S. helveticus* species. These two latter occupied the same branch, unlike *S. albidochromogenes* (Fig. 2). The topology of the ML and NJ MLSA trees as well as the 16S rRNA gene tree are in concordance (Figs 2 and S3). These results are consistent with the MLSA evolutionary genetic distances, which showed a value above the threshold of 0.007 for the assigning *Streptomyces* strains to the same species [41, 42] between strain HST21<sup>T</sup> and its close phylogenetic neighbours (Table S3). However, a genetic distance value of 0.0 % was obtained between *S. chryseus* DSM 40420<sup>T</sup> and *S. helveticus* DSM 40431<sup>T</sup> (Table S3).

The genomic DNA of strain HST21<sup>T</sup> was sequenced using Ion Torrent PGM (Personal Genome Machine) sequencer technology as described by Cortés-Albayay *et al.* [18] while the *S. albidochromogenes* DSM 41800<sup>T</sup>, *S. chryseus* DSM 40420<sup>T</sup> and *S. helveticus* DSM 40431<sup>T</sup> genomes were sequenced using Illumina next-generation sequencing technology (MicrobesNG). The RAST server was used for annotation of these genome sequences [43,44].

The genome sequence of strain HST21<sup>T</sup> had a size of 7.9 Mb and an *in silico* G+C content of 71.0 mol%. However, the type strains of *S. albidochromogenes* (accession number VBVBX00000000) and *S. flavidovirens* (accession number AUBE00000000) have genome sizes of 7.4 Mb and 7.0 Mb with *in silico* G+C contents of 70.5 mol% and 70.4 mol%, respectively.

The GGDC server with the recommended formula 2 [24] was used to estimate the dDDH values between the draft genome sequence of strain HST21<sup>T</sup> and its closest phylogenetic relatives, *S. albidochromogenes* DSM 41800<sup>T</sup>, *S. chryseus* DSM 40420<sup>T</sup>, *S. flavidovirens* DSM 40105<sup>T</sup> and *S. helveticus* DSM 40431<sup>T</sup>. The OrthoANIu algorithm of the ANI Calculator [45, 46] was used to calculate the ANI values between the strains cited above.

The dDDH values obtained between the genome of the HST21<sup>T</sup> and its closest relatives *S. albidochromogenes* DSM 41800<sup>T</sup> (35.6 %), *S. chryseus* DSM 40420<sup>T</sup> (36.5 %), *S. flavidovirens* DSM 40105<sup>T</sup> (47.2 %) and *S. helveticus* DSM 40431<sup>T</sup> (36.0 %), with which the 16S rRNA gene sequence

similarities values are above 99.0%, were well below the threshold of 70% for conspecific assignment [47]. These results are in concordance with the corresponding ANI values of 88.2%, 88.4%, 88.8% and 88.2%; values below the cut-off point of 95–96% for delineation of prokaryotic species [48–50].

The comparison of the dDDH and ANI values estimated between the pair of the closest phylogenetic neighbours of strain HST21<sup>T</sup> showed that only *S. chryseus* DSM 40420<sup>T</sup> (accession number VBVW00000000) and *S. helveticus* DSM 40431<sup>T</sup> (VBVY00000000) have dDDH (95.3%) and ANI (99.4%) values above the described thresholds of 70% and 96%, respectively. These results are coherent with their phylogenetic positions in the 16S rRNA gene and MLSA trees. Strains DSM 40420<sup>T</sup> and DSM 40431<sup>T</sup> had *anteiso*-C<sub>15:0</sub> and *iso*-C<sub>16:0</sub> as major fatty acids (>15%; Table S1). In addition, *S. chryseus* DSM 40420<sup>T</sup> and *S. helveticus* DSM 40431<sup>T</sup> contained DPG, PE, PI, GPL as major polar lipids, but only strain DSM 40420<sup>T</sup> had PME and PL while strain DSM 40431<sup>T</sup> showed unknown aminolipids (Fig. S1). In light of these findings, it is proposed that *S. helveticus* be recognized as a heterotypic synonym of *S. chryseus*. Therefore, an emended description of this species is proposed below.

In conclusion, strain HST21<sup>T</sup> showed phenotypic, genetic and genomic data distinct from its closest phylogenetic relatives and, consequently, it merits recognition as a new species, namely *Streptomyces altiplanensis* sp. nov.

## DESCRIPTION OF *STREPTOMYCES ALTIPLANENSIS* SP. NOV.

*Streptomyces altiplanensis* (al.ti.pla.nen'sis N.L. masc. adj. *altiplanensis* referring to the site in the Chilean Altiplano where the strain was isolated).

Aerobic, Gram-stain-positive actinobacterium which produces white aerial mycelium and a brownish substrate mycelia with diffusible pigment that is observed after 10 days of incubation at 28 °C on GYM media. It has rectiflexible spore chains in section with spiny spore surfaces. Strain HST21<sup>T</sup> is able to grow on GYM media and at a range of temperature between 28 and 37 °C; poor growth is observed at 25 and 45 °C. Optimal growth of strain HST21<sup>T</sup> is observed on GYM and ISP3 agar media, pH 9–11, after 10 days of incubation at 28 °C. Strain HST21<sup>T</sup> is able to metabolize sucrose, stachyose, raffinose, D-fructose, D-galactose (carbon sources); L-pyrogutamic acid, quinic acid, β-hydroxy-butyric acid, α-keto-butyric acid, butyric acid (organic acids); L-arginine (amino acid); and grow in the presence of aztreonam, lithium chloride and Tween 40 (inhibitory compounds) and sodium bromate, 1% sodium lactate (salts) (Table 1). Whole-cell hydrolysates of strain HST21<sup>T</sup> are rich in LL-diaminopimelic acid in its peptidoglycan and glucose and ribose in its cell-wall sugars. It is characterized by the presence of DPG, PME, PE, PI, GPLs and unknown lipids and phospholipids as polar lipids;

*anteiso*-C<sub>15:0</sub> and *anteiso*-C<sub>17:0</sub> as major fatty acids. The menaquinone profile contained MK-9(H<sub>6</sub>), MK-9(H<sub>8</sub>), MK-9(H<sub>4</sub>), MK-7(H<sub>2</sub>), MK-8(H<sub>2</sub>), MK-9(H<sub>2</sub>) and MK-10.

The genome size is 7.9 Mb with an *in silico* G+C content of 71.0 mol%. The type strain, HST21<sup>T</sup> (DSM 107267<sup>T</sup>=CECT 9647<sup>T</sup>), was isolated from hyper arid soil of the Salar de Huasco in the Atacama Desert, Chile. The GenBank accession numbers of the 16S rRNA gene and genome sequences of strain HST21<sup>T</sup> are KX130868.2 and RHMC00000000, respectively.

## EMENDED DESCRIPTION OF *STREPTOMYCES CHRYSEUS* KRASIL'NIKOV ET AL. 1965 PRIDHAM 1970 (APPROVED LISTS 1980)

The description is as given by Kämpfer [4] with the following modifications and additions after inclusion of *S. helveticus*. Spore chains in section are retinaculiaperti to spirales, but rectiflexible spore chains may also be common; spore surface is smooth. The major fatty acids are *anteiso*-C<sub>15:0</sub> and *iso*-C<sub>16:0</sub>. The polar lipid pattern comprises DPG, PE, PI, GPL, AL, L1–2 and PL. The genome size is 7.1–7.6 Mb with an *in silico* G+C content of 71.2–71.3 mol%. The GenBank accession number for the draft genome sequence is VBVW00000000.

The type strain is AS 4.1694=ATCC 19829=CBS 678.72=DSM 40420=ISP 5420=JCM 4737=NCIMB 10041=NRRL B-12347=RIA 1338=VKM Ac-200.

### Acknowledgements

Genome sequencing was provided by MicrobesNG (www.microbesng.uk), which is supported by the BBSRC (grant number BB/L024209/1). This project was supported by the School of Natural and Environmental Sciences at Newcastle University. I.N. is grateful to Newcastle University for a post-doctoral fellowship. C.C.-A. is grateful to CONICYT for a PFCHA/DOCTORADO BECAS CHILE/2016–21160585 fellowship and operational expenses. This work was also financially supported by the Basal Centres Programme of CONICYT (Chile) for funding the Centre for Biotechnology and Bioengineering, CeBiB (project FB0001) and FONDECYT 1110953; 11181773 grants.

### Conflicts of interest

The authors declare that there are no conflicts of interest.

### References

1. Waksman SA, Henrici AT. The Nomenclature and Classification of the Actinomycetes. *J Bacteriol* 1943;46:4.
2. Watve MG, Tickoo R, Jog MM, Bhole BD. How many antibiotics are produced by the genus *Streptomyces*? *Arch Microbiol* 2001;176: 386–390.
3. Angert ER. Alternatives to binary fission in bacteria. *Nat Rev Microbiol* 2005;3:214–224.
4. Kämpfer P. Genus I. *Streptomyces*. In: Whitman W, Goodfellow M, Kämpfer P, Busse H-J, Trujillo M et al. (editors). *Bergey's Manual of Systematic Bacteriology*, 2nd ed, vol. 5. New York: Springer; 2012. pp. 1455–1767.
5. Kroppenstedt R. Fatty acid and menaquinone analysis of actinomycetes and related organisms. In: Goodfellow M and Minnikin DE (editors). *Chemical Methods in Bacterial Systematics*. London: Elsevier Science & Technology Books; 1985. pp. 173–199.
6. Cortés-Albayay C, Silber J, Imhoff JF, Asenjo JA, Andrews B et al. The polyextreme ecosystem, salar de huasco at the Chilean

- altiplano of the atacama desert houses diverse *Streptomyces* spp. with promising pharmaceutical potentials. *Diversity* 2019;11:69.
7. Gause GF, Preobrazhenskaya TP, Sveshnikova MA, Terekhova LP, Maximova TS et al. *A guide for the determination of actinomycetes. Genera Streptomyces, Streptovorticillium, and Chainia*. Moscow: URSS, Nauka; 1983.
  8. Kudrina ES. In: Gauze G, Preobrazhenskaya TP and Kudrina ES (editors). *Problems of Classification of Actinomycetes-Antagonists*. Moscow: Publishing house of medical literature, Medgiz; 1957. pp. 1–398.
  9. Pridham TG, Hesseltine CW, Benedict RG. A guide for the classification of streptomycetes according to selected groups; placement of strains in morphological sections. *Appl Microbiol* 1958;6:52–79.
  10. Krasil'nikov NA, Korenyako AI, Nikitina NI. Actinomycetes of the yellow group. In: Krasil'nikov NA (editor). *Biology of selected groups of Actinomycetes (in Russian)*. Moscow: Publishing Firm Nauka; 1965. pp. 1–372.
  11. Shirling EB, Gottlieb D. Methods for characterization of *Streptomyces* species. *Int J Syst Bacteriol* 1966;16:313–340.
  12. Vaas LA, Sikorski J, Michael V, Göker M, Klenk HP. Visualization and curve-parameter estimation strategies for efficient exploration of phenotype microarray kinetics. *PLoS One* 2012;7:e34846.
  13. Vaas LA, Sikorski J, Hofner B, Fiebig A, Buddruhs N et al. opm: an R package for analysing OmnLog(R) phenotype microarray data. *Bioinformatics* 2013;29:1823–1824.
  14. Staneck JL, Roberts GD. Simplified approach to identification of aerobic actinomycetes by thin-layer chromatography. *Appl Microbiol* 1974;28:226–231.
  15. Lechevalier MP, Lechevalier H. Chemical composition as a criterion in the classification of aerobic actinomycetes. *Int J Syst Bacteriol* 1970;20:435–443.
  16. Minnikin DE, O'Donnell AG, Goodfellow M, Alderson G, Athalye M et al. An integrated procedure for the extraction of bacterial isoprenoid quinones and polar lipids. *J Microbiol Methods* 1984;2:233–241.
  17. Tindall BJ. Lipid composition of *Halobacterium lacusprofundi*. *FEMS Microbiol Lett* 1990;66:199–202.
  18. Cortés-Albayay C, Dorador C, Schumann P, Andrews B A et al. *Streptomyces huasconensis* sp. nov., an haloalkalitolerant actinobacteria isolated from a high altitude saline wetland at the Chilean Altiplano. *Int J Syst Evol Microbiol*;2019.
  19. Miller LT. Single derivatization method for routine analysis of bacterial whole-cell fatty acid methyl esters, including hydroxy acids. *J Clin Microbiol* 1982;16:584–586.
  20. Kuykendall LD, Roy MA, O'Neill JJ, Devine TE. Fatty acids, antibiotic resistance, and deoxyribonucleic acid homology groups of *Bradyrhizobium japonicum*. *Int J Syst Bacteriol* 1988;38:358–361.
  21. Sasser M. *Identification of Bacteria by Gas Chromatography of Cellular Fatty Acids*, Technical Note 101; 1990.
  22. Yoon SH, Ha SM, Kwon S, Lim J, Kim Y et al. Introducing EzBio-Cloud: a taxonomically united database of 16S rRNA gene sequences and whole-genome assemblies. *Int J Syst Evol Microbiol* 2017; 67:1613–1617.
  23. Meier-Kolthoff JP, Hahnke RL, Petersen J, Scheuner C, Michael V et al. Complete genome sequence of DSM 30083<sup>T</sup>, the type strain (U5/41<sup>T</sup>) of *Escherichia coli*, and a proposal for delineating subspecies in microbial taxonomy. *Stand Genomic Sci* 2014;9:2.
  24. Meier-Kolthoff JP, Auch AF, Klenk HP, Göker M. Genome sequence-based species delimitation with confidence intervals and improved distance functions. *BMC Bioinformatics* 2013;14:60.
  25. Meier-Kolthoff JP, Göker M, Spröer C, Klenk HP. When should a DDH experiment be mandatory in microbial taxonomy? *Arch Microbiol* 2013;195:413–418.
  26. Edgar RC. MUSCLE: multiple sequence alignment with high accuracy and high throughput. *Nucleic Acids Res* 2004;32:1792–1797.
  27. Stamatakis A. RAxML version 8: a tool for phylogenetic analysis and post-analysis of large phylogenies. *Bioinformatics* 2014;30: 1312–1313.
  28. Goloboff PA, Farris JS, Nixon KC. TNT, a free program for phylogenetic analysis. *Cladistics* 2008;24:774–786.
  29. Felsenstein J. Evolutionary trees from DNA sequences: a maximum likelihood approach. *J Mol Evol* 1981;17:368–376.
  30. Fitch WM. Toward defining the course of evolution: minimum change for a specific tree topology. *Syst Biol* 1971;20:406–416.
  31. Pattengale ND, Alipour M, Bininda-Emonds OR, Moret BM, Stamatakis A. How many bootstrap replicates are necessary? *J Comput Biol* 2010;17:337–354.
  32. Swofford DL. *PAUP\*: Phylogenetic Analysis Using Parsimony (\*and Other Methods*, Version 4.0. Sunderland: Sinauer Associates; 2002.
  33. Tamura T, Hayakawa M, Hatano K. A new genus of the order Actinomycetales, *Cryptosporangium* gen. nov., with descriptions of *Cryptosporangium arvum* sp. nov. and *Cryptosporangium japonicum* sp. nov. *Int J Syst Bacteriol* 1998;48 Pt 3:995–1005.
  34. Labeda DP, Dunlap CA, Rong X, Huang Y, Doroghazi JR et al. Phylogenetic relationships in the family Streptomycetaceae using multi-locus sequence analysis. *Antonie van Leeuwenhoek* 2017; 110:563–583.
  35. Busarakam K, Bull AT, Girard G, Labeda DP, van Wezel GP et al. *Streptomyces leeuwenhoekii* sp. nov., the producer of chaxalactins and chaxamycins, forms a distinct branch in *Streptomyces* gene trees. *Antonie van Leeuwenhoek* 2014;105:849–861.
  36. Idris H, Labeda DP, Nouioui I, Castro JF, del Carmen Montero-Calasanz M et al. *Streptomyces aridus* sp. nov., isolated from a high altitude Atacama Desert soil and emended description of *Streptomyces noboritoensis* Isono et al. 1957. *Antonie van Leeuwenhoek* 2017;110:705–717.
  37. Labeda DP. Taxonomic evaluation of putative *Streptomyces scabiei* strains held in the ARS Culture Collection (NRRL) using multi-locus sequence analysis. *Antonie van Leeuwenhoek* 2016;109:349–356.
  38. Kimura M. A simple method for estimating evolutionary rates of base substitutions through comparative studies of nucleotide sequences. *J Mol Evol* 1980;16:111–120.
  39. Le Roes-Hill M, Rohland J, Meyers PR, Cowan DA, Burton SG et al. *Streptomyces hypolithicus* sp. nov., isolated from an Antarctic hypolith community. *Int J Syst Evol Microbiol* 2009;59:2032–2035.
  40. Nouioui I, Carro L, García-López M, Meier-Kolthoff JP, Woyke T et al. Genome-based taxonomic classification of the phylum Actinobacteria. *Front Microbiol* 2018;9:9.
  41. Rong X, Huang Y. Multi-locus sequence analysis. Taking prokaryotic systematics to the next level. *Methods Microbiol* 2014;41:221–251.
  42. Rong X, Huang Y. Taxonomic evaluation of the *Streptomyces hygroscopicus* clade using multilocus sequence analysis and DNA-DNA hybridization, validating the MLSA scheme for systematics of the whole genus. *Syst Appl Microbiol* 2012;35:7–18.
  43. Aziz RK, Bartels D, Best AA, Dejongh M, Disz T et al. The RAST Server: rapid annotations using subsystems technology. *BMC Genomics* 2008;9:75.
  44. Overbeek R, Olson R, Pusch GD, Olsen GJ, Davis JJ et al. The SEED and the Rapid Annotation of microbial genomes using Subsystems Technology (RAST). *Nucleic Acids Res* 2014;42:D206–D214.
  45. Yoon SH, Ha SM, Lim J, Kwon S, Chun J. A large-scale evaluation of algorithms to calculate average nucleotide identity. *Antonie Van Leeuwenhoek* 2017;110:1281–1286.
  46. Lee I, Ouk Kim Y, Park SC, Chun J. OrthoANI: An improved algorithm and software for calculating average nucleotide identity. *Int J Syst Evol Microbiol* 2016;66:1100–1103.
  47. Wayne LG, Moore WEC, Stackebrandt E, Kandler O, Colwell RR et al. Report of the Ad Hoc committee on reconciliation of approaches to bacterial systematics. *Int J Syst Evol Microbiol* 1987;37:463–464.
  48. Goris J, Konstantinidis KT, Klappenbach JA, Coenye T, Vandamme P et al. DNA-DNA hybridization values and their

- relationship to whole-genome sequence similarities. *Int J Syst Evol Microbiol* 2007;57:81–91.
49. Richter M, Rosselló-Móra R. Shifting the genomic gold standard for the prokaryotic species definition. *Proc Natl Acad Sci USA* 2009;106:19126–19131.
50. Chun J, Rainey FA. Integrating genomics into the taxonomy and systematics of the Bacteria and Archaea. *Int J Syst Evol Microbiol* 2014;64:316–324.

**Five reasons to publish your next article with a Microbiology Society journal**

1. The Microbiology Society is a not-for-profit organization.
2. We offer fast and rigorous peer review – average time to first decision is 4–6 weeks.
3. Our journals have a global readership with subscriptions held in research institutions around the world.
4. 80% of our authors rate our submission process as 'excellent' or 'very good'.
5. Your article will be published on an interactive journal platform with advanced metrics.

**Find out more and submit your article at [microbiologyresearch.org](http://microbiologyresearch.org).**